Implication of an odorant-binding protein in precopulatory behaviour and interaction with the bacterial microbiota

Enisa Aruci

Université de Bourgogne

Ecole doctorale Environnement-Santé n°554

Centre des Sciences du Goût et de l'Alimentation

AgroSup Dijon, CNRS, INRAe, Université de Bourgogne

F-21000 Dijon, France

Thesis

Submitted in partial fulfillment of requirements for the degree of

Doctor of Life Sciences

Speciality: Biochemistry, molecular biology

Implication of an odorant-binding protein in precopulatory behaviour and interaction with the bacterial microbiota

Enisa Aruçi

20 January 2023

Composition of the jury

Mr. Moussian Bernard	Professor, University of Tübingen	Reviewer
Mrs. Parmentier Marie-Laure	Research director, Institute of Functional Genomics	Reviewer
Mr. Savary Stéphane	Professor, University of Burgundy	President of the jury
Mr. Billeter Jean- Christophe	Professor, University of Groningen	Jury member
Mrs. Wolfner Mariana	Professor, University of Cornell	Jury member
Mr. Robichon Alain	Doctor of philosophy	Invited
Mr. Ferveur Jean-François	Research director, The national Center for Scientific Research	Advisors
Mr. Briand Loïc	Research director, French National Institute for Agricultural and Environment Research	Advisors

Awakening is not a thing. It is not a goal, not a concept. It is not something to be attained. It is a metamorphosis. If the caterpillar thinks about the butterfly it is to become, saying “And then I shall have wings and antennae,” there will never be a butterfly. The caterpillar must accept its own disappearance in its transformation. When the marvellous butterfly takes wing, nothing of the caterpillar remains.

Alejandro Jodorowsky

Acknowledgments

The work that has been completed in the past three years would not have been possible without the help and support of a number of individuals who I would like to take this opportunity to express my deepest appreciation to below.

I am very thankful to Mrs Marie-Laure Parmentier and Mr Bernard Moussian who have agreed to evaluate this work thesis as well as to Mrs Mariana Wolfner, Mr Stéphane Savary, Mr Jean-Christophe Billeter and Mr Alain Robichon for being part of the thesis jury. I would like to sincerely thank you for your time and availability. It is undeniably a great and special honour for me.

I would also like to express my gratitude to my thesis committee members, Mr Alain Robichon and Mr Jean-Marie Heydel for all their guidance through this process; their extremely helpful, ideas, and feedback and for our discussions which have been absolutely invaluable.

The journey of this PhD has been a truly-life changing experience for me. I have learned many things both on a profession and personal level. For me, it was a process of building up myself and trying to understand what science means out of the university auditoriums. I am forever grateful the help of many people during this process.

First, I would like to thank my advisors, Mr Jean-François Ferveur and Mr Loïc Briand for their continuous support of my PhD study and for their patience, motivation and knowledge. Thank you for the scientific discussions that we had. They contributed to make me a better researcher. Mr Jean-François Ferveur, these three years would not have been the same without you. You motivated me through your passion and hard work. Thank you for all the advice that I needed especially when I was not feeling at my best. Thank you for helping me when I most needed it during my PhD. Mr Loïc Briand, thank you for believing in me since the beginning and for never saying no to my ideas. Unfortunately, we were not in the same building, but your support and encouragement were always there. Thank you to both of you, for your time during the past three years.

My heartfelt thanks also go out for the support and help I received from the engineers and the technicians of our team. I had the chance to work more closely with Mrs Lucie Moitrier, Mrs Isabelle Chauvel and Mr Stéphane Fraichard. Thank you for your help and your assistance

throughout my scientific experiments. I was able to learn new techniques from you and sharing time with you has been a great pleasure.

I would like to thank Mr Claude Everaerts, Mr Fabrice Neiers and Mr Nicolas Poirier. Thank you, Mr Claude Everaerts, for helping me every time I knocked on your door and for sharing your bio-informatics knowledge with me. Your help has been precious. Also, thank you for the hallway discussions. Thank you, Mr Fabrice Neiers, for helping in the projects of proboscis proteomic and for your time. Thank you, Mr Nicolas Poirier, for you time and you help at the beginning of my thesis.

I am also grateful for the precious time, professional or not, that I spent with you and other members of the team such as Mr Jean-Philippe Charles, Mr Stéphane Dupas, Mr Jérôme Cortot, Mrs Christine Belloir and Mr François Bousquet.

I would like to thank Mrs Karen Rihani and Mrs Laure Cazalé-Debat. Thank you for your time and your advice. You have motivated me throughout this process.

I would also like to thank Mr Georges Alves who gave me the opportunity to teach animal physiology to second year students of the University of Burgundy.

I would like to thank the collaborators who contributed to this research such as Mrs Deepa Agashe, Mrs Prathibas (NCBS, India), Mr Jean-Michel Saliou (University of Lille) and Mr Nicola Pernet (Cytometry platform, University of Burgundy). I am very grateful to all of you.

A very special thanks to Mr Mathieu Schartz, Mrs Lucile Marty, Mrs Caroline Peltier, Mrs Margot Glaz, Mrs Laura Arrazat and Mr Valentin Boichot. It has been a pleasure organizing the PhD student day with you and sharing this experience with you. Also, Mr Mathieu Schartz, thank you for helping me with the crystallography. Even though we did not obtain a crystal in the end, I was very happy to learn from you. Thank you, Margot Glaz, for being such a good friend during our PhD experience and for sharing your knowledge of binding assay with me.

I would like to thank all the members of the team, each and everyone with whom I exchanged and all the PhD students of CSGA for their time and for their nice moments. Very grateful for everyone that I met during congresses, conferences or others laboratories.

I would like to thank my family and dearest friends-family.

Thank you to the Berland family, for their support and for making me part of their family. Olivia and François, you were always supportive to me. Many thanks for helping us to build our apartment.

I would like to thank Léa, Marie, Sylvie and Fréderique, for being like a family to me when I had just arrived to France. It was a pleasure to be your roommate girls and to have the possibility to be friends with you. To the Souque family, thank you for your support and help.

I would like to thank, Hippolyte and Véronique, for their unconditional support and help. Hippolyte, I had the chance to be your babysitter and 8 years later, you are still a joy in my life. Thank you Véronique for being like a second mother to me and for your motivation.

Thank you, Mélanie, Amina, Pauline, Elise, Elodie and Kevin for being the good friends that you are. It was such a pleasure sharing the apartment with Pauline and Elise. It felt like a home away from home to me. Also, thank you Pauline for sharing your knowledge with me and trying to help when I needed it. Amina, I was lucky to share this journey with you and getting to know you better. Mélanie, Elodie, Elise and Kevin thank you for your support and for always cheering for me.

I would like to thank my dear friends, Xhilda, Najet, Fjona, Elma and Pegi. Xhilda, thank you for pushing me beyond my limits, for believing in me and for helping me every time it was hard to go on. You are such an important friend to me. Najet, thank you for being always optimistic and the sun when I most needed. Your help and support were always there.

This endeavour would not have been possible without the support of Antoine. Thank you for your presence and for your unconditional love and care during these years and especially during my PhD. You were always available with a hug to calm me down when this journey was hard and stressful. Thank you for supporting me, believing in me and teaching me not to be afraid of what the future holds.

I would like to thank my grandparents and especially, the ones that are not here anymore. It was not possible for me, to be in their last day, but I have their words always with me. I carry with me all the stories and advices.

This journey in France would not have been possible without, my uncle Lami, my mother and all the family who believed in me and encouraged me to follow my dreams.

Thank you, my dear uncle, for all the support, discussions and help that you gave me. You always believed in me and you are one of my favourite people.

Words cannot express my gratitude to my mother, the person who made all this possible. She literally sacrificed the days of her life to provide me and my brother with a better education. I can never thank you enough for all you have provided me with. Thank you for all the possibilities that you gave to me. I would like to dedicate this work of thesis to my mother.

Acknowledgments 2
List of abbreviation 11
Liste of figures and tables 13
State of the art 17
Introduction 18
Chapter I: 19
Chemoreception 19
1. The perception of the environment 20
2. The olfaction system anatomy 23
2.1. Vertebrate olfactory system 23
2.1.1. Receptors involved in the olfactory system of vertebrates 25
2.2. Insects olfactory system 27
3. The gustatory system anatomy 29
3.1. Vertebrates gustatory system 29
3.1.1. Taste receptors of vertebrates 31
3.2. Insects gustatory system 33
3.2.1. Receptors involved in the taste detection of insects 35
4. Perception of fatty acids 38
4.1. Structure of fatty acids 38
4.2. The synthesis and impact of fatty acids in organisms 39
4.3. Perception of fatty acids in vertebrates 41
4.4. Perception of fatty acids by insects 43
5. Perireceptor events 44
5.1. Odorant binding proteins (OBPs) 45
5.1.1 Structure of OBPs 45
5.1.2 Physiological roles of OBPs 46
Chapter 2: 49
Microbiota 49
1. Embryonic and larval development 50
2. The adult structure of *Drosophila melanogaster* gut and the physiology of foregut, midgut and hindgut 51
3. Definition of gut microbiota and influence on host's physiology 54
3.1. *Drosophila melanogaster*: a model to study host-microbe interactions 57
3.2. The impact of gut microbiota on the physiology of Drosophila 58
3.2.1. Gut microbiota and behaviour 58
3.2.2. Gut microbiota and metabolism 60

3.2.3 Gut microbiota and lifespan 60
Chapter 3: 62
Influence of OBPs and microbiota on development and physiological functions (nutrition and reproduction) 62
1. The impact of microbiota in larval development 63
2. The impact of gut microbiota in reproductive capacity 64
3. The impact of microbiota on OBPs 65
Objectives of my PhD thesis 67
Materials and Methods 69
1. Model of study: *Drosophila melanogaster* 70
A- *Drosophila melanogaster* life cycle 70
B- Maintenance 71
C- Lines tested 71
D- Eggs and adults' collection for experiments 71
2. Manipulation of the bacterium microbiota 72
3. Microbiome sequencing with 16S RNA 74
3.1. Dissection of Drosophila samples 74
3.2. DNA extraction from Drosophila samples 74
3.3. Determining the microbiome in the Drosophila samples 74
4. Quantification of OBPs expression in *Drosophila melanogaster* 75
4.1. Determination of the optimal housekeeping genes 75
4.2. mRNA expression of OBPs in the gut 77
4.3. mRNA expression of OBP56d in gustatory appendages 77
4.4. mRNA expression of OBPs after manipulation of microbiota 78
4.5. RNA extraction 78
4.6. Quantification of RNA by spectrophotometry 78
4.7. Reverse transcription (RT) 79
4.8. Determination of control housekeeping genes by using GeNorm method 79
4.9. Quantitative-polymerase chain reaction (q-PCR) 80
5. *In situ* hybridization on the gut, proboscis and reproductive organs *in toto* 81
5.1. General principle of *in situ* hybridization 81
5.2. Preparation of forward and reverse OBP56d probe 81
5.2.1. Polymerase chain reaction (PCR) 81
5.2.2. Insert purification 82
5.2.3. Use of the pGEM-T Easy expression vector 82
5.2.4. Bacterial transformation 83

5.2.5. Analysis of clones and identification of probes 83
5.2.6. Labelling of RNA probes (riboprobes) 84
5.3. Gut, reproductive organs and proboscis labelling procedures 84
6. Recombinant protein expression of OBPs in *E.coli* M15 bacteria 85
6.1. General principle of OBP56d and OBP56g proteins production 85
6.2. Culture media 86
6.3. Vector expression 87
6.4. Bacteria transformation 88
6.5. Recombinant protein expression 88
6.6. Purification by affinity chromatography on HisTrap™ HP 1 mL 89
(Ni-nitriacetic agarose acid) 89
6.7. Electrophoresis of peptides on polyacrylamide gel in the presence of sodium dodecyl sulphate (SDS-PAGE) 90
6.7.1. General principle of electrophoresis SDS-PAGE 90
6.7.2. Analyse SDS-PAGE protocol 91
7. Biophysical analysis: Circular dichroism for OBP56d 91
7.1. Circular dichroism principle 91
7.2. Circular dichroism procedure 93
8. Fluorescence affinity measurements 93
8.1. General principle of fluorescence affinity 93
8.2. Sypro orange fluorescence binding assay 94
8.3. Ligand screening using the competitive binding assay with Sypro orange 95
9. Crystallography 96
10. *OBP56d*⁻ mutant 97
10.1. The system CRISPR-Cas9 97
10.2. Plasmids construction 97
A- pU6-OBP56d-5' and pU6-OBP56d-3' plasmid procedure 98
i. Cloning of the guide sequences into the pU6-BbsIchiRNA plasmid 98
ii. Phosphorylation of oligonucleotides and realization of duplexes 98
iii. Linearization and purification of pU6-BbsIchiRNA 99
iv. Ligation, transformation and screening of transformants 99
B- pHD-DsRED plasmid protocol 99
i. Cloning of LHA and RHA sequences in the pHD-Dsred plasmid 99
ii. Genomic DNA (gDNA) extraction 99
iii. Reaction chain reaction (PCR) 100
iv. Purification of LHA and RHA inserts 101

v. Enzymatic digestion of the inserts and the pHD-DsRed plasmid 101
vi. Purification of the inserts and the pHD-DsredGAL4 plasmid on agarose gel 101
vii. Ligation of inserts and digested pHD-DsRed plasmid 101
viii. Bacterial Transformation 102
ix. Screening subclones by PCR 102
x. Preparation of plasmid DNA 102
C- Transgenesis 102
11. Behavioural assays 103
11.1. Preparation of flies 103
11.2. Courtship and copulation behaviours 104
11.3. Antennal ablation 105
11.4. Fecundity 105
11.5. Copulation frequency: direct and indirect measures 105
12. Statistics 106
Results 107
1. Expression of OBPs in the gut and gustatory appendages 108
1.1. Selection of OBPs 108
1.2. Quantification of OBPs mRNA expression in the gut 109
1.2.1. mRNA expression of OBP19b 109
1.2.2. mRNA expression of OBP56g 111
1.2.3. mRNA expression of OBP56d 115
1.2.4. OBPs expression in *Drosophila melanogaster* head and gut 118
1.3. The impact of fasting on mRNA expression of OBPs 120
1.3.1. OBP56g 120
1.3.2. OBP56d 122
1.4. mRNA expression of OBP56d in gustatory system 123
1.5. mRNA expression of OBP56d, OBP56e, OBP56a in the parts of gut 124
1.6. The impact of the bacterial microbiota on OBP56d and OBP56g mRNA expression 126
1.6.1. mRNA expression of OBPs in absence of microbiota 126
1.6.2. mRNA expression of OBPs after introducing bacteria in an axenic culture 128
1.7. Sequencing bacterial microbiome 131
2. Heterologous expression of OBPs using *E. coli* bacteria 134
2.1. Production and purification of OBPs 134
2.2. Biophysical analysis of recombinant OBP56d 135
2.3. Ligand-binding properties of *Drosophila melanogaster* OBPs 136
2.3.1. Binding affinities of OBPs to Sypro orange 136

2.3.2. Binding affinities of OBPs to tastant compounds 137
3. Expression pattern of OBP56d in *Drosophila melanogaster* 145
3.1. Proboscis mRNA expression *via in situ* hybridation 145
3.2. Gut mRNA expression *via in situ* hybridation 146
4. Reproduction-related tissue-specific expression and behaviours 149
4.1. Reproductive organs mRNA expression *via in situ* hybridation 149
4.2. Verification of the *OBP56d*$^{-}$ mutant 151
4.3. Involvement of OBP56d in reproduction-related behaviours 152
4.3.1. Copulation during two hours 152
4.3.2. Copulation with antennaless females 153
4.3.3. Fertility (after 2 hours and 12 hours long contact) 154
4.3.4. Fecundity 156
Discussion 159
Perspectives 168
Annexe 170
References 194
Abstract 215
Résumé 216

List of abbreviation

2MB2: 2-methylbut-2-enal

A. *pomorum*: *Acetobacter pomorum*

AA: Amino acids

ABC: ATP-binding cassette

ACBP: Acyl-CoA binding protein

ALA: α-Linolenic acid

Aldh: Aldehyde dehydrogenase

AMPS: Adult midgut progenitors

AMPs: Antimicrobial peptides

ASD: Autism sprectrum disorders

ASV: Amplicon sequence variant

ATP: Adenosine 5'-triphosphate

BCP: 1-romo-3-chloropropane

BSC: Biological safety cabinet

CD: Circular dichroism

CD36: Cluster of differentiation 36

cDNA: Complementary DNA

CHCs: Cuticular hydrocarbons

CSPs: Chemosensory proteins

*c*VA: 11-cis vaccenyl acetate

CYP 450: Cytochromes P450

DCSO: Dorsal cibarial organ

DHA: Docosahexaenoic acid

DRKs: Delayed rectifying potassium channels

DSBs: Double-strand breaks

DsRed: Discosoma Red

EBs: Enteroblasts cells

EC: Enterocyte cells

EE : Enteroendocrine cells

EOG: Electrophysiological recordings

EPA: Eicosapentaenoic acid

FABP: Fatty acid-binding proteins

FAs: Fatty acids

FC: Flow cytometry

FFA: Free fatty acid

FKh: HNF/Fork head

FPRs: Formyl peptide receptors

GG: Grueneberg ganglion

GPCR: G protein-coupled receptor

GRNs: Gustatory receptor neurons

GRs: Gustatory receptors

GSNs: Gustatory sensory neurons

GSTs: Glutathione transferases

HDR: Homology directed repair pathway

Hh pathway: Hedgehog pathway

HIS: *In situ* hybridization

I: Intermediate sensilla

ID: intellectual disability

IMD: Immune deficiency pathway

IPTG: Isopropyl β-D-1-thiogalactopyranoside

IRs: Ionotropic receptors

ISCs: Intestinal stem cells

JNK: c-Jun N-teminal kinase

KO: Knock out

L. *plantarum*: *Lactobacillus plantarum*

L: Left

L: Long sensilla

LA: Linoleic acid

LB: Luria broth

LB: Lysogeny broth

LCFA: Long chain fatty acids

LSO: Labral sensory organ

MRP: Multidrug resistance proteins

MRS: Man, Rogosa and Sharpe broth

NHEJ: Non-homologous end junction repair

NMR: Nuclear magnetic resonance

NST: Nuvleus of the solitary tract

OB: Olfactory bulb

OBPs: Odorant-binding proteins

OD: Optic density

OE: Olfactory epithelium

OPBs: Odorant-binding proteins

ORCs: Olfactory receptors cells

ORNs: Olfactory receptor neurons

ORs: Olfactory receptors

OSNs: Olfactory sensory neurons

Otop 1: Otoperin 1

PAM: Protospacer adjacent motif

PbN: Parabrachial nucleus

PBS: Phosphate-buffered saline

PCR: Polymerase chain reaction

PER: Proboscis extension response

Pgp: P-glycoprotein

PLC C: Phospholipase C

ppk: Pickpocket channel proteins

PUFA: Polyunsaturated fatty acids

q-PCR: Quantitative-polymerase chain reaction

R: Right

ROS: Reactive oxygen species

RTase: Reverse transcriptase

S: Short sensilla

SCCs: Solitary chemosensory cells

SDS: Sodium dodecyl sulphate

SFA: Saturated fatty acids

SNMP1: Sensory membrane neuron protein 1

SO: Septal olfactory organ of Masera

SOC: Super optimal broth medium with catabolic repression

Srp: Factor serpent

TAAR: Trace amine-associated receptor

TAG: Triglyceride

TLR5: Toll-like receptor 5

TM: Transmembrane domains

TRCs: Taste receptor cells

TRP: Transient receptor potential channels

UGTs: UDP-glycosyl transferases

VCSO: Ventral cibarial organ

VNO: Vomeronasal organ

VPM: Ventral posteromedial nucleus

XMEs: Xenobiotic metabolizing enzymes

Liste of figures and tables

Page

Figure I-1. The anatomy of the nasal activity in vertebrates. 20

Figure I-2. The olfactory neuroepithelium and a pathway for olfactory signal transduction. 22

Figure I-3. Structure of G protein-coupled receptors (GPCRs). 23

Figure I-4. The olfactory system of *Drosophila melanogaster* flies. 24

Figure I-5. The mouth and gustatory system of vertebrates. 26

Figure I-6. Taste receptors in mammalian. 29

Figure I-7. The gustatory system of *Drosophila melanogaster* flies. 30

Figure I-8. Schematic representation of Drosophila gustatory receptors. 34

Figure I-9. Key for fatty acids nomenclature. 35

Figure I-10. Metabolic pathway showing the synthesis of omega-6 and omega-3 fatty acids. 36

Figure I-11. Developmental transitions of the digestive tract in *Drosophila melanogaster*. 46

Figure I-12. The adult intestine and its cell types. 48

Figure M-1. *Drosophila melanogaster* cycle of life. 66

Figure M-2. Determination of the best housekeeping genes for our Rt-qPCR conditions. 72

Figure M-3. Plasmid map of pGEM-T Easy vector. 79

Figure M-4. The map of pQE-31 vector used for the insertion of OBP56d or OBP56g coding region. 83

Figure M-5. The OBP56d coding sequence. 84

Figure M-6. Principle of the purification of a recombinant protein by affinity chromatography. 86

Figure M-7. Origin of CD effect. 89

Figure M-8. Principle of the fluorescent binding assay. 90

Figure M-9. Schematic design of crystallography methods. 93

Figure M-10. The plasmid pHD-DsRED-LHA-RHA used for the construction of mutant OBP56d by CRISPR-Cas9. 96

Figure M-11. Device used to measure courtship and copulation behaviours. 100

Figure R-1. OBP19b mRNA expression in the head and in the gut of *Drosophila melanogaster* flies. 106

Figure R-2. mRNA expression of OBP56g in the head (left) and in the gut (right) of *Drosophila melanogaster* flies. 108

Figure R-3. Comparison of OBP56g mRNA expression in the head and in the gut of *Drosophila melanogaster* flies 110

Figure R-4. mRNA expression of OBP56d in the head (left) and in the gut (right) of *Drosophila melanogaster* flies. 111

Figure R-5. Comparison of OBP56d mRNA expression in the head and in the gut of *Drosophila melanogaster* flies. 113

Figure R-6. mRNA expression of OBPs in the head (A) and in the gut (B) of *Drosophila melanogaster* flies. 115

Figure R-7. Evaluation of fasting in the level of expression of OBP56g in the head (A) and in the gut (B) of *Drosophila melanogaster* flies. 117

Figure R-8. Evaluation of fasting in the level of expression of OBP56d in the head (left) and in the gut (right) of *Drosophila melanogaster* flies. 118

Figure R-9. OBP56d expression in the three gut regions of virgin males. 119

Figure R-10. OBP56d expression in the head deprived of sensory appendages (left) and in dissected proboscis (right) of *Drosophila melanogaster* female and male flies. 120

Figure R-11. Phylogenetic tree of OBPs family with alignment of amino acid sequences in 3 OBP56. 121

Figure R-12. Expression of OBPs in the three parts of the gut. 122

Figure R-13. Effect of bacterial microbiota elimination on OBP56d mRNA expression. 123

Figure R-14. Effect of bacterial microbiota elimination on OBP56g mRNA expression. 124

Figure R-15. mRNA expression of OBP56d resulting of four microbiota manipulations. 125

Figure R-16. mRNA expression of OBP56g resulting of four microbiota manipulations. 127

Figure R-17. Microbiome composition in control, axenic and mutant *OBP56d-* flies. 129

Figure R-18. Purification of recombinant OBPs. 130

Figure R-19. Biochemical characterization of the recombinant OBP56d. 131

Figure R-19. Biochemical characterization of the recombinant OBP56d. 132

Figure R-20. Sypro-Orange fluorescent binding assay. 134

Figure R-21. Binding properties of OBP56d and OBP56g revealed with a competitive fluorescent assay. 136

Figure R-22. Binding affinity of OBP56d for fatty acids. 137

Figure R-23. Binding affinity of OBP56g for fatty acids. 139

Figure R-24. Expression pattern of OBP56d in Drosophila proboscis in control females and males. 141

Figure R-25. OBP56d expression in virgin female gut. 143

Figure R-26. OBP56d expression in virgin male gut. 144

Figure R-27. OBP56d expression in the virgin female reproductive organs. 145

Figure R-28. OBP56d expression in the male reproductive organs. 146

Figure R-29. Quantification of OBP56d in mutant *OBP56d-* flies. 147

Figure R-30. Copulation kinetics in pairs of flies combining different genotypes. 149

Figure R-31. Fertility in couples of flies paired during 2 and 12 hours. 150

Figure R-32. Copulation frequency for 1h, 2h and 12h. 152

Figure R-33. Adult progeny produced by each type of mating pair. 153

Figure R-34. Adult progeny per tube for all pairs. 154

Table M.1. Forward and reverse primers for V3-V4 region of 16S rRNA. 70

Table M.2. List of potential housekeeping genes for different tissues in *D. melanogaster*. 75

Table M.3. List of forward and reverse primers of OBPs used for q-PCR. 77

Table M.4. Forward and reverse OBP56d his-1 probe primers. 78

Tableau M.5. Oligonucleotides used for the synthesis of guide sequences. 95

Table M.6. Oligonucleotides used for the synthesis of LHA and RHA homology arms. 97

Table M.7. Total number of homotypic and heterotypic pairs tested. 101

Table R.1. Relative mRNA-seq tissue-specific expression in *Drosophila melanogaster* adults. 104

Table R.2. Data show OBP19b expression in the complete Head (1) and Gut (2). 107

Table R.3. Data show OBP56g expression in the complete Head (1) and Gut (2. 109

Table R.4. Data show OBP56d expression in the complete Head (1) and Gut (2). 112

Table R.5. List of fatty acids tested with OBP56d and OBP56g. 140

State of the art

Introduction

Chapter I:

Chemoreception

1. The perception of the environment

All cellular life from bacteria to animals are sensitive to the chemical information, whether it comes from potential food, predators, the environment or other members of the same species. Here, I present some examples of chemical communication from bacteria, plants and animals.

In order to ensure survival, bacteria need to constantly adapt to changing environmental conditions (concentrations of nutrients or toxins, oxygen levels, pH, osmolarity and wavelength of light). They use a variety of signal transduction pathways like one- or two-component systems and chemoreceptor-based signalling cascades. These systems are referred as a chemotaxis or chemosensory systems (Ortega *et al.*, 2017; Porter *et al.*, 2011; Yang and Briegel, 2020). Another way to evaluate sensory signals is bacterial motility by using long, exquisitely thin appendages called type IV pili (Mattick, 2002). It is important for host colonization and other forms of complex colonial behaviour, like the formation of biofilms (Mattick, 2002; Semmler *et al.*, 1999). Bacteria communicate by a process called quorum sensing. They monitor the presence of other bacteria in their surroundings by producing and responding to signalling molecules (Bassler, 1999; Taga and Bassler, 2003).

Plants use pollen odour, leaf volatiles or caterpillar-damaged plants to protect themselves by attracting parasitic wasps as mechanisms for chemical communication (Azuma *et al.*, 1999; Bolter *et al.*, 1997; Dobson *et al.*, 1999; Raguso and Pichersky, 1999; Turlings *et al.*, 1995). A great variety of organic volatile compounds are released in the atmosphere by terrestrial plants (Knudsen *et al.*, 2006). Some studies showed that pollen emits odours for pollination, especially efficient in attracting insects and modulating their foraging behaviour. Odorant molecules from pollen odours include protective chemicals (like linalool, 3,7-dimethyl-1-6-octabien-3-ol) against pollen-feeding insect or pathogens, (Dobson *et al.*, 1999; Dobson and Bergstrom, 2000; Raguso and Pichersky, 1999). Plant leaves emit different types of molecules depending on the necessity of each plant. Leaves from *Mognoliaceae* emit volatile chemicals (terpenoids, benzenoids, fatty acid esters and hydrocarbons) to enhance specific pollinator interactions. When leaves are damaged, they emit volatile compounds such as for example, 3 (Z)-hexenal, 3(Z)-hexenol or terpenes to contribute to plant defence (Azuma *et al.*, 1999). Briefly, herbivore-injured plants provide chemicals that are easily detected by insects to limit the damage (Turlings *et al.*, 1995). Plant chemical communication is also involved in the movement, growth or in the development of plants (Fukano, 2017).

Animals use smell and taste, as chemical senses, to perceive their chemical environment. Chemicals present outside the organism that provide an information to the animal are called semiochemicals (pheromone, odorant and sapid molecules). Odorants molecules are detected by olfactory receptors (ORs) present on the cytoplasmic membranes of olfactory receptor neurons (ORNs). Sapid molecules are detected by gustatory receptors (GRs) present on the surface of gustatory receptor neurons (GRNs). These two systems can show similarities and differences, depending on the complexity of the animal species and its ecological niche.

Aquatic environment is more difficult to characterize than aerial environment given that compounds are dissolved into water. However, fishes possess both highly developed olfaction and taste systems. Fishes were used as animal models to study chemosensation (Hara, 1994).

A study carried out in goldfish showed that pheromones such as sex steroid, 17α, 20β-dihydroxy-4-pregnen-3-one (17, 20P), and metabolites of prostaglandin $F_{2\alpha}$ are involved in sexual interactions (Sorensen *et al.*, 1991). Authors used electrophysiological recordings (EOG) to detect the responses of these molecules on the surface of olfactory epithelium. The molecule 17, 20P, which is produced by females during ovulation, stimulates sperm and seminal fluid production in goldfish males. Also, during the reproductive behaviour, goldfish females release some prostaglandin metabolites that can be detected by male olfactory system. This compound stimulates male reproductive behaviour. EOG recordings showed that L-amino acids play an important role in feeding in teleost fishes. They may also serve as non-reproductive social cues in different fish species (Atema *et al.*, 1979; Saglio *et al.*,1985). Gustatory detection of L-amino acids was also observed in the facial taste system of the carp, *Cyprinus carpio L* (Marui *et al.*, 1983) by using EOG recordings. In fishes, the threshold for detecting tastant molecules is far lower than in other vertebrates such as amphibians or mammals. Amino acids and nucleotides are signals known as potent food source, while bile salts, pheromones and urine compounds are known for their effect in social and reproductive interaction in fishes (Hansen and Reutter, 2004). Another example revealing the importance of olfactory system is documented in the pacific salmon, *Oncorhynchus spp.* Salmons use their olfactory system to wander through the Pacific Ocean, to mate and to return in the place where they grew up with an amazing accuracy (Hasler and Scholtz, 1983). In addition to olfactory and gustatory systems, fishes possess a third chemoreceptive sensory system composed of solitary chemosensory cells (SCCs). SCCs resemble to taste buds and are found in a variety of fishes (Whitear, 1965). SCCs system is connected to the central nervous system

similarly to the gustatory system, and is mainly used for predator avoidance behaviour and not for feeding.

The importance of chemosensory perception was also often investigated in amphibians and mammals. To find partners and mate, animals must be able to locate and interpret species-specific chemical signals. The detection of odorants found in elephant urine can stimulate aggressive, defence or sexual behaviour (Rasmussen, 1988). For example, Asian elephant females release the (z)-7-dodecen-1-yl acetate in their urine during the preovulatory period (Rasmussen and Schulte, 1998) to attract sex partners. Other animals such as mice, produce urinary compounds to induce sexual behaviour or to find a mate (Yoshikawa *et al.*, 2013). Reptiles such as snakes and lizards often use chemical cues to find their mating partner. They use their tongue, as a chemosensory edge-detector to follow the pheromone trails of preys and of potential mates (Schwenk, 1995).

Another type of behaviour was identified between female rabbit and new-borns who are blind and use the odour signal 2-methylbut-2-enal (2MB2) to find mother nipples (Schaal *et al.*, 2003). 2MB2 plays the role of a pheromone that stimulates the behaviour of offspring to survive and have a normal development.

Olfactory and gustatory systems are also crucial for invertebrates survival and reproduction. Most insects use chemosensory perception during their preimaginal development and adult life. Insects exchange several molecules during their precopulatory behaviour (courtship). In some, but not all insects, cuticular hydrocarbons (CHCs) can play a role to induce or prevent sex-specific behaviours. In the *Drosophila melanogaster* species, males predominantly produce *cis*-7-tricosene (7-T) or *cis*-7-pentacosene (7-P), while females produce *cis*-*cis*-7-11-heptacosadiene (7.11-HD) and *cis*-*cis*-7-11-nonacosadiene (7.11-ND) (Ferveur, 1997). Female CHCs play a minor role in stimulating conspecific male precopulatory behaviour (Marcillac and Ferveur, 2004), while they strongly inhibit the courtship in males of the sibling species *Drosophila simulans* (Savarit *et al.*, 1999). On the other hand, male CHCs, and particularly 7-T, increases female receptivity (Grillet *et al.*, 2006) while it inhibits male-male homosexual behaviour (Ferveur, 1997; Ferveur and Sureau, 1996). Note that these CHCs often act in conjunction with other compounds such as the male pheromone 11 *cis*-Vaccenyl acetate (*c*VA; Billeter *et al.*, 2009; Duménil *et al.*, 2016; Laturney and Billeter, 2016). During copulation, Drosophila males transmits molecules on female flies that change her post-mating behaviour (Wolfner, 2002). In *D. melanogaster*, seminal proteins made in male accessory glands stimulate sperm storage, ovulation, egg production and reduce for a limited period of

time female receptivity to mating (Avila *et al.*, 2011; Herndon and Wolfner, 1995; Wolfner, 1997). *c*VA is a volatile compound with multiple reproduction-related functions: it is transmitted during copulation males to females of several Drosophila species (Brieger and Butterworth, 1970; Guiraudie-Capraz *et al.*, 2007). When females lay eggs impregnated with *c*VA in food, it attracts at a distance, and in synergy with food metabolite compounds, Drosophila male and female flies of several species (Bartelt *et al.*, 1985). Once flies have gathered on the food source they can perform at a close distance sex-specific behaviour (courtship/male-male aggressive behaviours). These behaviours are modulated by *c*VA acting in conjunction with other compounds including CHCs (Billeter and Levine, 2015).

In ants, CHCs are implicated in task decision (Greene and Gordon, 2003). A harvest ant task decision depends on its chemical interaction with other ants. For cockroach *Nauphoeta cinerea* male, the sex pheromone determines the status of males. Therefore, females decide to mate or not depending on the production of cockroach male pheromones (Moore *et al.*, 1997).

Outstanding progresses in our understanding of chemosensory systems was accomplished through many decades of research on a great variety of models. The molecular mechanisms of olfaction and taste has been the focus of thousands of studies, attempting to understand how these semiochemicals penetrate sensory organs, how they are transported to ORs and GRs and how the transduction machinery can translate the chemical information to an electric response transported from peripheral sensory neurons to the central nervous system (the brain).

2. The olfaction system anatomy

The olfactory system of animals allows them to perceive a multitude of volatile chemical substances. Such system plays an essential role in food search, territory labelling, predator detection and in other social and reproductive behaviours. The variety of odorous molecules that can be detected varies according to the sex and species, according in particular to OR number. In vertebrates, odorants are detected at the level of the nasal cavity where is located the olfactory epithelium (OE) containing ORs. In invertebrates, especially in insects, olfactory organs are borne by the antennae and maxillary palps located on the head. Odorants enter the pores of sensilla to reach olfactory receptors cells (ORCs).

2.1. Vertebrate olfactory system

In vertebrates, the detection of odorants occurs in the nasal cavity where the OE is located. The OE is common to all vertebrates while the vomeronasal organ (VNO) is only present in

most amphibia, reptiles and some mammals (but non-functional in human; Trotier, 2011). The sensory neurons of the VNO detect non-volatile chemical molecules and unlike the main olfactory system, it sends signals to the accessory olfactory bulb and then to the amygdala and the hypothalamus (Keverne, 1999). This process allows the detection of pheromones (volatiles or not) (Briand *et al.*, 2004). The septal olfactory organ of Masera (SO) and the Grueneberg ganglion (GG) are only found in a limited numbers of mammals (Bojsen-Møller, 1975; Kratzing, 1978) (**Figure I-1**). These two organs have been mostly studied in rodents. In mice, the GG is involved in the detection of alarm pheromones emitted by conspecifics under stress. The SO has not yet been sufficiently well studied for to know whether it contributes to pheromone detection (Brechbühl et al., 2008).

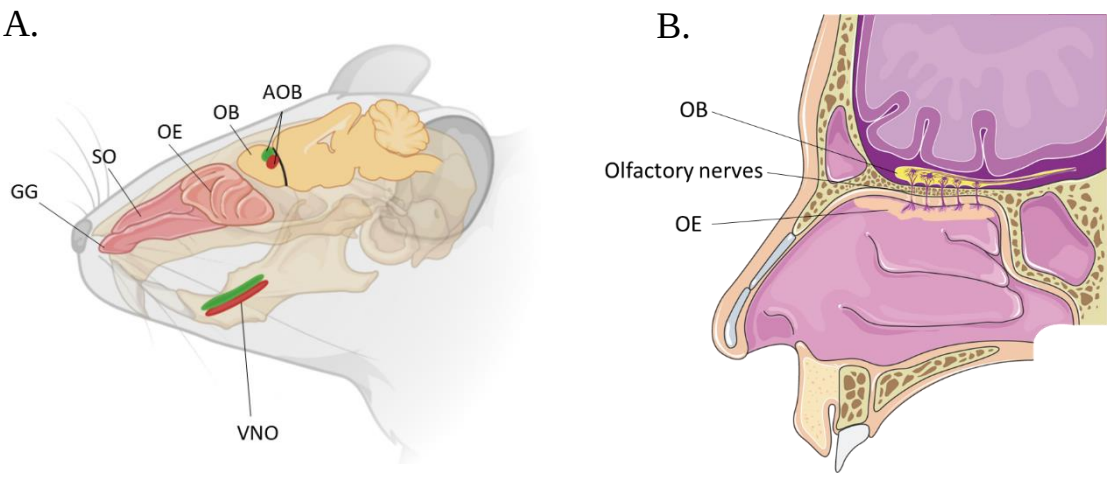

Figure I-1. The anatomy of the nasal activity in vertebrates.

A) The nasal cavity of the mouse contains several sensory organs: the Grueneberg ganglion (GG), septal organ of Masera (SO), vomeronasal organ (VNO), and olfactory epithelium (OE) that innervates the olfactory bulb (OB). The VNO neuroepithelium innervate the rostral and caudal divisions of the accessory olfactory bulb (AOB) respectively. B) The human nasal cavity contains only an OE that innervates the OB. The figure was created by using biorender and medical art.

2.1.1. Receptors involved in the olfactory system of vertebrates

After entering the nasal cavity, odorant molecules can either diffuse directly into the mucus covering the OE or be carried by transporter proteins called odorant binding proteins (OBPs) which facilitate their diffusion. Vertebrate OBPs belong to a large family of ligand carrier proteins called lipocalins. They are believed to transport the ligand molecules to deliver them to dedicated ORs. Odorants bind then to membrane receptors present on the cilia of the olfactory neurons (**Figure I-2**). These molecules are recognized by limited set of ORs. In turn, OR receptor may recognize several odorants. This highlights the problem of olfactory specificity. Each OSN expresses only one OR. From all these properties emerges the concept of a combinatorial code that allows mammals to detect thousands of odorant molecules (Malnic *et al.*, 1999).

The binding of the odorant molecule to the OR leads to a conformational change of the OR which in turn activates a specific G protein-coupled receptor (GPCR). ORs were first discovered in rodents (Buck and Axel, 1991). Downstream, a cascade of cAMP transduction pathway leads to the opening of an ion channel. Both the entry of cations and the exit of anions contribute to the depolarization of the neuron membrane. Such transduction of the chemical signal into an electrical signal induces the generation of an action potential which propagates to the olfactory bulb (OB), the first relay of olfactory information (Buck, 1996). The processed message is then transmitted to various regions of the brain.

Humans express ~ 380 ORs, while rodents express more than 1000 ORs. Differently fishes express a relatively small OR family of ~100 genes. GPCR-like ORs are found in all vertebrates and constitute a multigene family. The structure of GPCRs include seven transmembrane domains (TM) connected by three putative intracellular and extracellular loops and a conserved aspartate-arginine-tyrosine amino acid motif (**Figure I-3**). The N-terminal (NH_2) and C-terminal (COOH) ends are located in the extracellular and intracellular domains of the plasma membrane, respectively. The zone from TM3 to TM7 is a hypervariable region contributing to the selective binding of odorants (Abaffy *et al.*, 2006; Buck and Axel, 1991). OR genes are divided into two primary classes: Class I and Class II. Fish OR genes only belong to Class I genes while Class II genes are only found in terrestrial vertebrates (Glusman *et al.*, 2001; Zhang and Firestein, 2002). Mice ORs can recognize specific odorants (Mombaerts, 2004). In rodent, primate and fish, another type GPCR was identified: the trace amine-associated receptor (TAAR) family which is vertebrate-specific.

TAAR signalling is involved in the detection of volatile amines including pheromones (Dewan *et al.*, 2013; Liberles, 2015).

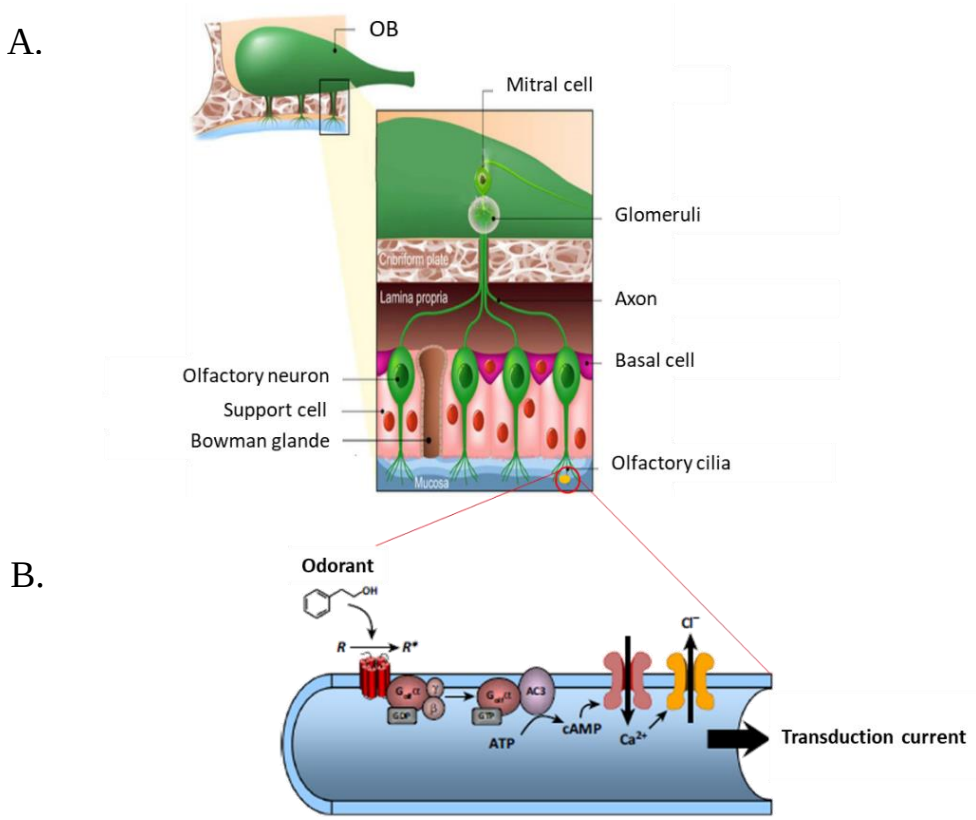

Figure I-2. The olfactory neuroepithelium and a pathway for olfactory signal transduction

A) The olfactory neuroepithelium. The initial events in odour perception occur in the nasal cavity. Odours interact with specific receptors on the cilia of olfactory sensory neurons. The signals generated by initial events are propagated by olfactory neurons to the olfactory bulb. B) A pathway for olfactory signal transduction. In this scheme the binding of an odorant molecule to an odour-specific transmembrane receptor leads to the interaction of the receptor with a GTP-binding protein. This interaction in turn leads to the release of the GTP-coupled α subunit of the G protein, which in turn stimulates adenylyl cyclase production inducing cAMP elevated levels. cAMP increase opens cyclic nucleotide-gated cation channels, thus causing an alteration in membrane potential (Adapted from Purves, 2004). The figure was created by using biorender and medical art.

A second multigene family of vomeronasal (VNO)-specific GPCRs was identified in $G_{\alpha 0}$ vomeronasal sensory neurons (VSNs). Studies showed the implication of V1Rs and V2Rs in mice reproductive behaviour (Herrada and Dulac, 1997; Kimchi *et al.*, 2007; Young *et al.*,

2010). Another GPCR family, consisting of members of the formyl peptide receptor (FPRs), was discovered in mice VNO. Mice VSNs express five distinct FPRs suggesting that they may contribute to pathogen sensing by the vomeronasal organ (Bufe *et al.*, 2012; Rivière *et al.*, 2009).

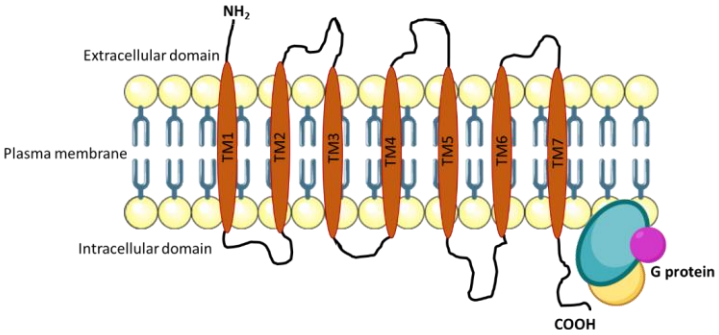

Figure I-3. Structure of G protein-coupled receptors (GPCRs)

The GPCRs are composed of seven transmembrane domains (TMs). The N-terminal (NH2) and C-terminal (COOH) extremities are respectively located in the extracellular and intracellular domain of the plasma membrane. The figure was created by using biorender and medical art.

2.2. Insects olfactory system

Insect olfactory organs are generally located on the head. They are represented by the maxillary palps and antennae in flies (**Figure I-4.A**). *Drosophila melanogaster* carries two aristate antennae composed of a thin arista, a second segment involved in auditory and mechanosensory functions and a third segment which is the main olfactory receptor organ (Shanbhag *et al.*, 1999). The third segment houses ORNs housed in the olfactory sensilla. Each sensillum houses from 1 to 4 ORNs and a single mechanosensory neuron. Each ORN is surrounded by three specialized cells, also called support cells (tormogen, trichogen and thecogen cells) (**Figure I-4.C**). These support cells secrete the sensillar lymph which protects ORNs and allows to transport ligand molecules to ORs (Vosshall and Stocker, 2007). Drosophila flies carry about 400 sensilla on each antenna and 60 sensilla on each maxillary palp. Antennae carry four olfactory sensilla types whose classification depends on their morphology: basiconic (club-shaped sensilla), trichoic (needle shape, thick walls), coeloconic (small, finshaped, double-walled) and intermediate sensilla (shape intermediate between

basiconic and trichoid sensilla) (Stocker, 1994; Vosshall and Stocker, 2007). Maxillary palps, carry only basiconic sensilla (Shanbhag *et al.*, 1999) (**Figure I-4.B**).

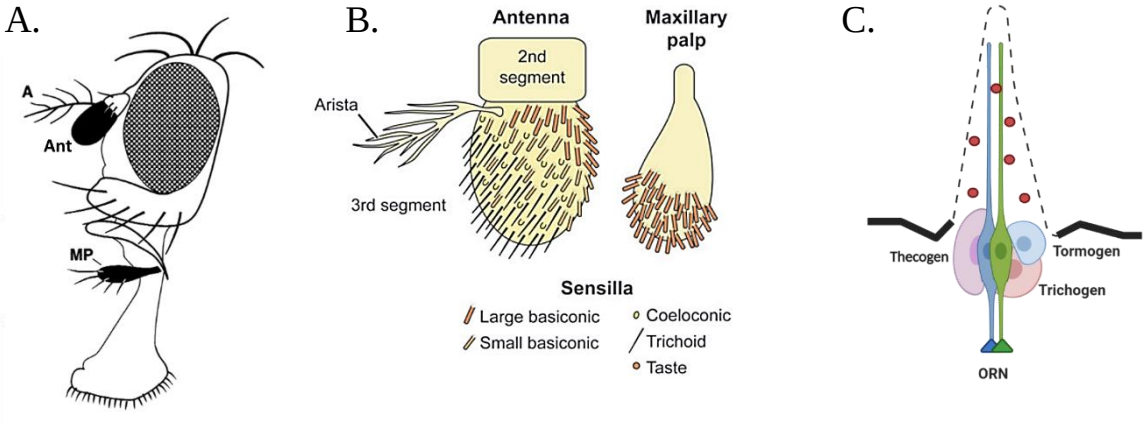

Figure I-4. The olfactory system of *Drosophila melanogaster* flies

A) Olfactory head appendages: antenna (Ant); arista, the third segment (A) and the maxillary palps (MP). (Figure from (Shanbhag *et al.*, 1999). B) Various types of sensilla and distribution in the olfactory organs. (Figure adapted from (Vosshall and Stocker, 2007)). C) Schematic drawing showing the internal structure of a olfactory sensillum. The figure was created by using biorender and medical art.

Odorant molecules enter the olfactory sensillum through the multipores of the sensillum cuticle. These ligands are often lipophilic and are taken in charge by carrier molecules such as the OBPs in the sensillar lymph. OBPs are believed to transport odorant molecules to ORs. In the Drosophila genome, 62 genes coding ORs have been identified while 2 ORs are produced by alternative RNA splicing. As in vertebrates, ORs are 7 TM proteins resembling GPCRs. However, these proteins have an inverted topology compared to vertebrates or nematodes ORs (Buck and Axel, 1991; Vosshall *et al.*, 1999; Robertson *et al.*, 2003; Vidal *et al.*, 2018).

In Drosophila larvae and adults, ORNs express the Or83b receptor. The gene encoding Or83b is the most conserved gene among insects; unlike other ORs, it is expressed in most ORNs. The common name Orco (Olfactory Receptor COreceptor) was proposed for Or83b in all insect species where it is found (Krieger *et al.*, 2003; Larsson *et al.*, 2004; Melo, 2004; Sato *et al.*, 2008; Vosshall and Hansson, 2011). ORCO acts as a chaperone protein that directs ORs to

the dendrite and its deletion disrupts behavioural and electrophysiological responses to many odorants (Larsson *et al.*, 2004). Similarly to the vertebrate olfactory system, studies revealed that Drosophila use a combinatorial OR code for odorants (Hallem *et al.*, 2006). Once the receptor is activated by the binding of its ligand, the ORN goes under a depolarization which generates an action potential. This signal is transmitted to a primary centre composed of several glomeruli forming the antennal lobe. In most cases, ORNs expressing the same receptor converge to the same glomerulus of the antennal lobe (Gao *et al.*, 2000; Vosshall *et al.*, 2000). Each basiconic and trichoid ORN of the antennae and each basiconic ORN of the maxillary palps possess a glomerular representation of odors with aliphatic and aromatic compounds activating distinct glomeruli. Based on these findings, a glomerular map of odorants molecules in the antennal lobe was established (Couto *et al.*, 2005).

Studies have also identified another gene family expressed in coeloconic sensilla called ionotropic receptors (IR) (Benton *et al.*, 2009). In adult antennae, 17 IRs are expressed and play an essential role in the perception of odorants such as amines, acids, pheromones and volatiles chemicals of food sources and oviposition sites (Benton *et al.*, 2009; Rimal *et al.*, 2019; Silbering *et al.*, 2011). IRs are also found in the gustatory system. ORNs expressing the gustatory receptors GR21a and GR63a, which are sensitive to CO_2 are considered as another ORN class that does not require OR83b. Electrophysiological and behavioural studies demonstrated that GR63a mutants do not respond to CO_2 (Benton *et al.*, 2006). The sense of smell is also mediated by GRs expressed in Drosophila olfactory appendages.

3. The gustatory system anatomy

The gustatory system is the second important chemosensory modality dedicated to food quality evaluation. In vertebrates, the gustatory system is located primarily on, the tongue, whereas in adult invertebrates, taste sensory organs are distributed all over the body. Five taste modalities have been described to detect: the sweet, the sour (acid), the bitter, the salty and the umami (amino acids) molecules. In the scientific world, there is still a debate to accept or not fatty acid taste detection as a sixth taste modality. All these taste modalities are present in vertebrates and invertebrates.

3.1. Vertebrates gustatory system

The mouth of vertebrates contains taste receptor cells (TRCs) located in the taste buds of the tongue and the palate epithelium. On the tongue, the taste buds are mounted in special folds

and protrusions called papillae. Three types of papillae are topographically organized on the tongue: fungiform (anterior surface of the tongue), circumvallate (back of the tongue) and foliate (sides of the tongue) (**Figure I-5.A**). In the fungiform papillae are found about ~ 10 of taste buds, in circumvallate about ~ 100 of taste buds and in fungiform papiellae about ~10 of taste buds (Yarmolinsky *et al.*, 2009). Each taste bud, depending on the species, contains 50–150 cells. Five basic taste modalities are commonly recognized: sour, salty, sweet, bitter, and umami (the taste of monosodium glutamate), and related tastants are detected by taste buds mainly localized on the tongue epithelium and rarely in the soft palate, pharynx, and upper oesophagus. Taste receptors have been identified for each taste modality. Taste buds are able to distinguish between different taste modalities through the interaction with different molecules or ions. Sweet, umami and bitter tastes are triggered by the binding of molecules to G protein-coupled receptors on the cell membranes of taste buds (Hoon *et al.*, 1999). Saltiness and sourness are perceived *via* ions entering taste buds (Chandrashekar *et al.*, 2006; Chang *et al.*, 2010; Servant *et al.*, 2020).

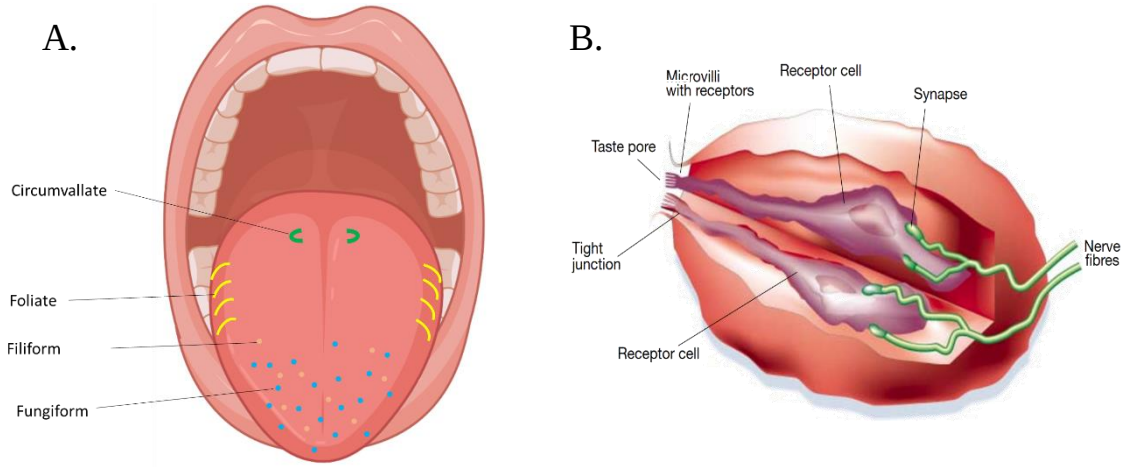

Figure I-5. The mouth and gustatory system of vertebrates

A) Distribution of three types of papillae on the tongue: fungiform (blue), circumvallate (green) and foliate (yellow). B) Structure of a taste bud with two receptor cells with apical microvilli and basolateral synapses. A taste bud has the shape of a bulb onion where the basal cell and the taste receptor cell are found inside. Taste bud have only one terminal pore where the GRs are located. (Figure modified from (Lindemann, 2001). The figure was created by using biorender and medical art.

Taste buds are composed of receptor cells that extend in the apical surface of the epithelium by microvillar structures through a taste pore (**Figure I-5.B**). This allows the direct contact with the chemicals present in the environment. Taste buds are at least divided in five classes based on taste. The taste buds on the tongue and palate are innervated by three afferent nerves: the chorda tympani, greater superficial petrosal, and glossopharyngeal nerves. These nerves carry taste information from the taste receptor cells to the nucleus of the solitary tract (NST) in the brain stem. From the NST, taste responses are transmitted and processed through the parabrachial nucleus (PbN) and the thalamus ventral posteromedial nucleus (VPM) to the primary gustatory cortex in the insula. Behavioural responses to food (and perceptions of flavour) are ultimately choreographed by the integration of gustatory information with other sensory modalities (such as olfaction, texture, etc) (Lindemann, 2001; Yarmolinsky *et al.*, 2009; Liman *et al.*, 2014).

3.1.1. Taste receptors of vertebrates

Gustatory receptors (GRs) were discovered in mammalian after ORs (Hoon *et al.*, 1999). Circumvallate papillae are located at the very back of the tongue (~100 for mice) to (~1000 to human) of taste buds, and are particularly sensitive to bitter substances. Foliate papillae are localized at the posterior lateral edge of the tongue and contain dozens to hundreds taste buds. They are particularly sensitive to sour and bitter substances. Fungiform papillae contain a single or a few taste buds and are located at the front of the tongue. They are thought to mediate much of the sweet taste modality.

Electrophysiological studies suggest that sour and salty tastants modulate taste cell function by direct entry of H^+ and Na^+ ions channels receptors whereas bitter, sweet and umami tastes are mediated by taste-specific GPCRs (Adler *et al.*, 2000; Chandrashekar *et al.*, 2006, 2000; Hoon *et al.*, 1999) (**Figure I-6**).

A. Bitter taste

Bitter taste allows animals to detect toxins that are primarily produced by plants in the environment. However, not all bitter-tasting compounds are toxic. In vertebrates, bitter chemicals are detected by a small family of receptors (T2Rs) that are structurally related to rhodopsin (Xu *et al.*, 2022). Their number is comprised between 3 to 49, depending on the species (Chandrashekar *et al.*, 2000; Matsunami *et al.*, 2000; Shi and Zhang, 2006). Humans have 25 T2R bitter receptors (Delompré *et al.*, 2022).

B. Sweet taste

Sweet taste receptor is a heterodimer receptor that is composed of the assemblage of two subunits, T1R2 and T1R3. Sweet taste is elicited by high sugar concentrations (100 – 500 mM), but also natural and artificial sweeteners (Belloir *et al.*, 2017). T1Rs are class C GPRCs which present a large N-terminal domain (**Figure I-6**). This domain is connected to transmembrane segments by a cysteine-rich domain that couples ligand binding to receptor activation (Adler *et al.*, 2000; Nelson *et al.*, 2001). Orthologs of the three T1Rs and of the T2R are present in the genomes of all vertebrates and the number of taste-detecting genes varies between animal species (Bachmanov *et al.*, 2014).

C. Umani taste

In humans, umami is only elicited by glutamate, while mice are sensitive to a wider range of L-amino acids (Laffitte *et al.*, 2016; Yamaguchi, 1967; Yarmolinsky *et al.*, 2009). The word umami comes from the Japanese language and means “delicious”, something that makes the taste even better. T1R1/T1R3 is widely recognized as the umami receptor since it responds to glutamate, but also possess all features of the umami detector.

D. Salt taste

The sodium-specific epithelial sodium channel (ENaC) is responsible of vertebrate salt perception (Chandrashekar *et al.*, 2010). The taste of salt is complex. First, because salt can be attractive or aversive depending on its concentration and secondly due to the variety of cations such as Li^+ or K^+ which may also be perceived salty.

E. Sour taste

Over the years, many sour receptors were proposed to be putative candidates, especially PKD2L1 (Chang *et al.*, 2010; Horio *et al.*, 2011). Today, a conserved gene family Otopetrin1 (Otop 1) has been found and accepted as a detector of acid-sensing taste. This gene family encodes a protein with 12 predicted TM domains (Tu *et al.*, 2018) which is required in acid-detecting taste receptor cells and is required for their Zn^{2+} sensitive proton conductance. Otop1 appears to be evolutionarily conserved from nematodes to humans. It was determined that Otop1 constitutes the proton current in acid-sensing taste receptor cells and that Otop1 was expressed in PKD2L1 cells implicated in sour transduction.

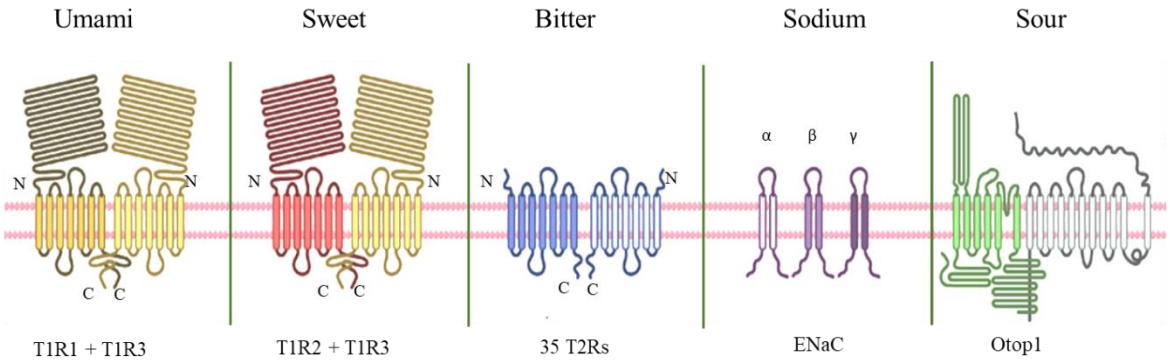

Figure I-6. Taste receptors in mammalian

Topology of bitter, sweet, umami, salty and sour receptors in mammalian. Umami, sweet and bitter receptors are G protein coupled receptors. Bitter receptors (35 total in mice) are Class A GPCRs, while sweet and umami receptors (two each) are Class C receptors, characterized by a large N-terminal domain forming a Venus flytrap structure. Sour and salty tastes modulate perception *via* ions channels receptors. (Figure modified from (Liman *et al.*, 2014)). The figure was created by using biorender and medical art.

3.2. Insects gustatory system

The gustatory system is the major chemical sensing system dedicated to the evaluation of the nutrient content of food. Thus, it allows insects to sort out and select nutritive compounds and avoid toxic ones. Taste allows invertebrates to assess and consume nutrients in a liquid or solid state. Invertebrate gustatory appendages include mouthparts, legs, or tentacles (in insects, spiders, lobsters, octopus), wing margins (flies), the tip of their abdomen and the ovipositor (in locusts, parasitic wasps, flies) and antennae (in bees, ants, wasps). The main taste organs of invertebrates are located in the mouthparts. In *Drosophila melanogaster*, the taste system is distributed over five body parts: the proboscis, the distal parts of the legs (tarsae), the wing margin, the ovipositor organ and the pharynx (**Figure I-7.A**). The proboscis is the major structure responsible for taste perception and harbors external and internal taste organs. The external part of the proboscis consists of two labial palps which merge at the level of the proximal part of the proboscis. The pharynx is the initial part of the digestive tract and it carries internal taste organs allowing Drosophila to detect to ingest food, or not, and to regurgitate toxic substances (Liman *et al.*, 2014; Stocker, 1994). The pharynx is composed of three distinct organs aligned along the wall (**Figure I-7.B**): the labral sensory organ (LSO), the ventral cibarial organ (VCSO) and the dorsal cibarial organ (DCSO). Taste sensilla

located on the tarsae and the labellum allow Drosophila to taste food even before ingestion (Dethier, 1971). *Drosophila melanogaster* males carry more sensilla on the tarsae of their forelegs (T1) than females (50 versus 37) (Montell, 2009). This sexual dimorphism is caused by the need that males have to detect the pheromones emitted by the females during courtship behaviour (Possidente and Murphey, 1989). Some of these tarsal sensilla are also involved in sex-specific detection of non-pheromonal substances such as sucrose (Meunier *et al.*, 2000). The two other pairs of legs also carry taste sensilla, 30 for T2 and 32 for T3. No sexual dimorphism has been noted on these legs. Each gustatory sensillum houses 2 to 4 GRNs. The sensilla of the ovipositor seems to be involved in the choice of the egg-laying site (Falk *et al.*, 1976; Yang *et al.*, 2008). The female ovipositor carries about 10 sensilla which remain poorly studied (Montell, 2009).

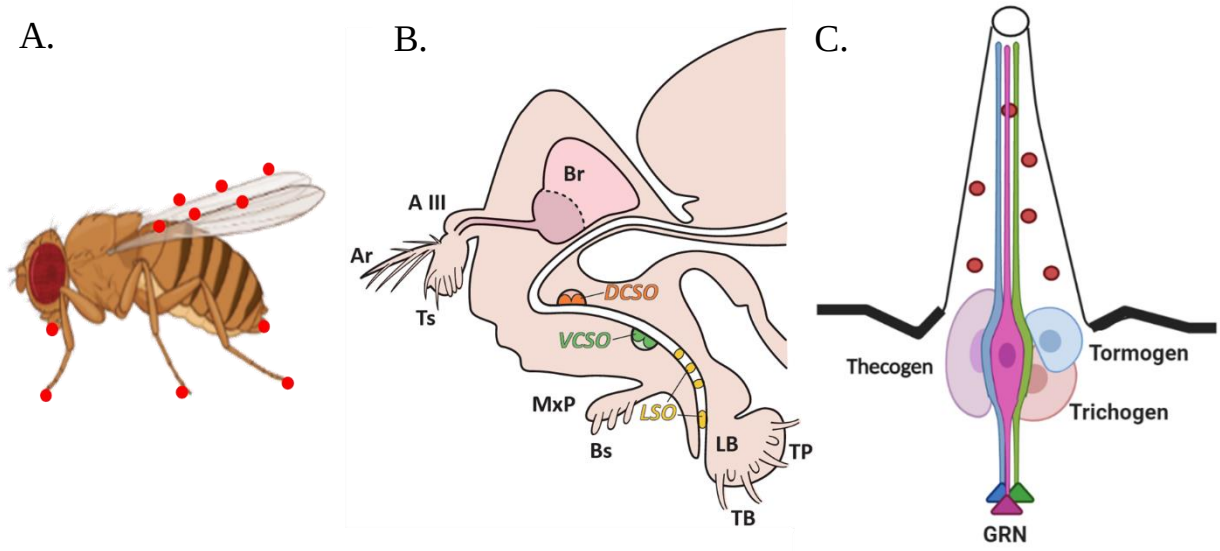

Figure I-7. The gustatory system of *Drosophila melanogaster* flies

A) Topological distribution of Drosophila fly gustatory organs. B) *Drosophila melanogaster* head with olfactory organs, antennae and maxillary palps (Mxp) and gustatory organs, proboscis with associated sensilla. Antennae include the 3rd antennal segment (A III), arista (Ar) covered with trichoid sensilla (Ts). Mxp is covered with basiconic sensillum (Bs). The labellum (LB) is covered with taste bristles (TB) and taste peg (TP) and contains three internal taste organs: (i) the labral sense organs (LSOs) in yellow; (ii) the ventral cibarial sense organ (VSCO) in green; and (iii) the dorsal cibarial sense organ (DSCO) in orange. Brain (Br). (Figure modified from (Stocker, 1994). C) Internal structure of a gustatory sensillum. The figure was created by using biorender and medical art.

The wings margins carry about 40 sensilla and each of them houses 4 GRNs (Montell, 2009). Taste sensilla located at the anterior wing margin respond to bitter and sugar stimuli and are important for exploration of ecological niches during flight (Houot *et al.*, 2017; Raad *et al.*, 2016). During their high beat frequency over plants and flowers, wings may create a vortex and help to volatilize substances without the need to contact the potential food surface and avoid to be intoxicated.

All gustatory organs are covered by sensilla. Each taste sensilla contains 2 to 4 GNRs, one mechanosensory neuron and three accessory cells (the trichogen, tormogen and thecogen cells). They are opened by one terminal pore (Shanbhag *et al.*, 1999) (**Figure I-7.C**). The LSO comprises 9 sensilla including 3 gustatory ones. Each LSO sensilla contains 1 to 8 GRNs (Gendre *et al.*, 2004; Montell, 2009). The VSCO comprises 3 sensilla housing 2 to 4 GRNs. The DCSO has 3 sensilla with 3 GRNs in each. Each labellum carries 31 taste sensilla. The taste sensilla of the external organs are classified according to their size, distribution and the number of sheltered GRNs. There are 3 types of sensilla according to their length: short (S), long (L) and intermediate (I). The S and the L have 4 GRNs while the I sensilla have only 2 (Siddiqi and Rodrigues,1980; Meunier *et al.*, 2003; Hiroi *et al.*, 2004; Thorne, 2005). Physiological studies revealed that each S and L sensilla contains a sugar-sensitive GRN (the S cells), a water-sensitive GRN (the W cell), a GRN activated by low salt concentrations (the L1 cell) and a GRN activated by high salt concentrations (L2 cell). Sensilla I possess a GRN sensitive to both sugar and low salt concentrations, and a GRN sensitive to high salt concentrations (Hiroi *et al.*, 2004).

3.2.1. Receptors involved in the taste detection of insects

Alike vertebrates, insects can detect the five taste modalities through dedicated GRs. Studies have identified 60 Drosophila genes encoding 68 taste receptors (Dunipace *et al.*, 2001; Robertson *et al.*, 2003; Scott *et al.*, 2001). These taste receptors have a structure with 7 TM domains (Sato *et al.*, 2008; Xu *et al.*, 2012). Studies on fly taste perception revealed that at least three families of receptors/channels are involved in gustatory detection: GRs, IRs and Transient Receptor Potential channels (TRP) (Dunipace *et al.*, 2001; Scott *et al.*, 2001). To survive, Drosophila can evaluate substances as diverse as sugars, many bitter molecules, amino acids, carbonation, salts, fatty acids, polyamines and water content of the food source (**Figure I-8**).

A. *Bitter taste*

Bitter taste in flies is detected by GRs and TRPs channels. Some GRs (GR66a, GR32a, GR33a, GR89a and GR39a) in the proboscis are required to respond to a large numbers of aversive chemicals indicating that they act as co-receptors (Lee *et al.*, 2009). Drosophila legs respond to bitter compounds either by activation of specific taste neurons and/or by inhibition of taste neurons activated by sugars and water (Meunier *et al.*, 2003).

TRP channels are involved in bitter compound detection. At least in one case, the GPCR signalling appears to be coupled to a TRP channel (TRPA1) (Kim *et al.*, 2010; Xu *et al.*, 2012; Zhang *et al.*, 2011). The TRPA1 channel is involved in the perception and the behavioural avoidance against aristolochic acid. However, it is not yet completely understood how GRs (which are GPCRs) function in addition to ionotropic channels.

Bitter compounds can suppress feeding by inhibiting sugar-sensitive GRNs (Jeong *et al.*, 2013; Meunier *et al.*, 2003). OBP49a binds directly to bitter compounds and then interacts with the sugar receptor GR64a on the cell surface of the GRNs to suppress its activity.

B. *Sweet taste*

Similarly to humans, flies are attracted to sugars (Hiroi *et al.*, 2004), but they respond more to disaccharides and oligosaccharides than to monosaccharides (Dahanukar *et al.*, 2007). Both fly sweet and bitter receptors belong to the GR family. In Drosophila, at least three receptors are required for sensing all sugars tested (except fructose): GR5a, GR64a, and GR64f (Dahanukar *et al.*, 2007; Jiao *et al.*, 2008; Slone *et al.*, 2007). These three receptors are co-expressed in the sugar-responsive GRNs of the labellum, along with five other related GRs that include the Gr-Sugar (Gr-S) clade (Dahanukar *et al.*, 2007; Jiao *et al.*, 2008). GR64a participates to the response to sucrose and maltose, while GR5a is needed for detection of trehalose and melezitose. GR64f is the co-receptor associated with GR5a and GR64a: its deletion affects the response to trehalose, sucrose, maltose and glucose (Dahanukar *et al.*, 2001, 2007). On the other hand, fructose is detected by a single GR named GR43a (Miyamoto *et al.*, 2012).

C. *Umami taste*

Many studies showed that amino acids (AAs) are required for larval growth, female fecundity or adult lifespan (Leitão-Gonçalves *et al.*, 2017; Yamada *et al.*, 2015). Physiological and electrophysiological responses of Drosophila labellum sensilla showed that the amplitude of male and female AA preference depends on the presence/absence of these AAs in their diet

(Toshima and Tanimura, 2012). None of the 19 common AAs tested stimulates action potentials in GRNs of sugar-responsive sensilla (Dahanukar *et al.*, 2007). Other AAs such as L-canavanine induced avoidance responses in flies (Mitri *et al.*, 2009). Gr8a and Gr66a are required for L-canavanine avoidance (Lee *et al.*, 2012). Specific IRs are also involved in AA detection: IR76b allows larvae to detect AAs during their development (Chen and Dahanukar, 2019; Croset *et al.*, 2016). IR76b is also present also in adults and involved in low salt concentration detection (see below).

D. Sour and carbonation taste

Fruit flies slightly prefer acidic foods, such as carbonated water, while they reject too acidic food (Fischler *et al.*, 2007). Some IRs (IR25a and IR76b) can play a role in the molecular basis of carbonation sensing (Charlu *et al.*, 2013). Behavioural and physiological analysis reveals that the avoidance to carboxylic acid is mainly mediated by a subset of bitter GRNs.

E. Salt taste

Flies are attracted to low salt concentrations (<100 mM NaCl). GRNs in L-type sensillum are activated at low concentrations. At higher salt concentrations (> 400 mM NaCl), GRNs in several S-type sensilla provide a dominant responses (Liu *et al.*, 2003; Zhang *et al.*, 2013). Two ENaC channels family members, the pickpocket channel proteins (ppk), ppk11 and ppk19, expressed in the terminal organ of Drosophila larvae are essential to sense low salt concentration (Liu *et al.*, 2003). IR76b is required for low-salt sensing in adult flies. The open states of IR76b and ENaC are well suited for low-salt sensors given the unusually low Na^+ compositions bathing the taste cells in both insects and mammals, relatively to the insect hemolymph or mammalian blood (Benton *et al.*, 2009; Canessa *et al.*, 1994).

F. Water detection

Flies also use their gustatory system to sense water. Studies based on the measure of proboscis extension response (PER) showed that PER to water depends on ppk28, a member of the DEG/ENac family of channels (Cameron *et al.*, 2010; Chen *et al.*, 2010). This channel, activated by low osmolarity, is required for water sensitivity (Inoshita and Tanimura, 2006).

G. Glycerol detection

The receptor required for glycerol sensing, Gr64e, belongs to the GR-S clade which also includes the three sugar receptors GR5a, Gr64a, and Gr64f. The ectopic expression of Gr64e in a heterologous chemosensory neuron conferred sensitivity to glycerol, indicating that Gr64e is directly involved in glycerol recognition (Wisotsky *et al.*, 2011). Pseudogenization

of Gr64e in two Drosophila species of the obscura group, *D. pseudoobscura* and *D. persimilis*, correlated with a loss of glycerol sensitivity in labellar sugar-sensing neurons. This receptor is required to feeding preference on beer or other fermenting yeast.

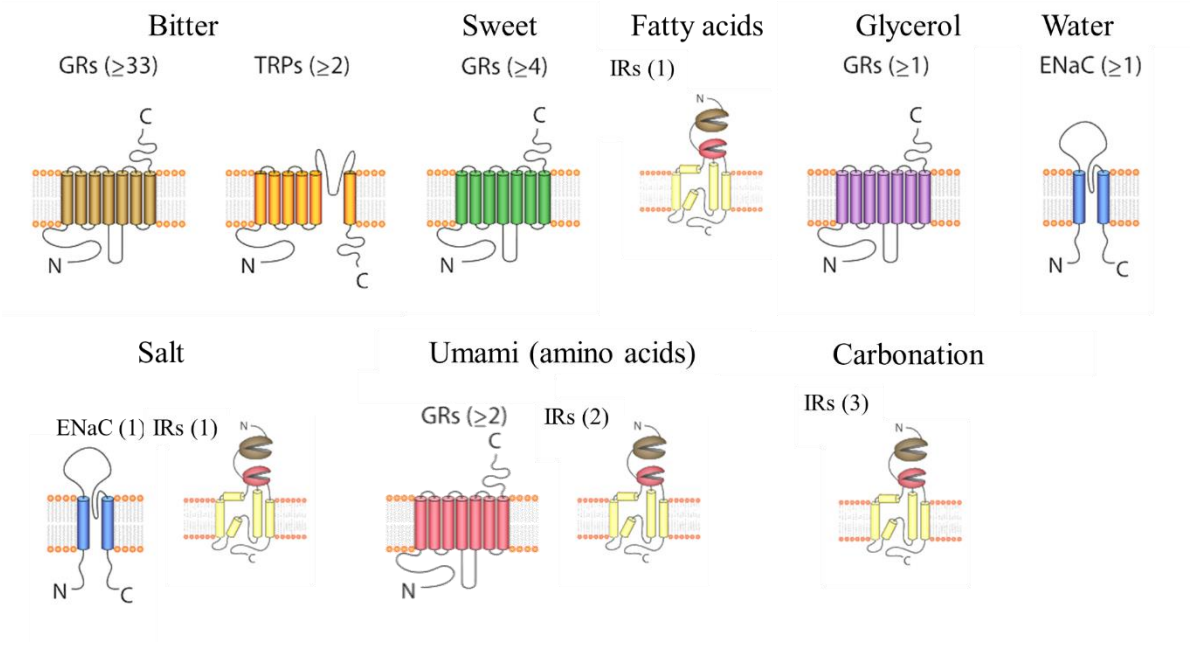

Figure I-8. Schematic representation of Drosophila gustatory receptors

Structure of Drosophila flies taste receptors involved in the detection of varied taste modalities. Gustatory receptors consist of 7 TM domains with an intracellular N-terminal domain and an extracellular C-terminal domain (Zhang *et al*.,2011) capable of forming ion channels with varied substrate specificities, allowing signal transduction. (Figure modified from (Liman *et al.*, 2014). The figure was created by using biorender and medical art.

4. Perception of fatty acids

4.1. Structure of fatty acids

Fatty acids (FA) are carbon chains with a methyl group at one end of the molecule (designated, ω) and a carboxyl group at the other end. The carbon atom next to the carboxyl group is called the α carbon, and the subsequent one the β carbon (**Figure I-9**). The letter n is often used to indicate the position of the double bond closest to the methyl end (Rustan and Drevon, 2005; Wakil *et al.*, 1983). FAs can be classified based on their chain length or on their number of double bonds. Based on their variable length they are called short-chain FA (2-4 carbon atoms), medium-chain FAs (6-12 carbon atoms), long-chain (14-18 carbon atoms)

and very long-chain FAs (derived from parental 18 carbon atoms). They can be further classified into saturated (SFAs: no double bond), mono-unsaturated (MUFAs: one double bond) and polyunsaturated (PUFAs: two or more double bonds). All FAs are involved in energetic, metabolic and structural activities. FAs may have *cis*- or *trans*- configuration, meaning this side of or the other side, respectively in term of spatial arrangement of atoms within molecules. The *cis*- FAs are thermodynamically less stable than the *trans*- forms. The *cis*- FAs have lower melting points than the *trans*- FAs or their saturated counterparts (Rustan and Drevon, 2005).

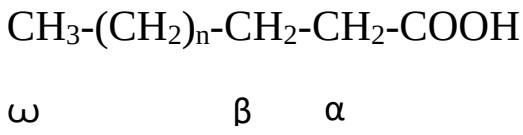

Figure I-9. Key for fatty acids nomenclature

Fatty acids are named according to chain length and number/position of double bond(s). One way to describe fatty acids is related to the methyl (ω) end. This is used to number the position of double bonds from the end of the fatty acid. The letter n is also often used to describe the ω position of double bonds.

4.2. The synthesis and impact of fatty acids in organisms

FAs represent 30–35% of total energy intake in many industrial countries. They are not only a source of energy, but very important in: i) signal-transduction pathways; ii) cellular fuel sources; iii) the composition of hormones and lipids; iv) membrane remodelling; v) the modification of proteins; and vi) energy storage within adipose tissue (specialized fat cells) in the form of triacylglycerols (de Carvalho and Caramujo, 2018). The pathway for FAs biosynthesis is highly conserved within the kingdoms of life, starting with the formation of malonyl-CoA by carboxylation of acetyl-CoA and further condensation of malonyl-CoA with acetyl-CoA with the release of CO_2 (Berg *et al.*, 2002). Free fatty acids (FFA) are taken up into cells mainly by protein carriers in the plasma membrane and transported intracellularly via fatty acid-binding proteins (FABP). FFA are activated (acyl-CoA) before they can be shuttled *via* acyl-CoA binding protein (ACBP) to mitochondria or peroxisomes for β-oxidation (formation of energy as ATP and heat), or to endoplasmic reticulum for esterification to different lipid classes. Acyl-CoA or certain FFA may bind to transcription factors that regulate gene expression or may be converted to signalling molecules

(eicosanoids). Glucose can be transformed to FAs if there is a surplus of glucose/energy in cells (de Carvalho and Caramujo, 2018; Nakamura and Nara, 2003).

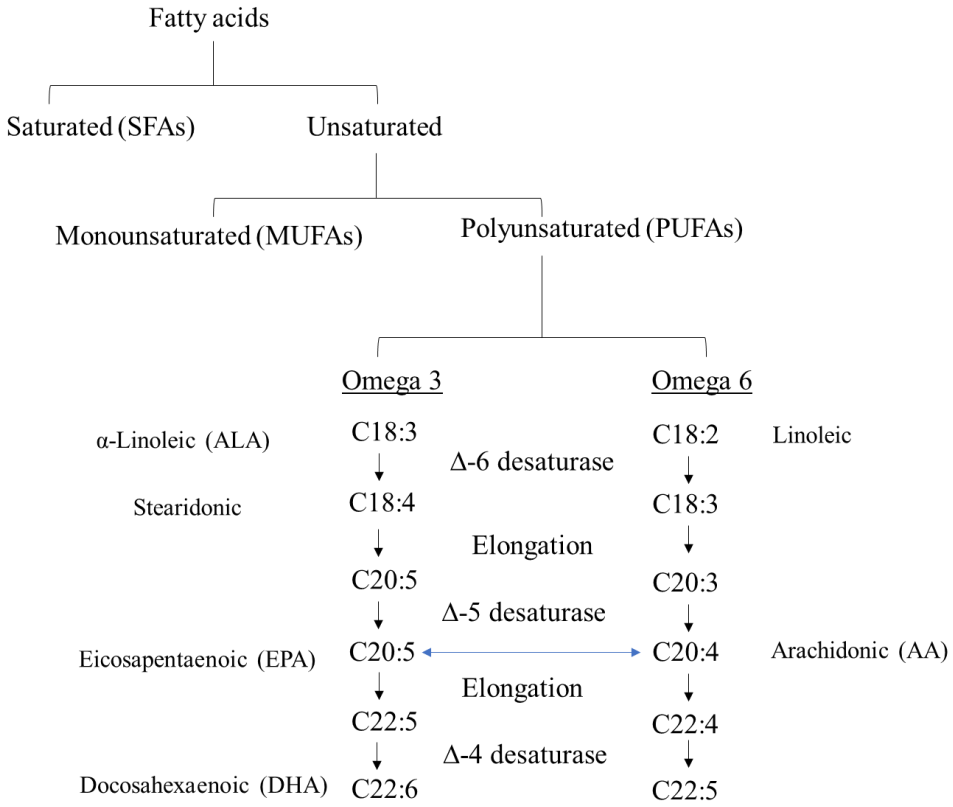

Figure I-10. Metabolic pathway showing the synthesis of omega-6 and omega-3 fatty acids

Fatty acids can be saturated or unsaturated, depending on the presence of double bonds. The unsaturated fatty acids are also divided into mono-unsaturated (MUFA) or poly-unsaturated fatty acids (PUFA). PUFAs are either ω-3 or ω-6 fatty acids. α-linolenic acid and linoleic acid are the precursors of ω-3 and ω-6 fatty acids, respectively, and are converted to different long chain PUFAs by sequential desaturation and elongation.

The most common SFAs are: palmitic acid (C16:0; animals, plants and microorganisms); stearic acid (C18:0; in animals and some fungi, and a minor component in most plants); myristic acid (C14:0; widespread occurrence), oleic acid (C18:1 ω-9; plants, animals and microorganisms) and palmitoleic acid (C16:1 ω-7; plants, animals and microorganisms) are the most common MUFAs. Linoleic acid and α-Linolenic acid cannot be synthetized by

animals and are precursor FAs for the pathway of ω-6 and ω-3 (**Figure I-10**), respectively (LA; C18:2 ω-6; plant and in animals is derived from dietary plant) and (ALA; C18:3 ω-3; found in plants and algae) (Nakamura and Nara, 2003; Rustan and Drevon, 2005). Even though, there is little doubt regarding the essential nature of ALA, yet the capacity of dietary ALA is the most important for the formation of LCFAs (Barceló-Coblijn and Murphy, 2009).

Eicosapentaenoic acid (EPA; C20:5 ω-3) and docosahexaenoic acid (DHA; C22:6 ω-3) are major FAs of marine algae, fatty fish and fish oils. Fishes have the ability to transform FA by metabolizing ALA and LA to long chain PUFAs and produce DHA and EPA. Nevertheless, in vertebrates, ALA and LA are taken from dietary source to synthetize PUFAs. By using desaturase enzymes and elongation, from ALA and LA, animals can produce EPA and DHA (de Carvalho and Caramujo, 2018).

Both ω-6 and ω-3 PUFA are essential for human nutrition, but not only, and a balance between the ingestion of ω-6 to ω-3 FAs is fundamental for maintaining health. Unbalanced diet favouring ω-6 PUFAs has prothrombotic and proinflammatory implications, which contributes to the prevalence of atherosclerosis, obesity and diabetes in human (Kang et al., 2003; Simopoulos, 2016, 2002). Omega-3 FAs have an anti-inflammatory action and are involved in the protection of heart diseases and brain development (Scott D. Doughman *et al.*, 2007; Wakil *et al.*, 1983). There is a ω-3/ω-6 ratio =1/5 that should be followed for a good health in humans but this ratio is very unbalanced due to the recent worldwide spreading of "western food" (Simopoulos, 2002).

Insects cannot synthesize PUFAs either. In Drosophila flies, they can synthesize lauric acid, myristic acid and stearic acid with the fatty acid synthase acting with malonyl-CoA (de Renobales and Blomquist, 1984). Based on the phase of development, on sex and age, the FA quantity necessary for physiological functions varies (Green and Geer, 1979).

4.3. Perception of fatty acids in vertebrates

Vertebrates can sense many qualities of food including fat. Several studies have focused on fatty acid perception in mammals, in particular in humans and rodents (Gaillard *et al.*, 2008; Johnson *et al.*, 1999; Tsuruta *et al.*, 1999). Defining fat as a sixth sense is still an open question, but experiments showed that fat should be detected to promote its consumption. Rats prefer long chain fatty acids (LCFA) fluids to a control solution of 0. 3% xanthan gum.

Their order of LCFA preference is: linolenic acid > linoleic acid > oleic acid. In these experiments, four LCFA derivatives were not preferred compared to LCFA, but LCFA derivatives were preferred over the control. These studies suggest that rats select LCFA based on olfactory or on gustatory cues related both to their carbon chain length and the presence of a carboxylate group (Tsuruta *et al.*, 1999). On the other hand, humans are capable to discriminate stearic, oleic and linoleic acids (Chale-Rush *et al.*, 2007).

In rat gustatory cells, delayed rectifying potassium channels (DRKs) were identified as FA receptors. Once, the PUFAs bind DRKs, gustatory cell depolarization was elicited (Gilbertson *et al.*, 1997). FFA stimulus induce taste receptor depolarization while K^+ channels represent the mechanism by which fat is detected in rat fungiform papillae.

The Cluster of Differentiation 36 (CD36) is another factor proposed for FA detection (Baillie *et al.*, 1996; Gaillard *et al.*, 2008). CD36 knock-out mice showed no longer preference for linoleic acid. Also, when FAs were deposited on the tongue of wild mice, with their oesophagus ligated to avoid ingestion, there showed a rapid increase of bile flow and of pancreatic secretions (Laugerette *et al.*, 2005). The level of secretions depends on FA length and on the number of insaturations. The fact that CD36 is involved in oral LCFA detection raises the possibility that lingual fat perception is linked to feeding dysregulation. Additionally, cells expressing CD36 responded to linoleic acid by increasing their intracellular concentration for both Ca_2^+ and inositol-triphosphate (Gaillard *et al.*, 2008). The ‘‘calcium taste’’ of Ca_2^+ ions is attractive to deprived-calcium animals, but is rejected by satiated-calcium animals. The aversive response to Ca_2^+ requires a functional T1R3 receptor, a subunit shared by umami and sweet taste receptors (Tordoff *et al.*, 2008).

Two fat-sensitive GPCRs, GPR40 and GPR120, are required for FA preference in mice whereas GPR120 is expressed in human taste receptor cells (TRCs) (Galindo and Smith, 2001; Cartoni *et al.*, 2010; Liu *et al.*, 2011). GPR120 has an important affinity for LCFAs. GPR40 and GPR120 are expressed in the taste buds of the tongue, brain and pancreas. GPR40 is expressed in the pancreas and GPR120 in the intestine. Depending on their identity, these GPCRs are activated by saturated or unsaturated FAs with C1 to C22 chain length (Briscoe *et al.*, 2003; Le Poul *et al.*, 2003; Hirasawa *et al.*, 2005; Cartoni *et al.*, 2010). Most mammals detect fat with TRCs with K^+ channels sensitive to PUFAs, CD36, GPR40 and GPR120.

4.4. Perception of fatty acids by insects

FAs are crucial nutrients for insects such as Drosophila larva and adult (Fougeron *et al.*, 2011). The behavioural response was of larvae and adults to the saturated FA (Myristic acid, C14:0; Palmitic acid, C16:0; Stearic acid, C18:0) and unsaturated FA (Oleic acid, C18:1; LA, C18:2; ALA, C18:3) was measured. Larva showed attraction to unsaturated FAs and a strong repulsion against SFAs. Differently, adults preferred SFAs: they laid more eggs and showed a longer life span when ingesting these FAs compared to unsaturated FAs.

In general, insects show contrasted reponses to FAs. They are attracted to lactic acid, myristic acid or nonadecylic acid (Bosch *et al.*, 2000; Smallegange *et al.*, 2009). Electrophysiological studies showed that the olfactory neurons respond to different FAs. The antennae of *Anopheles aegypti* and *Anopheles gambiae* respond to compounds ranging from C3:0 to C6:0. Those of *A.gambiae* responds to C5:0-C10:0 (Qiu *et al.*, 2006).

There is not much information about FAs receptors in flies. Flies are attracted by the taste of long or short chain FAs, except when the concentrations are very high (Masek and Keene, 2013). Low FA concentrations induce an appetitive signal. FAs perception is performed through sugar-GRNs which depends of phospholipase C (PLC) signalling (Masek and Keene, 2013). Mutant flies for PLC fail to respond to FAs: this function can be rescued by ectopic *norpA* expression in sweet-sensing neurons. FA detection might be mediated through sugar-GRNs with a GPRCs. Alike mammals, Drosophila PLC pathway in sweet-sensing neurons is a conserved molecular signalling pathway that confers attraction to fatty acids (Masek and Keene, 2013).

The Gr64e implication in glycerol detection is essential for the behavioural and electrophysiological responses to FAs (hexanoic acid, octanoic acid, oleic acid and LA) (Kim *et al.*, 2018; Wisotsky *et al.*, 2011). To determine which of the six GRs in the GR64 cluster is (are) required for FA sensing, PER responses to hexanoic acid were measured in flies carrying mutations for each of the six genes of the cluster and GR64e was identified in FA sensing (Kim *et al.*, 2018). Although both GR64e and PLC are required for FA detection in sweet GRNs, it is unclear how they function together. Also, IR56d is required in sugar-GRNs to mediate behavioural responses to FAs (Ahn *et al.*,2017).

5. Perireceptor events

In vertebrates, olfactory sensory neurons (OSNs) and gustatory sensory neurons (GSNs) are surrounded, respectively by the mucus in the nasal cavity and the saliva and the mucus in taste buds. In invertebrates, OSNs and GSNs are surrounded by the sensillar lymph filling olfactory and gustatory sensilla. "Perireceptor events" are the biochemical mechanisms allowing volatile and non-volatile chemicals from the outside environment to interact with the internal sensory receptor (Getchell *et al.*, 1984). Since these compounds need to be solubilized before being transported to their sensory receptor, three protein families present in the aqueous fluid are dedicated to this function: xenobiotic metabolizing enzymes (XMEs), chemosensory proteins (CSPs) and odorant binding-proteins (OBPs).

External substances such as pesticides, plant toxins, sapid and odorant molecules and drugs can penetrate and circulate inside the organism. When these molecules enter the body (by inhalation, ingestion or physical contact), they must be eliminated to prevent their accumulation or they should be transformed to facilitate their elimination to stop intoxication. The elimination of molecules by xenobiotic metabolizing enzymes (XMEs) occurs in three phases (Xu *et al.*, 2005). The phase I-detoxification includes cytochromes P450 (CYP), carboxylesterases, aldehyde dehydrogenases or even alcohol dehydrogenases. Their action consists to graft a functional group (OH, NH2, etc.) to lipophilic xenobiotics through oxidation, reduction and hydrolysis reactions, thus increasing their polarity (Anzenbacher and Anzenbacherová, 2001). Phase II enzymes (UDP-glycosyl transferases (UGTs) and glutathione transferases (GSTs) (Heydel *et al.*, 2010) graft hydrophilic residues to make compounds more soluble (GSTs and UGTs), while carboxylesterases catalyse the hydrolysis of xenobiotics containing 41 esters, leading to their detoxification (Heydel *et al.*, 2013, 2010). Phase III-enzymes actively export the conjugated toxins out of the cell using ATP-binding cassette (ABC) and other transmembrane transporters such as P-glycoprotein (Pgp) or multidrug resistance proteins (MRP) (Jones and George, 2004).

CSPs are small soluble polypeptides (~140 amino acids) identified across several insect orders. They show a broad tissue distribution likely due to their expression both in sensory and non-sensory organs involved in varied developmental functions (Brito *et al.*, 2016; Pelosi, 2005). However, there is no clear evidence that they participate in olfaction or in taste. Nevertheless, 4 Drosophila CSPs were identified and they may be involved in the storage and release of pheromonal molecules. The number of CSPs varies across species (Pelosi *et al.*,

2006). OBPs are the main object of my PhD thesis and I develop their functions and diversity below.

5.1.Odorant binding proteins (OBPs)

OBPs were first discovered by two research groups in the 1980's. In insects, they were discovered in the antennae of the moth *Antheraea Polyphemus* while in vertebrates, they were found in the cow olfactory mucosa (Pelosi *et al.*, 2006, 1981; Steinbrecht, 1998; Vogt and Riddiford, 1981). In insects, but not in vertebrates, a larger number of OBPs was discovered after genome sequencing and 40 years of research have allowed us to better understand their functions in chemoreception, although some remain to be discovered.

5.1.1 Structure of OBPs

A. Vertebrate OBPs

In vertebrates, OBPs are members of the lipocalin superfamily (Flower, 1996; Flower *et al.*, 2000). Lipocalins are widely distributed and form an heterogenous group of proteins in animals, plants and bacteria. X-ray crystallography or nuclear magnetic resonance (NMR) solved their 3D structure. Structural studies of rat OBP1 and OBP3 (Nespoulous, 2004; Portman *et al.*, 2014), pig OBP (Vincent *et al.*, 2000) and bovine OBP (Bianchet *et al.*, 1996; Tegoni *et al.*, 1996) helped to gain a better understanding of OBP vertebrates structure.

The lipocalin fold is a highly symmetrical all-β structure dominated by a single eight-stranded antiparallel β-sheet closed back on itself to form a continuously hydrogen-bonded β-barrel forming the calyx. The calyx has two—closed and opened— ends which differ in structure and function (Flower *et al.*, 2000). In addition, one large α-helix is attached to the C-terminus of the calyx and another smaller α-helix, called 3^{10} - helix, is attached to the N-terminus. Different ligand types can bind to lipocalin proteins due to the diversity of the binding cavity and the structural variation of the omega-type loop (Vincent *et al.*, 2000). Although vertebrate OBPs have been classified mainly as transport proteins, it appears now that members of the lipocalin family can fulfil an unsuspected variety of functions.

B. Insects OBPs

Insect OBPs are small soluble proteins, composed of 150 AAs with a molecular weight ranging from 13 to 20 kDa. They are secreted in large quantity in the sensillar lymph. OBPs are produced by the three types of support cells (tormogen, thecogen and trichogen cells).

These support cells are located at the base of each sensory sensilla (Larter *et al.*, 2016). According to the Flybase database, the *Drosophila melanogaster* genome has 52 OBP-encoding genes. The number of OBP-coding genes is highly variable between insect species, ranging from 12 to 100 in some mosquito species (Jennifer S. Sun *et al.*, 2018).

Classical OBPs consist of six highly conserved cysteines, linked together by disulfide bridges and spaced apart by a conserved number of amino acids (Rihani *et al.*, 2021; Scaloni *et al.*, 1999). These disulfide bridges give OBP its specific three-dimensional structure composed of 6 alpha helices and a hydrophobic docking site (Gonzalez *et al.*, 2019; Leal *et al.*, 1999). Insect OBPs have been divided in five groups depending on the number of conserved cysteines: (1) Classic OBPs with typical six-cysteine signature, (2) Dimer OBPs containing two six-cysteine signatures, (3) Plus-C OBPs with two additional conserved cysteines plus one proline, (4) Minus-C OBPs that lost two conserved cysteines and (5) Atypical OBPs with 9–10 cysteines and a long C-terminus (Hekmat-Scafe, 2002; Zhou *et al.*, 2004).

The spatial and temporal expression pattern of *Drosophila melanogaster* OBPs were reported in several studies. Some data revealed that OBPs are expressed both in larva and adults while others are only expressed in either life stage. Moreover, the analysis of OBP expression in olfactory and gustatory appendages revealed that some OBPs are expressed in both appendage types, while others are only expressed in either one (Galindo and Smith, 2001; Hekmat-Scafe, 2002).

5.1.2 Physiological roles of OBPs

Various biochemical roles have been proposed for OBPs, including solubilization of odours and pheromonal molecules in sensillar lymph, transport of odours through the lymph to dedicated receptors, removal of noxious compounds from the lymph, and de-activation of odours following receptor activation (Heydel *et al.*, 2013; Pelosi, 1994; Steinbrecht, 1998; Jennifer S. Sun *et al.*, 2018). These hypotheses were mainly based on studies dealing with *in vitro* binding assays, behavioural measurements and electrophysiological recordings associated to knockdown of OBPs.

In *Drosophila melanogaster*, OBP76a, also named LUSH, solubilizes and transports the sex pheromone 11-*cis*-vaccenyl acetate (*c*VA) to its receptor (Laughlin *et al.*, 2008). *c*VA is an important pheromone in aggregation and many aspects pertaining to reproduction. The exact mechanism of *c*VA detection is still debated, but the *c*VA/LUSH interaction with the sensory

membrane neuron protein 1 (SNMP1 homologous to the CD36 vertebrate factor) is necessary to transport and release the *c*VA pheromone (Gomez-Diaz *et al.*, 2013).

A recent study showed that OBP28a, one of the most abundant OBPs in *Drosophila melanogaster*, is not only necessary for the transport of the tested odorants molecules, but also serves to dampen the quantitative variation of odours according their concentration in the environment (Gonzalez *et al.*, 2019). Thus, OBP28a plays a buffering role likely to avoid receptor saturation.

Two closely related OBPs (OBP57d and OBP57e) are required for the detection of hexanoic and octanoic acids. These two compounds are involved in the preference and identification of an oviposition site of a Drosophila species endemic to Seychelles islands (*D. sechellia*; Harada *et al.*, 2012, 2008).

Recently, an unexpected role of OBP59a in humidity sensing was revealed. The moisture-sensing sensillum in the Drosophila antenna expresses OBP59a. Mutants lacking this protein showed increased desiccation resistance (Jennifer S. Sun *et al.*, 2018). OBP59a is an exceptionally well-preserved protein and its function is essential for insect survival.

Another study demonstrated that the interaction between OBP49a (specifically expressed in the Drosophila taste system) and the sugar receptor GR64a resulted in the suppression of the attractive response to sugar combined with a bitter molecule (Jeong *et al.*, 2013).

Another study showed that the suppression of the expression of OBP56h led to a reduction in the latency lap between courtship initiation and copulation start (Shorter *et al.*, 2016). This phenomenon was linked a decreased production of a cuticular pheromone (5-tricosene), which impacts courtship initiation in males (Ferveur and Sureau, 1996).

Another study, carried out in our laboratory, deciphered the role of OBP19b. Rihani and co-workers demonstrated that OBP19b is required for the peripheral sensing of specific AAs, including the essential L-phenylalanine (Rihani *et al.*, 2019).

These studies revealed that OBPs can have multiple functions. Through the years, researchers realized that OBPs are not only ligand transporters. New insights were proposed for OBPs implication in the host - gut microbiota interaction. A recent study showed that the microbiota is involved in the development and functioning of the immune system of two diptera species, Glossina (tsetse fly) and Drosophila (Benoit *et al.*, 2017). In particular, this study revealed that symbiotic bacteria help flies to maintain immune system homeostasis.

Insects establishing an endosymbiosis with bacteria seem to better resist to dehydration and/or to exposure to infections caused by environmental microbes after cuticular injury. The *Wigglesworthia* bacterium regulates the expression of OBP6 in the intestine of intra-uterine tsetse fly larvae whose ortholog OBP28a was found in Drosophila (Benoit *et al.*, 2017). This process seems to be necessary and sufficient to induce expression of the hematopoietic transcription factor RUNX in adults and to provide substantial benefits for the host organism. These results provide clear insight into the mechanisms underlying host-symbiont interactions.

The microbial community contributes to the healthy shape of organisms. Under-nutrition shorten the lifespan of Drosophila. A protein-deficient diet (0.1% yeast extract), was sufficient to induce AA extraction from a nutrient-poor diet and thus increase the protein flux ingested (Yamada *et al.*, 2015). The fungal microbiota plays also a role in energy harvest and contributes to host health. The quality of yeast provided in the diet of juvenile Drosophila strongly changes food and olfactory preferences in resulting adults (Grangeteau *et al.*, 2018).

The next chapter introduces the microbiota and its impact on organisms.

Chapter 2:
Microbiota

1. Embryonic and larval development

The digestive tract of *Drosophila melanogaster* is divided in three parts: the foregut, the midgut and the hindgut (Demerec, 1950). The foregut and hindgut originate from ectoderm while the midgut originates from the endoderm during the embryonic gastrulation phase. Maternal factors and transcription factors such as GATA transcription factor Serpent (Srp) and the HNF/Fork head (FKh) highly conserved during evolution, allow cell type specification through the action of proneural proteins and Notch signaling pathway (**Figure I-11**). The proneural proteins promote enterocyte (EC) while Notch signaling promotes enteroendocrine (EE) (Takashima *et al.*, 2011; 2013). The balance between proneural activity and Notch signaling activity determines the cellular composition of the midgut.

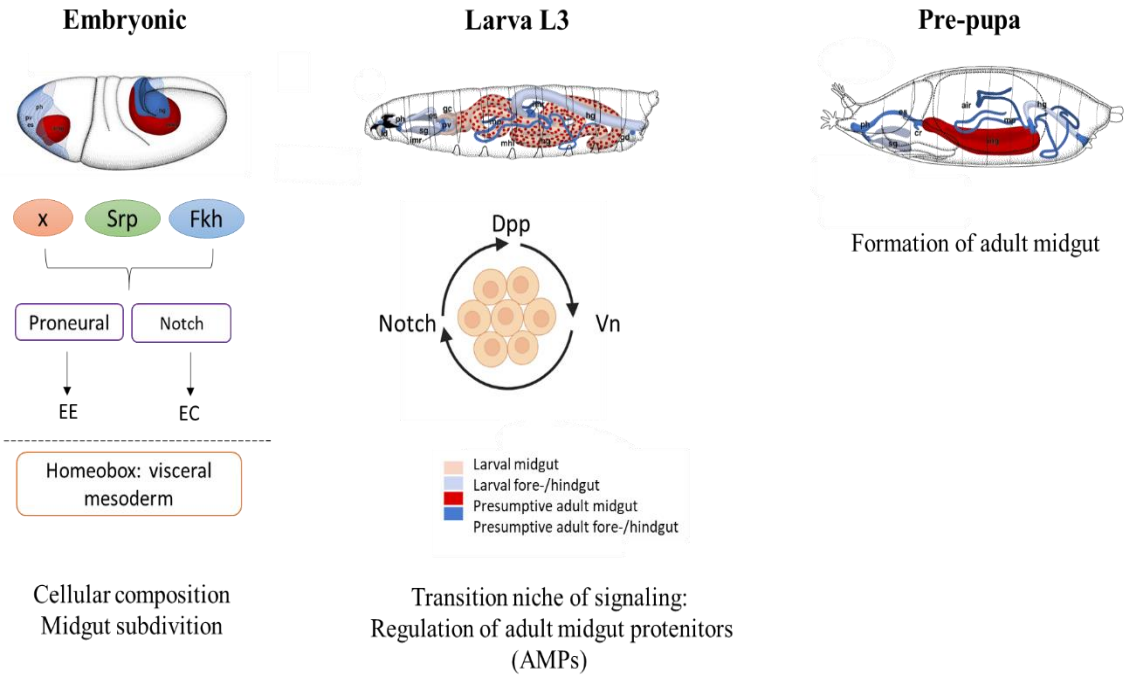

Figure I-11. Developmental transitions of the digestive tract in *Drosophila melanogaster*

Development of digestive tract from embryonic phase to pupal phase. Embryonic stage: proneural activity and Notch signalling activity determine the cellular composition and midgut subdivision. Larva L3: transition niche of signalling with undifferentiated cells (AMPs). Pre-pupa: AMPs are regulated by a transient niche in the larval midgut and niche cells go on to differentiate during metamorphosis, spending out between the newly forming adult gut and the degenerating larval midgut and forming a transient pupal epithelium. (Embryonic, Larva L3 and pre-pupa picture taken from Atlas of Drosophila development).

The Homeobox (Hox) genes in the visceral mesoderm promote the subdivision of the midgut endoderm in anterior-posterior axis. During the larval phase, the adult midgut progenitors cells (AMPs) form clusters of proliferation, undifferentiated cells that are attached to the basal surface of the larval gut epithelium. During the complete metamorphosis phase, complex interaction spreads out between the newly forming adult gut and the degenerating larval midgut thus forms a transient pupal epithelium (Miguel-Aliaga *et al.*, 2018).

2. The adult structure of *Drosophila melanogaster* gut and the physiology of foregut, midgut and hindgut

The adult Drosophila gut consists of a tube lined by an epithelial monolayer consisting of four cell types: intestinal stem cells (ISCs), absorptive ECs cells, secretory EEs cells and enteroblasts (EBs) (**Figure I-12.B**). This epithelium is surrounded by visceral muscles and protected toward the lumen both by secreted mucus and by a chitinous layer called "peritrophic matrix" (Hegedus *et al.*, 2009). Anatomical specializations and regional subdivisions also define the future functions of the gut including ingestion, storage, digestion, absorption and defecation.

The foregut contains the oesophagus, crop and proventriculus (also known as cardia). After food evaluation by the three internal taste organs included in the proboscis (LSO, VCSO and DCSO), the foregut ensures the transit from the oesophagus to the crop. The crop is a diverticulated structure, unique to Dipteria, made with a complex array of valves and sphincters allowing the « *in and out* » transit of nutrient of the crop into the midgut. It is composed of four main structures: (*i*) epithelial cells producing the cuticular lining of the crop system, (*ii*) the cuticular intima, (*iii*) a pair of crop nerve bundles emanating from the *corpora cardiaca* and (*iv*) the crop muscles of the duct and lobes.

Studies suggest that the crop (**Figure I-12.A**) is involved in early digestion, detoxification, regurgitation and vomiting, microbial control and/or food storage (Stoffolano and Haselton, 2013). The size of the crop can differ between flies. The cardia is a complex bulb-shaped organ composed of three epithelial layers producing the peritrophic matrix. It is a major site of antimicrobial peptide production and it may regulate the entry of ingested food into the midgut (Tzou *et al.*, 2000).

The midgut is the larger portion of intestine with an average length of 6 mm in flies. It possesses both digestive and absorptive functions for nutrients. The Malpighian tubules are

located between the midgut and hindgut. They serve as excretory organs and do not belong to the intestine. The midgut is subdivided into the anterior, middle and posterior midguts. However, morphologically and molecularly, the midgut is subdivided into 10-14 regions (Buchon *et al.*, 2013; Dutta *et al.*, 2015) (**Figure I-12.A**).

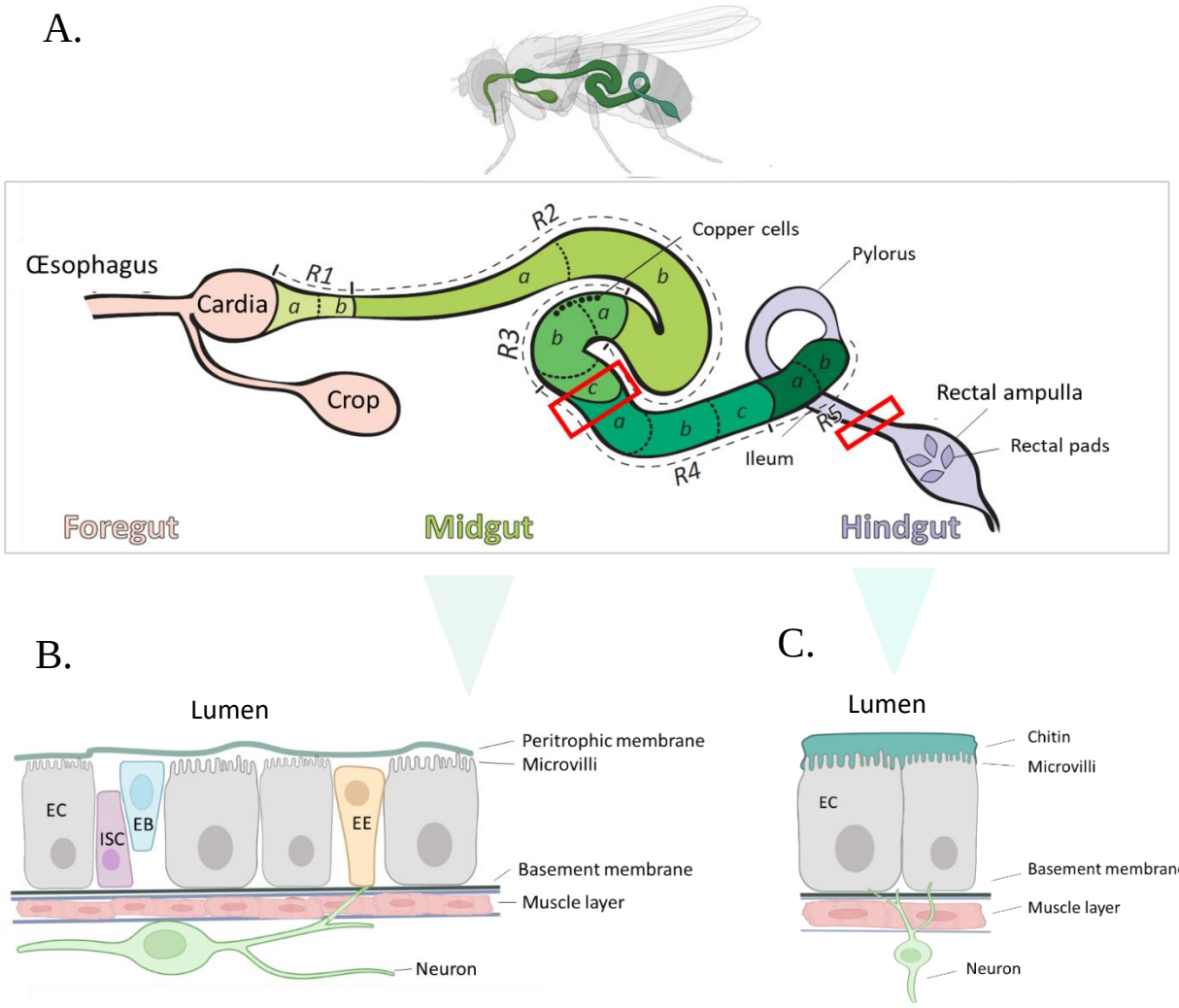

Figure I-12. The adult intestine and its cell types.

A) Anatomical and morphological parts of the digestive tract. Presentation of gut from oesophagus to hindgut. There are three parts: the foregut composed of crop and cardia; the midgut composed of 5 regions (R1 -R5) which can be subdivided where Copper cell region is found; the hindgut composed of the pylorus, ileum and rectal ampulla (4 rectal pads). B) General cellular composition of the midgut. Four cell types: intestinal stem cells (ISCs), absorptive cells (ECs), secretory cells (EEs) and enteroblasts (EBs). The epithelium in this part is protected by achitinous layer called peritrophic matrix. C) General cellular composition

of hindgut. Mostly contains absorptive cells (ECs) surrounded by a dense chitinous layer. The figure was created by using biorender and medical art.

The midgut is the major site for digestion and absorption of nutriments. The anterior midgut is composed of R1a, b and R2a, b. From R1 to R3, are located the enzymes involved in the breakdown of sugars. In the R2 region, occurs the digestion of fatty acid and triglycerides that continues to R3 region. The middle midgut region contains the R3 region subdivided in R3a, b and c. R3a, b is known as Copper cell region which produces gastric acid with a pH 2-4. The role of region R3c remains unclear. The posterior midgut contains R4a, b, c and R5a, b, c with a pH 7-9. These regions serve to absorb fatty acids, complex and simple carbohydrates and vitamins. All regions of the midgut contain ISCs able to regenerate all cell types of their particular region with a 1-2 weeks turnover.

The hindgut consists of three major regions, the pylorus, ileum and rectum (Hartenstein, 2005) (**Figure I-12.A**). The pylorus region is highly innervated both by the peripheric and central nervous systems. Such innervation may enable the pylorus to function as an intestinal checkpoint for further passage of gut contents (Cognigni *et al.*, 2011; Miguel-Aliaga *et al.*, 2008). Downstream the posterior midgut, the cell structure is different mainly due to pH change. While in the posterior midgut, the pH range between 7 and 9, it drops down to 4 - 5 in the hindgut. Cells of the hindgut pyloric epithelium or ileum epithelium (**Figure I-12.C**) contact the lumen through an electron-dense chitinous layer (Murakami and Shiotsuki, 2001). The pylorus is also an important zone of interaction between the Drosophila host environment and its microbiota. However, the hindgut-specific microbe interaction remains to be investigated. In addition, the cuticle of the pyloric region of several insects is thought to host enriched microbial communities (Elzinga, 1998). The pylorus is also implicated in innate immune response *via* melanin production (Wang *et al.*, 2018). Melanisation acts as a defence response mediated in part via the JNK signalling pathway. The crucial role of melanin in hindgut immunity was discovered in Drosophila as well as in other insects (Wu *et al.*, 2015). For example, honeybees infected with a pathogenic bacterium activate melanin formation in their pylorus. When silkworms are fed with a pathogenic bacteria, prophenoloxidase, a component of the melanisation process, is activated in the faeces (Wu *et al.*, 2015). Drosophila flies fed with toxic compounds activate a melanisation response in the hindgut (Takashima *et al.*, 2011; Wu *et al.*, 2015). This pylorus reaction is thought to be the ultimate response of defence to clear off the host from pathogenic bacteria or other toxic elements.

The ileum and the rectum are two major regions involved in the reabsorption of water, Na^+, Cl^- and K^+ ions, and nutrient recycling. These hindgut regions are specialized in ion and water transport. The rectum acts as the final site of reabsorption: it is composed of four rectal papillae, also known as rectal pads. This structure was first described in honeybees, almost three centuries ago (Swammerdam, 1737). Both Drosophila males and females contain a four cone-shaped papillae structure, which projects into the intestinal lumen (Bodenstein, 1950). The rectal pads are sexually dimorphic in some species and highly adapted to each type of diet. Moreover, the rectal papillar structure was found to be conserved between Drosophila, mosquitos and ants (Hopkins, 1967; Wigglesworth, 1972). Rectal pads are crucial in Drosophila ion balance regulation. Similarly, to the pylorus, the rectum is one of the most highly innervated regions of the Drosophila intestinal tract. The innervation plays a role in the final step of excretion following reabsorption, defecation and also, in insulin metabolism (Cognigni *et al.*, 2011; Patrick *et al.*, 2006). Some neurons produce insulin suggesting a cross-talk between metabolic signalling and hindgut functions (Miguel-Aliaga *et al.*, 2008).

The idea that stem cells in the hindgut could be involved in injury of intestine is not accepted by all the scientific community. An hypothesis increasingly accepted suggests that pylorus cells leave a quiescent state to enter into S phase as a response to injury or toxin (Cohen *et al.*, 2018; Sawyer *et al.*, 2017). This response does not involve repair by cell division and creation of new cells, but involves, instead, the enlargement of cells that remain subsequently to injury. These processes are known as wound induced polyploidization and compensatory cell proliferation.

3. Definition of gut microbiota and influence on host's physiology

A community of microbes that colonizes a niche is called « microbiota ». The microbiota is composed of bacteria, archea, protists, fungi and viruses. The total biomass of microbes on Earth is estimated to represent ~ 70 gigatons of carbon (Gt C) of bacteria ; 7 Gt C of archea ; 4 Gt C of protists ; 12 Gt C of fungi and 0.4 Gt C of viruses (Bar-On *et al.*, 2018). The discovery of microbes on extreme environments, like acidic lakes or hypersaline brines has increased even more our scientific curiosity to better understand their characteristics (Rothschild and Mancinelli, 2001; Uma *et al.*, 2020). All plants and animals live in close association with microbial organisms.

In plants, the soil was identified as the main driver of bacterial community composition. The microbiota of plants is known for its importance on healthy growth and development of the

host, on water loss and in preventing or favouring roots (Fürnkranz *et al.*, 2012; Kõiv *et al.*, 2015; Sturz, 1995). For example, the bacterial community of potatoes is recruited from the soil and partly inherited across generations to allow the best development of the plant (Buchholz *et al.*, 2019). Other results also showed that seeds act as a source, or reservoir for transmitting microorganisms (Abdelfattah *et al.*, 2021). In the rhizosphere (on plant roots), bacteria are abundantly present and some of them stimulate plant growth. These plant-growth-promoting rhizobacteria (PGPRs) can fix nitrogen and improve plant growth when the nitrogen is absent from the soil (Bloemberg and Lugtenberg, 2001). Co-evolution mechanisms have allowed the symbionts to adapt to their hosts and reciprocally to benefit from abundant nutrients and of the shelter provided by their host (Abdelfattah *et al.*, 2021; Buchholz *et al.*, 2019).

Microbiota is found in all animals and most studies have focused on the understanding of gut microbiota functions. The composition of gut microbiota is shaped both by diet and host phylogeny (Groussin *et al.*, 2017; Hale *et al.*, 2018; Nishida and Ochman, 2018). Between the host and the microbes, three types of symbiosis have been identified. (1) "Parasitism" where the parasitic microbes infect host's tissues. Some infections by parasites can be lethal for the host organisms (Blaser and Parsonnet, 1994; Westwood *et al.*, 2010). (2) "Commensalism" where microbes benefit from their host, without affecting it. Most gut-associated microbes are classified as commensals because they are not known to be harmful to their host (Cremon *et al.*, 2018). However, classification of a microbe as being a commensal is not definitive. (3) "Mutualism" when microbes provide a benefit to their host. For years, researchers have described the influence of mutualistic symbionts in different organisms, mostly in mice and humans, using many parameters.

Human gastrointestinal tract is thought to contain $3x10^{14}$ microorganisms, a number 10 times larger than the human cells amount (MetaHIT Consortium; (Qin *et al.*, 2010). This highlights the importance to study human gut microbiota. In humans and mice, the development of obesity correlates with brutal shifts in the relative abundance of the two dominant bacterial phyla in the gut, the *Bacteroidetes* and the *Firmicutes* (Ley *et al.*, 2005; Turnbaugh *et al.*, 2009). Obese mice have 50% fewer *Bacteroidetes* and more *Fircutes* than mice with a regular weight. Similar results were found in the human faecal microbiota (Duncan *et al.*, 2008). The gut microbiota regulates host energy balance and storage (Turnbaugh *et al.*, 2008, 2006). Energy metabolism in mice and humans can be significantly impacted by the presence, composition and metabolic actions of the gut microbes. These results showed that our gut

microbiota depends on our diet which can therefore promote, or not, the occurrence of obesity (Al-Assal *et al.*, 2018; Shen *et al.*, 2013). The transfer of gut microbiota from obese mice (ob/ob) to axenic wild type mice leads to an increase of the fat mass (Turnbaugh *et al.*, 2009). This experiment was the first to demonstrate a causal relationship between microbiota composition and variation of host weight. The gut microbiota is involved in the metabolic syndrome that increases the individual's risk of developing type 2 diabetes and cardiovascular disease (Vijay-Kumar *et al.*, 2010). Furthermore, supplementation with *Akkermensia muciniphila* bacteria to mice fed on a high-fat diet reduces their fat mass and improves their sensitivity to insulin (Everard *et al.*, 2013). Mice genetically deficient for the Toll-like receptor 5 (TLR5), a factor of the innate immune system expressed in the gut microbiota, showed hyperlipidaemia, insulin resistance and increased adiposity compared to the controls. Therefore, the alteration of the gut microbiota composition resulting from loss of TLR5 induced the occurrence of a metabolic syndrome in these mice (Everard *et al.*, 2013).

The microbiota is also involved in the initiation, progression and dissemination of cancer (Roy and Trinchieri, 2017). Inflammation modifies the gut microbiota which in turn affects the progression of colorectal cancer. High-throughput sequencing revealed that inflammation modifies gut microbial composition in colitis-susceptible interleukin-10–deficient mice (Arthur *et al.*, 2012). Also, monocolonization with the commensal *Escherichia coli,* induced by inflammation, promoted invasive carcinoma. *Escherichia coli* were found in a significantly high percentage of inflammatory diseases and in colorectal cancer patients. Microbiota transplant, the injection of a donor of faecal microbiota to a deficient patient, is a highly efficient therapy used to cure different pathologies (Zhou *et al.*, 2017).

The link between the gut microbiota and social behaviour also received an important attention. Gut microbiota is increasingly recognized as a potential modulator of brain functions. This effect is mediated via the gut-brain axis and involves metabolic, nutritional, endocrine and immunological aspects (Baothman *et al.*, 2016; Foster and McVey Neufeld, 2013; Martin and Mayer, 2017). A different composition of gut microbiota was noted between two mice models characterized either by their dominance or submissiveness (Agranyoni *et al.*, 2021). Thus, the gut microbiota determines the social behaviour of mice and induces metabolic and inflammatory changes in their adipose tissue (Agranyoni *et al.*, 2021).

Several studies speculated on a potential interaction between gut microbiota and Autism Spectrum Disorders (ASD). Moreover, some *Bifidobacteria and Lactobacilli* species can induce positive effects on anxiety, depression, cognition and autism-related behaviours

(Cryan and Dinan, 2015). Furthermore, babies born from a caesarean-section show less diversity of gut microbiota than babies vaginally delivered (Arboleya *et al.*, 2018). The genital passage is crucial for babies to acquire a rich microbial colonization beneficial for future health. Furthermore, autistic children have a distinct and less diverse gut microbial community structure compared to non-autistic children (Kang *et al.*, 2013). In hospitals, a current trend consists to cover caesarean-section new-born baby with a blanket wore by their mothers. Moreover, human gut microbiota from autism spectrum disorder promotes altered behaviours in mice (Sharon *et al.*, 2019). This suggests that a mechanism involved in the production of microbial metabolites in the gut can affect brain function and regulate behaviour. A *trans*-species experiment consisting to transfer the gut microbiota of depressive human patients to axenic mice caused depressive-like behaviour in recipient mice (Chevalier *et al.*, 2020).

If mouse is a powerful vertebrate model to study gut microbiota, simpler animal models allow researchers to investigate molecular and genetic factors underlying host-microbiota interactions. The zebra fish *Danio rerio* which has a small size and a high fecundity is a favourable vertebrate model to study microbiota effects. The nematode worm *Caenorhabditis elegans* is an invertebrate of choice to decipher host-microbiota interactions (Douglas, 2019).

In my PhD thesis, I used the fruit fly *Drosophila melanogaster* as a model to study the interaction between host and bacteria in several nutritional and reproductive conditions.

3.1. *Drosophila melanogaster*: a model to study host-microbe interactions

Drosophila became a laboratory model in the early 1900's, especially in experimental genetics with Thomas Hunt Morgan and his talented students (Sturtevant, Bridges and Müller) at Columbia University. In the recent decades, Drosophila has been used as a model to study interaction with microbes (Ludington and Ja, 2020). This species can be infected by fungi, viruses, protozoans or bacteria (Chandler and James, 2013; Davoodi *et al.*, 2019; Mussabekova *et al.*, 2017). During my thesis, I focused on interactions with bacteria. The fruit fly, like all invertebrates does not have an adaptive immune system and defends itself against all types of infections through its innate immune system (Imler, 2014). This system is based on the production of antimicrobial peptides (AMPs), reactive oxygen species (ROS) and the activity of circulating cells including dedicated phagocytes (Lemaitre and Hoffmann, 2007). The immune response of *Drosophila melanogaster* to pathogenic bacteria (gram + ; gram -) is provided by four signalling cascades: the Toll pathway, the immune deficiency

(IMD) pathway, the c-Jun N-terminal kinase (JNK) pathway and the (Hedgehog) Hh pathway (Buchon *et al.*, 2014; Cohen *et al.*, 2020; Gobert *et al.*, 2003; Kleino and Silverman, 2014; Lemaitre and Hoffmann, 2007).

More precisely, during my PhD thesis, I was interested to study the effect of interactions between Drosophila and symbiotic microbes. Some bacteria strains were shown to not permanently colonize the fly gut, but they rather showed a transient symbiotic interaction, from the food to the gut (Blum *et al.*, 2013; Storelli *et al.*, 2018). However, such transient symbiotic bacteria can influence the biology of their host and in turn these bacteria can be influenced by their host. Also, some strains show a stable colonization allowing them to persist in the gut.

The composition of Drosophila gut microbiota varies between lab-reared flies and wild flies (Miguel-Aliaga *et al.*, 2018; Téfit *et al.*, 2018). Also, the stability and the dynamics of bacteria in the gut was shown to differ between wild and laboratory flies (Obadia *et al.*, 2017). The selection of microbes present in the intestine is influenced by the host diet during its complete development. This raises the question on antifungal or antimicrobial conservatives used in most laboratory to keep the fly food. Drosophila can also influence microbiota with its immune system. AMPs and ROS pathways can kill both symbiotic and pathogenic bacteria indiscriminately (Storelli *et al.*, 2018).

However, studies comparing wild-caught and laboratory fly stocks showed that *Drosophila melanogaster* gut is an environment with a low bacterial diversity (1-30 species). The most commonly found species are members of three major families: *Lactobacillacecae* (e.g. *Lactobacillus*, *Leuconostoc*), *Acetobacteraceae* (e.g. *Acetobacter*, *Gluconobacter*) and *Enterobacteriaceae*. Yeasts such as *Hanseniaspora* or *Saccharomyces* are also found. (Chandler *et al.*, 2011; Newell and Douglas, 2014; Wong *et al.*, 2011). The different parts of the gut host different bacterial strains which may help to maintain microbial diversity (Obadia *et al.*, 2017).

3.2. The impact of gut microbiota on the physiology of Drosophila

3.2.1. Gut microbiota and behaviour

The gut microbiota can modify the feeding behaviour of flies. While Drosophila raised in conventional food showed an appetence for the 6 types of food, seeded or not with bacteria, their highest preference was for food containing *Acetobacter*. The microbial preference of

germ-free flies was dramatically altered. Such flies preferred food with *Lactobacillus* and they showed an increased foraging in unseeded food (Wong *et al.*, 2017). Flies raised in mono-association with *Acetobacter pomorum* or with *Lactobacillus plantarum* showed increased preferences for food seeded with the corresponding bacteria. The feeding behaviour was influenced by their microbiota identity. Food choice assay performed with larvae revealed that the early-life microbial exposure influences host microbial preferences (Wong *et al.*, 2017). In order to understand the preferences for bacteria strains, authors used the PER assay. Their data suggested that olfaction plays an important role in Drosophila microbial preferences and that chemosensory mechanisms underlying taste may play a role for microbe detection (Wong *et al.*, 2017). Drosophila detects and prefers microorganisms growing together in co-culture (*Saccharomyces cerevisiae* and *Acetobacter malorum*) than separate-culture mixture (Fischer *et al.*, 2017). Drosophila fly mutant for ORCO (co-receptor for all olfactory receptor gene products) and OR42b showed a significant reduction in olfactory attraction to the co-culture suggesting that OR42b enables Drosophila to distinguish the co-culture. However, not all microbial strains elicit olfactory attraction.

To further understand the molecular basis of a metabolic cross-feeding relationship, the symbiotic relationship between *Acetobacter pomorum* and *Lactobacillus plantarum* was investigated. In amino acids deficient diet, *Lactobacillus plantarum* produces lactate which is used by *Acetobacter pomorum* (Henriques *et al.*, 2019). The commensal bacteria needs to provide relatively high amounts of dietary isoleucine (amino acids) (between 25 and 50% of the original amounts in the holidic medium) to directly suppress yeast appetite. This result suggests that one or more molecules derived from *Acetobacter pomorum* lactate metabolism can produce amino acids and alters food choice by supressing yeast appetite (protein preference) in Drosophila.

The gut microbiota can also influence its hosts social behaviour. Drosophila KO for the histone demethylase KDM5 gene (*kdm5-/-*) show a reduced social behaviour. Flies deficient in *kdm5* display gut dysbiosis, abnormal social behaviour and aberrant immune activation (IMD pathway) (Chen *et al.*, 2019). These mutant flies showed a different composition of their microbiota compared to the wild type flies. Proteobacteria and *Lactobacillus plantarum* have very low level of expression in *kdm5-/-* mutant flies. By treating germ-free *kdm5* flies or *kdm5-/-* with antibiotic or with *Lactobacillus plantarum*, authors reduced the expression of IMD pathway and partially rescued the intestine permeability, and the defective social behaviour. Loss-of-function in kmd5a, b or c genes were found in human patients suffering of

intellectual disability (ID) or ASD. The data suggest that KMD5 demethylase affects social behaviour through the gut-microbiome brain axis and that *Lactobacillus plantarum* shows a causal relationship between the microbiota composition and social behaviour (Chen *et al.*, 2019).

3.2.2. Gut microbiota and metabolism

Gut microbiota can influence the metabolism, more specifically energy metabolism. A study showed that the removal of gut microbiota decreased mitochondrial activity and adenosine 5'-triphosphate (ATP) levels in the whole-body (Gnainsky *et al.*, 2021). Axenic females recolonized by bacteria or supplemented with riboflavin revealed a clear increase level of mitochondrial activity and ATP production. Riboflavin is a precursor of flavine mononucleotide and flavine adenine dinucleotide (FMN /FAD), the active form of riboflavin required for mitochondrial reactions. More precisely, *Acetobacter* increases the mitochondrial activity of Drosophila by providing FAD^{+}. These authors showed that gut bacteria removal reduced riboflavin levels and decreases the levels of metabolites in the citric acid cycle, glycolysis and electron transport chain pathways. These changes were accompanied by global reduction in ATP. These findings uncovered a bacterial-mitochondrial axis revealing how gut microbiota can impact energy metabolism (Gnainsky *et al.*, 2021; Wong *et al.*, 2014).

Elimination or perturbation of the microbiota can also alter metabolic indices, such as elevated lipid and carbohydrate levels (Ridley *et al.*, 2012). Axenic flies showed high levels of glucose and triglyceride (TAG) compared to axenic flies treated with different *Acetobacteraceae* and *Lactobacillaceae* strains (Newell and Douglas, 2014). These results were observed in another study where TAG and glucose levels were higher in axenic flies (Dobson *et al.*, 2015) compared to flies raised on regular food. Douglas team found out a link between acetic acid and microbial effects on fly TAG and protein content. They quantified the acetic acid content of the flies colonized with different microbial taxa. Three compounds were detected in adults: acetic, butyric and propionic acids which are also the three dominant short chain fatty acids in mammalian intestine (Cummings et al., 2004). This finding suggests that acetic acid is mostly produced by *Acetobacteraceae* and can reduce the TAG levels of flies (McMullen *et al.*, 2020).

3.2.3 Gut microbiota and lifespan

The influence of gut microbiota was also investigated on Drosophila lifespan. Many studies already documented changes in fly lifespan as a result of various factors, including diet, host

genetics, and gut microbiome composition. All combination between *Lactobacillus plantarum, Acetobacter tropicali* and *Acetobacter orientalis* or the use of one of this bacteria can shorten lifespan. Differently, mono-association with *Lactobacillus brevis* or *Acetobacter pasteurianus* had no effect (Gould *et al.*, 2018). This report concluded that the interactions between bacteria can impact Drosophila lifespan. Generally, interactions between bacteria become weaker and even negative when their diversity increases (Gould *et al.*, 2018).

Another study showed that the presence of *Acetobacter aceti* in the gut microbiota increases age-related gut dysfunction and shortens lifespan (Obata *et al.*, 2018). The use of antibiotics killing *Acetobacter*, but not *Lactobacillus*, revealed that *Lactobacilus plantarum* promotes Drosophila longevity.

Dietary conditions can influence microbes' impact on its host physiology. When added on a protein-deficient diet (0.1% yeast extract), microbes such as *Issatchenkia orientalis,* extended fly lifespan by 148% compared to the axenic control. This effect was due to an improved capacity to harvest amino acids in a poor diet. No similar effect on the lifespan was found on highly nutritive diet (0.5% yeast extract) (Yamada *et al.*, 2015). Compared to *Saccharomyces cerevisiae,* only *I. orientalis* consistently induced the greatest benefit to fly lifespan. Therefore, the addition of *I.orientalis* on a highly nutritive diet (5% yeast extract) induced a reduction of longevity (Keebaugh *et al.*, 2019). In conclusion, a single microbial species can be beneficial or deleterious to fly lifespan.

Chapter 3:

Influence of OBPs and microbiota on development and physiological functions (nutrition and reproduction)

1. The impact of microbiota in larval development

The presence and the amount of specific yeasts and bacteria in the diet can affect the development of Drosophila larvae. Drosophila larvae go through three larval instars (L1, L2 and L3) and their body mass increases about 200-fold during this period before reaching the "critical weight" allowing late L3 to undertake their complete metamorphosis (Tennessen and Thummel, 2011).

On a poor-yeast diet (8 g/l), axenic Drosophila larvae show a growth delay of 3 days compared to control larvae (Storelli *et al.*, 2011). No growth difference was observed between axenic and control larvae on a rich-yeast diet (80 g/l). The fungal microbiota significantly lengthened the duration of larval stages.

The fungal microbiota is also beneficial since it allows Drosophila to extract amino acids from a nutrient-poor diet and thus increase the protein flux ingested (Yamada *et al.*, 2015). Moreover, the quality of the yeast provided in the diet of juvenile Drosophila can strongly change the food preference of resulting adults (Grangeteau *et al.*, 2018). Interestingly, the later study revealed that larvae growing on a yeast-deprived diet rarely reach adulthood, but in case they could survive, their life span was greatly extended.

The effects induced by three live yeast species (*Saccharomyces cerevisiae*; *Hanseniaspora uvarum* and *Metschnikowia pulcherrima*) added in the preimaginal diet were compared on Drosophila adult behaviour and fitness (Murgier *et al.*, 2019). *Hanseniaspora uvarum*-rich diet tended to shorten the "egg-to-pupa" period of development while *Metschnikowia pulcherrima*-rich diet induced higher larval lethality compared to other diets. Also, the quality of the juvenile diet affected adult food choice preference and longevity (Murgier *et al.*, 2019).

The production and impact of acetoin, a pheromone-like substance produced as a metabolite by gut microbiota in Drosophila, was investigated in larvae (Farine *et al.*, 2017). A bidirectionnal curve with an earlier increased production of acetoin level (during L1-L2) was followed by an acetoin decrease during L3. This bidirectionnal effect was shown to be linked to microorganisms associated with the egg envelope (chorion; increase) and microbes inside the egg (decrease). Larvae derived from dechorionated eggs produced no, or very little acetoin amounts. However, decreased acetoin level still existed in larvae resulting of dechorionated eggs indicating that internal egg bacteria were still able to metabolize acetoin. While dechorionated-derived larvae showed no response to acetoin-rich food, control larvae

(producing substantial amounts of acetoin) showed a clear preference to acetoin-rich food. Very differently, larvae previously exposed to a high level of acetoin showed a repulsive behaviour against this substance. The presence and activity of microbiota during developmental stages is likely involved in this acetoin "production-preference" response (Farine *et al.*, 2017). The microorganisms involved in such an effect remain unknown.

The larval gut contains stem cells called Adult Midgut Precursor (AMPs) which differentiate into epithelial cells and the adult ISCs during metamorphosis, forming a transitory "pupal gut" that ensures the integrity of the intestinal barrier during metamorphosis. Around adult emergence, adult ISCs become active to establish the adult midgut. The *L.plantarum* bacteria stimulates the production of ROS in enterocytes, which increases the number of the AMPs and intestinal tissue growth. Axenic larvae show an important size variability compared to control larvae (Reedy *et al.*, 2019).

The genome sequencing of *A.pomorum* revealed the presence of 14 genes involved in pyrroloquinoline quinone–dependent alcohol dehydrogenase (PQQ-ADH). *A.pomorum* can modulate insulin/insulin-like growth factor signalling (IIS) in Drosophila. This pathway regulates host homeostatic programs underlying developmental rate, body size, energy metabolism, and intestinal stem cell activity. Larvae colonized with any of the 14 mutant strains showed severe deregulation of development and metabolic homeostasis (Shin *et al.*, 2011).

2. The impact of gut microbiota in reproductive capacity

The gut microbiota of *Drosophila melanogaster* can influence fecundity together with post-mating responses. Both female and male microbiome status influence egg laying (Delbare *et al.*, 2020). Many transcripts differ in abundance between axenic and control virgin females and even a higher number of transcripts is altered after mating. Authors compared transcript abundance between "axenic females mated to axenic males" and "axenic females mated to control males". They found that 136 transcripts showed significant quantitative differences. Male microbiome status did not affect post-mating transcript abundance in control females, but had a major effect on axenic females. This suggests that post-mating changes observed in the female transcriptome are influenced by the male microbiota (Delbare *et al.*, 2020).

Another impact of gut microbiota was observed in Drosophila mating preferences. However, these data remain strongly controversial. Authors argue that antibiotic-treatment decreased fly

mating preference compared to untreated strains (Sharon *et al.*, 2010). They hypothesize that *Lactobacillus plantarum* is a candidate inducing mating preference based on the observation that symbiotic bacteria change the levels of cuticular sex pheromones. However, the number of flies tested in most experiments was far too low to assess any conclusion (n=2-3). Moreover, an independent research group was not able to reproduce these data concluding on an absence of evidence for the mating preference of flies with different microbiome (Leftwich *et al.*, 2017; Selkrig *et al.*, 2018).

Other studies revealed that Drosophila fed on a culture depleted in amino acids and with no/inappropriate microbiome showed a decreased egg laying activity and an increased yeast appetite (Piper *et al.*, 2014). In particular, flies treated with 5 bacteria taxa laid much more eggs than flies raised on a diet without amino acids and and without bacterial pre-treatment (Leitão-Gonçalves *et al.*, 2017). Flies kept on a full holidic diet and pretreated with the five bacteria did not show any increased yeast feeding compared to germ-free controls. The microbiota may suppress yeast appetite.

The reduced fecundity can be rescued by symbiotic bacteria (Delbare *et al.*, 2020; Gnainsky *et al.*, 2021). The gut microbiota can increase mitochondrial activity in axenic flies and this is due to the fact that mitochondrial genes are regulated by *Acetobacter* (Gnainsky *et al.*, 2021). The supplementation of axenic females with *Acetobacter* fully restored oogenesis. The activity of aldehyde dehydrogenase (Aldh) was lower in axenic flies. These results suggest that reduced mitochondrial functions observed in axenic females led to downregulation of ovarian Aldh and that gut microbiota promoted oogenesis restauration (Gnainsky *et al.*, 2021).

Experiments carried out with germ-free flies of both sexes were mono-infected with *A.pomorum* or *L.plantarum*: their mating duration, short term (72h) offspring and offspring body mass were measured (Morimoto *et al.*, 2017). Males infected with *L.plantarum* showed longer mating duration compared to males infected with *A.pomorum*. A tendency on the number of offspring in all mating was seen when at least one fly was infected with *L.plantarum.*

3. The impact of microbiota on OBPs

During the 40 years scientific research on OBPs, the knowledge on their importance in chemoreception has considerably grown together with the diversity of their functions. The primary function of OBPs is too bind, solubilize and transport hydrophobic stimuli to

chemoreceptors across the aqueous sensilla lymph (Rihani *et al.*, 2021). Recently, new insights on OBP involvement into the mechanisms of host-symbiont interactions were discovered. A study already mentioned above revealed that *Wigglesworthia* bacterium regulates the expression of OBP6 in the intestine of intra-uterine region of the tsetse fly larvae (Benoit *et al.*, 2017). This process was shown to be necessary and sufficient to induce the expression of the hematopoietic transcription factor RUNX in flies after cuticular injury.

This is the only insect study linking microbiota and OBPs. Moreover, very few reports dealt with OBPs expressed in the Drosophila gut. This is why our PhD thesis project aimed at unravelling the relationship between microbes, OBP and physiological functions such as nutrition and reproduction in *Drosophila melanogaster*.

Objectives of my PhD thesis

The goal of my PhD thesis was to decipher novel function(s) of taste- and gut-expressed OBPs. This is why I first selected OBPs expressed in the gut and then I checked for their presence in internal reproductive organs. I also investigated the possible impact of microbiota on OBP expression. I focused most of my project on the OBP56d, but for some aspects I also studied OBP56g.

Our strategy consisted to perform analysis at different biological levels using the complementarity offered by a variety of methodologies. We principally used genetics, molecular biology, biochemistry, microbiology, histology and ethology.

In particular, we quantified the mRNA levels in whole flies, or in dissected parts of flies (tagmas or organs). We also used different procedures to compare feeding effect (in flies starved during different periods) or of microbes (in flies raised on antibiotics or on food supplemented with single bacteria species, or with fly guts). We attempted to detect the tissular expression of OBP56d using both *in situ hybridization* and tagged proteins.

We measured the presence of proteins in different genotypes/manipulated flies and performed a proteomic screen on the main gustatory organ of the fly: the proboscis that we compared between the sexes (Publication: Aruçi *et al.*, 2022). We tried (in collaboration with the NCBS laboratory, in Bangaluru, India) to sequence and determine the abundance of bacteria species hosted in the gut or present on the cuticle of differently manipulated flies.

We grew the two OBPs in bacteria heterologous system to obtain enough purified proteins which were tested in biochemical assays. In these assays, performed with a fluorescent competitor, we screened representative compounds of many chemical families. We also performed behavioural tests with adults to measure their copulatory ability, fertility and fecundity.

Materials and Methods

1. Model of study: *Drosophila melanogaster*

A- *Drosophila melanogaster* life cycle

Drosophila melanogaster is an holometabolous insect used as a study model in biology for more than a century. Its short life cycle (**Figure M-1**), the inexpensive aspect of its maintenance and the large number of individuals yielded by each line made it a model of choice for conducting genetic studies. Its genome fully sequenced in 2000 (Adams *et al.*, 2000) identified 13600 genes. The genome segregates on four pairs of chromosomes. In nature, *Drosophila melanogaster* feeds and grows on decaying fruits, and has a close contact with microorganisms. This makes *D. melanogaster* a perfect model to study host-microbiota interactions and mechanisms.

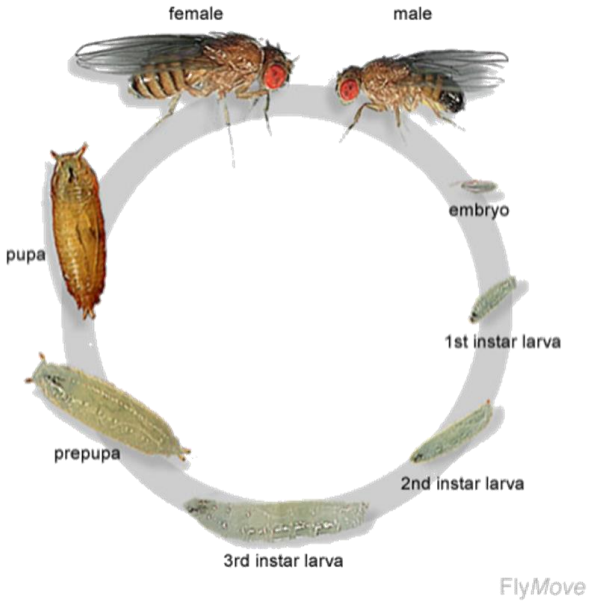

Figure M-1. *Drosophila melanogaster* cycle of life

The complete metamorphosis allows the transition from last larval stage to adult life. Embryonic development is followed by 3 larval cycles, which are mostly growth phases. At 25°C, it takes 4 days for freshly laid eggs to reach the 3rd larval stage. The transition between larval stages is made by a moult. When the third instar larva reaches a sufficient weight, it forms a pupa, inside which the larval structures are degraded and the adult structures develop through metamorphosis (4 days). Adult tissues are formed from cells groups also called imaginal discs. Adults can reproduce 16 hours after emergence. The full developmental cycle (from egg to egg) at 25°C in a non-limiting nutrient environment lasts 12 days (Stocker and Gallant, 2008) (Figure modified from internet site Flymove: http://flymove.uni-muenster.de/).

B- Maintenance

All *D. melanogaster* lines, except those used for the microbiota experiment, were kept in a room at 24 ± 0.5 °C and 65 ± 5% relative humidity with a 12 hours light/dark cycle. Strains were raised on the standard David medium culture (1.5% agar-agar, 10% brewer's yeast, 9% corn flour, 0.4% methyl para-hydroxy-benzoate) ensuring the development of larvae and adults. The transfer of adults in fresh food culture vials every 2-3 days allowed us to expand the stocks and avoid overcrowding. Beside the vials kept at 24 ± 0.5 °C for experiments, a duplicate of each line was maintained at 18 °C as a back-up.

C- Lines tested

The control line used during this project was the *white*^{1118} (*w*$^{-}$) line. This line was used for (*i*) the development of the microbiota experiment, (*ii*) the Quantitative-Polymerase Chain Reaction (q-PCR) experiment, (*iii*) mapping or labelling tissues and (iv) behavioural experiments. We also used the *OBP56d*$^{-}$ mutant. To produce this mutant *(See section 10. OBP56d*$^{-}$ *mutant*), the complete coding region of OBP56d was deleted and the Discosoma Red (DsRed) marker sequence was added in order to screen the flies. Transgenesis was performed by the Bestgene Inc company (California, USA).

D- Eggs and adults' collection for experiments

Eggs were collected from petri dishes sprinkled with agar apple juice. The medium was composed of 800 ml water and 24 g agar. After its sterilization, 26.4 g of sugar, 200 ml of apple juice and 1.6 g of anti-fungal agent were added. The culture was divided into several petri dishes. Every 2 h, petri dishes were replaced with fresh plates. In this way, females were stimulated with the apple juice to lay more eggs to obtain enough eggs in the desired embryonic stage (stages 2 or 3). We used distilled water to collect eggs subsequently used for microbiota manipulation or for transgenesis. For microbiota manipulation, collected eggs were immediately dechorionated.

We were unsuccessful in producing the *OBP56d-LexA mutant*. We wanted to built this transgene to benefit of the binary expression of *LexA/LexAOP* and manipulate the *OBP56d* gene simultaneously to the use of GAL4/UAS transgenes (for co-labelling). We were unsuccessful despite two attempts with Bestgene Inc and our own transgenesis work: we injected 1035 embryos in our laboratory. Briefly, eggs were collected using the same methods

as described above. However, we only obtained a low percentage of surviving larvae and no adult. For this reason and for time limitation reasons, to obtain a complete mutation for the *OBP56d*$^{-}$ coding region, we send material to the Bestgene Inc Company which was successful after several attempts.

We used 4-days old in our molecular biology experiment and 4 to 7-days old in behavioural tests. Flies to be dissected were kept in tubes by groups of 10 under fasting conditions of different durations (0 h, 2 h, 16 h, 30 h) and 16 h L-Phe (16 h of fasting in presence of the L-Phenylalanine amino acid; L-Phe). The latter condition was performed to see whether L-Phe can impact OBP expression. This is based on a previous study showing that OBP19b is necessary for the detection of essentials amino acids, such as L-Phe (Rihani *et al.*, 2019).

More precisely, a cotton was placed in the bottom of an empty glass vial and, depending on the external humidity, we added between 700 µl (high humidity) to 1 ml (low humidity) water. Therefore, flies had only water to drink during their fasting period. Virgin flies subjected to fasting were collected the next morning. Since we also tested mated females and, in this case, we check for copulation to be sure obtaining mated females, kept in similar conditions as described above. For the molecular biology experiments, 10 females and 10 males together were put in each vial and separated two days before dissection.

For behavioural tests see Section *11.1 Preparation of adults flies.*

2. Manipulation of the bacterium microbiota

To generate axenic lines, embryos were dechorionated for 3 min in 3% bleach and then washed for 2 min in 70% ethanol followed by 2 min in distilled water. Dechorionated embryos were placed in vials filled with the medium enriched with the antibiotic mixture. More precisely, standard medium was autoclaved for 21 min at 120 °C, distributed in sterile glass vials closed by cotton plugs and then exposed to ultraviolet radiation for 15 min under the biological safety cabinet (BSC). The antibiotic mixture was added in the food when its temperature cooled down below 50 °C. The antibiotic mixture included the 4 following antibiotics: Tetracycline (50 µg/mL), Streptomycin (100 µg/mL), Rifampicin (200 µg/mL) Ampicillin (50 µg/mL). The mixture of the 3 formers antibiotics was previously tested (Sharon et al., 2010) and Ampicillin was added to cover as broadly as possible the spectrum against anaerobic bacteria. Antibiotic-food vials were constantly kept under the BSC throughout the whole experiment. After two generations spent on antibiotic-rich food, axenic

4 days old flies were used for the quantification of OBP56d and OBP56g mRNA. The absence of bacteria in treated lines was regularly tested by gridding axenic flies in sterile 1x Phosphate-buffered saline (PBS) and spreading 100-200 µL of such suspension on LB (Lysogeny broth) or MRS (Man, Rogosa and Sharpe broth) plates. After 48 hours incubation at 37 °C, the plates were checked to verify for presence/absence of bacterial growth on the media.

To test the effect of individual bacteria species, we separately reinplanted two bacteria species in the axenic medium: *Acetobacter pomorum* (A.*pomorum*) (DSM 11825, LTH 2458) and *Lactobacillus plantarum* (L.*plantarum*) [ATCC; *L.plantarum* 39 (IAM 12477)]. *A.pomorum* was cultivated in reinforced acetic acid ethanol medium (RAE medium; **Annex M.1**) at 30 °C for 48 h with orbital agitation (180 rev.min^{-1}). It was cultured in 200 ml medium using 500 ml flasks. *L.plantarum* was cultivated in 10 ml MRS broth (**Annex M.2**) as a static culture in 14 ml tubes at 37 °C for 24 h. To prepare gnotobiotic flies, vials with sterilised standard medium were inoculated with the desired bacterial species before transferring flies into this food. The number of bacteria added per tube was estimated by flow cytometry (FC) (**Annex M.3**), a technique used to detect and measure physical and chemical characteristics of cell or particle populations. We used the Live/Dead BacLight ^{TM} Bacterial Viability Kit (ThemoFisher Scientific, #L7012) to determine the number of live and dead bacteria by using fluorescent marking. The number of bacteria added per tube was as follows: *A.pomorum* 8.62 x10^{8} bacteria/ml and *L.plantarum* 8.53 x 10^{7} bacteria/ml. More precisely, 1 ml culture with *A.pomorum* or *L.plantarum* inoculates was centrifuged (5000 x g, 10 min). The pellet was washed three times with 1xPBS and the cells re-suspended in 50 µl 1xPBS. The same volume of sterile bacterial media was centrifuged and the PBS obtained after three washes was used as control medium. Fifty microliters of cell suspension were added to each fly culture tube and allowed to dry for 2 h before receiving flies (Henriques *et al.*, 2019). Bacteria counting *via* FC was repeated twice, each assay consisting of 6 biological replicates.

Two additional microbiota manipulations were tested through the transfer of whole guts dissected out of control flies. First, 30 male or female guts were dissected in 1xPBS. Then, they were grinded and 100 µl of the resulting suspension was added in each vial containing sterilised standard medium. Two hours later, axenic flies were transferred in these vials. Our control experiment, consisting of sibling flies kept in standard medium vials, ran in parallel next to the BSC in similar temperature, humidity and light conditions.

3. Microbiome sequencing with 16S RNA

3.1. Dissection of Drosophila samples

Virgin females and males of the control, axenic and mutant lines were dissected. The microbiome either of the whole body or of the whole gut were sequenced by using 16S rRNA. Tissues were dissected in lysis buffer and 6 biological replicates were prepared. Each of them contained 10 fly bodies or guts. This step was prepared in our laboratory while the sequencing part of the experiment was carried out in collaboration with Prof. Deepa Agashe and Dr. Prathibas at NCBS (National Center for Biological Sciences, Bangaluru, India).

3.2. DNA extraction from Drosophila samples

All samples were centrifuged at 10.000 rpm for 10 min. Each tube contained ~1 mL of lysis buffer with 10 bodies or guts. We added 1 mL lysis buffer to ensure that tissues were always immersed in the buffer during the transport between France and India. Then, only ~300 µL of the supernatant with the samples was taken. The samples were gently crushed with a sterile pestle and 20 µL proteinase K was added. All tubes were placed at 56 °C for overnight incubation. The next day, 200 µL of the AL buffer were added and placed at 56. °C for 30 min. Then, the procedure provided by the Qiagen DNEASY blood & tissue kit was followed step by step. Finally, the DNA was eluted by using sterile nuclease free water (30 µL/sample). All the samples were stored at -20 °C until further processing.

3.3. Determining the microbiome in the Drosophila samples

The DNA concentration of samples was quantified with the Qubit 3 fluorometer (Invitrogen, ThermoFisher Scientific Inc.). The V3-V4 region of 16S rRNA was amplified using standard illumina primers (**Table M.1**). The underlined bases indicate the adapter overhang.

Table M.1. Forward and reverse primers for V3-V4 region of 16S rRNA

V3-V4 primers	Sequence
Forward	TCGTCGGCAGCGTCAGATGTGTATAAGAGACAGCCTACGGGNGGCWGCAG
Reverse	GTCTCGTGGGCTCGGAGATGTGTATAAGAGACAGGACTACHVGGGTATCTAATCC

The amplicons were sequenced by using the Illumina Miseq platform (300 x 2 paired end reads). To analyse the dataset, the DADA-2 pipeline was used for extracting the good quality reads and generates an amplicon sequence variant (ASV) table. The primer sequences were trimmed and only reads with ≥ 97% sequence identity were retained. The identification of taxonomy was done by using the Silva reference databases (training set v138).

4. Quantification of OBPs expression in *Drosophila melanogaster*

The thorax was *a priori* considered as the control tissue based on the assumption of a low OBP expression in this body tagma. The head and the gut constituted our experimental tissues where we aimed to quantify the mRNA of OBPs. The expression of the genes of interest was compared with that of two internal housekeeping genes. We performed a preliminary screening of OBPs in Flybase to select those showing an important expression in the gut. Only three OBPs found in Flybase (OBP56g, OBP56d and OBP18a) and one (OBP19b), which was recently studied in our laboratory, were retained for our initial investigation.

Virgin or mated females and virgin males of the control line were dissected. We tested 4 to 6 biological replicates, each one containing pooled dissected tissue from 10-15 individuals. Tissues were dissected in 1xPBS RNA sterilized solution and placed directly in 300 µL Trizol before storage at – 80 °C until RNA extraction.

4.1. Determination of the optimal housekeeping genes

GeNorm software was used to determine the most stable housekeeping genes (reference targets) from a set of tested candidate reference genes in a given sample panel. From this, a gene expression normalization factor was estimated for each sample based on the geometric mean of user-defined number of reference genes. GeNorm is a module integrated in qbase^{+} software for real-time PCR data analysis. For q-PCR, we tested 12 reference targets with different samples representing the conditions. The high reference stability was Tub-3 and MnF (**Figure M-2.B**). The optimal number was always between 2 to 3 regard the conditions we tested (**Figure M-2.A**).

A.

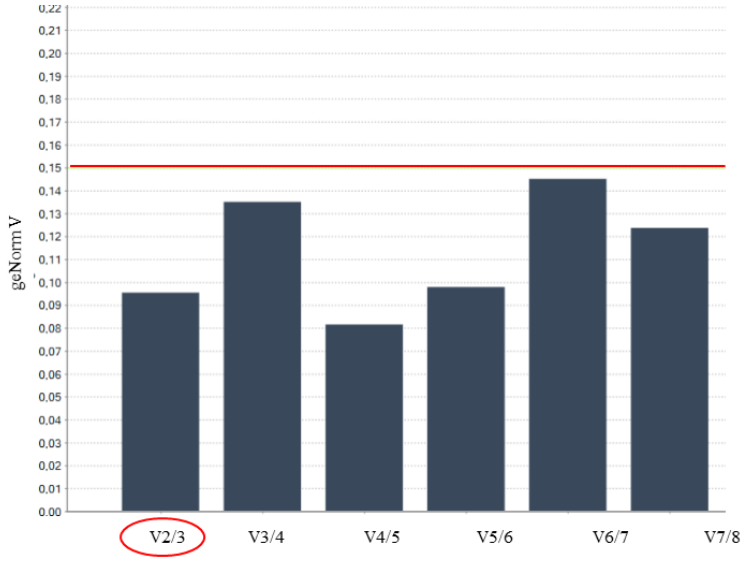

B.

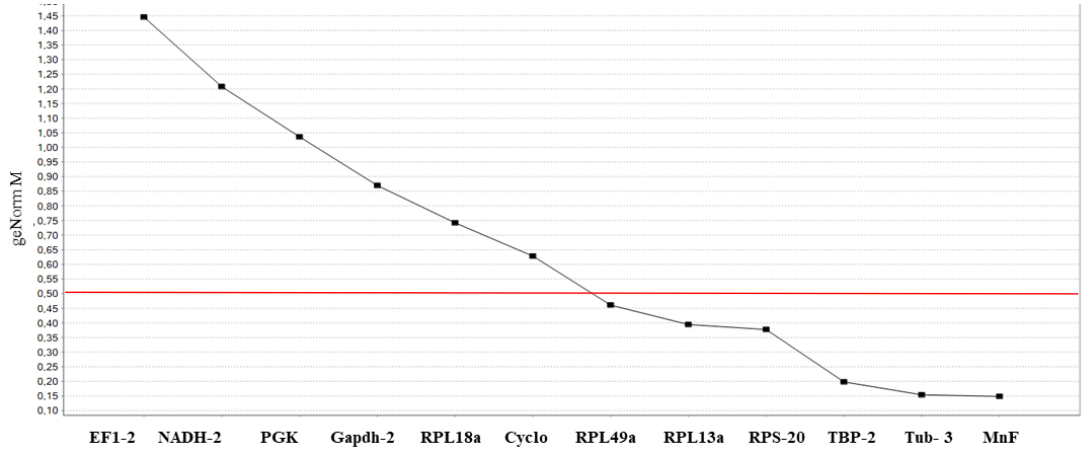

Figure M-2. Determination of the best housekeeping genes for our Rt-qPCR conditions

A) Determination of the optimal number of reference targets. Twelve reference targets were tested. The optimal number of reference targets is 2 (geNorm V<0.15 when comparing a normalization factor based on the 2 or 3 most stable targets). As such, the optimal normalization factor can be calculated as the geometric mean of reference targets Tub-3 and Mnf. B) Average expression stability of housekeeping genes. High reference stability (average geNorm M ≤ 0.5). Twelve candidate reference targets were tested on a total set of 12 samples.

4.2.mRNA expression of OBPs in the gut

The expression of three OBPs (OBP56d, OBP56g and OBP19b) was separately evaluated in the head, thorax and gut. We could not evaluate the expression of OBP18a because the primers used were not specific to OBP18a after testing them on q-PCR plates. Due to the limited time allowed for a PhD thesis in France (3 years), we decided not to not duplicate our attempt with OBP18a.

Flies were kept fasting under different duration to study the impact of nutrition on OBP expression *(see Section 1.D. for collection of flies).* Virgin/mated females and virgin males of the w^{1118} control line were dissected. First, we tested 2 h, 16 h and 16 h L-Phe fasting conditions. Once, OBPs expression was determined in these three groups, our further studies only focused on OBP56g and OBP56d. Two new fasting conditions: “no fasting” and “30 h fasting” were tested in virgin females and virgin males.

The expression level of OBPs was not impacted by fasting duration. For this reason, *in situ* hybridization was performed on flies subjected to 16 h fasting to avoid the autofluorescence of food potentially remaining in the gut.

Based on our preliminary data and to localize more precisely the gut region associated with OBP expression, we dissected the gut of virgin males into three parts: the foregut, midgut and hindgut.

Next, we aimed to obtain an antibody against OBP56d to study the expression of its protein. OBP56d sequence shows similarity with OBP56e and OBP56a sequences. For this reason, the level of expression of each of these OBPs was separately evaluated in the three gut parts. Due to their protein similarity, we determined the best part of the OBP56d sequence for the production of a polyclonal anti-body. However, the Company (ProteoGenix SAS, Schiltigheim, France) was unable to produce such OBP56d anti-body.

4.3.mRNA expression of OBP56d in gustatory appendages

OBP56d expression was measured in the head deprived of its principal sensory appendages (antenna and proboscis with maxillary palps) and in dissected proboscis of virgin females and males of the control line. More precisely, we cut off the head deprived of these appendages to indirectly measure OBP56d expression in the brain. OBP56d expression was also evaluated in female and male proboscis deprived of maxillary palps.

4.4.mRNA expression of OBPs after manipulation of microbiota

OBP56d and OBP56g mRNA expression was measured in flies raised on standard medium and in axenic culture. This experiment was triplicated for OBP56d and duplicated for OBP56g. This allowed us to evaluate how the (quasi total) absence of bacteria could affect OBPs expression. We also compared axenic virgin females and males resulting of four microbiota manipulations: (1) axenic culture enriched with *A.pomorum*, (2) axenic culture enriched with *L.plantarum*, (3) sterilized standard culture enriched with control female guts or (4) sterilized standard culture enriched with control male guts. This experiment was only preformed one time.

4.5.RNA extraction

Tubes containing tissues suspended in 300 µL of Trizol were defrosted on ice. Two to three beads (2.00 mm RNAse free Zirconium Oxide Beads, NextAdvance) were added in the tubes which were placed in the TissueLyser (Qiagen) (3min x 30sec at 30 Hz) to lyse all tissues and cells. The samples were then incubated at room temperature for 5min to allow the separation of total RNA. A volume of 50 µL BCP (1-bromo-3-chloropropane, Sigma) was added to the homogenate and mixed several times for 10min at room temperature.

A first centrifugation at 12,000 g for 15 min at 4 °C allowed us to separate the organic and aqueous phases. The supernatant containing the RNA was transferred to a new tube and precipitated with 250 µL isopropanol before incubation at room temperature for 7 min. Samples were centrifuged at 16,000 g for 10 min at 4 °C and the resulting pellet was washed twice with 500 µL 75% ethanol and each time centrifuged at 16,000 g for 3 min at 4 °C. The pellet was air-dried and re-suspended in RNAse-free water.

4.6.Quantification of RNA by spectrophotometry

RNA concentration was measured by spectrophotometry (UV/Vis spectrometry, SPECTROstar microplate reader from BMG LABTECH). The OD260/280 and OD260/230 ratios are used to assess the purity of the RNAs. The samples are considered pure if the OD260/280 ratio is comprised between 1.8 and 2.0. Below 1.8 value, the samples may be contaminated and were therefore discarded. The OD260/230 ratio which is an indicator of phenolic contamination can be used as a secondary measure of RNA purity. RNA with a 2.0 – 2.2 ratio was considered pure. The quality of total RNA was evaluated by electrophoresis with 1% agarose gel. Samples were stored at – 80 °C.

4.7.Reverse transcription (RT)

The reverse transcription reaction consists of making complementary DNA (cDNA) from mRNA by reverse transcriptase (RTase). One µg RNA was digested by DNAse I enzyme with DNAse buffer for 30 min at 37 °C followed by 10 min at 65 °C where 1 µl EDTA was added. This step allowed us to digest the genomic contaminants of the DNA as well as to stop the enzymatic DNAse reaction. The iScript™ Reverse Transcription Supermix Kit and protocol were used for reverse transcription experiment. The reaction mix contained 10 µL total RNA (500 ng of digested RNA), 4 µL RT buffer (5X) and 1 µL Reverse Transcriptase iScript enzyme. The reverse transcriptase program consisted of the 3 following steps: (1) Priming (5 min at 25 °C), (2) Reverse transcription (20 min at 46 °C) and (3) Reverse transcription inactivation (1 min at 95 °C).

4.8. Determination of control housekeeping genes by using GeNorm method

GeNorm is a method of choice for high-throughput and accurate expression profiling of selected genes. It identifies the most stable control genes expressed in a given set of tissues. It also allowed us to determine the minimum number of genes required to obtain a reliable normalization factor (Vandesompele *et al.*, 2002). We evaluated 10 housekeeping genes from different abundance and functional classes in various Drosophila tissues (**Table M.2**). Their ranking was determined according to expression stability and a gene expression normalization factor was calculated for each sample based on the geometric mean of a defined number by the use of control genes. The optimal number of control genes for the given samples was determined *via* the gene expression normalization factor (geNorm V<0.15).

Table M.2. List of potential housekeeping genes for different tissues in *D. melanogaster*

Housekeeping genes	Forward (5'-3')	Reverse (5'-3')
EF 1	GAT-CTT-CTC-CTT-GCC-CAT-CC	GCG-TGG-GTT-TGT-GAT-CAG-TT
NADH	GCC-CGT-ATC-AAG-TAC-TGC-CA	AAA-CCC-TCT-AGA-TGC-CCT-GG
PGK	CGA-GAA-ACT-GGT-GGA-GAA-GG	CGA-AGT-TGG-GGA-ACT-CAA-AG
TBP	TGC-AGA-GTT-ACC-AGC-CAT-CG	CGT-CTG-GTG-GAT-GTT-GCT-CA
RPL 18a	GCA-AGC-CAG-CAC-TGA-ATA-CG	TGC-TGG-CAC-TCA-GGA-TGG-TT
Tub 3	TGT-CGC-GTG-TGA-AAC-ACT-TC	AGC-AGT-AGA-GCT-CCC-AGC-AG
RPL 49a	CCC-AAG-GGT-ATC-GAC-AAC-AG	GTT-CGA-TCC-GTA-ACC-GAT-GT
Cyclo	GTC-GCT-GTG-ATT-CGT-AGT	GAG-ACT-GCT-GAA-CAA-TGC
MnF	GAG-CAG-AAG-ACC-CCC-TAC-CT	AAT-GAA-ACC-CTG-ACG-TGG-AC
Actine	TCC-AGT-CAT-TCC-TTT-CAA-ACC	CAA-ATT-CAA-GGC-GTG-AAA-ACT

4.9. Quantitative-polymerase chain reaction (q-PCR)

Quantitative PCR (q-PCR) is an *in vitro* method that allowed us to determine the relative quantity of the mRNA level of a target gene compared to that of a control gene. After producing the cDNA from the mRNA reverse transcription reaction, a specific nucleotide sequence was amplified using a pair of primers flanking the target region. q-PCR allowed us to determine a threshold cycle (Ct: cycle threshold) for which the PCR product reached a given quantity. A fluorophore (Low ROX SYBR Green MasterMix dTTP blue, Eurogentec) was used: its signal proportionally increased with the quantity of amplified product during the reaction.

The q-PCR reaction kit contains a mixture of 5 µL Takyon Low ROX SYBR MasterMix dTTP blue, 4 µL cDNA mixture diluted to $1/10^{th}$ and 1 µL Primer Forward and Primer Reverse diluted to $1/40^{th}$. The expression of the different OBPs was tested (**Table M.3**). We used the QuantStudio Real-Time PCR software v1.2, Thermofisher which allowed us to quantify the transcript level for each OBP gene of interest.

The q-PCR program is composed of four steps: (i) polymerase activation (3 min at 95 °C), (ii) denaturation (40 cycles, 10 sec at 95 °C), (ii) hybridization/elongation (40 cycles, 30 sec at 60 °C), (iii) new denaturation cycle (15 sec at 95 °C), (iii) one cycle (1 min at 60 °C). At the end, a melting curve was produced providing us with the possibility to verify that a single product has indeed been amplified. For each condition, 4 to 6 biological replicates were used and each sample was deposited in technical duplicates. Negative controls without cDNA or primers were also deposited on the same plate. To calculate the PCR efficiency, a $1/10^{th}$ cascade dilution range was performed at 4 points from a cDNA mixture. The undiluted sample was composed of a mixture of equivalent amounts of all the cDNAs which were used for the experiment. A value close to 2 is an optimal efficiency for PCR. Plates with 384 wells were used to do simultaneously many measurements and thus reduce the plate bias factor.

Table M.3. List of forward and reverse primers of OBPs used for q-PCR

OBPs	Forward (5'-3')	Reverse (5'-3')
OBP19b	CAC-GAG-ACC-AAG-TGC-TTC-C	CTC-GTT-ATA-CTG-CAA-CTG-ATC-CTC
OBP56d	TCT-ACC-GAA-AAT-GAA-GTT-CCT-GAT	CAT-CGG-ATA-GTT-GCA-GCT-CAG
OBP18a	CGA-GGA-TCT-CAA-GAG-GAC-CA	AGA-TTG-GTG-ACG-CCA-TCG
OBP56a	CCC-CAA-CGT-TCT-AAC-AAG-TCA	TCG-CTC-AGA-TTA-AGG-GAC-GA
OBP56g	CTG-CCT-TTC-AGG-AAT-TTT-GG	CCG-TTC-TTC-TTG-AGG-CAA-T
OBP49a	GTC-ATC-ATC-ATC-CGC-ATC-C	CCG-GTT-TTG-ATA-GAT-TCC-AGT-T
OBP56e	TGC-AGC-TCT-ATC-TTT-GGC-ATC	GGC-CTT-GGC-TCT-CTG-CTT
OBP57b	AGG-CTC-CCG-AAG-AAC-TTT-GT	GGA-TGG-CCA-GCC-TTA-AAT-G
OBP57e	TTC-TGT-GCG-CAA-ATG-TTC-TC	TGG-CCA-ATT-CTC-CAT-CAC-TT
OPB69a	GTC-AGT-TCA-TGT-GGA-ACT-CAG-AA	GCA-CTT-GAC-GGT-TTC-ATA-AGC

5. *In situ* hybridization on the gut, proboscis and reproductive organs *in toto*

5.1. General principle of *in situ* hybridization

The localization of OBP56d in the gut was investigated by using *in situ* hybridization (HIS). HIS is a method that allowed us to localize a specific single-stranded target nucleic sequence on a histological section of tissue or isolated cells. This technique is based on the complementarity of nucleic bases. The complementary sequence to the target is called "probe". The probe can be labelled either with a radioactive isotope, with an enzyme or with a fluorescent substance, permitting its easy detection to localise a DNA or RNA molecule, the double-stranded sequence, in the case of DNA, should be denatured to obtain a single strand. The next step consists to choose a complementary probe to target the sequence and label the probe to visualize the labelled tissue. After the revelation of the probe, the labelling highlights the location of the desired target within an entire organism, a set of cells, in a cell compartment or on a specific chromosome.

5.2. Preparation of forward and reverse OBP56d probe

5.2.1. Polymerase chain reaction (PCR)

Two pairs of primers used for OBP56d were designed and tested by a simple polymerase chain reaction (PCR) at 60 °C on the cDNA extracted from the gut. The cDNA was mixed with the reactive solution (20 mM Tris-HCl pH 8.4; 50 mM KCl; 3 mM $MgCl_2$) supplemented with 4 dNTPs, specific primers and 1U of Taq Polymerase. The cDNA was

denatured for 2 minutes at 95 °C followed by three others steps: (i) denaturation (30 sec, 95 °C), (ii) hybridization of the primers (30 seconds, at the Tm of the oligonucleotides) and (iii) polymerization (30 seconds at 72 °C). This cycle was repeated 35 times. The reaction was terminated with an extension step of 5 minutes at 72 °C. After passage on agarose gel, the primer pair OBP56d his-1 was kept for the rest of the experiment (**Table M.4**).

Table M.4. Forward and reverse OBP56d his-1 probe primers

OBP56d his-1	Sequence
Forward	AGT-TCC-TGA-TTG-TCC-TCT-CCG
Reverse	GAT-TTG-GCG-CTT-AGA-TGT-GGG

5.2.2. Insert purification

The amplified fragment was purified using the Wizard SV Gel α PCR Clean up system kit (Promega) to eliminate the template and the primers. The mixture was filtered by centrifugation on a column that absorbs DNA at high ionic strength (KI>4 M). After two washes with ethanol, the insert was eluted with 50 µL of ultrapure water and quantified by spectrophotometry (1 unit of OD at 260 nm is equivalent to 50 µg of DNA/mL).

5.2.3. Use of the pGEM-T Easy expression vector

The purified insert was introduced into pGEM-T Easy vector (**Figure M-3**) by a T4 DNA ligase (pGEM-T Easy Vector Systems, Promega). The preparation of a 10 µL-reaction mixture contains 3 U T4 DNA ligase (3 U/µL), 5 µL of 2X Rapid Ligation Buffer (60 mM Tris-HCl pH 7.8; 20 mM $MgCl_2$; 20 mM DTT; 2 mM ATP; 10% polyethylene glycol (v /v)), 50 ng pGEM-T Easy vector and the insert to be ligated. It was left overnight at 4 °C with an 3/1 insert/vector molar ratio.

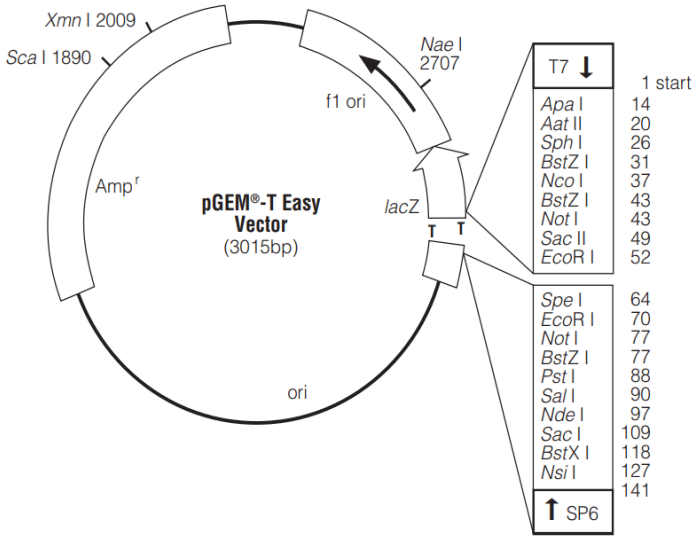

Figure M-3. Plasmid map of pGEM-T Easy vector

T7: T7 promoter; SP6: SP6 promoter; Ampicillin: ampicillin resistance gene; lac z: start codon; lac ori: lac operator; f1 ori: phage f1 region; T: multiple cloning site with restriction sites shown above (Promega 2000-2013, USA).

5.2.4. Bacterial transformation

A bacterial transformation was carried out with cells of the DH5α competent strain. The ligation products were added to 100 µL DH5α competent cells and incubated for 30 min on ice. After a heat shock (42 °C for 45 sec), transformed cells were returned on ice for 3 min, then incubated at 37 °C for 30 min in 800 µL LB and cultured on solid medium (LB/Agar 15 g/L; Ampicillin 100 µg/mL) for 16 h at 37 °C.

5.2.5. Analysis of clones and identification of probes

Recombinant bacteria were cultured (16 h, 37 °C, 180 rpm) in 5 mL LB supplemented with ampicillin (100 µg/mL). The DNA plasmid of the subclones was extracted and purified by a Miniprep *via* Wizard Plus SV Minipreps DNA purification system (Promega).

The quality of the subcloning procedure was checked by digesting the DNA of the subclones with *EcoRI*, the restriction sites of which are found on both sides of the insertion site. Then the clones containing the insert were digested by *NcoI* and *SpeI* and sent (50 – 100 ng) for sequencing by the Eurofins MWG Operon Company to ensure the integrity of the sequences and determine the insert orientation.

5.2.6. Labelling of RNA probes (riboprobes)

Labelling both the forward and reverse probes was carried out by *in vitro* transcription according to the procedure provided by the Roche kit (Dig RNA labelling kit, Roche). Once synthesized, digoxigenin-labelled riboprobes were measured by spectrophotometry at 260 nm and analysed on a 1% agarose gel.

5.3. Gut, reproductive organs and proboscis labelling procedures

i. **Dissection:** Before dissecting, flies were kept fasting for 16 h to avoid the auto-fluorescence of food remaining in the gut. Dissection of the gut and reproductive organs was performed on the sterilized solution 1X PBS. The proboscis was dissected in 1 X PBS; 0,03% Triton X-100 solution; Labellum were pierced with a minute needle.

ii. **Fixation of the gut and reproductive organs:** Tissues were fixed in PFA4%/1X PBS; 0.03% Triton X-100 for 45 min at room temperature then washed for 5 min in 1X PBS 0.03% Triton X-100 at room temperature. Tissues were then incubated for 10 min in 0.2M HCl 0.03% Triton X-100 and washed for 5 min in 1X PBS 1% Triton X-100.

Fixation of the proboscis: Tissues were fixed in PFA 4%/Na_2CO_3 0.1M pH 9.5 0.03% Triton X-100 over night (~16 h). We pierced the labellum to allow a better penetration of the solution inside tissues. The next day, tissues were washed for 5 min in 1X PBS 0.03% Triton X-100 at room temperature. Then, tissues were incubated for 10 min in 0.2 M HCL 0.03% Triton X-100 and washed for 5 min in 1X PBS 1% Triton X-100.

iii. **Pre-hybridization:** The pre-hybridization buffer was added and left for at least 5 h at 55°C to block all non-specific sites. The pre-hybridization buffer was composed of: 50% deionized formamide, SSC (Saline-sodium citrate) X4, Denhardts 5X, tRNA at 0.25 mg/ml, Heparin 0.05 mg/ml, Tween 0.1% and water.

iv. **Hybridization:** At the end of the pre-hybridization, the hybridization buffer was added. It had the same composition as the pre-hybridization buffer except that both the forward and reverse probes were added with a 1 µg/ml final concentration for 16 h at 55°C. The next day, these tissues were washed with SSC 0.1X 0.03% Triton X-100 for 4 X 15 min at 60°C to remove non-specific RNA-RNA hybrids and non-hybridized probes and they were washed for 10 min with 1X PBS 0.03% Triton X-100.

v. **Immunodetection:** Tissues were incubated in a blocking solution (Blocking Reagent from the Tyramide signal amplification kit) at 1% in PBS 0.03% Triton X-100 for 5 h at room temperature. Next, they were incubated with an antibody directed against digoxigenin coupled with a peroxidase (anti-Dig-HRP) diluted to 1/100 in the blocking solution for 48 h at 4°C. Anti-Dig antibody can detect anti-sense mRNA/riboprobe complexes.

vi. **Amplification:** In order to amplify the signal detected by the anti-Digoxigenin antibody, tissues were incubated in a solution containing Tyramide-CF488a molecules (Tyramide amplification kit from BIOTIUM) diluted to 1/2000 in Tyramide amplification Buffer Plus for 1 h away from light at room temperature. A peroxidase molecule coupled to the anti-Dig antibody can bind several tyramide molecules coupled to the CF488 fluorochrome allowing signal amplification. The tissues were again washed with PBT for 5×10 min and then mounted between slide and cover slip in a Vectashield H-1200 + Dapi (Vector) mounting medium.

Labelled tissues were visualized under a Leica SP8 laser scanning confocal microscope. Resulting images were analysed with the ImageJ software (Software, NIH, Bethesda, MD, USA).

The OBP56d-Flag transgenic line was obtained (Bestgene Inc company) for immunolabeling experiment. This transgene was supposed to indicate the expression of the OBP56d protein in the fly tissues. Even though, the insertion of tag flag was checked, the line did not work properly. Data obtained are not shown in the present thesis report given that experiments performed both on the control and the transgenic lines showed similar labelling. Thus, we were unsuccessful to determine the tissular localisation of the OBP56d protein.

6. Recombinant protein expression of OBPs in *E.coli* M15 bacteria

6.1. General principle of OBP56d and OBP56g proteins production

Both OBP56d or OBP56g proteins were produced as recombinant forms using the bacterium *Escherichia coli* (*E. coli*) as a heterologous expression system. The complementary DNA (cDNA) encoding the protein was inserted into the pQE31 plasmid and introduced into thermocompetent *E.coli* cells. For this, embrittlement by chemical treatment was carried out at the level of the membrane of the bacteria in order to create pores facilitating the entry of the

plasmid into the cells during the heat shock. During this “transformation” phase, the bacteria with the plasmid integrated will multiply. The overproduction of recombinant proteins can be toxic for bacteria. For this reason, the expression of the recombinant protein was suppressed during an early step to promote a “healthy” bacterial growth. The concentration of bacteria in the culture medium was estimated by spectrophotometry at 600 nm (OD600 nm). Once the optical density at 600 nm reached a value between 0.5 and 0.7, a chemical inducer, isopropyl β-D-1-thiogalactopyranoside (IPTG), was added to the culture medium. IPTG binds the protein called "lac repressor" which suppressed the expression of OBP56d or OBP56g by binding to the promoter site. The RNA polymerase of *E.coli*, an enzyme that polymerizes RNA molecules by reading DNA was then recognized by the promoter site, which triggered protein expression. At the end of production, the soluble protein was extracted from the lysed cells. The lysate supernatant was then loaded onto a suitable affinity chromatography column to purify the desired protein.

6.2.Culture media

The super optimal broth medium with catabolic repression (SOC) was used during the bacterial transformation phase. The Luria broth (LB) culture medium consists of 10 g/L of tryptone, 5 g/L of yeast extract and 10 g/L of sodium chloride with a pH adjusted to 7.2 with sodium hydroxide. This medium was used during the preculture phase. The agar medium was obtained by adding 15 g of agar per LB liter. This medium was used for petri dishes preparation. The terrific broth (TB) culture medium consists of 12 g/L of tryptone, 24 g/L of yeast extract, 9.4 g/L of dipotassium hydrogen phosphate (K_2HPO_4) and 2.2 g/L of dipotassium hydrogen phosphate (KH_2PO_4). This richer medium was used during the culture given that it allows an optimal production of OBP56d and OBP56g.

6.3. Vector expression

The pQE31-rOBP3 plasmid (**Figure M-4**) was used for the construction of the pQE31-OBP56d plasmid or of pQE31-OBP56g. The rOBP3 protein coding sequence was replaced by the OBP56d or OBP56g coding sequence fused to a 6-histidines tag located at the N-terminus.

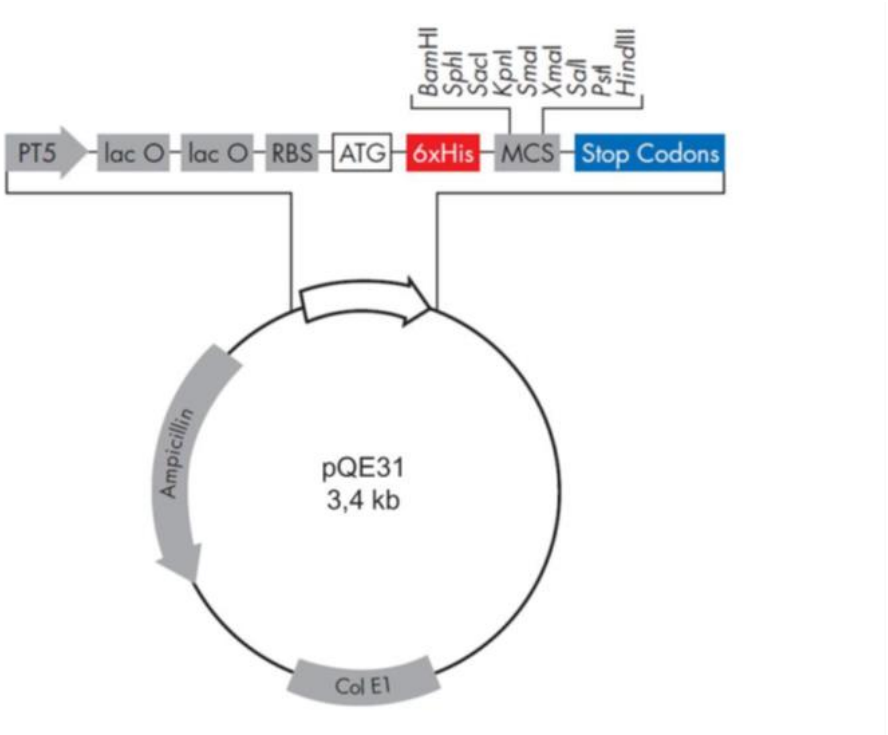

Figure M-4. The map of pQE-31 vector used for the insertion of OBP56d or OBP56g coding region.

PT5: promoter T5, lac O: lac operator, RBS: ribosome-binding site, ATG: start codon, 6xHis: tag sequence of 6 histidine, MCS: multiple cloning site restriction, Stop Codons, Col E1: origin replication of Col E1, Ampicillin: ampicillin gene resistance. (Source: The QIA expressionist).

The construction of the pQE31-OBP56d/56g plasmid was carried out by inserting the DNA sequence coding for OBP56d/56g at the level of the *BamHI* and *HindIII* restriction sites of the pQE31 vector. Below we show, as an example, the OBP56d coding sequence (**Figure M-5**).

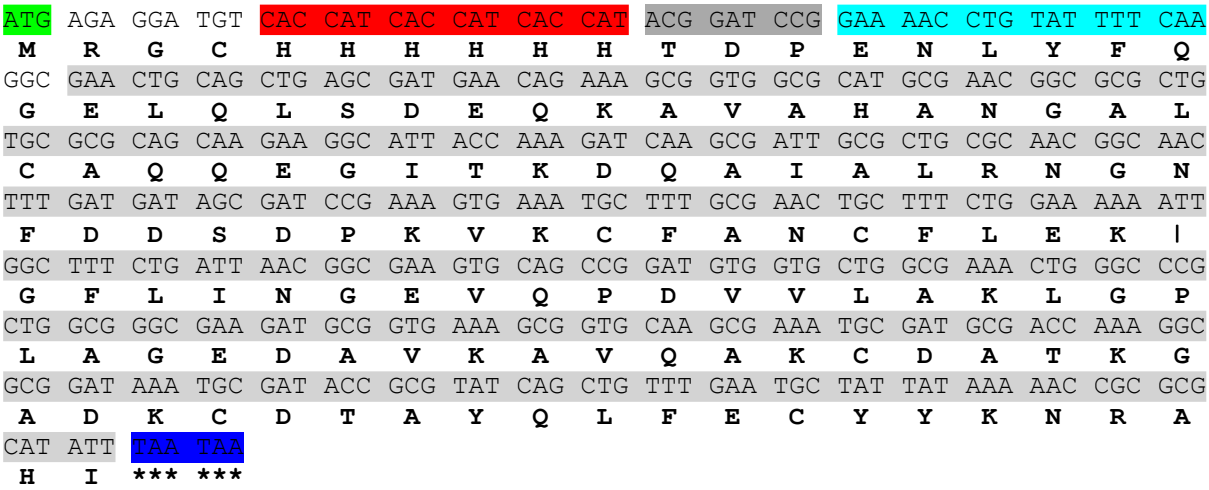

Figure M-5. The OBP56d coding sequence

The amino acid sequence of the recombinant OBP56d protein is shown in capital letters with the corresponding protein sequence at the bottom. The initiation codon (ATG) is highlighted in green, the BamHI restriction site in dark grey, the cleavage site called “TEV protease” is highlighted in light blue, the nucleic sequence encoding the 6-histidine tag in red and the DNA sequences encoding OBP56d inserted into the vector in grey. Stars indicate the stop codon. The code used to indicate the protein sequence is the one-letter code specified by the IUPAC - IUBMB Joint Nomenclature Committee.

6.4. Bacteria transformation

One µL plasmid at 20 ng/µL was brought into contact with 20 µL of heat-competent *E. coli* M15 bacteria previously thawed on ice. This cell suspension was incubated for 20 min on ice and placed 40 sec in a water bath at 42 °C, then immediately it was returned on ice for 5 min. A volume of 250 µL of SOC medium (Invitrogen, **Annex M.4**) was then added to the cells. The mixture was then incubated for 1 h at 37 °C and shaked at 200 rpm, then 5 µL, 20 µL and 150 µL of the solution were spread on a LB agar medium supplemented with the ampicillin antibiotic at 100 µg/mL final and kanamycin at 25 µg/mL final. Petri dishes were incubated for 24 h at 37 °C.

6.5. Recombinant protein expression

A preculture of 25 mL liquid LB supplemented with kanamycin (25 µg/mL final) and ampicillin (100 µg/mL final) antibiotics was inoculated with a colony from the transformation step described above and incubated overnight at 37 °C under stirring at 220 rpm. One litter of the TB medium was inoculated with 20 mL of the preculture. When the OD600 nm reached a

value between 0.4 and 0.5, a final 0.2 mM of IPTG was added and the culture was placed at 30 °C. After 6 h incubation, the culture was stopped and then centrifuged at 4200 g for 20 min at 4 °C. The pellet was resuspended with 30 mL of lysis buffer (50 mM sodium phosphate, 300 mM NaCl and 20 mM Imidazole pH 7.5) then frozen at -20 °C

6.6. Purification by affinity chromatography on HisTrap™ HP 1 mL (Ni-nitriacetic agarose acid)

The cell suspension obtained at the end of the previous step was subjected to ultrasound for 2 min on ice with 5 sec pulses every 3 sec at 60 W (2 repetitions). The soluble fraction was separated from cell debris and inclusion bodies by centrifugation at 20,000 g for 45 min at 4 °C. The supernatant was collected and filtered (1.2 µm and 0.45 µm porosity filter) then loaded onto a 1mL HisTrap™HP column (GE Healthcare) equilibrated with 5 mL of a buffer composed of 50 mM sodium phosphate, 300 mM of NaCl and 20 mM of imidazole at pH 7.5 (buffer A), then 5 mL of the same buffer but containing 500 mM of imidazole at pH 7.5 (buffer A) and finally 10 mL of the first buffer (**Figure M-6**). The equilibration and loading were performed in a fume cupboard using a peristaltic pump with a column flow rate of 1 mL/min. After loading the protein on the loop column for at least 1 h, successive washes in 50 mM ammonium acetate buffer supplemented with 20% ethanol and 30% acetonitrile were carried out to clean the protein (Brulé *et al.*, 2020). The protein was eluted on Akta Prime with a 20 mL linear gradient ranging from 20 mM to 500 mM imidazole (in buffer of 50 mM sodium phosphate, 300 mM NaCl, pH 7.5). The protein was dialyzed in 6-8 kDa bags twice against 100 mM phosphate buffer pH 7.5 supplemented with 5% acetonitrile and then twice against 100 mM phosphate buffer pH 7.5 lacking acetonitrile. Each dialysis was carried out for at least 2 hours at 4 °C in 500 mL buffer. The protein was then aliquoted in 4 mL portions and stored at -20°C. The protein concentration was determined by UV-visible absorption spectrophotometry using its molar extinction coefficient at 280 nm (ε280 OBP56d = 6.335 $M^{-1}.cm^{-1}$; ε280 OBP56g = 2.980 $M^{-1}.cm^{-1}$) and its molecular mass (M OBP56d= 14.884 kDa; M OBP56g= 13.646 kDa).

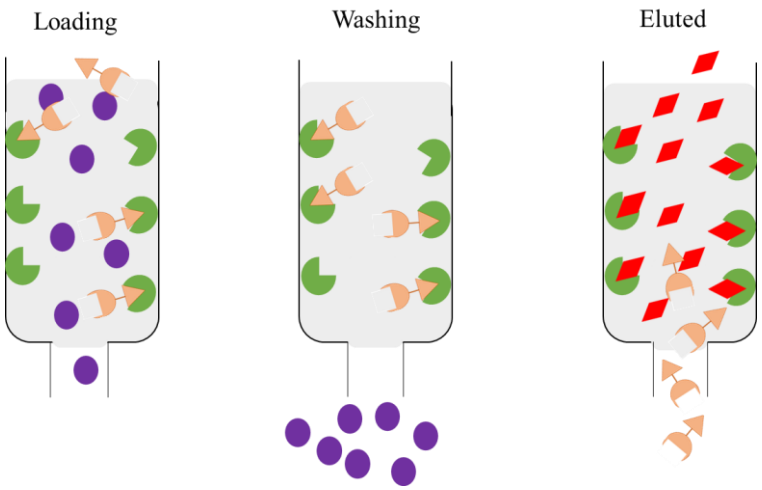

Figure M-6. Principle of the purification of a recombinant protein by affinity chromatography

The supernatant containing the recombinant protein and the impurities is loaded into a chromatographic column containing a functionalized resin. The recombinant protein, which was produced with a tag binds specifically to the column. The resin was then washed with the buffer to remove impurities. The protein was then eluted by the addition of a competing agent which in turn bind to the column.

6.7. Electrophoresis of peptides on polyacrylamide gel in the presence of sodium dodecyl sulphate (SDS-PAGE)

6.7.1. General principle of electrophoresis SDS-PAGE

The samples to be analysed were deposited in the wells of a polyacrylamide gel subjected to an electric field. The migration of proteins depends on many parameters: their size, shape, and charge, the strength of the electric field, the temperature of the system, the pH, the type of ions presents and the buffer concentration. The mesh of the polymer gel makes it possible to discriminate the proteins according to their volume, which itself depends on their size and their folding: the larger the proteins are, the more difficult they move in the gel and therefore the slower is their migration speed. The protein charge defines the direction of migration: negatively charged proteins migrate towards the cathode (+) while positively charged proteins

migrate towards the anode (-). The sodium dodecyl sulphate (SDS) is a strong ionic detergent. It is added to the protein deposition solution and to the polyacrylamide gel to perform so-called SDS-PAGE electrophoresis. SDS molecules bind to proteins non-covalently with a constant ratio of 1.4 g of SDS to 1 g of protein. Since SDS is negatively charged, the overall charge of the proteins on which it binds becomes negative and their charge to mass ratio is identical, with the SDS masking the intrinsic charges of the protein to be analysed. In addition, SDS denatures proteins which are in the shape of fully unfolded chains instead of adopting a tertiary structure. Their migration rate then depends essentially on their size, which permit to measure their molecular mass. At the end of the electrophoresis, the acrylamide gel is immersed in a solution containing Coomassie blue, a protein-specific dye. After rinsing the gel and fixing the proteins, the proteins are revealed in the form of blue bands.

6.7.2. Analyse SDS-PAGE protocol

In order to detect the presence of OBP56d and OBP56g and to control their purity, during purification, a sample was taken from the following fractions: the supernatant before loading onto the column, the fraction not retained and the elution fractions. The separation gel was composed of 14% acrylamide, 8.75 mL 40% bis-acrylamide, 6.25 mL 1.5 M Tris-HCl at pH 9, 0.1% SDS, TEMED 0.2% and 0.1% ammonium persulfate and 9.5 mL water. The concentrating gel was composed of 14% acrylamide, 1.25 mL 40% bis-acrylamide, 2.5 mL 0.5 M Tris-HCl at pH 9, 0.1% SDS, TEMED 0.15 % and 0.1% ammonium persulfate and 6.05 mL water. Migration was performed using TGS buffer (25 mM Tris, 192 mM Glycine, 0.1% SDS, pH 8.3). The “Precision plus protein Dual Xtra” marker (BioRad) was used as a molecular weight marker. The migration was carried out for 40 min at 90 mA at a 200 V voltage regulated with an ST 606 600 V-600 mA generator (Amilabo). The gel was rinsed with distilled water, then stained with Bio-SafeTM Coomassie (Bio-Rad) for 1 hour until band revelation. The gel was then washed with distilled water for 1 hour. Gels were imaged using the ChemiDoc XRS gel analyser (Bio-Rad) coupled with Image Lab software.

7. Biophysical analysis: Circular dichroism for OBP56d

7.1. Circular dichroism principle

Circular dichroism (CD) spectroscopy is a form of light absorption spectroscopy that measures the difference in absorbance of left-handed (L) and right-handed (R) circularly polarized light ($\Delta A = AL – AR$). Briefly, if the two components are not absorbed or absorbed

to equal extents, a radiation polarised in the original plane is generated. An elliptically polarised radiation occurs if (L) and (R) are absorbed to different extents (**Figure M-7**). CD is an effective method for rapidly evaluate protein secondary structure, folding and binding properties (Greenfield, 2006). Folded proteins generate highly asymmetrical secondary structural elements such as α-helix, β-sheet that have characteristic CD spectra. α-helical proteins have negative bands at 222 nm and 208 nm and a positive band at 193 nm. Proteins with well-defined antiparallel β-pleated sheets (β-helices) show negative bands at 218 nm and positive bands at 195 nm, while disordered proteins show very low ellipticity above 210 nm and negative bands near 195 nm (Kelly et al., 2005). Since secondary structures are sensitive to their environment (temperature or pH), circular dichroism allowed us to follow secondary structure changes according to the variation of environmental conditions or after protein interaction with other molecules. The far-UV CD bands of proteins (between 180 to 260 nm) derive primarily from the peptide bonds and reflect the secondary structure of the protein, whereas the chirality of aromatic amino acids is measured in the near-UV. The absorbance difference ΔA measured by the spectropolarimeter is usually converted to molar ellipticity (deg.cm^2.dmol^{-1}): [θ] = 100 x θ / (m x d); θ is the ellipticity degree, m is the molar concentration and d is the pathlength (cm) (Kelly *et al.*, 2005).

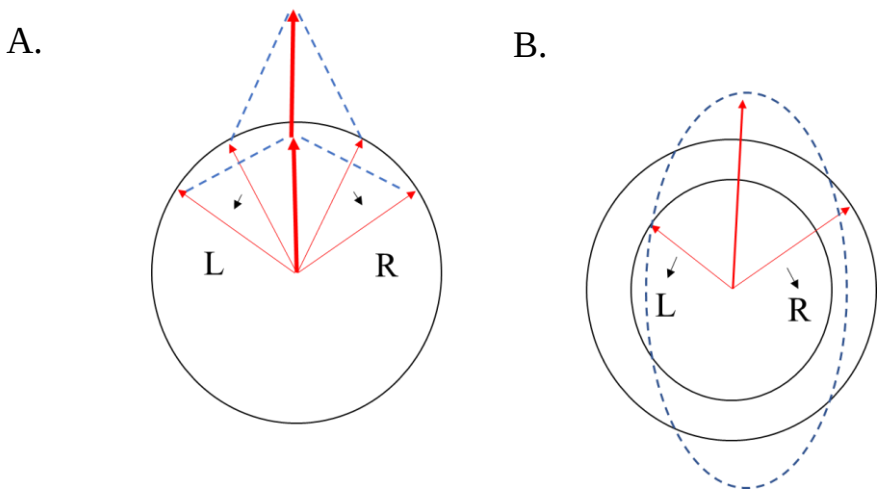

Figure M-7. Origin of CD effect

The left (L) and right (R) circularly polarised components of plane polarised radiation: (A) the two components have the same amplitude; When combined, they generate plane polarised radiation; (B) the components are of different magnitude and their resultant (dashed line) is elliptically polarised.

7.2. Circular dichroism procedure

We used circular dichroism to check the protein folding of OBP56d. CD spectra of OBP56d were recorded using a JASCO J-815 spectropolarimeter equipped with a Peltier temperature control system (JASCO MPTC-490S) using a 0.1 mm thick quartz cell. Measurements were performed with a protein concentration of 1.2 mg/mL in 50 mM NaF buffer, pH 7.5. Unlike NaCl buffer, NaF buffer absorbs very little in the wavelengths and does not interfere with the signal emitted by the proteins (Miles and Wallace, 2016). OBP56d was prepared at ~ 48 µM and plated into 0.1mm thick slides. Ten accumulations of measurement were recorded for each spectrum over a range of 180-260 nm at 20 °C with a data pitch of 0.5 nm and a scanning speed of 50 nm/min. The buffer contribution was corrected and converted into molar ellipticity. A K2D deconvolution algorithm on DichroWeb program was used to estimate the secondary structure content (http://dichroweb.cryst.bbk.ac.uk/html/home.shtml).

8. Fluorescence affinity measurements

8.1. General principle of fluorescence affinity

The OBP to be studied was brought into contact with a fluorescent probe. The fluorescent probe is a molecule which binds to the cavity of the OBP. Its fluorescence quantum highly depends on the environment in which it is found. Fluorescence is low in a polar medium and high in a hydrophobic medium. Thus, the fluorescent probe fluoresces strongly in the OBP pocket and very weakly in the aqueous medium where the protein is solubilized. It is therefore possible to detect the probe that binds to the OBP by measuring the resulting fluorescence. When a ligand is added, it can eventually compete with the probe in the OBP hydrophobic pocket. If the fluorescent probe is chased out, it induces decreased fluorescence level (**Figure M-8**).

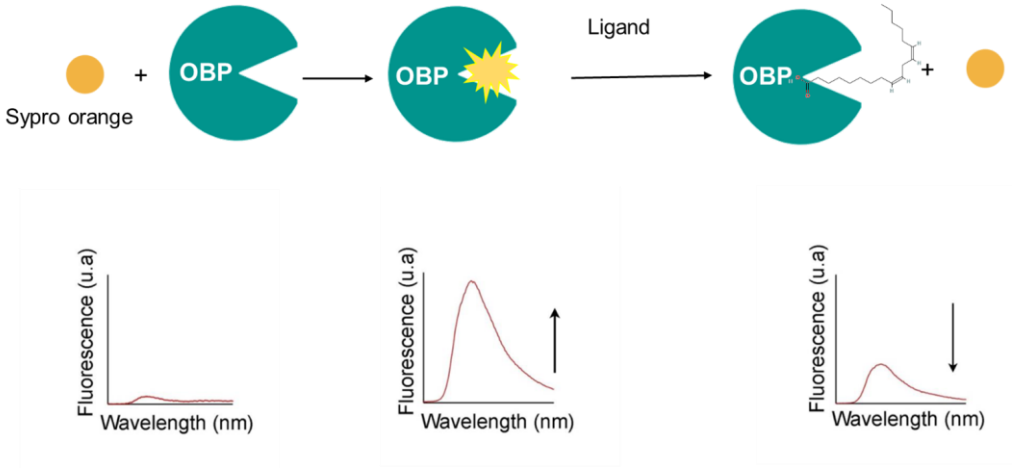

Figure M-8. Principle of the fluorescent binding assay

The fluorescent probe is highly fluorescent in the OBP cavity but becomes weakly fluorescent when chased out from this cavity. The OBP ligand displaces the fluorescent probe present in the OBP cavity, inducing in a decreased fluorescence. The figure was created by using biorender.

8.2. Sypro orange fluorescence binding assay

The binding measurements with the Sypro Orange probe (5000X concentrated in DMSO, ThermoFisher) were carried out in three quartz cuvettes (optical path: 10 mm) containing 1 mL of OBP56d or of OBP56g at a 2 µM concentration in a phosphate buffer (50 mM sodium phosphate, pH 7.5), with a Cary Eclipse spectrofluorometer (Agilent Technologies) equiped with magnetic stirring and a Peltier effect temperature regulator (Brulé *et al.*, 2020). A bandwidth of 5 nm was used for excitation and emission. The control tank contained 1 mL of 50 mM sodium phosphate buffer at pH 7.5. The spectra were recorded between 500 and 700 nm with an excitation wavelength at 490 nm. Additions of Sypro from a 100X stock solution were added to the cuvettes and the fluorescence was measured at 580 nm. The fluorescence intensities at the maximum fluorescence emission were plotted against Sypro orange concentration. The hyperbolic titration curves were adjusted and the value of the dissociation constant of the complex OBP/Sypro (K_{Sypro}) of OBP56d and OBP56g were calculated using the Sigmaplot software via a nonlinear regression for a unique binding site:

$$f = B_{max} \times abs(x) / K_{Sypro} + abs(x)$$

In this equation, f corresponds to the fluorescence intensity, abs(x) represents the Sypro orange concentration, K_{Sypro} is the dissociation constant of the fluorescent probe and B_{max} the maximum specific binding.

8.3. Ligand screening using the competitive binding assay with Sypro orange

We measured OBP56d or OBP56g affinity to representative molecules of several chemical families to test their putative ligand ability. Compounds were tested in µmolar range with respect to the physiological concentration ranges hypothetically sensed by Drosophila larvae or flies.

Displacement measurements of the Sypro Orange fluorescent probe by competition with taste and odorant molecules were carried out. The molecules were added in solutions with increasing concentrations (0, 0.5, 1, 2, 5, 10, 15, 25 and 40 µM). Each cuvette contained 2 µM of OBP56d or of OBP56g and Sypro 1X or 0.6X dissolved in 50 mM sodium phosphate buffer at pH 7.5. In three tanks, we added the molecule to be tested. In the control cuvette, we added 50 mM sodium phosphate buffer, or 100% methanol or 0.4% methanol depending on the solvent used for the tested molecule. Spectra were recorded for each molecule and for each addition with the fluorescence measured at 580 nm.

The fluorescence values obtained were processed to be expressed in relative fluorescence (Fr) according to the following equation:

$$F_r = (F_m/F_i) \times 100$$

Then, relative fluorescence data were processed using SigmaPlot software. The dissociation constant (K_D) of each compound was calculated according to the corresponding IC_{50} values (the concentration of ligands halving the initial fluorescence value of Sypro orange) using the following equation:

$$K_D = [IC_{50}] / (1 + [Sypro] / K_{Sypro})$$

where [Sypro] is the free concentration of Sypro at this concentration and K_{Sypro} is the affinity constant of the probe for the protein. The reported K_{sypro} values are the average of three measurements performed on three independent technical replicates (Zhu *et al.*, 2017).

9. Crystallography

This technique permits to represent the 3D structure of molecules by determining atomic arrangement in a solid crystal. It is useful to clearly understand the binding phenomenon between the ligand and the protein based on physico-chemical properties. Crystal growth assays were undertaken with OBP56d and OBP56g samples with a purity level ~ 90% as estimated on SDS-PAGE gel. Two methods are available: micro-batch, suspended drop vapor diffusion and seated drop vapor diffusion, micro-seeding. We tested OBPs alone with different buffers or, in order to increase the stability of the protein, we also tested the OBP/ligand complex.

We used the technique of the seated drop which is a vapor diffusion method. A drop of the solution containing the molecule, buffer, and precipitants was sealed in a container with a reservoir containing a hygroscopic solution (**Figure M-9**). Water in the drop diffuses to the reservoir, slowly increasing the concentration and allowing a crystal to form. If the concentration was to rise more quickly, the molecule would simply precipitate out of the solution, resulting in disorderly granules rather than an orderly and usable crystal. A progressive gas exchange between the drop containing the protein and the reservoir was allowed. The crystal growth conditions tested come from instructions provided by the commercial kits Wizard Classic (kits 1 to 4) and Jena BioScience (JBS kits 1 to 5). Despite several attempts, we could not obtain a crystal neither for OBP56d or for OBP56g.

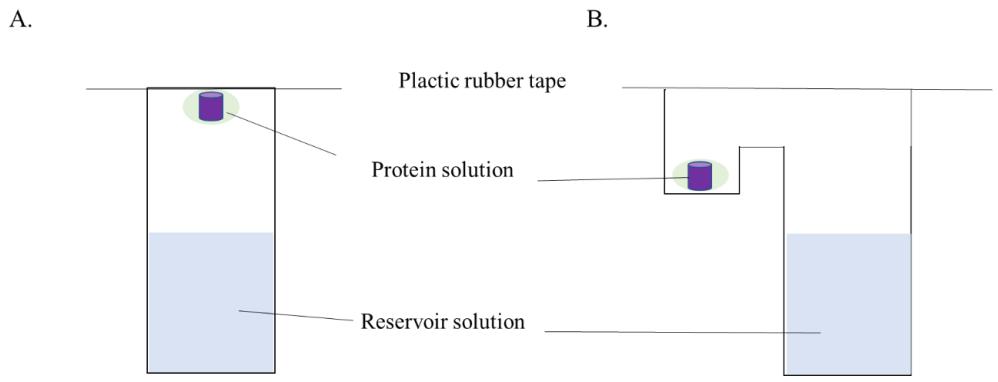

Figure M-9. Schematic design of crystallography methods

A) Protein crystallization by hanging drop diffusion: the protein drop is placed on a coverslip above the precipitating agent reservoir. B) Protein crystallization in a sitting drop: the drop of protein and precipitating agent are deposited in a second reservoir next to the precipitating agent solution

10. *OBP56d*$^{-}$ mutant

10.1. The system CRISPR-Cas9

The CRISPR-Cas9 system creates deletions in DNA with great efficiency. It is an editing technique that makes possible to add or delete genes in the genome (Doudna and Charpentier, 2014). This system was first discovered in bacteria as a defence mechanism against phages. It is composed of the Cas9 protein which is a multifunctional protein with two nuclease domains generating a double-strand break. The site to be cleaved requires a match between the crispr RNA (crRNA) sequence and the DNA sequence, and the presence of a short PAM (Protospacer Adjacent Motif). PAM sequences are short sequences of three nucleotides of NGG type, which serve as a binding site for the Cas9 enzyme. PAM sequences are essential for the recognition of target sequences by Cas9. The CRISPR-Cas9 system that we used, requires a unique guide RNA (sgRNA) to recruit and direct Cas9 nuclease activity to the target DNA sequence of the gene to cut out. This sgRNA includes both crRNA which determines the DNA target site by Watson-Crick pairing and tracrRNA (small trans-activation RNA) which binds to Cas9.

The breakdown of DNA double chains triggers repair by two general cellular repair pathways: (i) non-homologous end junction (NHEJ) repair and (ii) homology-directed repair (HDR). We used HDR pathway to replace the OBP56d sequence by DsRED sequence because it allowed us to obtain precise modifications including deletions, sequence substitutions or defined insertions.

10.2. Plasmids construction

HDR pathway required to design and built 3 different plasmids. First, two plasmids containing both guide RNA 5' and guide RNA 3' were designed. Target sites should generate double-strand breaks (DSBs) close to the location of the expected modification. They must be as specific as possible to minimize potential off-target mutagenesis. Target sites were identified from the reference *D. melanogaster* genome using the FlyCRISPR site. Once PAM sequences were identified, their localisation was verified to avoid strongly condensed or not easily accessible regions of the genome (Mavrich *et al.*, 2008). Target sequences were cloned into the pU6-BbsIchiRNA plasmid to allow the synthesis of the guide RNA.

To design the third plasmid, we used pHD-DsRED plasmid in which we introduced left homology arm (LHA) and right homology arm (RHA). To do that, we needed to add primers

located at the left and at the right of the region to be cleaved. Also, the primers should be located at 3 or 4 pairs of bases away from the PAM sequences, to allow a precise amplification of LHA and RHA. The sequences of the *AaRI* and *SapI* restriction sites were added to the ends of the primers allowing the amplification of LHA and RHA, respectively. These sites allowed us to directionally clone each of the homology arms into the pHD-DsRED plasmid.

A- pU6-OBP56d-5’ and pU6-OBP56d-3’ plasmid procedure

These plasmids made possible to transcribe the guide RNA-5’and RNA-3’which recognized the sequences of OBP56d and recruited the nuclease Cas9 (necessary to cleave the double-stranded DNA upstream of the PAM sequences).

i. Cloning of the guide sequences into the pU6-BbsIchiRNA plasmid

The oligonucleotide duplexes corresponding to the guide sequences was cloned into the pU6-BbsIchiRNA plasmid upstream of the Cas9 endonuclease recognition sequence (tracrRNA) at the level of the *BbsI* restriction sites. The oligonucleotide duplexes were designed to generate ends compatible with these restriction sites. The produced constructs were named pU6-OBP56d-5’ and pU6-OBP56d-3’.

ii. Phosphorylation of oligonucleotides and realization of duplexes

For subsequent ligation of the duplexes into the plasmid, the oligonucleotides must have a phosphate at their 5' end. To the pairs of complementary oligonucleotides (**Tableau M.5**) for which the duplex (10 µM each) was obtained, T4-DNA Ligase buffer and PolyNucleotide Kinase (PNK) were added. The reaction mixture was incubated for 30 min at 37 °C, before being brought to 95 °C for 5 min to inactivate the PNK and denature the oligonucleotides. It was left to cool down slowly at room temperature to promote the slow hybridization of the oligonucleotides, and to obtain oligonucleotide duplexes.

Tableau M.5. Oligonucleotides used for the synthesis of guide sequences

Oligonucliotides	Sequence
Guide 3’ sens	CTT-CGA-TTA-TCA-CAC-AGG-AGA-ATA-T
Guide 3’ antisens	AAA-CAT-ATT-CTC-CTG-TGT-GAT-AAT-C
Guide 5’ sens	CTT-CGA-GGG-CCA-ATT-ATA-GGT-ACA-A
Guide 5’ antisens	AAA-CTT-GTA-CCT-ATA-ATT-GGC-CCT-C

iii. Linearization and purification of pU6-BbsIchiRNA

The pU6-BbsIchiRNA plasmid was digested with *BbsI* for 1 hour at 37 °C then purified.

iv. Ligation, transformation and screening of transformants

The linearized and purified pU6-BbsIchiRNA plasmid was ligated to the oligonucleotide duplexes, then the ligation products were inserted into competent bacteria. Given the small size of the insert (25 pb), the validation of the clones was carried out directly by sequencing. To do this, we cultured a few colonies from which the plasmids were extracted and purified before being sent for sequencing (Eurofins genomics).

B- pHD-DsRED plasmid protocol

The plasmid serving as a matrix for homologous recombination was designed from the pHD-DsRed plasmid modified by adding the two homology RHA and LHA arms. The sequence encoding the DsRed fluorescent protein allowed us to select the mutants in which the homologous recombination was inserted.

i. Cloning of LHA and RHA sequences in the pHD-Dsred plasmid

The plasmid serving as a template for homologous recombination was constructed in the pHD-DsRed plasmid by cloning the homology arms (LHA and RHA) obtained by PCR amplification from the genomic DNA extracted from the vas-cas9 strain. The plasmid was generated by performing two successive cloning reactions. The first arm homology LHA was inserted in SapI by digestion while the second arm homology RHA was inserted in AaRI by digestion. The final plasmid was pHD-DsRed-LHA-RHA (**Figure M-10**).

ii. Genomic DNA (gDNA) extraction

Ten flies were grounded in 200 µl of a solution of 1% Tris, 1% SDS, 0.5 M EDTA pH 8.0. The grinded material was incubated at 70 °C for 30 min. After adding 30 µl of a solution potassium acetate 8 M, the homogenate was incubated on ice for 30 min before being centrifuged (15 min., 4 °C, 15000 g). The DNA was precipitated with 100 µl isopropanol then centrifuged for 10 min at 4 °C at 13000 g. The pellet was washed with 70% ethanol, dried and resuspended in 20 µl milliQ water. The gDNA was digested with RNase A for 25 min at 37 °C. The gDNA was quantified by spectrophotometry.

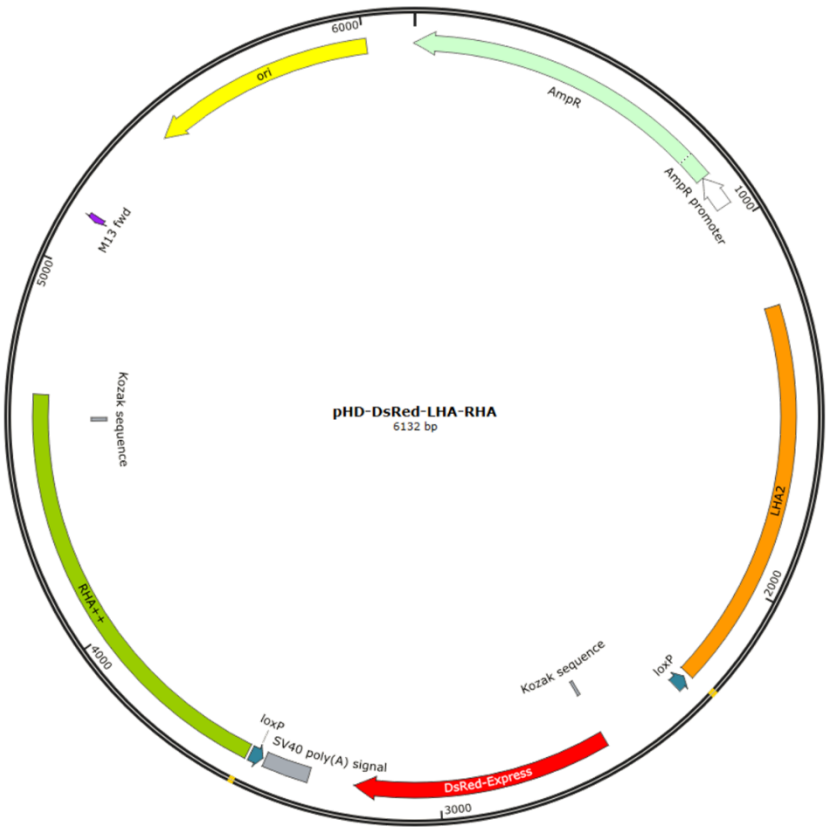

Figure M-10. The plasmid pHD-DsRED-LHA-RHA used for the construction of mutant OBP56d by CRISPR-Cas9

The plasmid structure: loxP sites on the bacteriophage P1 recombines DNA between specific sequences; RHA+++: right homology arm; LHA: left homology arm; DsRed: the sequence to be integrated in the genome; AmpR: confers resistance to ampicillin.

iii. Reaction chain reaction (PCR)

The gDNA was mixed with the reaction buffer, to which the 4 dNTPs (2 mM), the specific primers (10 µM) (**Table M.6**) and 2U of Taq polymerase have been added. The gDNA was denatured for 5 min at 95 °C followed by a cycle of denaturation (30 s, 95 °C), hybridization of the primers (1 min, +/- 5 °C of the Tm of the primers) and a polymerization step (2 min, 72 °C). This cycle was repeated 35 times. The reaction was completed by an elongation step of 10 min at 72 °C.

Table M.6. Oligonucleotides used for the synthesis of LHA and RHA homology arms

Oligonucleotides	Sequence	Length of amplicon (bp)
LHA sens	AGTCCACCTGCAGTCTCGCCTTTGATAACCGCACTTGAC	1142
LHA antisens	AGTCCACCTGCAGTCTTATGGTATCGAAACTGTTGAATT	
RHA sens	AGTCGCTCTTCATATTCCTGTGTGATAATCTGTCTGTGA	1000
RHA antisens	AGTCGCTCTTCAGACACAAAGGCTGATGTCGAGCA	

iv. Purification of LHA and RHA inserts

After their amplification by PCR, inserts were purified to eliminate all traces of primers and template using a kit (SV Gel, Promega). Each reaction mixture was filtered by centrifugation on a column which adsorbs DNA. After two washes with ethanol, the DNA was eluted with 50 µL of elution buffer and quantified using a spectrophotometer at 260 nm.

v. Enzymatic digestion of the inserts and the pHD-DsRed plasmid

The reaction mixture consists of 1µg of the PCR product (or plasmid pHD-DsRed), enzyme buffer (1X), 1 µL of each restriction enzyme (AaRI, SapI, 10U/µL – ThermoFisher). The digestions were incubated at 37 °C for 2 h.

vi. Purification of the inserts and the pHD-DsredGAL4 plasmid on agarose gel

All of the digested sequences were deposited on a 1% agarose gel. The band of interest was cut out and then purified using a kit (Wizard SV Gel, Promega). The DNA was extracted from the gel and filtered through a high affinity column. After washing, the DNA was eluted with 50µL of milliQ water and dosed by spectrophotometry.

vii. Ligation of inserts and digested pHD-DsRed plasmid

The necessary quantity of purified inserts was brought into contact with 50 ng of plasmid pHD-DsRed (previously prepared), one unit of T4 DNA ligase (Promega) and associated 10X buffer for 16 h at 4 °C.

viii. Bacterial Transformation

The ligation products were added to 50 µL of competent bacteria. After 1h incubation on ice, bacteria were subjected to a thermal shock (42 °C, 45 s). Then, they were incubated in 450 µL LB at 37 °C and stirring for 1h30. Next, they were inoculated on a selective solid medium (LB/agar, Ampicillin 100 µg/L) and cultured for 16 h at 37 °C.

ix. Screening subclones by PCR

We carried out directly a PCR from the colonies to quickly determine the recombinant clones. For this, a fraction of each colony was sampled and deposited separately in a mix composed of the specific primers of the insert and the PCR. The remaining fraction was seeded in 5 mL of LB associated with 100 µg/L of ampicillin. Only recombinant colonies (amplification of the insert by PCR) were cultivated to extract and purify the plasmids.

x. Preparation of plasmid DNA

After centrifugation (8000 g, 5 min) of the cultures containing the transformed bacteria, the plasmid DNA was extracted from the bacteria by alkaline lysis and purified on an anion exchange column (Plasmid Mini kit, QIAGEN). The column loaded with plasmid DNA was washed and then elution was carried out by passing a solution at low salt concentration. DNA was concentrated by precipitation with isopropanol then resuspended in a buffer (10mM Tris-HCl, pH 8.5) and assayed by spectrophotometry at 260 nm. In order to verify the presence of the insert, part of the plasmid DNA was digested with the appropriate restriction enzymes. The analysis of the fragments was carried out by electrophoresis on a 1% agarose gel. To ensure the integrity of the cloned sequences, the plasmids were sequenced by Eurofins Genomics.

C- Transgenesis

Each plasmid DNA construction was purified on a column (Wizard Plus SV Promega kit), then 1µg of the plasmids pU6-OBP56d-3' and pU6-OBP56d-5' were added to 5 µg of plasmid pHD-DsRed-LHA-RHA before being precipitated with 300 mM sodium acetate in 1% ethanol overnight at -20 °C. After 1 hour centrifugation (14,000 g), the pellet was resuspended in 10 µL Ultrapure water for injection. This step was only performed in our laboratory when we attempted to transform embryos. Otherwise it was taken in charge by the Bestgene Inc Company (USA) with the plasmid we sent there.

In the Bestgene company, plasmids purified and concentrated in the previous step were injected into embryos that had not yet been cellularized. The injection was made at the germinal pole, where reproductive cells arise. The CRISPR-Cas9 system led to the recombination of the coding part of OBP56d by the DSRed sequence with the gDNA of the germ cells in various stages. The balanced line BDSC # 51324 (*$w^{1118:}$ vas-Cas9 III*) was used to generate the OBP56d mutant. Adults resulting from injected embryos (G0) were crossed with a line containing the Curly *(CyO)* balancer to identify, in the G1 progeny, individuals having incorporated the DSRed transgene. To stabilize transgenic individuals, each potential carrier of the transgene was crossed in two successive generations to eliminate the Cas9-encoding transgene and to provide a balancer chromosome. Then, potential mutant lines were sent to us and the integrity of sequences adjacent to the recombining site verified by sequencing.

11. Behavioural assays

11.1. Preparation of flies

The main goal of our behavioural experiments consisted to determine the influence of the OBP56d protein in the ability of female and male flies to court, copulate and reproduce. Accordingly, we successively tested these abilities in pairs of flies prepared as follows. Flies were screened under light CO_2 anaesthesia and collected in the morning 1-6 hours after emergence from pupal case. They were kept 4 to 7 days until the behavioural test. Virgin females were kept in groups of five, while virgin males were isolated in a fresh food vial. Males kept isolated show higher behavioural activity than males kept in groups (Svetec and Ferveur, 2005). Beside the *OBP56d^{-}* mutant line, we used two control lines (control line 1 = *w^{-}* line; control line 2 = vas-cas9 line #51324 used to generate the *OBP56d^{-}* mutant line). Behavioural experiments were always performed during the same period of the day (8h30-11h30). Behavioural tests were performed under white light in a observation chamber consisting of a plate pierced with a hole used to introduce the flies covered with a watch glass (1.6 cm^3). Briefly, tester males were individually aspirated (without anaesthesia). After 5 min, a female fly was introduced and both the courtship and copulation behaviours shown by each pair were noted (**Figure M-11**).

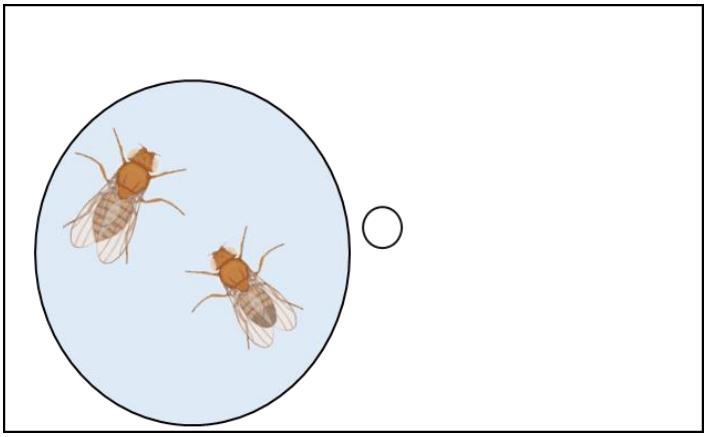

Figure M-11. Device used to measure courtship and copulation behaviours.

Equipment used for the courtship behaviour. A plate pierced with a hole was used to introduce the flies covered with a watch glass (1.6 cm3). The male was introduced first and 5 min later, a female fly was introduced.

11.2. Courtship and copulation behaviours

Courtship is the behavioural ritual exhibited by Drosophila flies before copulation. Copulation occurs only if both flies reciprocally accept their courting partner. We observed the courtship behaviour in heterosexual pairs of flies combining the two controls and the *OBP56d*$^{-}$ mutant lines. The courtship behaviour was first observed between homotypic pairs (Female x Male of the same line: Ctrl1 x Ctrl1; Ctrl2 x Ctrl2; *OBP56d*$^{-}$ x *OBP56d*$^{-}$). Then, we observed heterotypic crosses (Ctrl1 x *OBP56d*$^{-}$; Ctrl2 x *OBP56d*$^{-}$; *OBP56d*$^{-}$ x Ctrl1; *OBP56d*$^{-}$ x Ctrl2) (**Table M.7**). Each pair was given a maximum of 2 hours during which we noted whether courtship occurred (we did not note precisely each courtship step but only courtship initiation) and we measured the latency to copulate as well as copulation duration. All tests were simultaneously performed, but we carried out these experiments during two separate periods and the data were pooled. Using the latency of copulation, we plotted the cumulated copulation frequency as a function of time during 2 h. Copulation frequencies were statistically compared between genotype pairs.

Table M.7. Total number of homotypic and heterotypic pairs tested

Virgin females x Virgin males	Number of mating pairs
Ctrl1 x Ctrl1	86
Ctrl2 x Ctrl2	80
OBP56d- x OBP56d-	100
Ctrl1 x OBP56d-	60
Ctrl2 x OBP56d-	60
OBP56d- x Ctrl1	68
OBP56d- x Ctrl2	58

11.3. Antennal ablation

In preliminary tests, we attempted to measure the influence of chemosensory signals detected by fly antenna. Therefore, we bilaterally ablated antenna in female flies and tested their courtship and copulatory behaviours. Two-days old flies were surgically operated with Moria Worst microscissors (#17000; Moria,France) and left 2 days to recover before the behavioural test. Only flies which behaved like intact flies were kept for the courtship/copulation experiment. The test was performed with pairs of flies under similar experimental conditions as those described above.

11.4. Fecundity

We also counted the fecundity of individual females based on the adult offspring emerging from each vial. Progeny was counted twice 12 and 17 days after oviposition. We also took into account the sex ratio of the progeny.

11.5. Copulation frequency: direct and indirect measures

All mated females resulting from this experiment were kept individually in fresh food vials and allowed to oviposit for approximately 5 days before being discarded. These vials were kept under standard conditions. We first determined the fertility of each mated female (presence/absence of progeny). These data allowed us to establish a correspondence between copulation frequency and fertility frequency. In an additional experiment, we wondered whether pairs kept together for longer period of time (12 h) would increase their copulation frequency? Accordingly, pairs of flies were placed in fresh food vials (overnight) and after 12

h (next early morning) males were removed. 12-14 days later, we noted for the presence/absence of adult progeny in each vial. The progeny frequency in this "12-hours long experiment can be considered as a reliable indicator (proxy) of copulation given that we determined the relationship between copulation and fertility copulation in the 2 hours long copulation test.

12. Statistics

RT q-PCR data was analysed first by LinRegPCR (version 2020.0). Once Cq were normalized by LinRegPCR, data were analysed based on the procedure described in a previous study (Ganger *et al.*, 2017). The efficiency and the Cq for each well were taken into consideration. The efficiency-weighted $\Delta Cq(w)$ values were used to calculate a normalized relative expression ration based on the conditions of the experiment.

To test the impact of the microbiota, the NCBI used PERMANOVA (Permutational analysis of variance) using the function 'Adonis' in the package 'Vegan'. To visualize sample clustering based on bacterial community composition, Bray-Curtis distances between samples were calculated and performed Canonical Analysis of Principal Coordinates based on Discriminant Analysis (CAPdiscrim) using the R package 'Biodiversity R'. This test is based on the significant clustering and estimated classification success by permuting the distance matrix 1000 times, and estimating the probability of finding the observed differences by chance. Next, data were plotted with the two dominant linear discriminants (LD) used to visualize clusters on a planar representation. For each cluster, ellipses reflect 95% confidence intervals using the function 'Ordiellipse' in the R package 'Vegan'.

Genus-level distribution of the microbiome in the whole body or gut was calculated based on all the ASVs clubbed which fell into single genus (identification of bacteria) and remaining rare ASVs of multiple genus were clubbed as "others". Then, the relative abundance of each genus depending on groups was calculated (i.e. relative to the total reads in each sample).

The statistical analyses and graphic presentations were carried out with XLSTAT (version 2022.2.1) and Graph Pad Prism (version 8.0).

Results

1. Expression of OBPs in the gut and gustatory appendages

1.1. Selection of OBPs

During my thesis, we quantified the expression of OBPs mRNA in the digestive system of *Drosophila melanogaster*. After the identification of the OBPs mostly expressed in the digestive system (based on mRNA-seq data from Flybase), we selected fewer OBPs for further studies (**Table R.1**). According to Flybase, OBP19b did not show a significant expression level in the digestive system. However, the preliminary results obtained in our laboratory showed that (1) it was expressed in the detection of L-Phenylalanine in the peripheral gustatory system (proboscis) and (2) its expression in the gut could be affected by fasting (K.Rihani, unpublished data). The 16h + L-Phe fasting treatment was carried out specially for OBP19b, to detect for any impact on level of expression given its high affinity for L-Phe amino acid (Rihani *et al.*, 2019). However, the OBP19b showed no, or extremely low expression in the gut. This treatment was also tested on other OBPs. The OBP19b, OBP18a and OBP56g are expressed in the gustatory system, while OBP56d is expressed in the olfactory and gustatory system of adults (Galindo and Smith, 2001). The transcription levels of these OBPs were quantified using RT-qPCR.

Table R.1. Relative mRNA-seq tissue-specific expression in *Drosophila melanogaster* adults. The age of flies was 4 days (Data base of Flybase).

OBPs	Head Virgin female	Head mated female	Head male	Intestine (mix F+M)
OBP19b	+	+	++	-
OBP56g	+++	++	+++	++++
OBP56d	+++	+++	+++	++
OBP18a	+	+	+++	++

- = no/extremely low expression ; + = very low expression ; ++ = moderate expression ; +++ = high expression ; ++++ = very high expression

1.2. Quantification of OBPs mRNA expression in the gut

The statistical analysis was based on a previous study (Ganger *et al.*, 2017). In Flybase, the transcription levels of different OBPs in the gut is provided in mix sexes samples (females + males). For this reason, we decided to quantify OBP level of expression in the gut according to the sex and mating status (virgin/mated). The expression of OBP19b, OBP56g and OBP56d was determined in virgin females, mated females and virgin males. We decided to be careful on the status of females given potential post-mating effects on OBP expression. These three groups of Drosophila flies were kept fasting during 2h, 16h or 16h L-Phe (16h of fasting in presence of L-Phe). Then, mRNA expression of the three OBPs was quantified. This was compared with the level of the two selected housekeeping genes (Tub-3 and MnF). The thorax was arbitrarily chosen as a reference tissue (with the "1" value), after determining the low expression of OBPs. The variation of OBP expression in the other tissues was compared to this reference tissue. Therefore, our graphs show the fold change $R=10^{-(\Delta\Delta Cq)}$ in the complete head and in the whole gut compared to the thorax reference.

1.2.1. mRNA expression of OBP19b

In the three groups, OBP19b expression was higher in the head than in the gut (**Figure R-1**). This is supported by previous data revealing the expression of OBP19b in the complete head (Galindo and Smith, 2001; Hekmat-Scafe, 2002; Rihani *et al.*, 2019). No significant difference of expression was detected between the heads of virgin females, mated females and virgin males for the three fasting treatments (2h, 16h and 16h L-Phe; **Table R.2. Head**; p - value = 0.051). Also, OBP19b showed no difference of expression in the gut between females and males (**Table R.2. Gut**) (p-value = 0.715) in three conditions of fasting. Here, we can at least conclude that fasting duration did not impact the level expression of OBP19b in the head or in the gut. OBP19b level of expression, either in the head or in the gut, was not impacted by female mating status (**Figure R-1**).

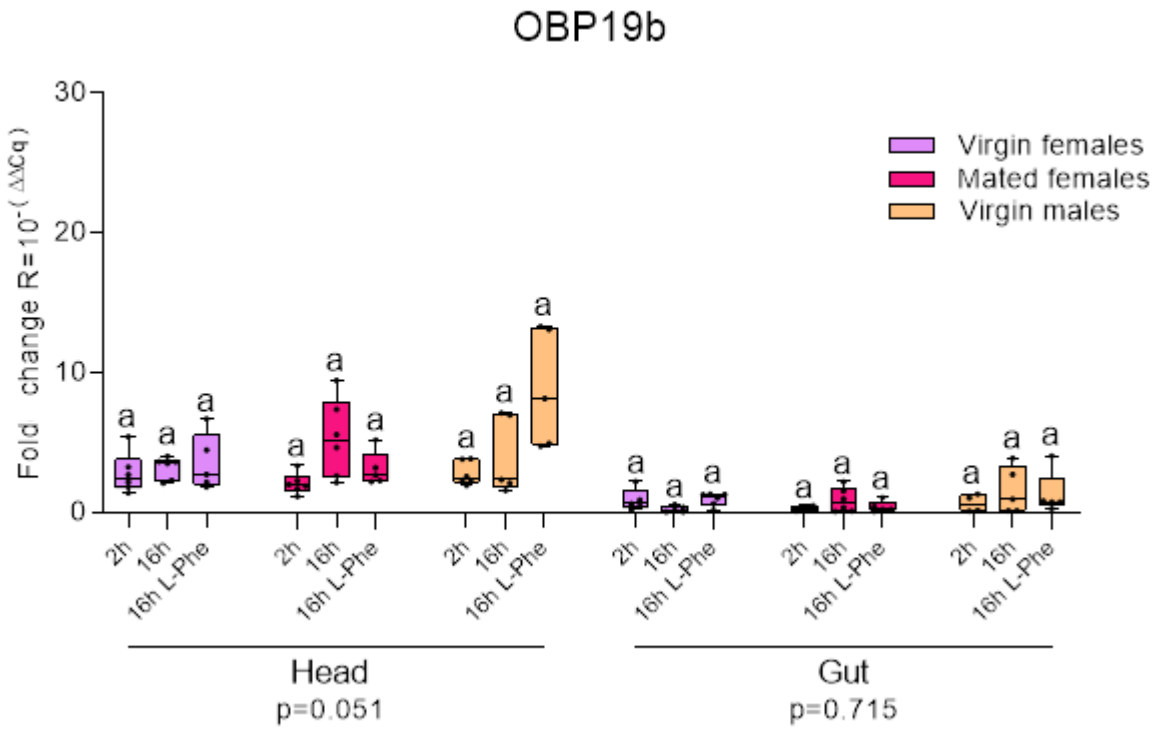

Figure R-1. OBP19b mRNA expression in the head and in the gut of *Drosophila melanogaster* flies

The thorax was used as a reference tissue (level of expression = 1) to compare the variation of OBP19b in the head and gut. The variation was compared between three fasting treatments: 2h, 16h and 16h with L-Phe. Data are shown as box plots which represent mRNA expression in two different tissues. Kruskal-Wallis test was applied for each tissue independently by indicating different letters that determine significant differences or not. Data were tested with Kruskal Wallis test, post-hoc Conover-Iman with Bonferroni correction, Head p= 0.051 N=5-6; Gut p=0.715 N=4-6. Non-significant difference was detected between samples

Table R.2. Data show OBP19b expression in the complete Head (1) and Gut (2). For each group and condition, the sample size, mean, standard deviation and SEM are shown. The comparison between data was carried out using a Kruskal-Wallis test, post-hoc Conover-Iman with Bonferroni correction.

	Virgin female			Mated female			Virgin male		
Head	2h	16h	16h L-Phe	2h	16h	16h L-Phe	2h	16h	16h L-Phe
Sample size	6	6	5	6	6	5	6	5	5
Mean	2.79	3.19	3.57	2.05	5.29	3.10	2.76	4.01	8.84
Standard deviation	1.44	0.8	2.02	0.73	2.79	1.24	0.85	2.78	4.2
SEM (±)	0.59	0.33	0.9	0.3	1.14	0.55	0.35	1.24	1.88

	Virgin female			Mated female			Virgin male		
Gut	2h	16h	16h L-Phe	2h	16h	16h L-Phe	2h	16h	16h L-Phe
Sample size	5	6	4	4	6	5	4	5	5
Mean	0.87	0.97	0.83	0.29	0.86	0.39	0.65	1.55	1.31
Standard deviation	0.79	1.82	0.55	0.18	0.87	0.39	0.62	1.68	1.54
SEM (±)	0.35	0.74	0.28	0.09	0.35	0.17	0.31	0.75	0.69

1.2.2. mRNA expression of OBP56g

The OBP56g showed significantly higher expression in the head of virgin/mated females than in males (**Figure R-2. Head**) (p-value <0.001-0.0001), except for the expression of 16h L-Phe in mated females (p-value > 0.05). No difference was observed for 16h L-Phe compared to the expression of males in all fasting conditions. OBP56g expression in the head was at least ~ 90 times more important in females (virgin/mated) than in males (**Table R-3. Head**).

In the head, under the "16h" and "16h L-Phe" fasting conditions, virgin females showed a higher expression of OBP56g than mated females. No significant difference were observed for 2h, and 16h fasting conditions (p-value > 0.05) in three groups, but only between 2h or 16h and 16h L-Phe fasting ($p < 0.0001$) in virgin and mated females. The presence of L-Phe during 16h fasting, in virgin females induced higher expression while in mated females it induced the lowest expression. We can not conclude whether this difference is induced by the presence of L-Phe or by the status of females, but there is apparently an impact of the addition of L-Phe during the fasting period. For time limitation reasons, this difference was not further explored.

The OBP56g expression was significantly higher in the gut of virgin males for the three fasting conditions compared to mated females (**Figure R-2. Gut**) (p-value < 0.001-0.0001). For 2h fasting, virgin male gut expression was significant higher compared to fasting treatments of virgin females (p-value<0.0001). No difference for 16h of fasting in males was found compared to virgin females (p-value > 0.05). Male guts subjected to 16h L-Phe showed significantly higher expression compared to 16h or 16h L-Phe conditions in virgin females or mated females (p-value <0.001-0.0001). We can conclude that OBP56g showed higher expression in the male guts than in female guts (**Table R.3. Gut**).

Fasting duration did not affect OBP56g expression in the gut of virgin females, mated females or virgin males (p-value > 0.05).

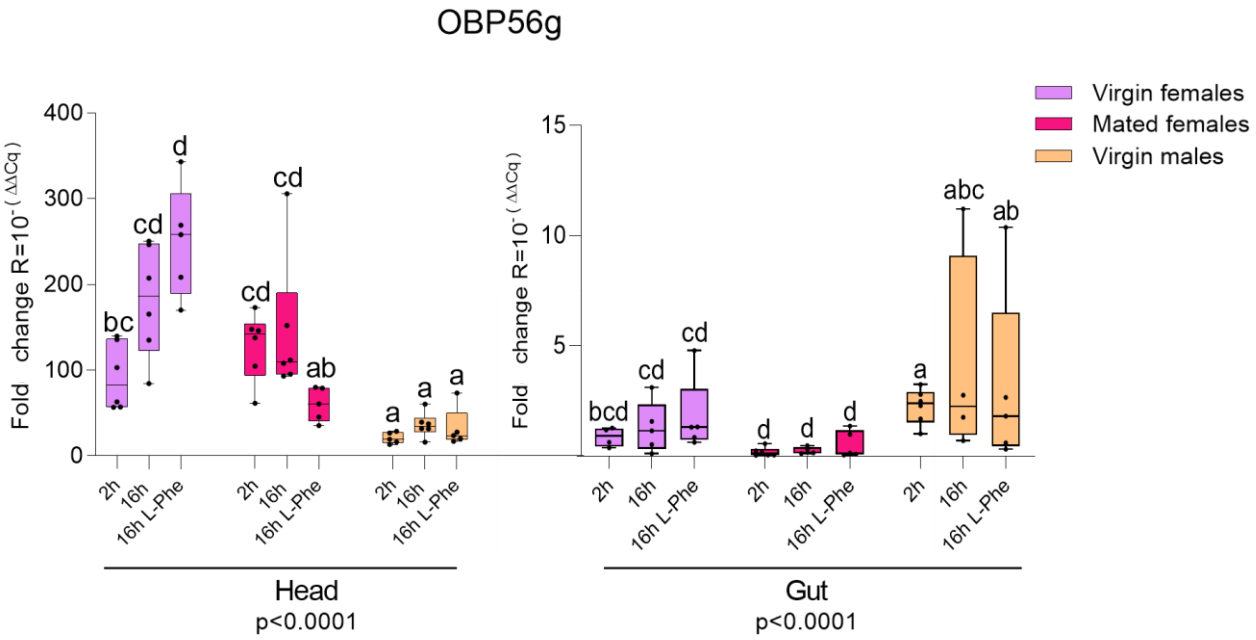

Figure R-2. mRNA expression of OBP56g in the head (left) and in the gut (right) of *Drosophila melanogaster* flies

The thorax was used as a reference tissue (level of expression = 1) to compare the variation of OBP56g in the head and gut. The variation was compared between three fasting treatments: 2h, 16h and 16h with L-Phe. Data are shown as box plots which represent mRNA expression in two different tissues. Kruskal Wallis test was applied for each tissue independently. Different letters indicate significant differences. Data were tested with Kruskal Wallis test, post-hoc Conover-Iman with Bonferroni correction: Head p<0.0001 N=5-6; Gut p=0.001 N=4-6.

Table R.3. Data show OBP56g expression in the complete Head (1) and Gut (2). For each group and condition, the sample size, mean, standard deviation and SEM are presented.

	Virgin female			Mated female			Virgin male		
Head	2h	16h	16h L-Phe	2h	16h	16h L-Phe	2h	16h	16h L-Phe
Sample size	6	6	5	6	6	5	5	6	5
Mean	92.6	181.6	250.0	128.6	144.4	60.2	21.0	36.2	32.5
Standard deviation	39.1	65.5	65.6	39.6	81.8	19.8	6.5	14.4	23.2
SEM (±)	15.9	26.7	29.3	16.2	33.4	8.9	2.9	5.9	10.4

	Virgin female			Mated female			Virgin male		
Gut	2h	16h	16h L-Phe	2h	16h	16h L-Phe	2h	16h	16h L-Phe
Sample size	4	5	5	6	5	5	6	4	5
Mean	0.9	1.3	1.8	0.2	0.3	0.5	2.3	4.1	3.2
Standard deviation	0.4	1.2	1.7	0.2	0.2	0.6	0.8	4.8	4.1
SEM (±)	0.2	0.5	0.8	0.1	0.1	0.3	0.3	2.4	1.9

In all fasting conditions, OBP56g expression in the three groups was significantly higher in the head than in the gut (**Figure R-3**) (p-value= 0.001).

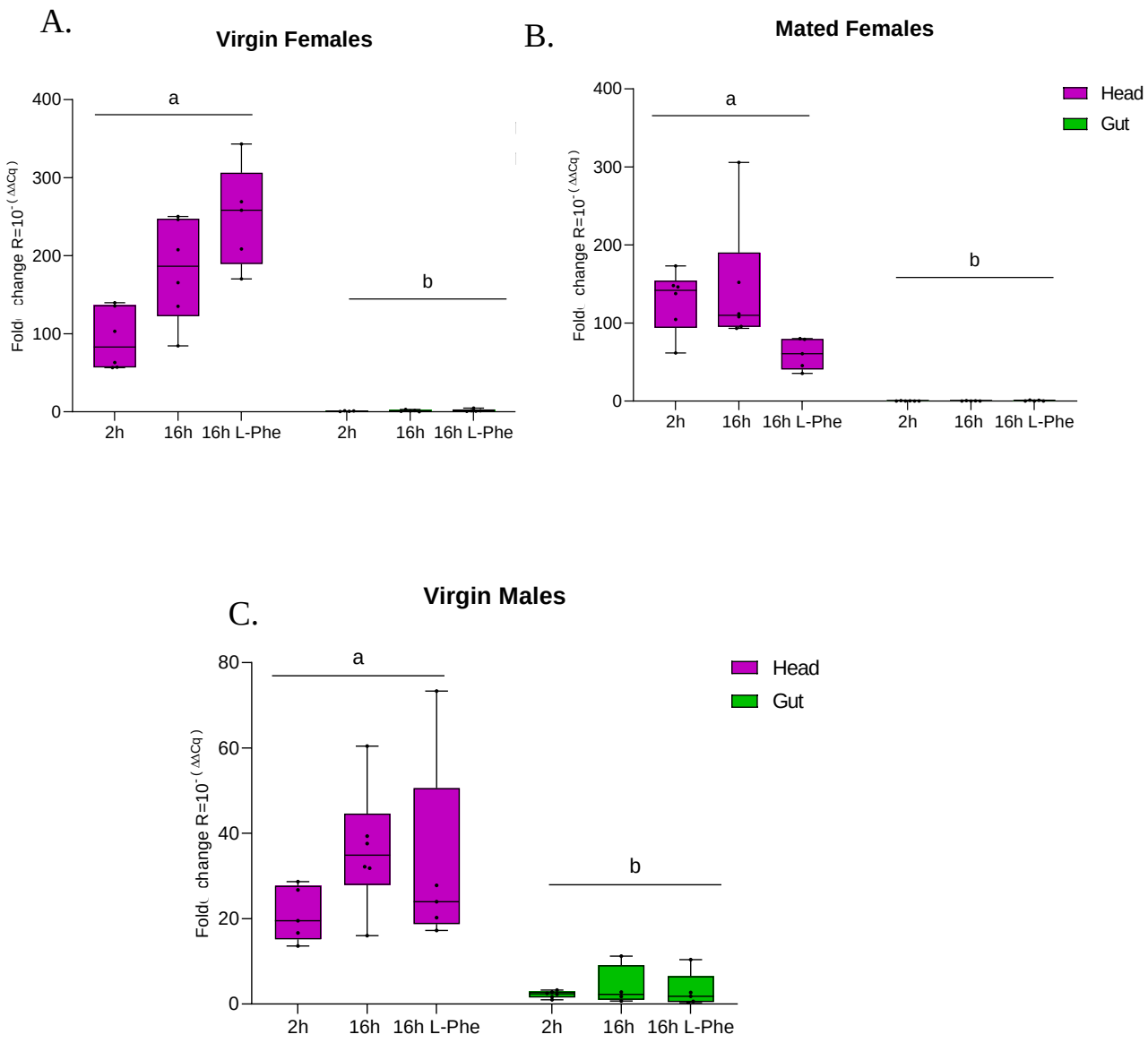

Figure R-3. Comparison of OBP56g mRNA expression in the head and in the gut of *Drosophila melanogaster* flies

The thorax was used as a reference tissue (level of expression = 1) to compare the variation of OBP56g in the head and gut. The variation was compared between three fasting treatments: 2h, 16h and 16h with L-Phe. Data are shown as box plots which represent mRNA expression in two different tissues. Kruskal Wallis test was applied for each group. Different letters indicate significant differences. Data were tested with Kruskal Wallis test, post-hoc Conover-Iman with Bonferroni correction: Virgin females Head (a), Gut (b) p-value <0.0001 N=4-6; Mated females, Head (a), Gut (b) p-value < 0.0001 N=5-6; Virgin males, Head (a), Gut (b) p-value < 0.0001 N=4-6.

1.2.3. mRNA expression of OBP56d

Head expression of OBP56d showed a tendency to be higher in females than in males (**Figure R-4**). For the 16h fasting condition, the level of expression significantly decreased in virgin males compared to virgin/mated females (p-value<0.01-0.001). In females, the level of OBP56d expression was not influenced by post-mating changes (**Table R.4. Head**). It was no impact of fasting duration for each of these groups.

OBP56d expression was significantly higher in the gut of males than the gut of virgin/mated females (**Figure R-4**). In the three fasting conditions, gut expression was higher in males compared to females (p-value < 0.0001). Fasting duration did not influence the level of OBP56d expression (**Table R.4. Gut**). Furthermore, OBP56d showed a sexually dimorphic expression in the gut.

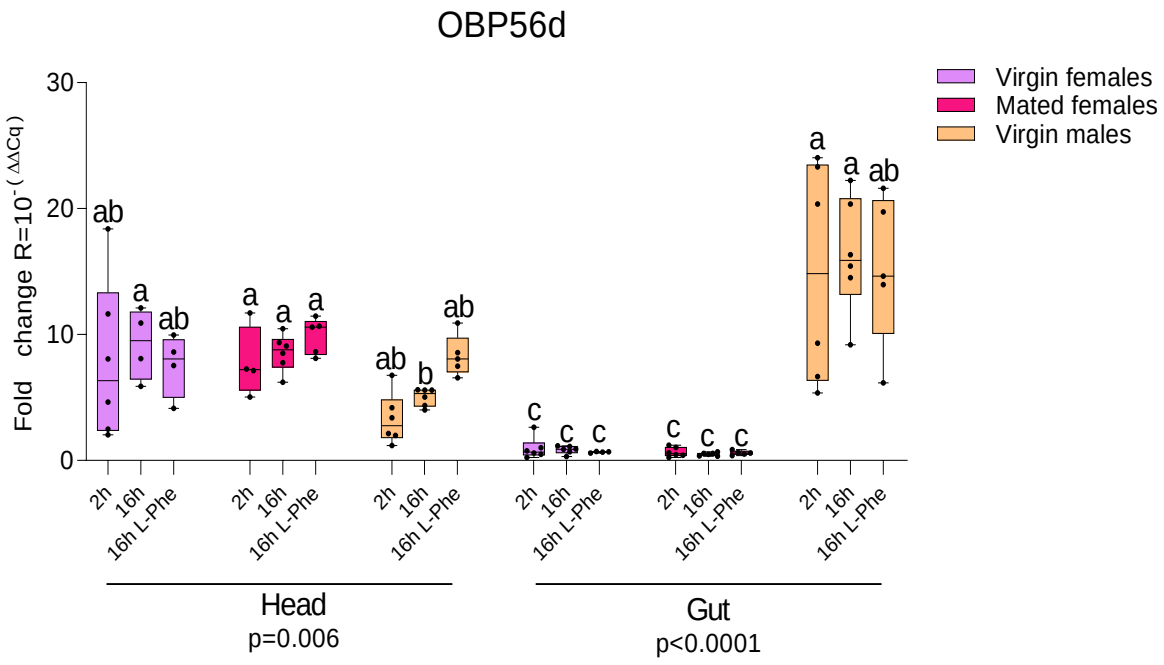

Figure R-4. mRNA expression of OBP56d in the head (left) and in the gut (right) of *Drosophila melanogaster* flies

The thorax was used as a reference tissue (level of expression = 1) to compare the variation of OBP56g in the head and gut. The variation was compared between three fasting treatments: 2h, 16h and 16h with L-Phe. Data shown as box plots represent mRNA expression in two different tissues. Kruskal Wallis test was applied for each tissue independently. Different letters indicate significant differences. Data were tested with Kruskal Wallis test, post-hoc Conover-Iman with Bonferroni correction: Head p=0.006 N=4-6; Gut p<0.0001 N=5-6. Head ns=nonsignificant p > 0.05, p=0.01 or p=0.001; Gut (right; a, abc, ab, bcd, cd, d) ns=nonsignificant, p=0.001 and p<0.0001.

Flybase indicates that OBP56d was less expressed than OBP56g, our data suggest an opposite trend.

Table R.4. Data show OBP56d expression in the complete Head (1) and Gut (2). For each group and condition, the sample size, mean, standard deviation and SEM are presented.

	Virgin female			Mated female			Virgin male		
Head	2h	16h	16h L-Phe	2h	16h	16h L-Phe	2h	16h	16h L-Phe
Sample size	6	6	4	4	6	5	6	6	5
Mean	7.9	10.2	7.6	7.8	8.6	9.9	3.3	5.0	8.3
Standard deviation	6.3	2.7	2.5	2.8	1.5	1.4	2.0	0.7	1.6
SEM (±)	2.6	1.1	1.2	1.4	0.6	0.6	0.8	0.3	0.7

	Virgin female			Mated female			Virgin male		
Gut	2h	16h	16h L-Phe	2h	16h	16h L-Phe	2h	16h	16h L-Phe
Sample size	6	6	4	4	6	5	6	6	5
Mean	1.0	0.8	0.7	0.7	0.5	0.6	14.8	16.3	15.2
Standard deviation	0.9	0.3	0.1	0.4	0.1	0.2	8.7	4.6	6.0
SEM (±)	0.4	0.1	0.0	0.2	0.1	0.1	3.5	1.9	2.7

In all fasting conditions, females showed a significantly higher expression of OBP56d in the head than in the gut (**Figure R-5.A/B**). Meanwhile, males showed a higher expression in the gut for all fasting conditions compared to females. Their expression was significantly important for 2h and 16h fasting compared to females (**Figure R-5.C**).

OBP56d has a very important expression in the gut compared to OBP56g, respectively for 2h fasting (14.8 ± 3.5; 2.3 ± 0.3), for 16h fasting (16.3 ± 1.9;4.1 ±2.4) and for 16h fasting with L-Phe (15.2 ± 2.7; 3.2 ± 1.9) treatments.

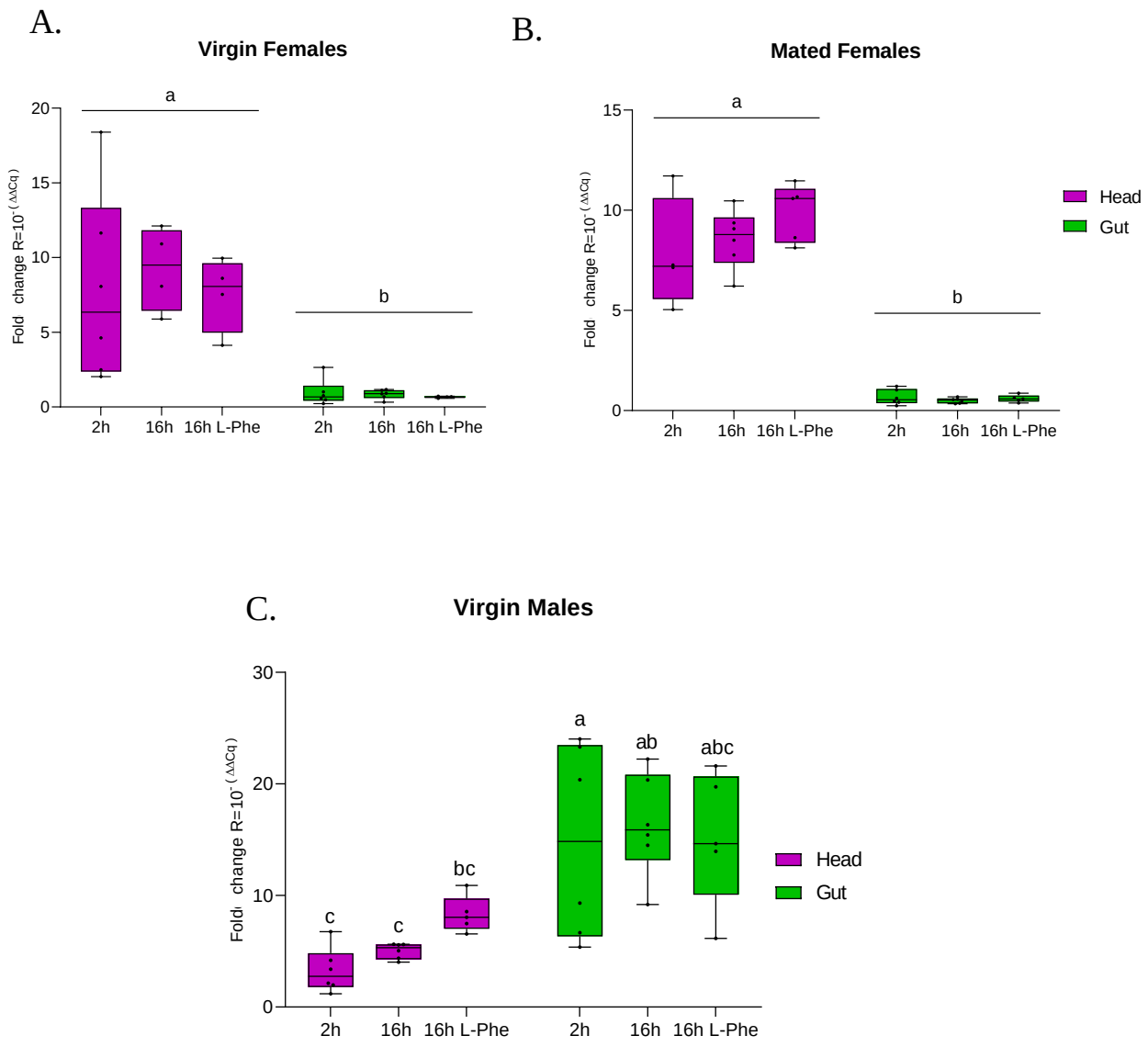

Figure R-5. Comparison of OBP56d mRNA expression in the head and in the gut of *Drosophila melanogaster* flies

The thorax was used as a reference tissue (level of expression = 1) to compare the variation of OBP56g in the head and gut. The variation was compared between three fasting treatments: 2h, 16h and 16h with L-Phe. Data are shown as box plots which represent mRNA expression in two different tissues. Kruskal Wallis test was applied for each group. Different letters indicate significant differences. Data were tested with Kruskal Wallis test, post-hoc Conover-Iman with Bonferroni correction: Virgin females, p-value < 0.0001 N=5-6; Mated females, p-value < 0.0001 N=5-6; Virgin males, p-value =0.003 or p-value < 0.0001 N=4-6.

1.2.4. OBPs expression in *Drosophila melanogaster* head and gut

Given our interest in studying mechanisms linking the peripheral gustatory system with the gut, we focused on both OBP56g and OBP56d which both showed a relatively high expression in the gut. We gave up with the study of OBP19b since our preliminary data found no significant expression of this OBP in the gut.

OBP56g was more highly expressed in the head of females than in males with no influence of fasting duration (**Figure R-6.A**). Conversely, in the gut OBP56d was more expressed in males than in females (**Figure R-6.B).** Also, females showed a relatively higher OBP56d expression in their head than males.

We further studied OBP56g and OBP56d since they showed a substantial expression level in the fly gut. No significant impact was observed on post-mating level of OBP expression in females. We continued working only with virgin females. For the part of this study, we also measured two extreme fasting conditions: “no fasting” or “30h fasting duration”. The two treatments, only tested in virgin females and virgin males.

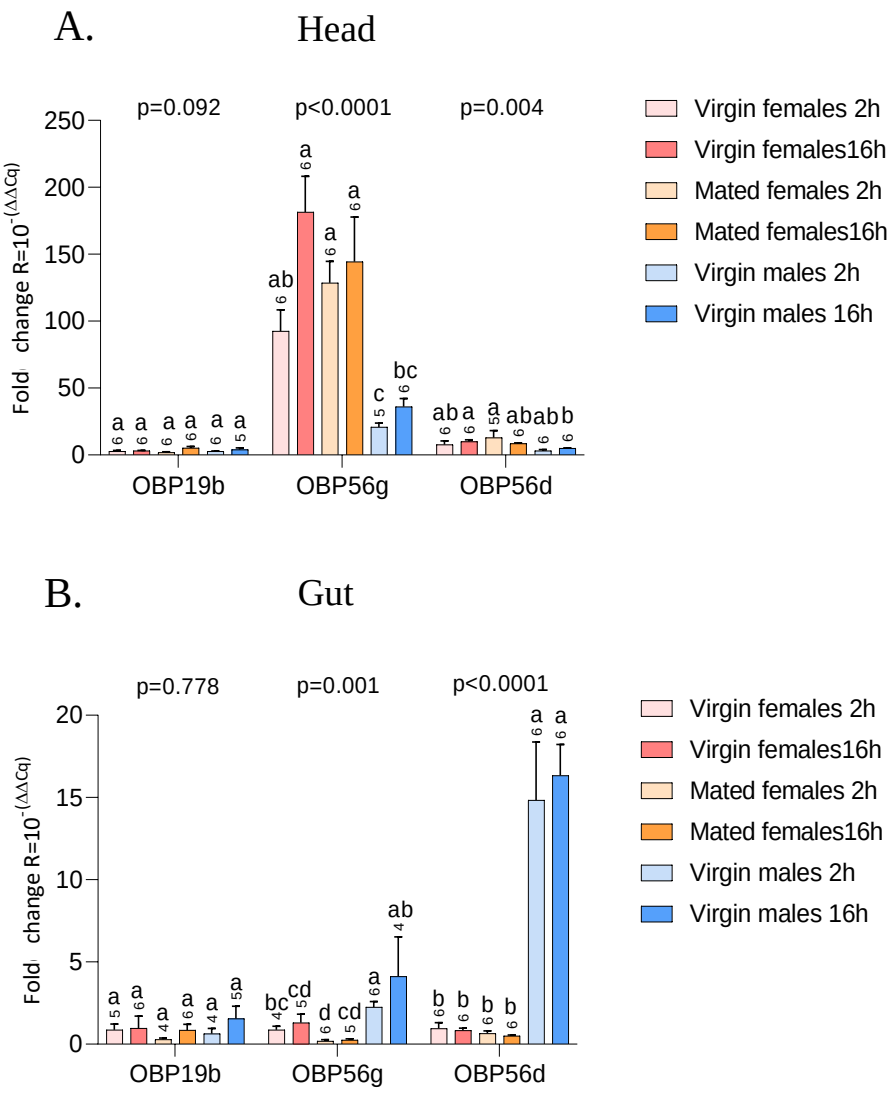

Figure R-6. mRNA expression of OBPs in the head (A) and in the gut (B) of *Drosophila melanogaster* flies

The thorax was used as a reference tissue (level of expression = 1) to compare the variation of OBPs in the head and gut. OBP variation was compared between three fasting treatments: 2h and 16h. Kruskal Wallis test was applied for each OBP-group/condition independently. Different letters indicate significant differences. Data were tested with Kruskal Wallis test, post-hoc Conover-Iman with Bonferroni correction: For the Head: OBP19b: p-value= 0.092; OBP56g: p-value<0.0001 and OBP56d: p-value=0.004). For the Gut: OBP19b: p-value=0.778; OBP56g: p-value=0.001; OBP56d: p-value< 0.0001).

1.3. The impact of fasting on mRNA expression of OBPs

1.3.1. OBP56g

In the head of virgin females, OBP56g expression was significantly increased by “no fasting” and “30h fasting” compared to 2h and 16h fasting conditions, respectively (**Figure R-7.A**) (p-value < 0.0001). Meanwhile, OBP56g expression was very low in the head of males compared to the head of females. This suggests that the highly sexually dimorphic expression of OBP56g in female head could be induced by 30h fasting.

Conversely, OBP56g mRNA expression was higher in the gut of males than in that of females (**Figure R-7.B**) (p-value <0.05-0.0001). In male gut, no difference of expression was induced by fasting duration whereas in the gut of non-fasting females, OBP56d level of expression significantly decreased compared to 2h or 16h fasting conditions.

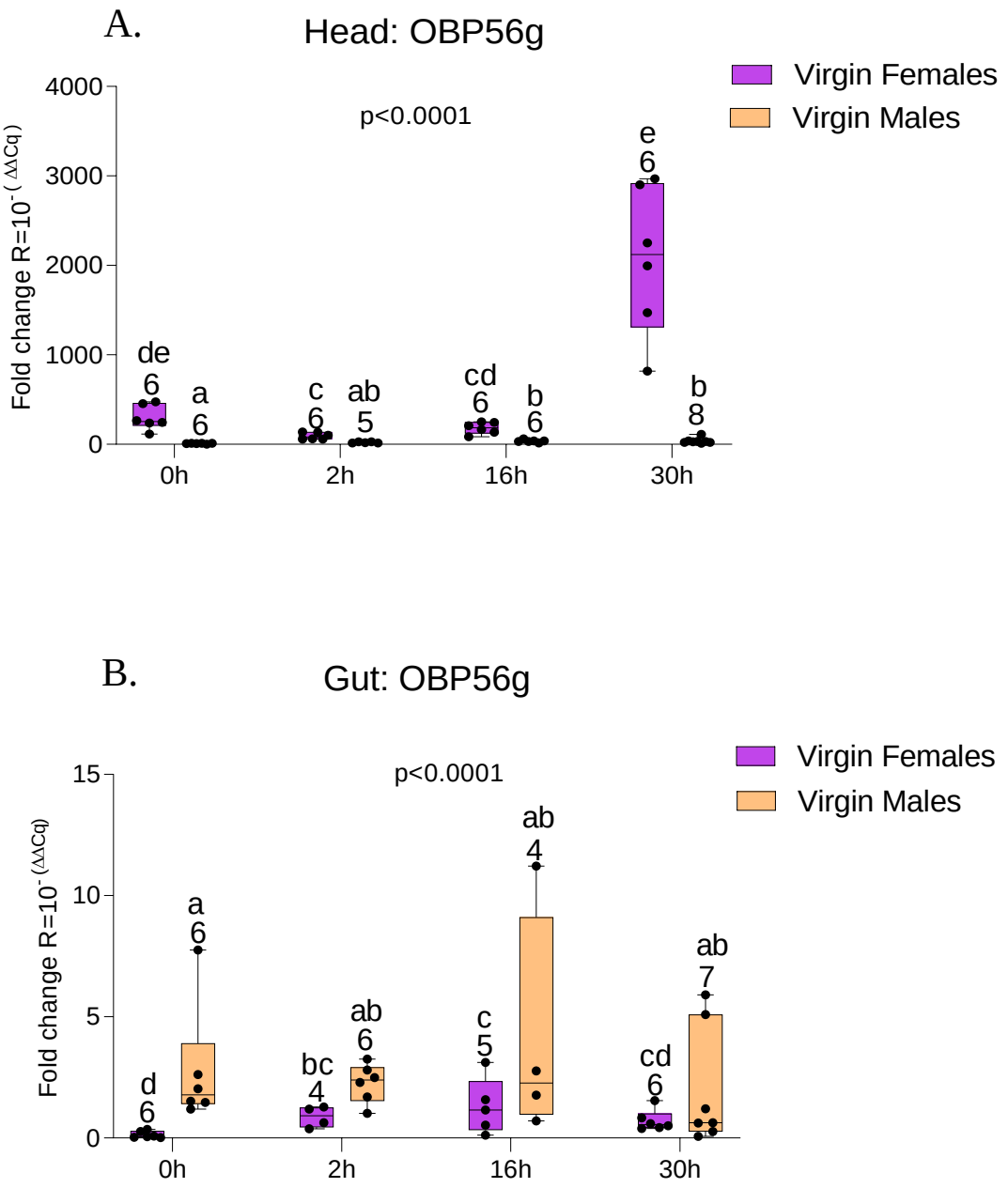

Figure R-7. Evaluation of fasting in the level of expression of OBP56g in the head (A) and in the gut (B) of *Drosophila melanogaster* flies

The thorax was used as a reference tissue (level of expression = 1) to compare the variation of OBP56g in the head and in the gut. The variation was compared between four fasting treatments: 0h, 2h, 16h and 30h. Data are shown as box plots which represent mRNA expression in two different tissues, head (A) and gut (B). Kruskal Wallis test was applied for each tissue. Data were tested with Kruskal Wallis test, post-hoc Conover-Iman with Bonferroni correction: Head $p<0.0001$ N=5-8; Gut $p<0.0001$ N=4-7. Different letters indicate significant differences.

1.3.2. OBP56d

The level of OBP56d expression was more important in female heads than in male heads (**Figure R-8**). Moreover, the head of females, but not of males, showed a quantitative variation related to fasting treatment (p-value = 0.001).

In the gut, OBP56d showed higher expression in males than in females (Kruskal Wallis test: p-value < 0.0001). No variation related to fasting duration was detected in either sex. Given such a strong sex-biased difference of OBP56d expression in the gut, we decided to investigate more precisely the region(s) of the male gut where this OBP was present.

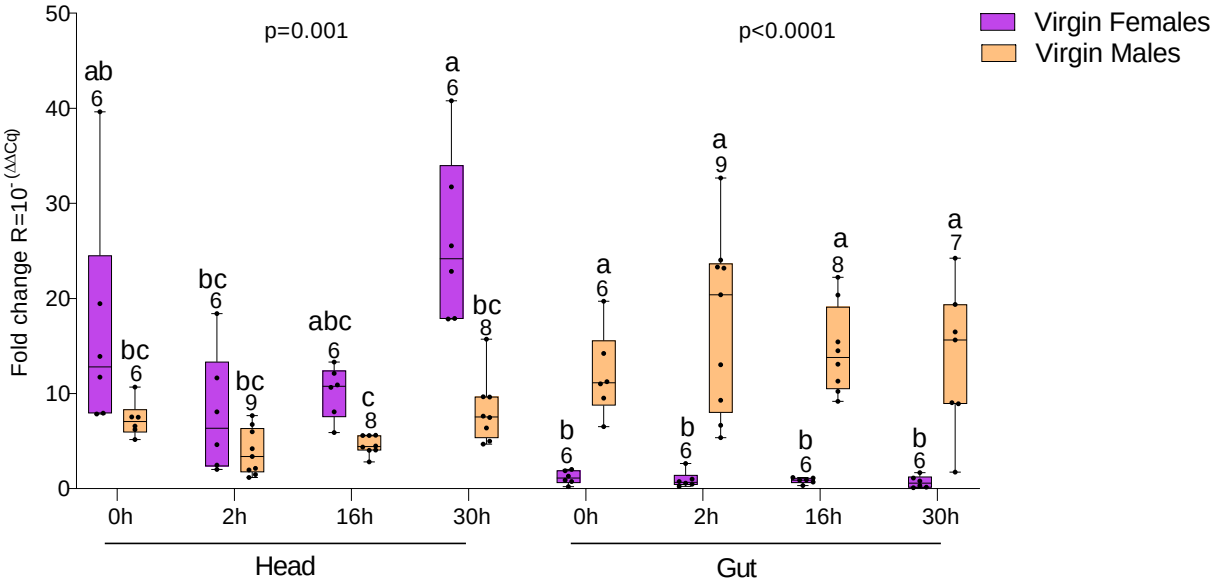

Figure R-8. Evaluation of fasting in the level of expression of OBP56d in the head (left) and in the gut (right) of *Drosophila melanogaster* flies

The thorax was used as a reference tissue (level of expression = 1) to compare the variation of OBP56d in the head and gut. The variation was compared between four fasting treatments: 0h, 2h, 16h and 30h. Data are shown as box plots which represent mRNA expression in two different tissues. In each tissue, Different letters indicate significant differences. Kruskal Wallis test was applied, with post-hoc Conover-Iman and Bonferroni correction. For the Head: p=0.001 N=6-8; For the Gut p<0.0001 N=6-8.

1.3.2.1. Expression of OBp56d in the parts of gut

We dissected the male gut into the three main portions (foregut, midgut and hindgut), and measured OBP56d expression in each portion, after 2h fasting. OBP56d appeared to be highly expressed in the hindgut, much more significantly than in the two other regions where its expression was very low (p-value = 0.001) (**Figure R-9**).

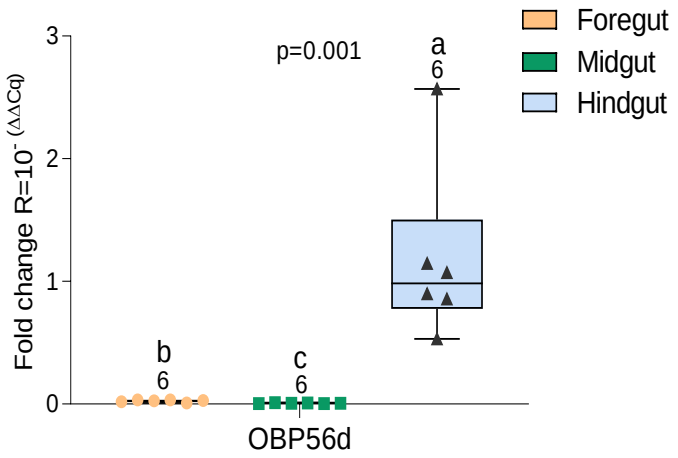

Figure R-9. OBP56d expression in the three gut regions of virgin males

The whole gut was used as a control tissue (level of expression = 1) and compared to OBP56d level in each of its three regions. Data were obtained in males subjected to 2h fasting. Data were tested with Kruskal Wallis test, post-hoc Conover-Iman with Bonferroni correction, p=0.001 N=6. Different letters indicate significant differences.

1.4.mRNA expression of OBP56d in gustatory system

Since we knew that OBP56d is expressed in the head with appendages, we needed to measure its expression in the proboscis (peripheral gustatory system). No inter-sex difference of expression was found in the head deprived of its appendages (**Figure R-10**; p-value = 0.857). This suggests that the OBP56d is no, or very poorly, expressed in the brain. Differently, OBP56d expression was relatively high in the proboscis of both sexes, with a tendency—but no statistical difference—for females to show a higher level than males (**Figure R-10**; p-value = 0.114). Since this experiment is based on 4 replicates for each sex, it will require to increase the number of samples to determine whether there is, or no, a sex difference for OBP56d quantitative expression in the proboscis.

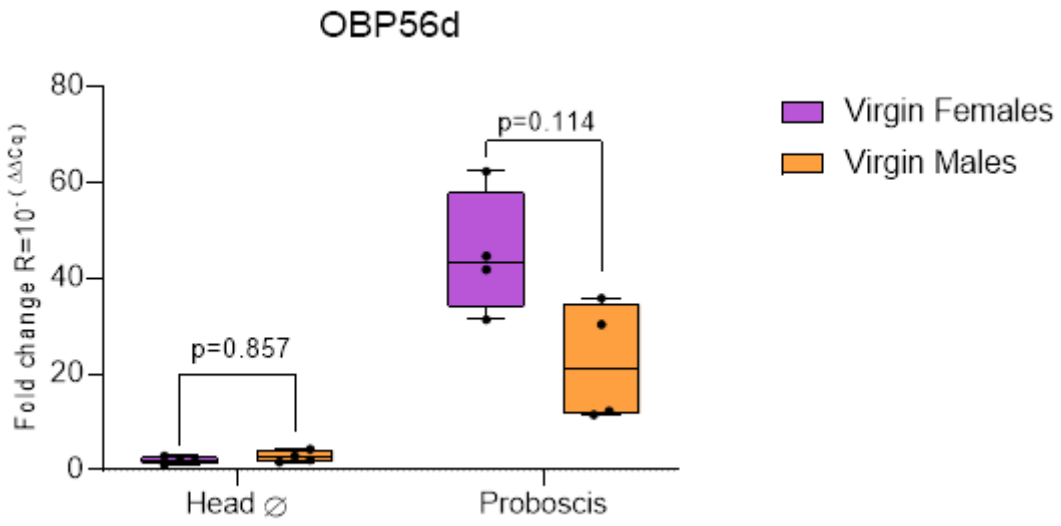

Figure R-10. OBP56d expression in the head deprived of sensory appendages (left) and in dissected proboscis (right) of *Drosophila melanogaster* female and male flies.

Thorax was used as a control tissue (level of expression = 1) to compare the variation of OBP56d in the head without appendages and in the proboscis. The variation was measured in virgin females and males after 16h fasting. Mann-Whitney test was applied for each tissue For the Head without appendages p=0.857 N=4; For the proboscis p=0.114 N=4.

1.5.mRNA expression of OBP56d, OBP56e, OBP56a in the parts of gut

Our next step aimed to obtain an antibody to detect the OBP56d protein in the fly body. Even though OBP56e and OBP56a, according to Flybase, do not have a substantial expression in gut, these OBPs show a high molecular similarity with OBP56d (**Figure R-11.A**). A multiple sequence alignment was performed to determine the similarity of their amino acid sequence. OBP56d has 38.17 % sequence resemblance with OBP56a and 63.36 % with OBP56e (**Figure R-11.B**.).

We verified the expression of OBP56e and OBP56a in the three parts of the gut, to indirectly validate the reliability of a potential antibody raised against OBP56d. Surprisingly, OBP56a and OBP56e were also expressed in the hindgut similarly to OBP56d (**FigureR-12**) (Kruskal Wallis test: OBP56d p-value = 0.001; OBP56a p-value = 0.002; OBP56e p-value = 0.002). Based on these differences and similarities, the Proteogenix SAS company proposed to design

a 15 amino acids peptide, the sequence of which covered the region showing the highest divergence between OBP56d and both OBP56e and OBO56a. It was necessary to choose a sequence as specific as possible to obtain the highest affinity in such designed polyclonal antibodies. The polyclonal antibody against OBP56d raised in two rabbits did not work and showed no specificity.

A.

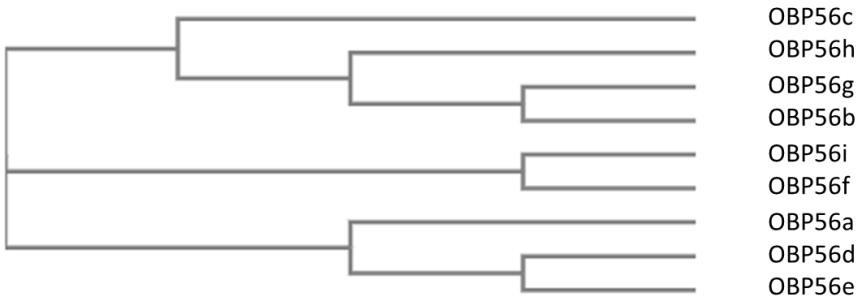

B.

```
OBP56a      MNSYFVIALSALFVTLAVGSSLNLSDEQKDLAKQHREQCAEEVKLTEEEKAKVNAKDFNN      60
OBP56d      MKFLIVLSVIL----AISAAELQLSDEQKAVAHANGALCAQQEGITKDQAIALRNGNFDD      56
OBP56e      MKVFFVFAALA----ALSLASAGLTDSQKAEAKQRAKACVKQEGITKEQAIALRSGNFAD      56
            *:  :*::           :.  *:*.**  *: .   *.::  :*:::   :.  :* :

OBP56a      PTENIKCFANCFFEKVGTLKDGELQESVVLEKLGALIGEEKTKAALEKCRTIKGENKCDT      120
OBP56d      SDPKVKCFANCFLEKIGFLINGEVQPDVVLAKLGPLAGEDAVKAVQAKCDATKGADKCDT      116
OBP56e      SDPKVKCFANCFLEQTGLVANGQIKPDVVLAKLGPIAGEANVKEVQAKCDSTKGADKCDT      116
               ::*******:*: * : :*::: .*** *** : **  .* .  ** : ** :****

OBP56a      ASKLYDCFESFKPAPEAKA 139   38.17 %
OBP56d      AYQLFECYYKNRAHI---- 131
OBP56e      SYLLYKCYYENHAQF---- 131   63.36 %
            :  *:.*: . :
```

Figure R-11. Phylogenetic tree of OBPs family with alignment of amino acid sequences in 3 OBP56.

A) Phylogenetic tree of OBP56s family. B) Clustal Omega was used as a program for multiple sequence alignment by using FASTA form of protein sequence for OBPs. A percentage of identity was presented for OBP56e and OBP56a compared to OBP56d. Symbols indicate: " * " positions which have a single, fully conserved residue, " : " conservation between groups of strongly similar properties, " . " conservation between groups of weakly similar properties. Red colour used for small and hydrophobic residue (AVFPMILW), blue colour used for acidic residue (DE), magenta colour used for basic and not H residue (RK) and green colour used for hydroxyl, sulfhydryl, amine and G residu (STYHCNGQ). The frame indicates the region chosen for antibody design.

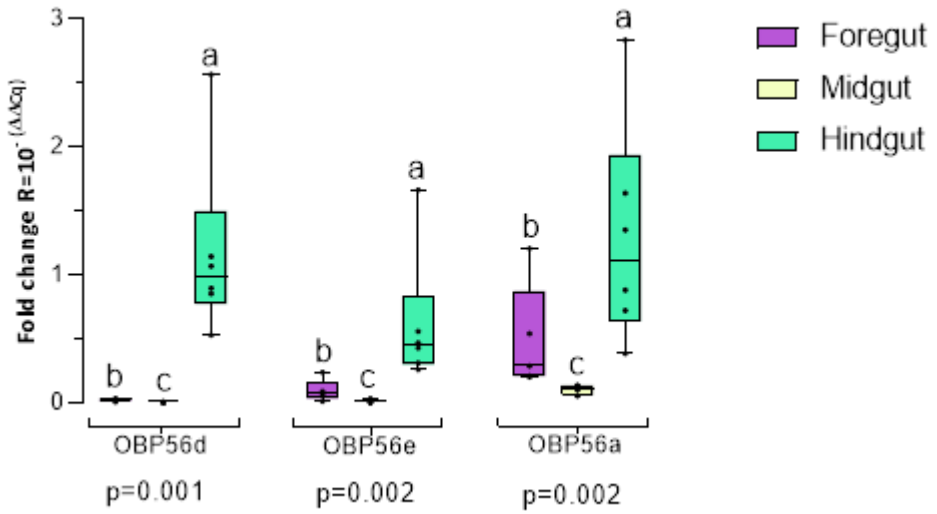

Figure R-12. Expression of OBPs in the three parts of the gut

The whole intestine was used as a control tissue (level of expression = 1) to compare the variation of OBP56d, OBP56e and OBP56a in its three regions. The variation was measured in virgin males after 2h fasting. Data are shown as box plots which represent mRNA expression in two different tissues. Kruskal Wallis test was applied in each tissue. Kruskal Wallis test, post-hoc Conover-Iman with Bonferroni correction was applied for each tissue. Different letters indicate significant differences for OBP56d: p-value ≤ 0.001, for OBP56e and OBP56a: p-value ≤ 0.01.

1.6. The impact of the bacterial microbiota on OBP56d and OBP56g mRNA expression

1.6.1. mRNA expression of OBPs in absence of microbiota

We manipulated the bacterial microbiota of lines by adding a mix of antibiotics in the diet of our experimental lines and during 2 generations. After these two generations spent on antibiotic-rich diet, we measured by RT-qPCR the expression level of OBP56d and OBP56g in the gut of resulting “axenic” flies.

To eliminate as much as possible the bacterial microbiota of flies, we used a large antibiotics spectrum (*see Material and methods*). Also, all these tests were carried out under a BSC. Moreover, we ran a control experiment in the same room, under the same conditions, in parallel to the experiment axenic lines. We measured the OBP56d expression in the head and in the gut of flies. In the gut of axenic virgin males flies, the expression of OBP56d

significantly decreased compared to the gut of untreated male flies (p-value = 0.006) (**Figure R-13**). This means that it was an impact of the absence of bacterial microbiota for the expression of OBP56d in the males gut. No similar effect was observed in females gut or in in the heads of females and males.

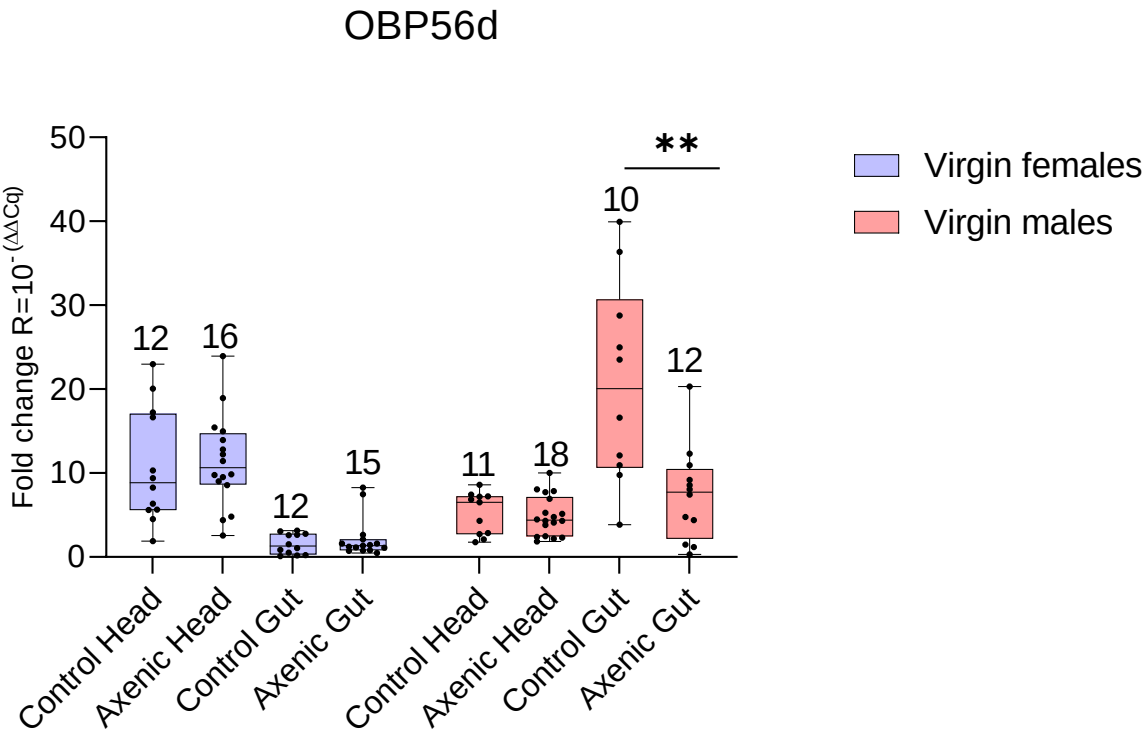

Figure R-13. Effect of bacterial microbiota elimination on OBP56d mRNA expression

4 days old flies were dissected after 2h fasting. Box plots show mRNA expression in females (left) and males (right). Mann-Whitney test was applied for each group-tissue to compare the mRNA expression in control and axenic culture. In Virgin females head and gut and in male head:, p-value >0.05; In virgin males gut: p-value < 0.01. Each experiment was triplicated.

OBP56g expression was also measured by RT-qPCR in axenic flies maintained in similar conditions. The level of expression significantly decreased in virgin female heads maintained in axenic culture compared to control female heads (p-value = 0.027). The absence of microbiota did not affect OBP56g expression in male heads or in the gut of both sexes (**Figure R-14**).

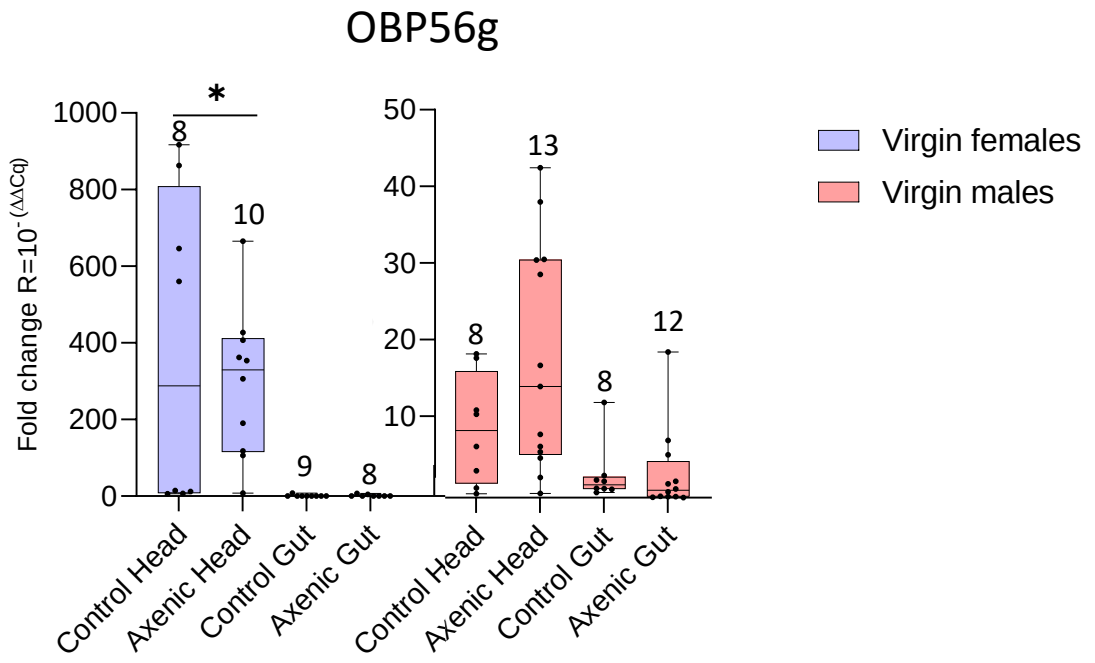

Figure R-14. Effect of bacterial microbiota elimination on OBP56g mRNA expression

4 days old flies were dissected after 2h fasting. Box plots show mRNA expression in females (left) and males (right). Mann-Whitney test was applied for each group-tissue to compare the mRNA expression in control and axenic culture. In virgin females head: p-value ≤ 0.05; For all other comparisons: p-value > 0.05. This experiment was duplicated.

1.6.2. mRNA expression of OBPs after introducing bacteria in an axenic culture

We further investigated the impact of the bacterial microbiota, in four experimental conditions. In the two first conditions, we separately introduced two types of bacteria (*A.pomorum* and *L.plantarum*) in the diet (sterilized medium) of experimental lines during two generations. In the two other conditions, we added in sterilized medium whole grinded guts of females or of males. In the four conditions, this was the diet provided to experimental lines during two generations. Axenic flies were maintained in similar conditions as described above and further tested the mRNA expression of OBPs by RT q-PCR.

There was no significant variation of OBP56d mRNA expression in the head or in the gut of female flies in the four experimental conditions compared to control or axenic gut (**Figure R-15.A**).

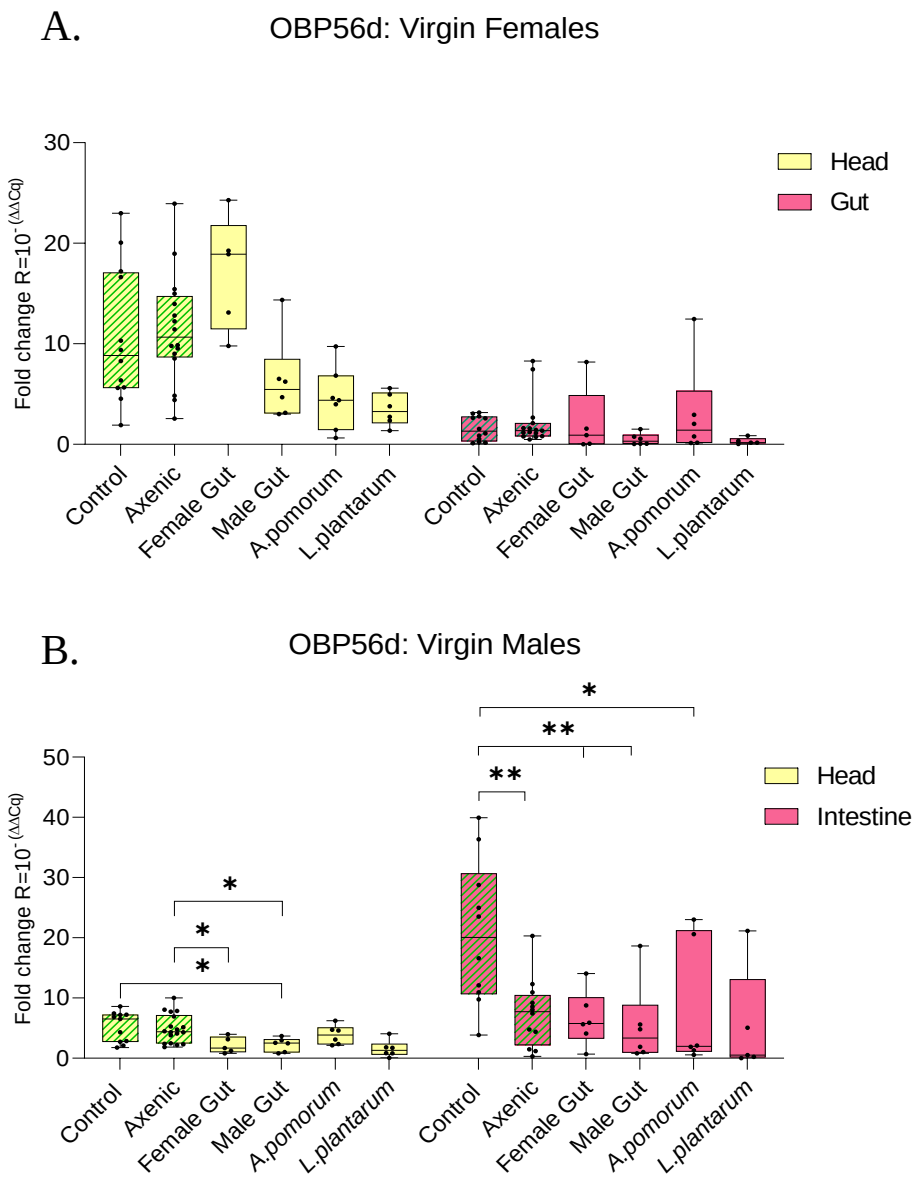

Figure R-15. mRNA expression of OBP56d resulting of four microbiota manipulations

4 days old flies were dissected after 2h fasting. Box plots show mRNA expression in the head (left) and gut (right). OBP56d expression in flies raised on control or axenic culture was compared in lines raised on axenic food added with female guts, male guts, *A.pomorum* or *L.plantarum*. Mann-Whitney test was used to compare the expression. A) Expression of OBP56d in virgin females. No significant effect for the head of for the gut. B) Expression of OBP56d in virgin males. In virgin males head, p-value < 0.05; In virgin males gut, p-value ≤ 0.01. Each experiment was only performed once.

In male heads, OBP56d expression was significantly decreased in “male gut medium” condition compared to control line. Also, both in “male gut medium” or “female gut medium” conditions compared to axenic culture the expression of OBP56d in the head was decreased (**Figure R-15.B**). Meanwhile, OBP56d gut expression was significantly decreased in the absence of microbiota. The expression of OBP56d in female gut, male gut and *A.pomorum* condition was decreased compared to control culture.

OBP56 expression could not be evaluated in the head of virgin females because we had not enough quantity of RNA left. No difference of expression was observed in the gut of virgin females between conditions (**Figure R-16.A**).

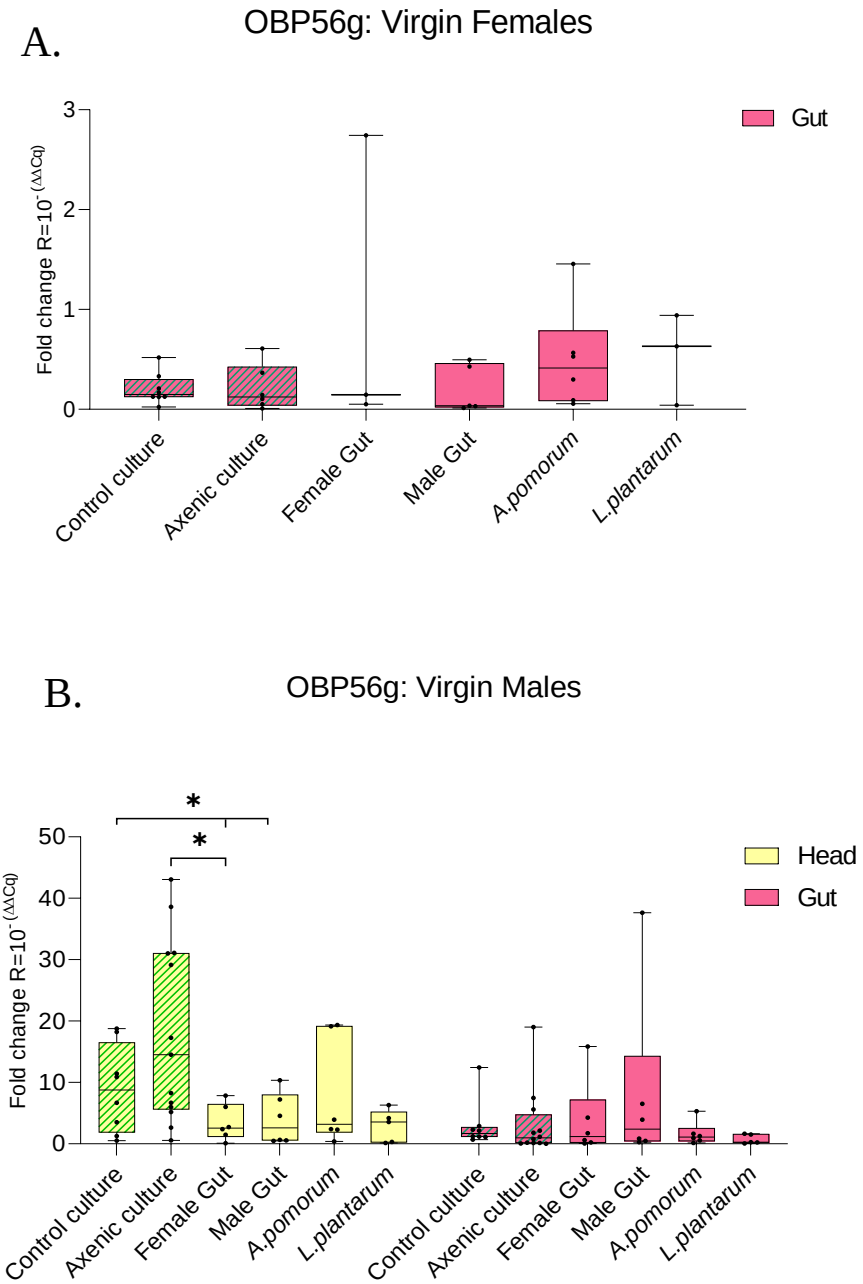

Figure R-16. mRNA expression of OBP56g resulting of four microbiota manipulations

4 days old flies were dissected after 2h fasting. Box plots show mRNA expression in the head (left) and gut (right). OBP56g expression in flies raised on control or axenic culture was compared in lines raised on axenic food added with female guts, male guts, *A.pomorum* or *L.plantarum*. Mann-Whitney test was used to compare the expression. A) Expression of OBP56g in virgin females. In virgin female gut: p-value > 0.05 B) Expression of OBP56g in virgin males. In virgin males head: p-value < 0.05; In virgin males gut: p-value > 0.05. Each experiment was only performed once.

In male heads, OBP56g expression was significantly decreased on the "female gut medium" compared to axenic and control culture. The head level of OBP56d expression decreased in "male gut medium" compared to axenic culture. No effect was found in male guts after testing these conditions (**Figure R-16.B**).

1.7. Sequencing bacterial microbiome

To better grasp the impact of microbiota on OBP56d and OBP56g expression, we aimed to determine the identity of bacteria present in the gut of our flies. We also needed to compare bacteria composition between the whole body and dissected guts. This work was carried out in collaboration with Prof. Deepa Agashe and Dr. Prathibas at NCBS (National Center for Biological Sciences, Bangaluru, India) and the analysis was done by these researchers.

We compared control flies raised in regular and in axenic conditions and *OBP56d*$^{-}$ mutant flies raised in standard conditions. Unfortunately, the fact that the flies of our control w^{1118} line were contaminated with *Wolbachia* introduced a major bias in the data analysis. Indeed at least 95 % of female and male flies were infested with Wolbachia (**Figure R-17.A**). This intracellular bacterium can modify the gut commensal microbiome and therefore induce physiological changes in Drosophila (Simhadri *et al.*, 2017). This may explain why, in our case, we did not detect *Lactobacillus plantarum* and very few *Acetobacter* in our control flies raised on regular diet. The composition of body and gut microbiome were similar in females and males.

The bacterial microbiome of axenic flies was very different from that found in control flies (see above). This was mainly due to strongly decreased occurrence of Wolbachia in the fly bodies and total absence in their guts. This effect was likely due to the use of Tetracyclin (in the antibiotic mix used to generate axenic lines) known to eliminate Wolbachia. Despite the

absence of *Wolbachia* neither the *A.pomorum* or the *L.plantarum* bacteria were detected (**Figure R-17.B**). *Acinetobacter* was present both in the body and in the gut of flies. *Izhakiella* was found in the gut. This gram-negative bacterium belongs to the Enterobacteriaceae family and has been often found in the Drosophila gut. *Izhakiella* was the dominant bacteria in our axenic flies.

Unfortunately, our preliminary data for mutant flies remain to be confirmed and specially those for female bodies which are missing due to a technical problem (**Figure R-17.C**). We believe that this will be done soon, so the complete data could be integrated in the final version of this PhD thesis.

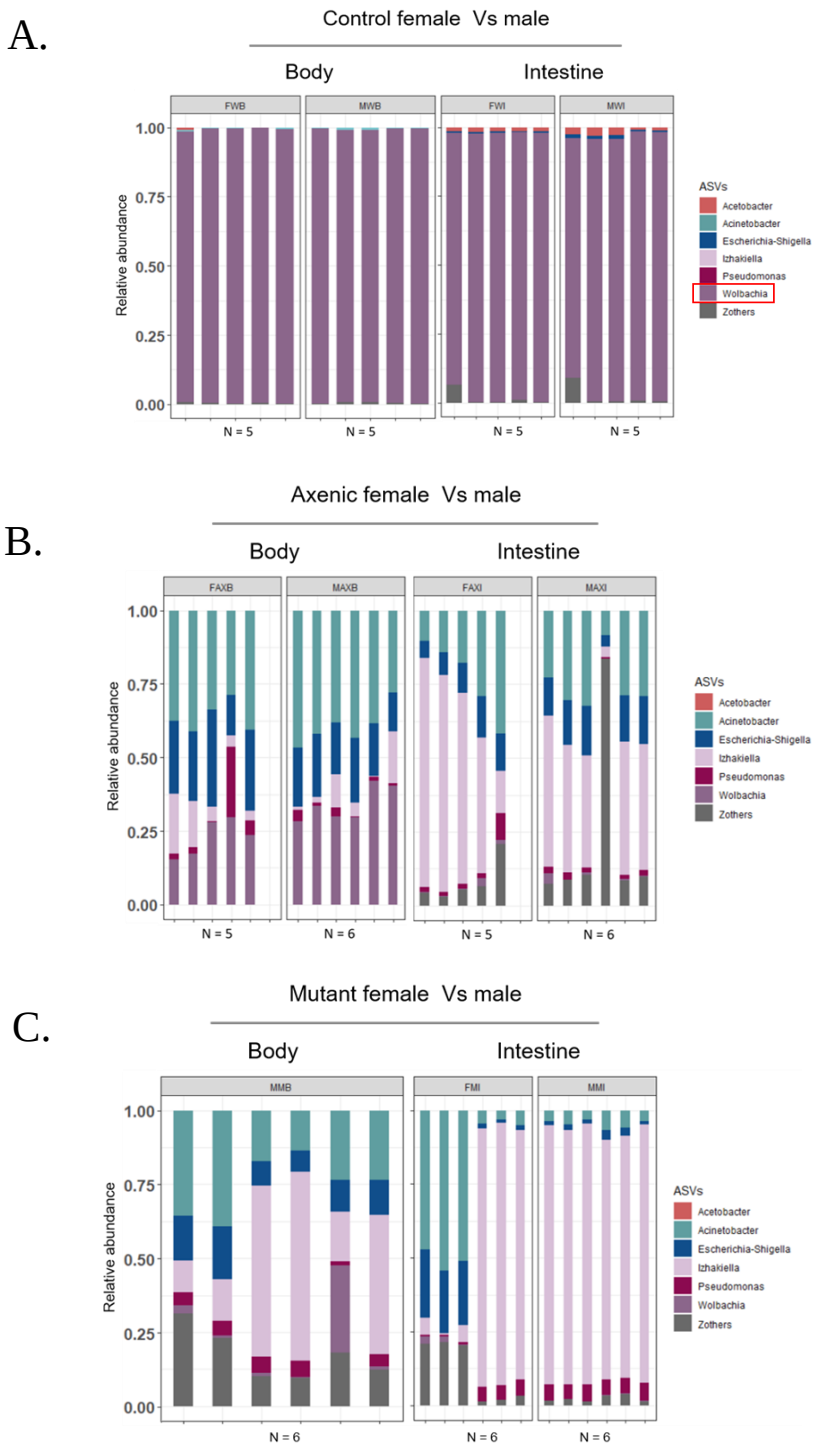

Figure R-17. Microbiome composition in control, axenic and mutant *OBP56d-* flies.

The bacteria present in the body and in the gut were sequenced (sample size n=5-6). Non-fasting 4 days old flies were tested. The microbiome composition was evaluated in control, axenic and mutant *OBP56d-* flies. The data is presented in relative abundance of identified species from 0 to 1 (meaning 0 to 100% of presence).

2. Heterologous expression of OBPs using *E. coli* bacteria

2.1. Production and purification of OBPs

For each recombinant OBP, a single band, corresponding to the expected molecular mass of the purified protein, was observed on SDS-PAGE. The culture was set at 37°C for 2 to 3 hours and after the optic density, OD at 600nm reached between 0.5 to 0.6, the chemical inducer IPTG was added to the culture medium. The TB culture was placed at 30°C for 6h. These were the optimal conditions after testing several combinations of cultures and temperatures. Both OBP56d and OBP56g were produced under similar conditions. They were purified in HisTrap^{TM}HP 1mL column as explained in (*Section 6 of Materials and Methods*). The elution fractions were collected and analysed by SDS-PAGE (**Figure R-18**).

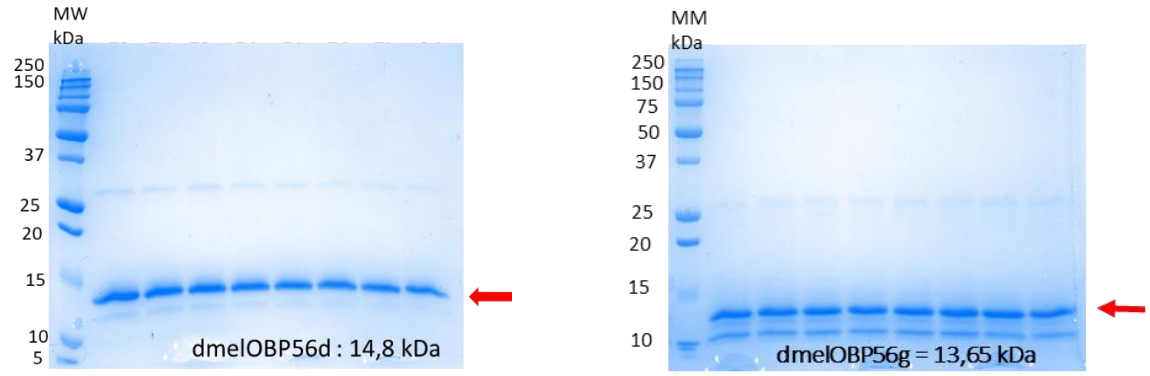

Figure R-18. Purification of recombinant OBPs

OBP56d and OBP56g were purified from cell culture supernatant using metal ions immobilized on the chromatography. The eluted franctions were collected and analysed using SDS-PAGE. Proteins were stained using Bio-SafeTM Coomassie (Bio-Rad). The MW (kDA) lane shows the molecular weight standard 5-250 kDa (Precision plus protein Dual Xtra" marker, Bio-Rad). Different fractions of purified protein were collected and evaluated SDS-PAGE gel. The red arrow indicates the presence of OBPs after migration.

A single band, corresponding to the expected molecular mass of the OBPs was observed on SDS-PAGE. To estimate the level of OBP product, the concentration of purified proteins from culture supernatant was determined using UV absorbance at 280 by using its molar extinction coefficient at 280 nm (ε280 OBP56d = 6.335 M-1.cm-1; ε280 OBP56g = 2.980 M-1.cm- 1) and its molecular mass (M OBP56d= 14.884 kDa; M OBP56g= 13.646 kDa). For OBP56d and OBP56g, we obtained around 8mg/L and 1mg/L, respectively. To remove the second band, we tried further purification by gel filtration, but the OBP quantity lost was very high

while the unwanted band was still there. We estimated that the quality was very good in these conditions and therefore that it was possible to test binding affinity of these OBPs.

2.2.Biophysical analysis of recombinant OBP56d

Circular dichroism (CD) spectrometry is widely used to estimate the secondary structure content of proteins. The far-UV CD spectrum (**Figure R-19**) of OBP56d revealed two positive peaks (195.5 nm and 255 nm) and a negative one (210 nm). This secondary structure corresponds to 20 % of α-helices, 30 % of β-helices, 15 % loop and 33.6 % not structured. These values are expected for secondary structures of insects OBPs with a 3D structure making a pocket formed by five or six α-helices (Briand *et al.*, 2001; Zhou, 2010). These data indicate that OBP56d was properly folded.

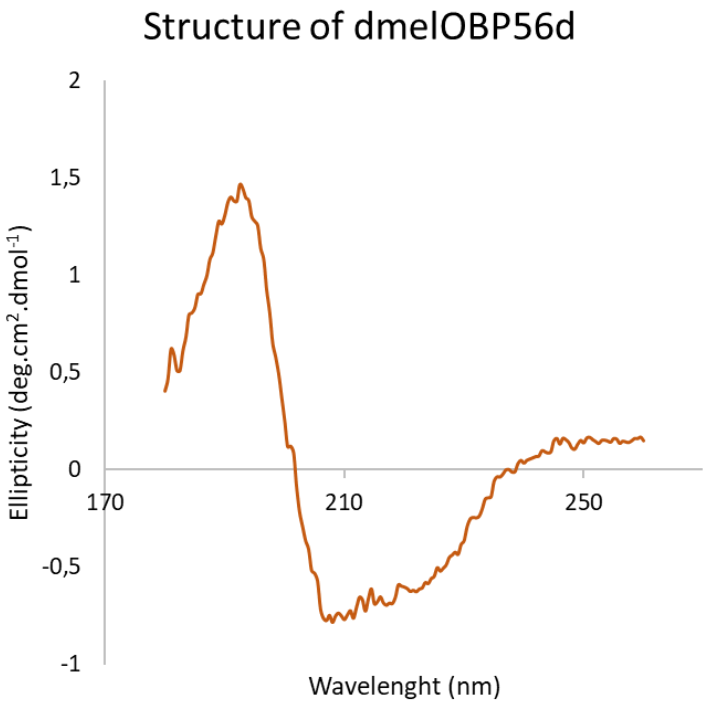

Figure R-19. Biochemical characterization of the recombinant OBP56d.

Characterization of OBP56d folding based on circular dichroism spectroscopy. Far-UV circular dichroism spectrum of OBP56d measured from 180 to 260 nm. The protein concentration was 1.2mg/mL in 50mM NaF pH 7.5.

2.3.Ligand-binding properties of *Drosophila melanogaster* OBPs

2.3.1. Binding affinities of OBPs to Sypro orange

We investigated the binding affinities of the two purified OBPs using the Sypro orange probe (Steinberg, 2009). OBP56g and OBP56d bound the fluorescent Sypro orange probe. NPN and 1-AMA probe were tested with both OBPs, but they did not show binding affinities (Pelosi et al., 2006). The spectra were recorded between 500 and 700 nm with an excitation wavelength of 490 nm (**Figure R-20.A**). The control tank with Sypro Orange showed a low fluorescence and the complex OBP – Sypro Orange showed high fluorescence when put in contact. The maximum emission shifted to 580 nm with a quantum yield increase of 10-fold for OBP56d and OBP56g. The saturation for OBP56d was at 2.08 µM of Sypro Orange (**Figure R-20.B**); For OBP56g it was at 1.2µM of Sypro Orange (**Figure R-20.C**).

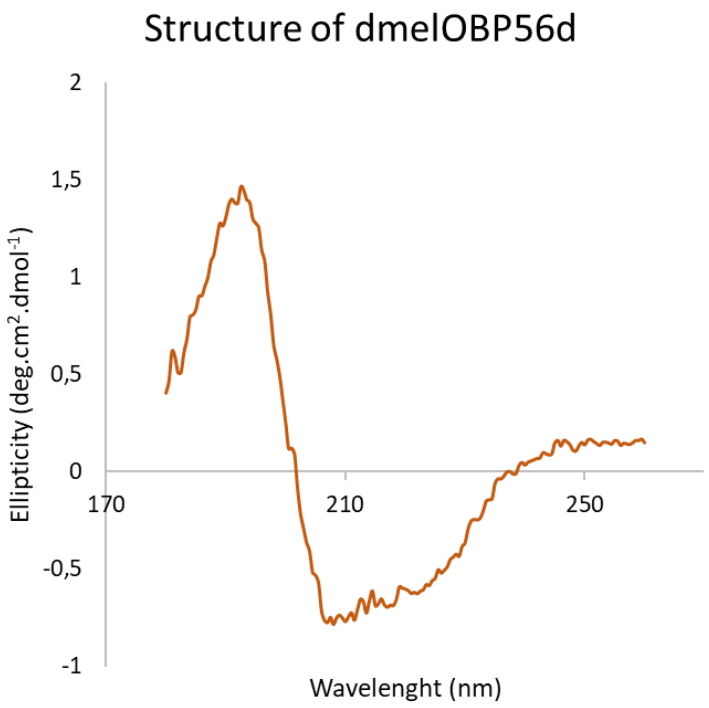

Figure R-19. Biochemical characterization of the recombinant OBP56d.

Characterization of OBP56d folding based on circular dichroism spectroscopy. Far-UV circular dichroism spectrum of OBP56d measured from 180 to 260 nm. The protein concentration was 1.2mg/mL in 50mM NaF pH 7.5.

2.3.2. Binding affinities of OBPs to tastant compounds

1.*A- Determination of fluorescent probe of OBPs*

First, we determined the probe that had an affinity for OBPs. We measured the probe alone and the complex OBP-probe. In our case, Sypro Orange was the probe that had an affinity for both OBPs. This was presented by the augmentation of fluorescence intensity in the presence of OBP (**Figure R-20.A**). We measured the dose-response of the Sypro Orange probe in presence of each OBP to determine the point of saturation, indicating the amount of probe to use for each case (**Figure R-20.B.C**).

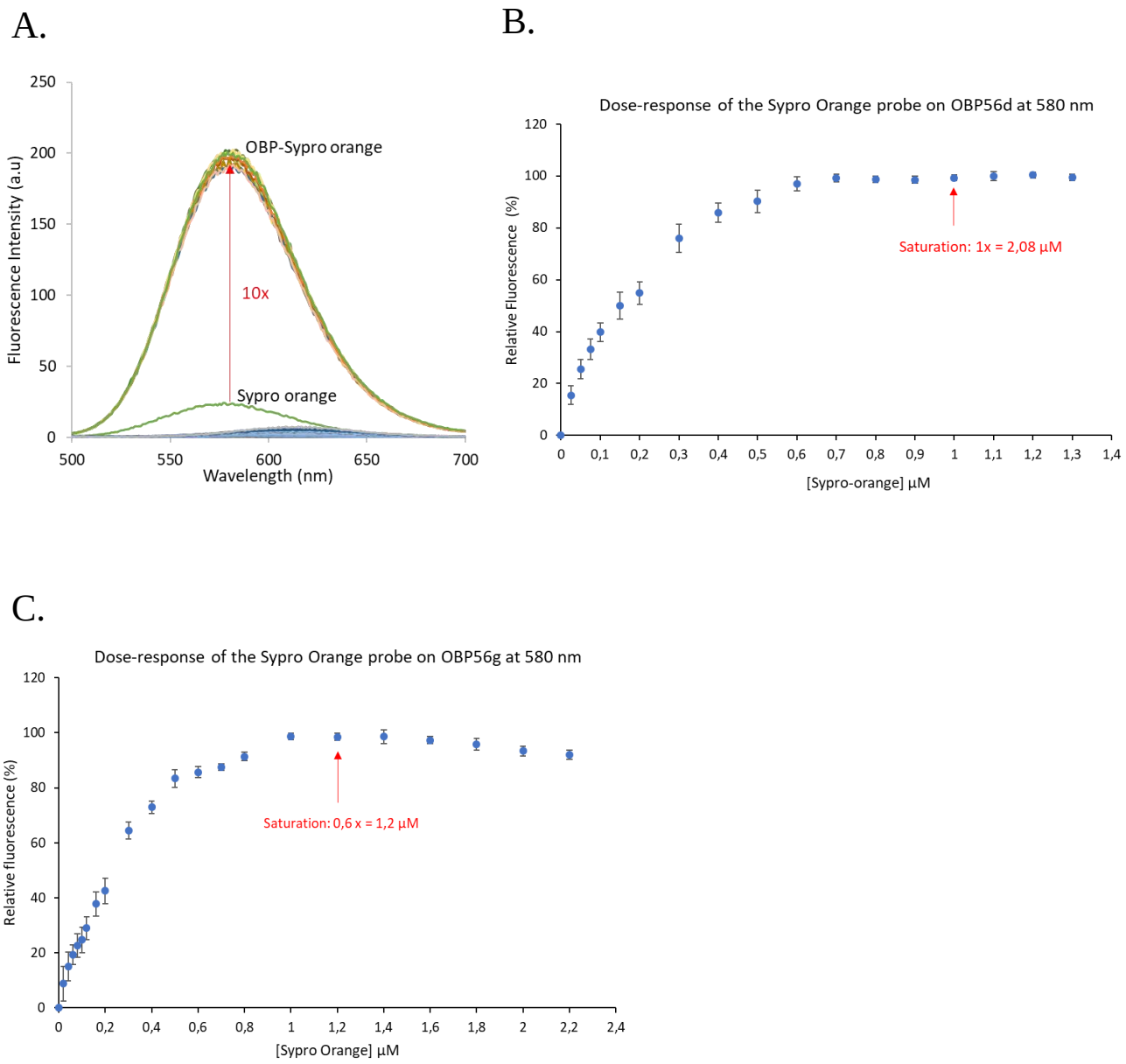

Figure R-20. Sypro-Orange fluorescent binding assay

A) Presentation of emission shift between the control tank (Sypro-Orange) and the three tanks (Complex OBP - Sypro-Orange). Spectra recorded at 25°C of 1X or 0.6X Sypro-Orange in presence of 2µM OBP56d or OBP56g. B) Dose-response of the Sypro-Orange probe on OBP56d at 580nm. Saturation of solution at 2.08µM of Sypro-Orange (1X). C) Dose-response of the Sypro-Orange probe on OBP56g at 580nm. Saturation of solution at 1.2µM of Sypro-Orange (0.6X).

2. B- Screening of molecules via competitive binding assay

A large spectrum of tastants molecules was tested with OBP56d and OBP56g. These compounds represent several classes of chemical structures which possess distinct taste qualities.

Their affinity was tested in a competitive binding assay with the fluorescent Sypro Orange probe in tanks. We ran a control tank where the solvent used for the tested molecule was added. For the other three tanks the compound tested was added with increasing concentrations (0, 0.5, 1, 2, 5, 10, 15, 25 and 40µM).

Dissociation constants for Sypro Orange were calculated using the software Sigma plot. Dissociation constants of the competitors were calculated by the equation K_D = IC50/ (1 + [Sypro Orange]/$K_{Sypro\ Orange}$), where IC_{50} is the concentration of ligands halving the initial fluorescence value of Sypro Orange, [Sypro Orange] is the free concentration of Sypro Orange, and $K_{Sypro\ Orange}$ is the dissociation constant of the complex OBP/Syro Orange. The obtained K_D was converted in $1/K_D$ (10^6). Based on the K_D bitter molecules, amino acids, triglycerides, sugar, pheromones or antibiotics did not show affinity for OBP56d (**Figure R-21.A**). Differently, fatty acids, like α-Linolenic acid and Palmitoleic acid showed a high affinity for OBP56d and for OBP56g (**Figure R-21.A.B**).

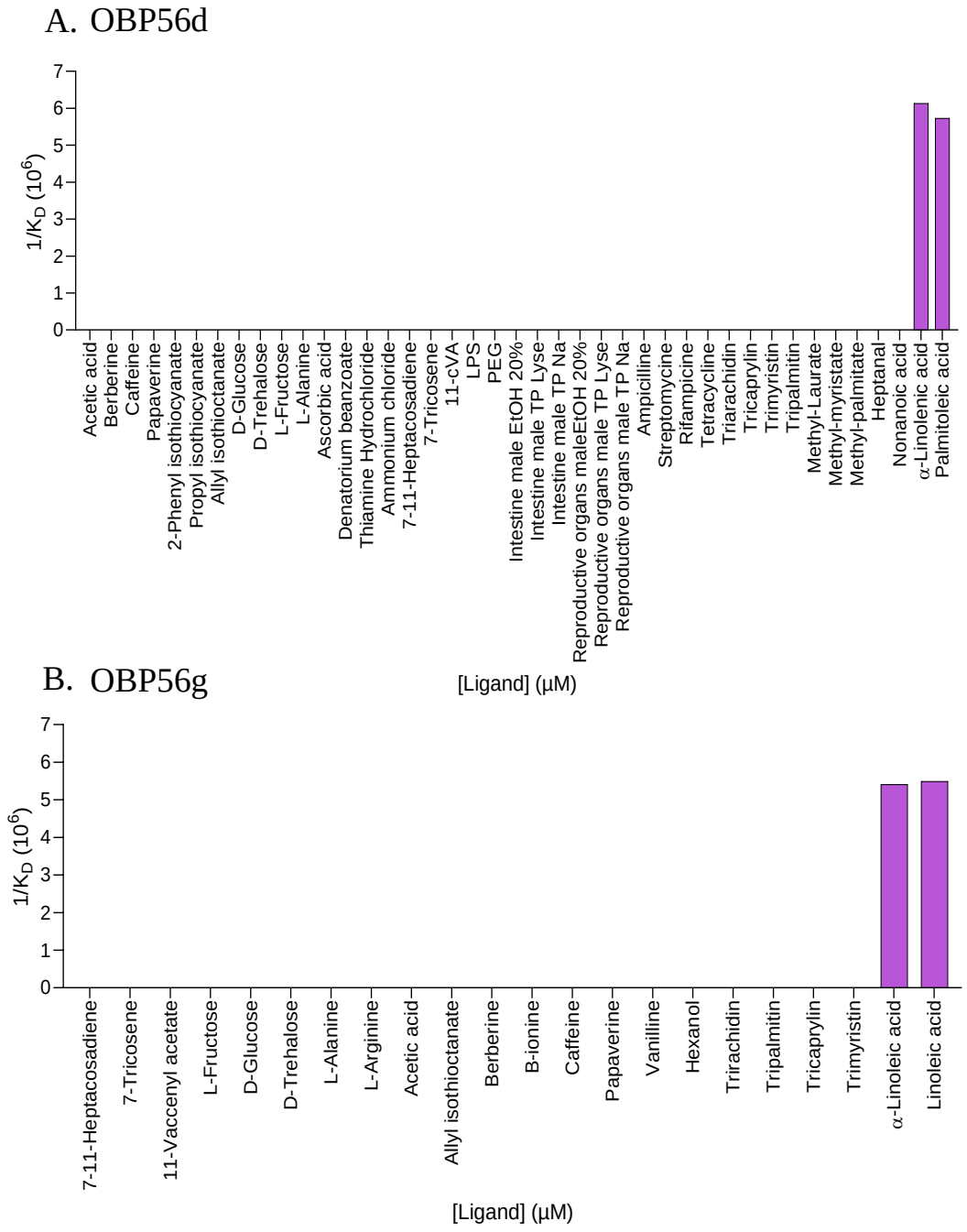

Figure R-21. Binding properties of OBP56d and OBP56g revealed with a competitive fluorescent assay.

The fluorescent displacement of the fluorescent Sypro-Orange probe by various tastant compounds was evaluated for OBP56d. Binding assays were performed at 25°C in four tanks (one control and three independent replicates with the OBP - Sypro-Orange complex). The data are presented in $1/K_D$. A) Biding affinity of OBP56d. Among 40 ligands tested, only α-Linolenic acid (Polyunsaturated fatty acids) and Palmitoleic acid (Monounsaturated fatty acids) showed an affinity for OBP56d. B) Binding affinity of OBP56g. Among 22 ligands tested, only α-Linolenic acid (Polyunsaturated fatty acids) and Palmitoleic acid (Monounsaturated fatty acids) showed an affinity for OBP56g.

3. C- Binding ability of OBPs to fatty acids

Given the unexpected binding ability of OBPs to these fatty acids (FAs), we tested a wider FA range (with varied carbon length chain, number of unsaturation and presence of a methyl group) (**Table R.5**). The fluorescence displacement was calculated for each ligand tested at 15µM. A reduction (at least > 20%) in the fluorescence intensity of the OBP56d – Sypro Orange complex was observed with Myristic acid, Palmitic acid, Palmitoleic acid, Oleic acid, Stearic acid, α-Linolenic acid, Linoleic acid, Arachidonic acid, Eicosapentaenoic acid (EPA), Docosahexaenoic acid (DHA) and Docosanoic acid (**Figure R-22**). OBP56d had an affinity for long chain fatty acids ≥ C14 with the higher fluorescent displacement for Palmitic acid, Oleic acid, Linoleic acid and DHA.

With OBP56g, bitter molecules, amino acids, triglycerides, sugar or pheromones did not show any affinity. Based on the K_D affinity, OBP56g showed an affinity for similar FAs as for OBP56d (**Figure R-23**).

OBP56g showed a substantial affinity for Butanoic acid, Oleic acid, Linoleic acid, Arachidic acid, EPA and DHA. The fluorescent displacement at 15µM for Oleic acid, Linoleic acid, EPA and DHA was lower than for OBP56d. OBP56g had more affinity for Butanoic acid and Arachidic acid than OBP56d (**Figure R-23)**.

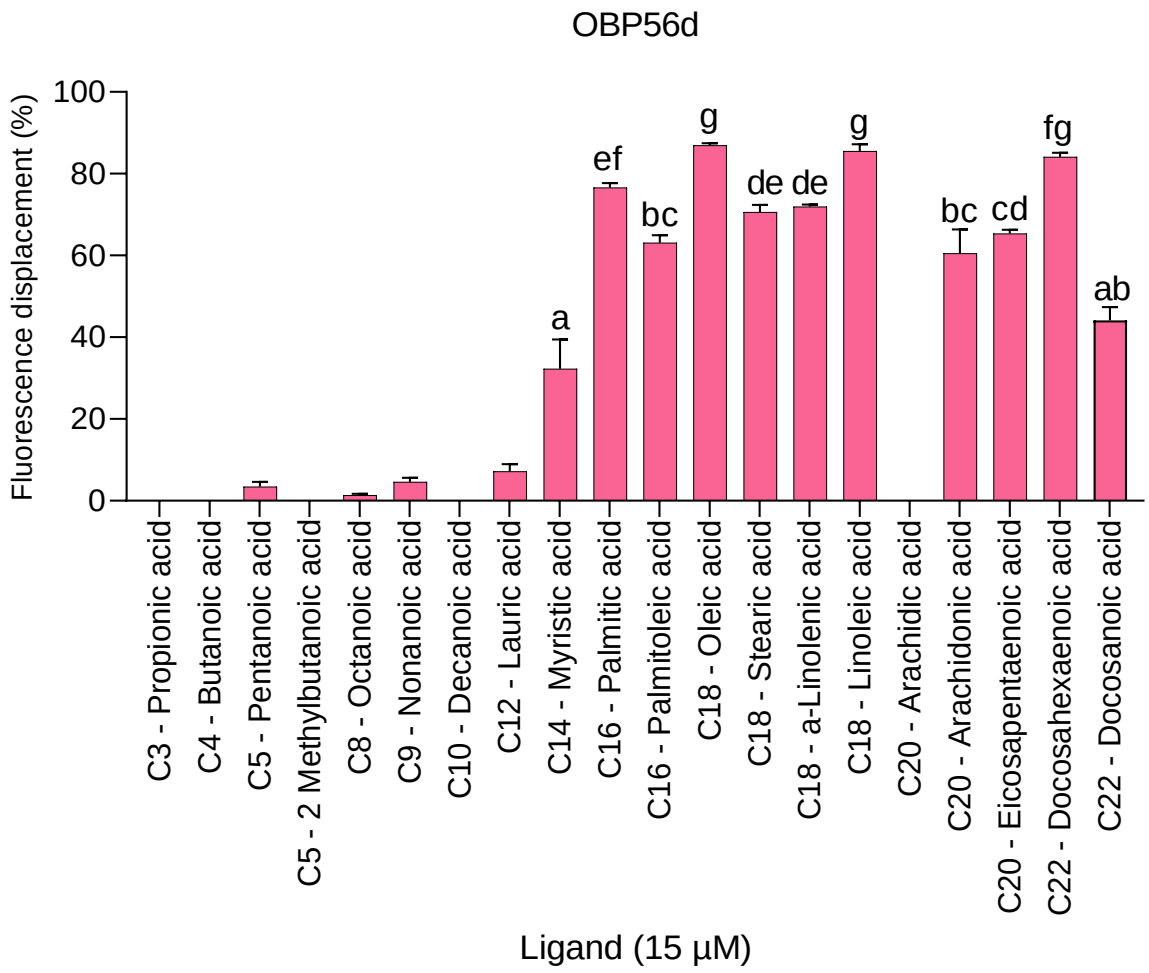

Figure R-22. Binding affinity of OBP56d for fatty acids

The fluorescent displacement of the fluorescent Syrpo-orange probe by various fatty acids (FAs) at the final concentration of 15µM was evaluated in OBP56d. A binding affinity of OBP56d was shown above C12 chain length FA. Only ligands that induced at least 20 % of fluorescence displacement were taken in account for Kruskal-Wallis test, post-hoc Conover-Iman, Bonferroni correction. Different letters indicate significant differences. Each ligand was tested in biological triplicates. Palmitic acid, Oleic acid, Linoleic acid and DHA showed the most important binding (with a fluorescent displacement > 80%).

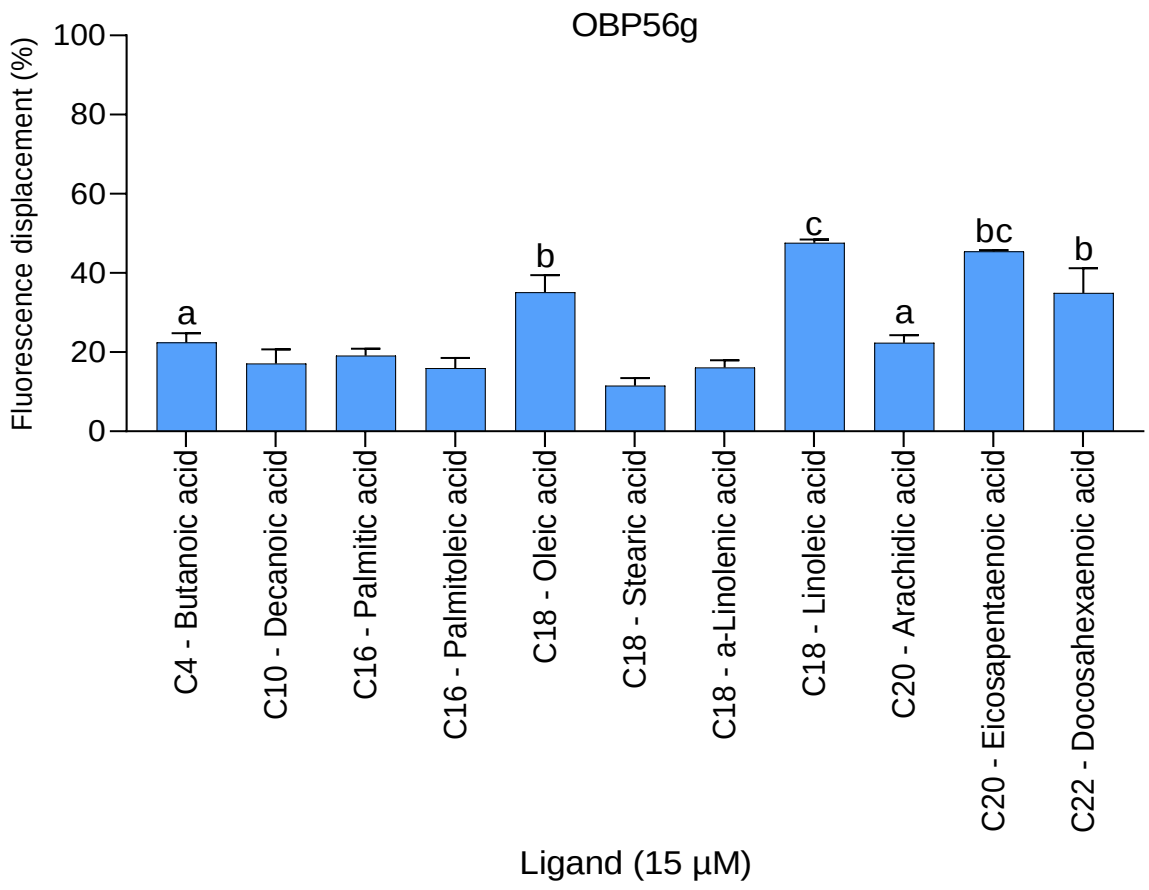

Figure R-23. Binding affinity of OBP56g for fatty acids

The fluorescent displacement of the fluorescent Syrpo-orange probe by various fatty acids compounds at the final concentration of 15µM was evaluated in OBP56g. Only the ligands that induced at least 20 % of fluorescence displacement were taken in account for Kruskal-Wallis test, post-hoc Conover-Iman, Bonferroni correction: Different letters indicate significant differences. Each ligand was tested with three independent replicates. Oleic acid, Linoleic acid, EPA and DHA showed the most important binding.

Table R.5. List of fatty acids tested with OBP56d and OBP56g.

The carbon length chain, the number of unsaturations, the IC50 (one-half of fluorescence value of Sypro Orange) and K_D of OBPs (dissociation constant) for each fatty acid tested was presented in the table.

			OBP56d		***OBP56g***	
Fatty acids	**C chain**	**Number unsaturations**	**IC_{50}**	**K_D**	**IC_{50}**	**K_D**
Propionic acid	3	0	ND	ND	-	-
Butanoic acid	4	0	ND	ND	28.26	90482
Pentanoic acid	5	0	123.8	35.5	3.06	2.58
Octanoic acid	8	0	ND	ND	-	-
Nonanoic acid	9	0	13.02	24.6	-	-
Decanoic acid	10	0	ND	ND	-	-
Lauric acid	12	0	56.1	115.4	-	-
Myristic acid	14	0	18.5	30.4	-	-
Palmitic acid	16	0	2.2	2.8	2.3	2.14
Palmitoleic acid	16	1	3.2	4.3	12.78	39.72
Oleic acid	16	1	2.4	2.2	6.57	4.11
Stearic acid	18	0	3.2	3.1	6.72	6.59
α-Linolenic acid	18	3	1.68	1.78	11.58	21.69
Linoleic acid	18	2	4.8	7.5	6.98	11.33
Arachidic acid	20	0	ND	ND	1.91	1.58
Arachidonic acid	20	4	7.6	14.1	-	-
Eicosapentaenoic acid	20	5	4.7	6.5	21.57	11.08
Docosahexaenoic acid	22	6	4.2	5.6	10.31	3.1
Docosanoic acid	22	0	17.7	15.4	-	-

3. Expression pattern of OBP56d in *Drosophila melanogaster*

3.1. Proboscis mRNA expression *via in situ* hybridization

Given that our transcriptional study (RT-qPCR) revealed that OBP56d was highly expressed in the proboscis and in the gut of males, we attempted to determine its expression profile by immunolabelling of these tissues. Proboscis labelling in 4 days old virgin females or virgin males of the *w-* line was visualized with a Leica sp8 confocal microscope. The images show that OBP56d was expressed in both sexes but we can not detect any obvious difference of mRNA expression in the proboscis (**Figure R-24.A.B**).

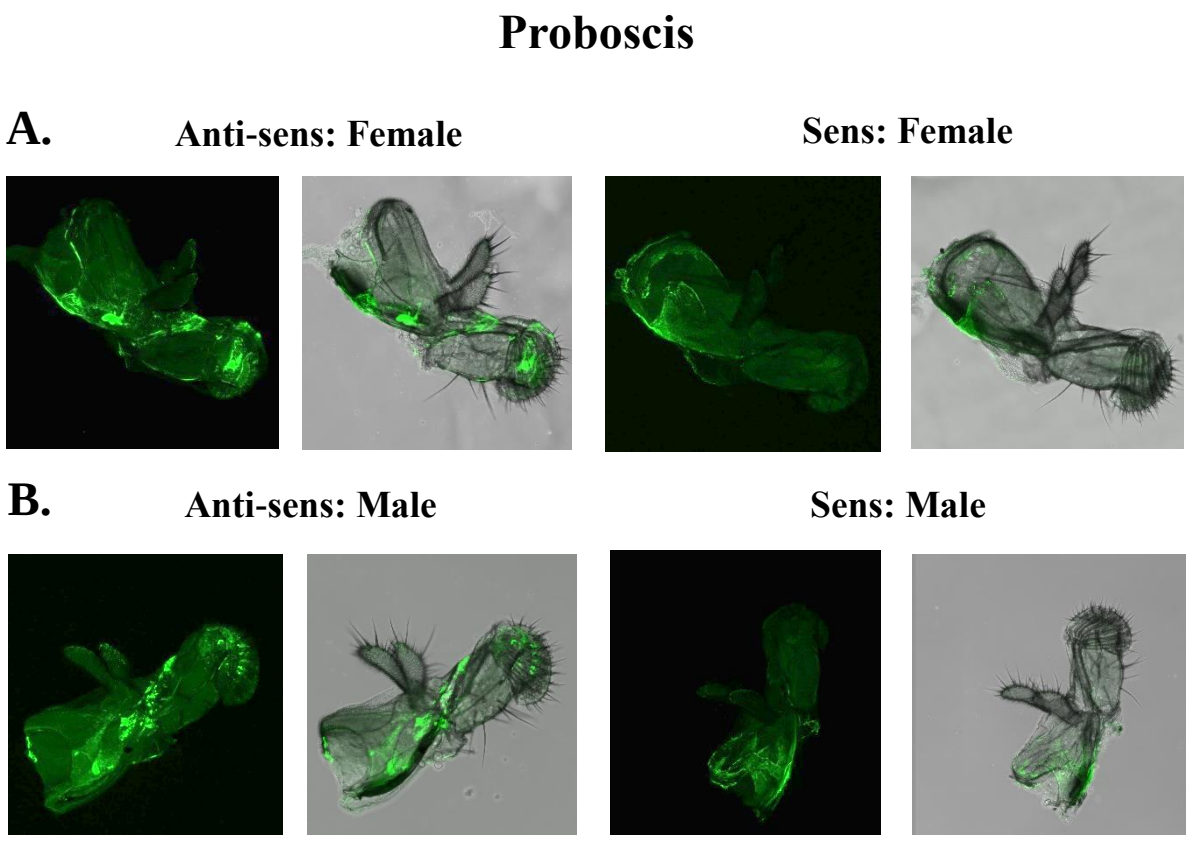

Figure R-24. Expression pattern of OBP56d in Drosophila proboscis in control females and males

4 days old flies were dissected after 16h fasting. The anti-sens probe detects mRNA expression of OBP56d while the sens probe serves as a control. A) OBP56d expression in female proboscis. B) OBP56d expression in male proboscis.

3.2. Gut mRNA expression *via in situ* hybridation

Given that our RT-qPCR data indicated that OBP56d is expressed in the male hindgut, we needed to confirm these data with the immunolabelling approach. We used the OBP56d probe similar as that used for the proboscis to map the tissue-specific expression of the OBP. We used the dissected gut of flies subjected to 16h fasting (to avoid the autofluorescence of food remaining in the gut).

The expression profile of OBP56d was observed in the foregut, midgut and hindgut of virgin females and virgin males. In virgin females, there was only a faint expression of OBP56d in the hindgut (**Figure R-25**).

In virgin males, clearly defined expression was only found in the hindgut and more precisely in the rectal ampulla (**Figure R-26**). This observation somewhat confirmed our RT-qPCR data.

The mRNA expression of OBP56d, visualized by immunolabelling, was also searched in the gut of females and males after copulation but no obvious difference of expression was observed when compared with same-sex virgin flies (data not shown). Given that the mRNA expression in the male hindgut was close to male internal reproductive organs, we thought to evaluate the expression of OBP56d in the reproductive organs.

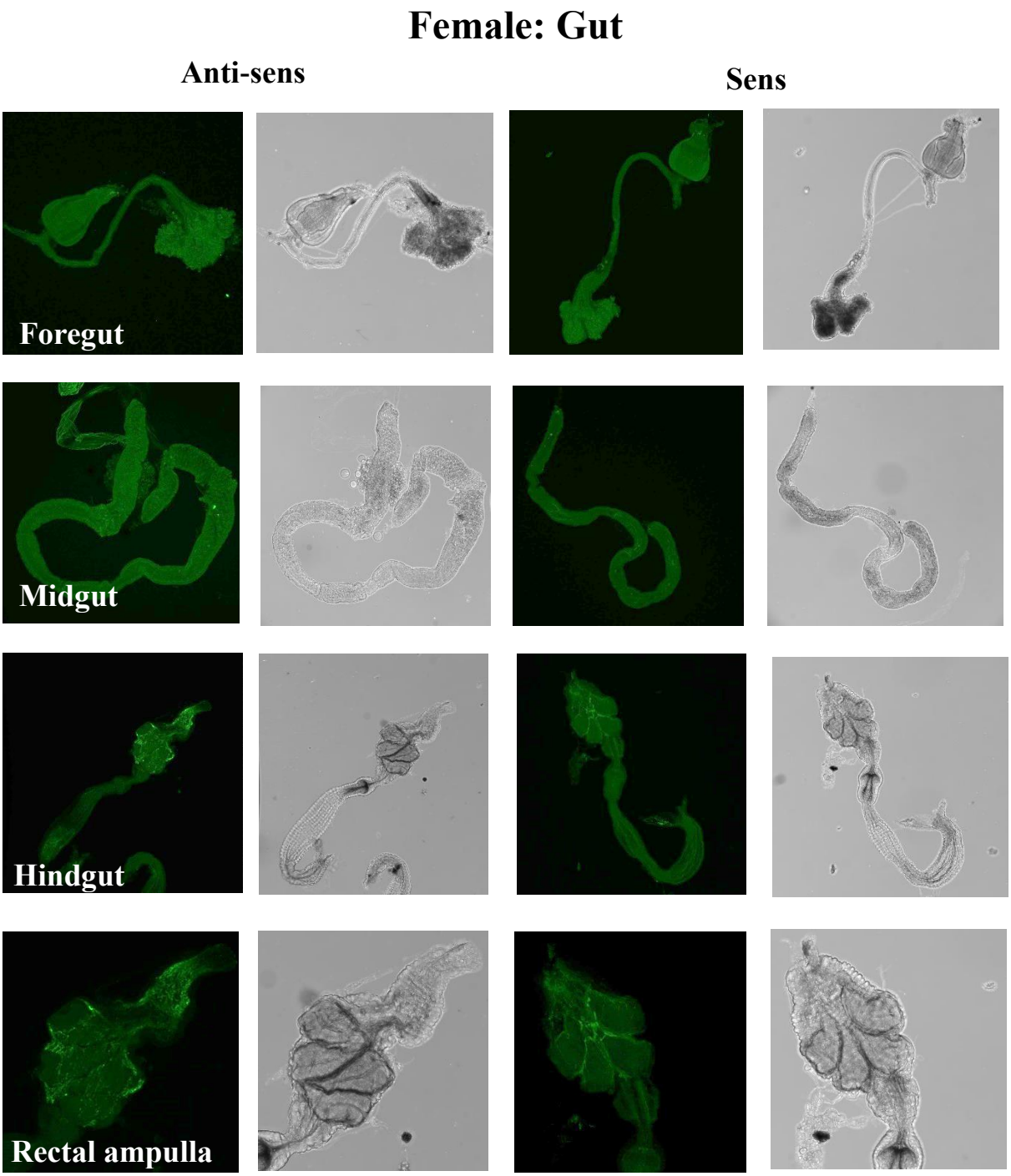

Figure R-25. OBP56d expression in virgin female gut

4 days old flies were dissected after 16h fasting. Photomicrographs show the three parts of the gut (from top to bottom): the foregut, midgut and hindgut with a focus on the rectal ampulla.

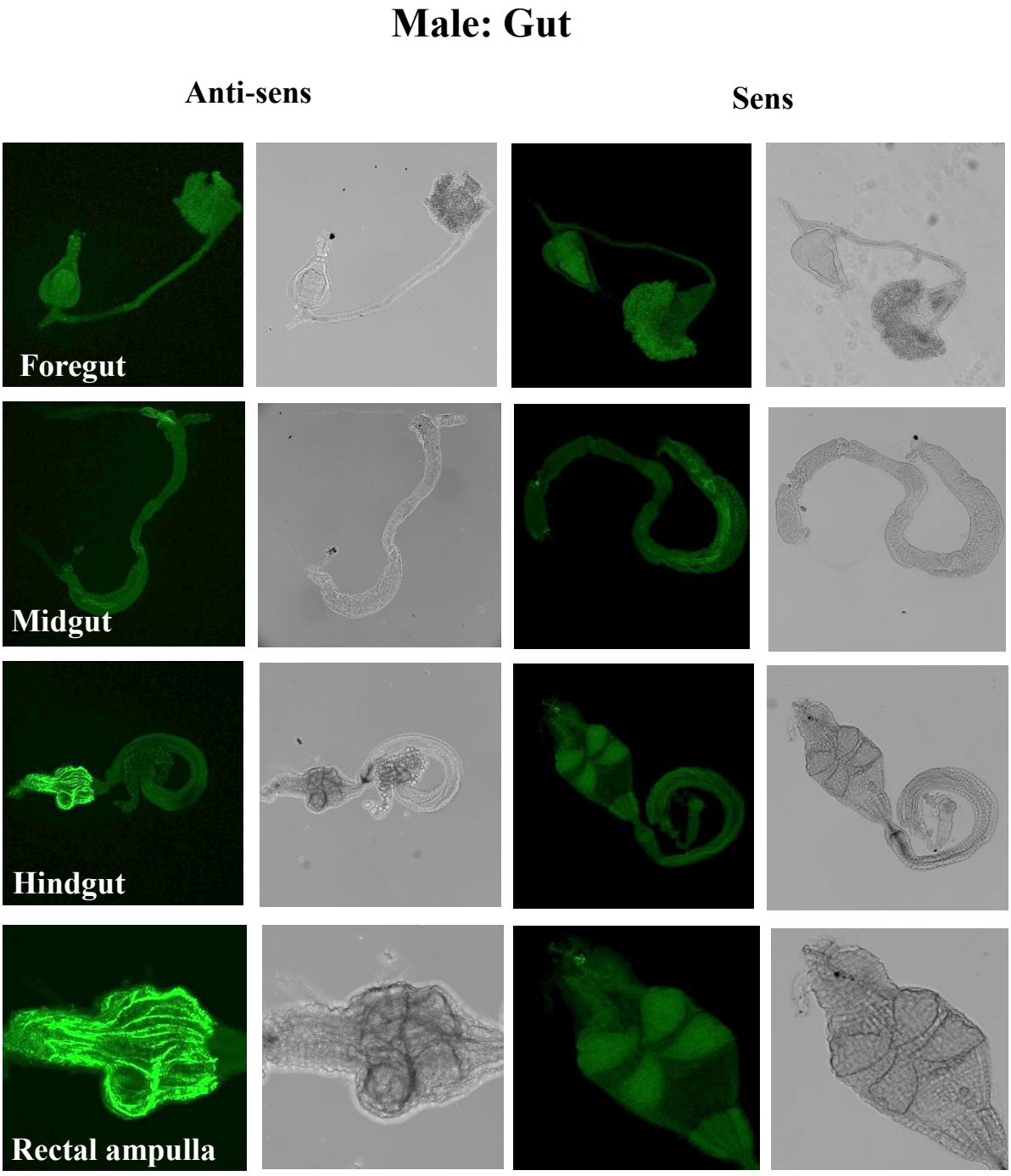

Figure R-26. OBP56d expression in virgin male gut

4 days old flies were dissected after 16h fasting. Expression pattern of OBP56d in the three parts of the gut (from top to bottom): the foregut, midgut and hindgut with a focus on the rectal ampulla.

4. Reproduction-related tissue-specific expression and behaviours

4.1. Reproductive organs mRNA expression *via in situ* hybridization

By using the same immunolabelling procedure as described above, we mapped OBP56d expression in male and female reproductive organs. First, no OBP56d expression was observed in female reproductive organs (virgin or mated; data not shown) (**Figure R-27.A.C**).

In male reproductive organs, OBP56d expression was found in the testes (**Figure R-28.A.B**). OBP56d expression pattern showed no difference in the reproductive organs of virgin and mated males. To localize OBP56d expression in the testes, we used Dapi coloration (**Figure R-28.C**). This indicated that OBP56d is expressed in the cytoplasm of testis cells.

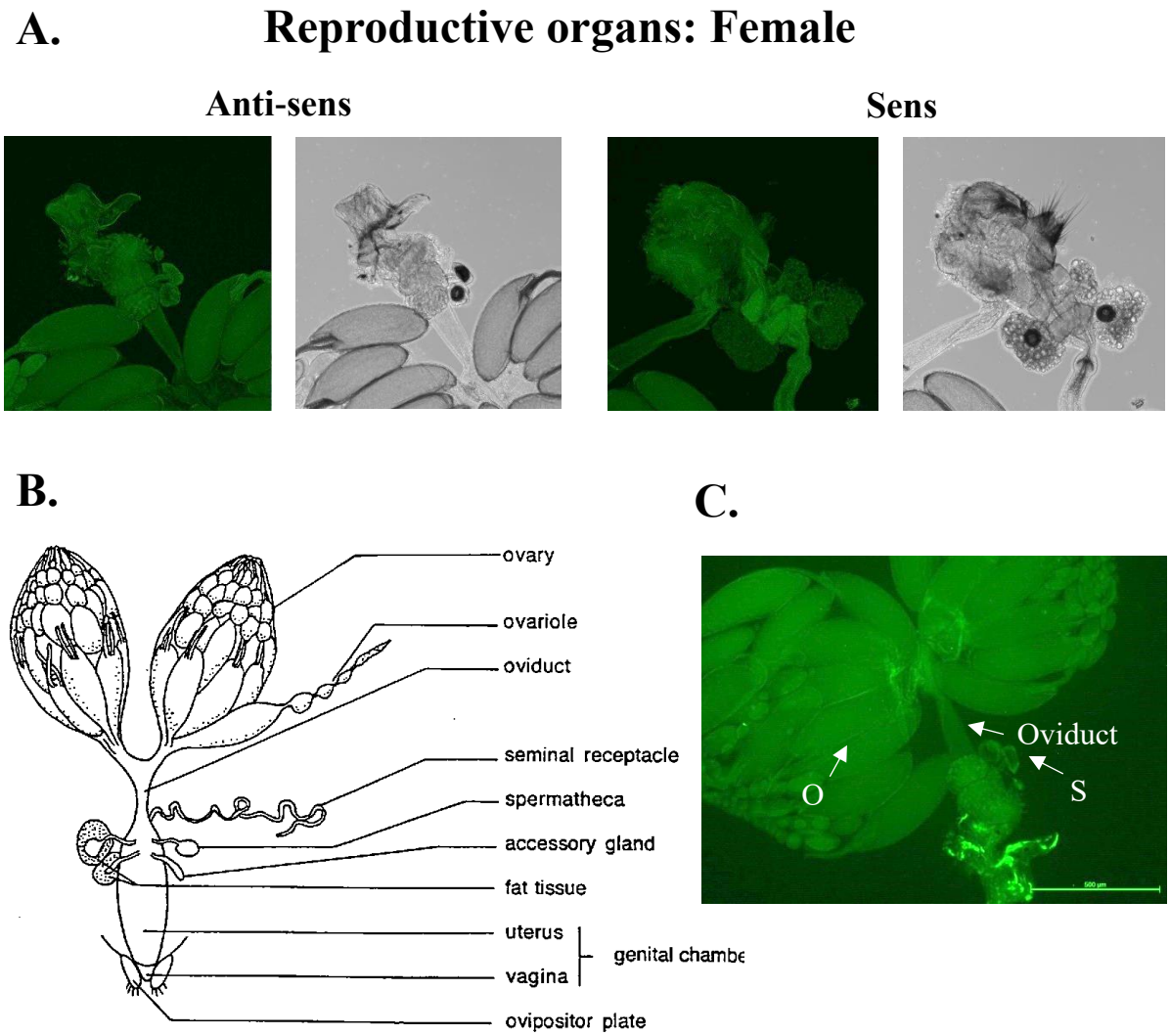

Figure R-27. OBP56d expression in the virgin female reproductive organs

4 days old flies were dissected after 16h fasting. A) Expression pattern of OBP56d in the reproductive organs. B) Schematic organization of the reproductive organs in female *Drosophila* (from Demerec book). C) Photo showing the ovary, oviduct and spermatheca.

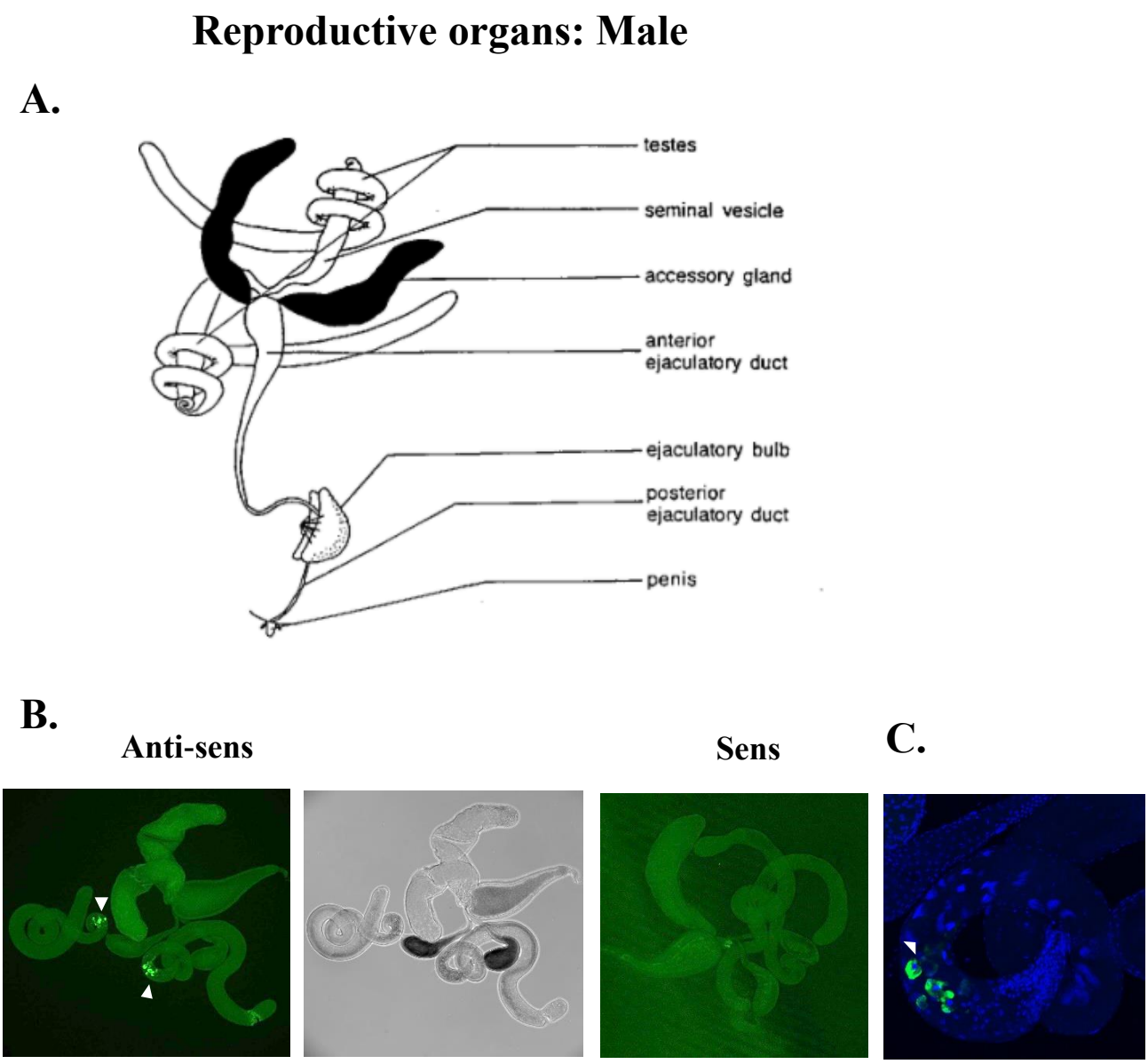

Figure R-28. OBP56d expression in the male reproductive organs

4 days old flies were dissected after 16h fasting. A) Schematic organization of the reproductive organs in male *Drosophila* (from Demerec book). B) Expression pattern of OBP56d in the reproductive organs. C) Photo showing the fluorescence in the cytoplasm of testis cells (using a Dapi coloration).

4.2. Verification of the *OBP56d*$^{-}$ mutant

For the following experiments carried out in this "Reproduction" section, we used an OBP56d^{-} mutant which was generated by the Bestgene Company. We obtained it relatively late during the thesis (Spring 2022) due to the difficulties to generate this mutant. Basically, it was deleted for the complete coding sequence of the OBP56d gene. We first verified that OBP56d was not expressed in the mutant and quantified the mRNA expression level both in *w*$^{-}$ and in the provided "mutant" lines (**Figure R-29.A**). No OBP56d expression was detected either in the head or in the gut of flies compared to the control line. To confirm this finding, we also performed an immunolabelling experiment in the male hindgut (**Figure R-29.B**). No expression pattern of OBP56d in the male hindgut was detected when using OBP56d probe in mutant males. This indicates that the OBP56d^{-} mutant is a null mutant for the OBP56d gene. Therefore, we were confident to use this mutant line in our further experiments.

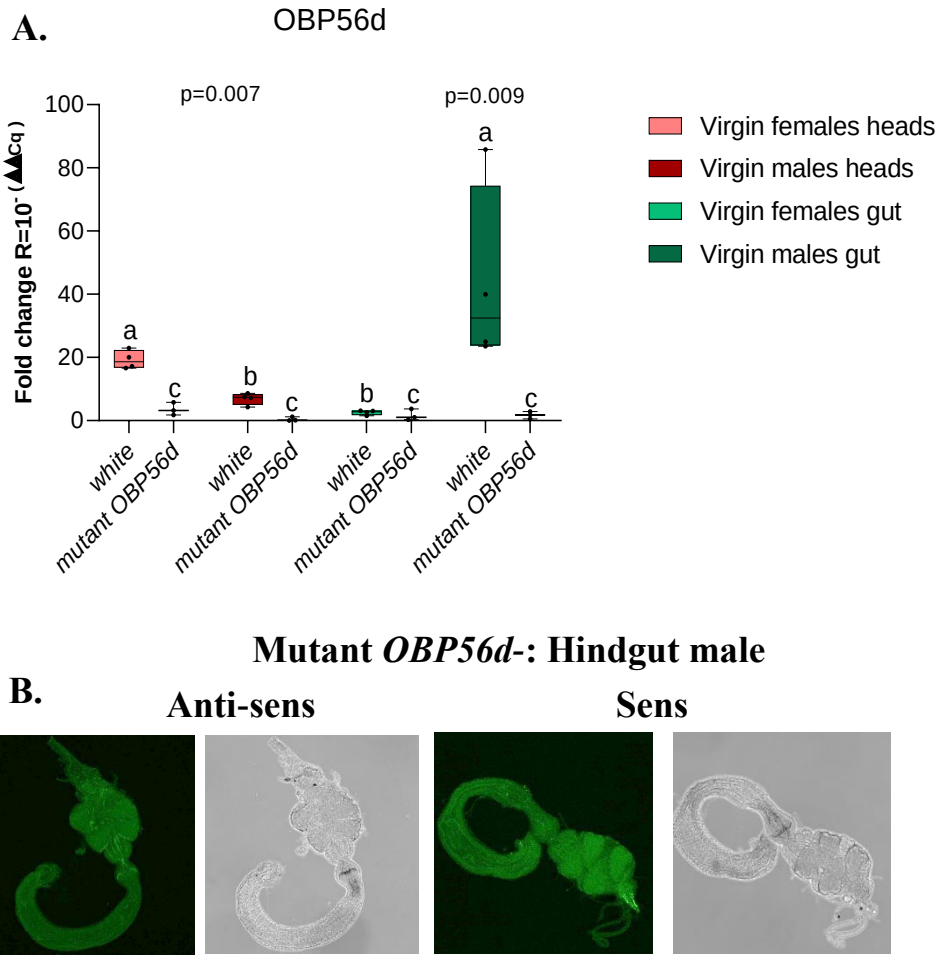

Figure R-29. Quantification of OBP56d in mutant *OBP56d-* flies

4 days old flies were dissected after 2h fasting. A) OBP56d expression was measured in w^- and mutant flies. Kruskal-Wallis test, post-hoc Conover-Iman with Bonferroni correction was used. Different letters indicate significant differences. statistics are shown above each sex. B) In situ hybridization with OBP56d probe in the male hindgut. 4 days old flies were dissected after 16h fasting.

4.3. Involvement of OBP56d in reproduction-related behaviours

4.3.1. Copulation during two hours

To assess the function of OBP56d in the testis and/or in the rectal ampulla as well as in the proboscis, we decided to measure the courtship and copulatory behaviours of OBP56d$^-$ mutant flies. These mutant flies were either tested in homotypic pair (a mutant female with a mutant male) or in heterotypic pairs (one mutant fly with a control fly of the other sex). In parallel experiments, we also tested pairs of control flies. (Note that all the mating pairs presented here always show the cross in the "female x male" order). Mutant flies as well as flies of the two control lines have white eyes: the first line (Ctrl1) was the w^- (^{w1118}) line while the second control line tested (Ctrl2) was the line originally used by the Bestgene Company to generate the mutant line.

We first looked at the courtship behaviours of all pairs tested. Nearly 95% showed elements of courtship ritual during the first 10 min of observation. No obvious difference between pairs of genotypes were detected (data not shown). When looking at copulation behaviour, we found significant difference between pairs of genotypes. These differences started during the first minutes of the copulation test and were amplified during the two-hour long observation period. Homotypic pairs of control flies (Ctrl 1 and Ctrl2) showed a high frequency of copulation during 2h (89.5% and 80%, respectively) whereas homotypic pairs of mutant flies show decreased copulation frequency compared to Ctrl1 and Ctrl2 pairs (34.5% and 25%, respectively) (**Figure R-30**).

To determine whether the OBP56d$^-$ mutation affected female or male copulatory behaviour, we performed heterotypic crosses. Pairs involving Ctrl1 or Ctrl2 females crossed with OBP56d$^-$ mutant males show copulation frequencies similar to those shown by homotypic Ctrl1 and Ctrl2 pairs (p-value >0.05). However, in reciprocal crosses involving mutant females with Ctrl males, the copulation frequencies were far much lower than those observed in homotypic Ctrl pairs (p-value $<10^{-15}$). More precisely, after two hours 41.2% mutant females copulated with Ctrl1 males while 20.7% mutant females copulated with Ctrl2 males.

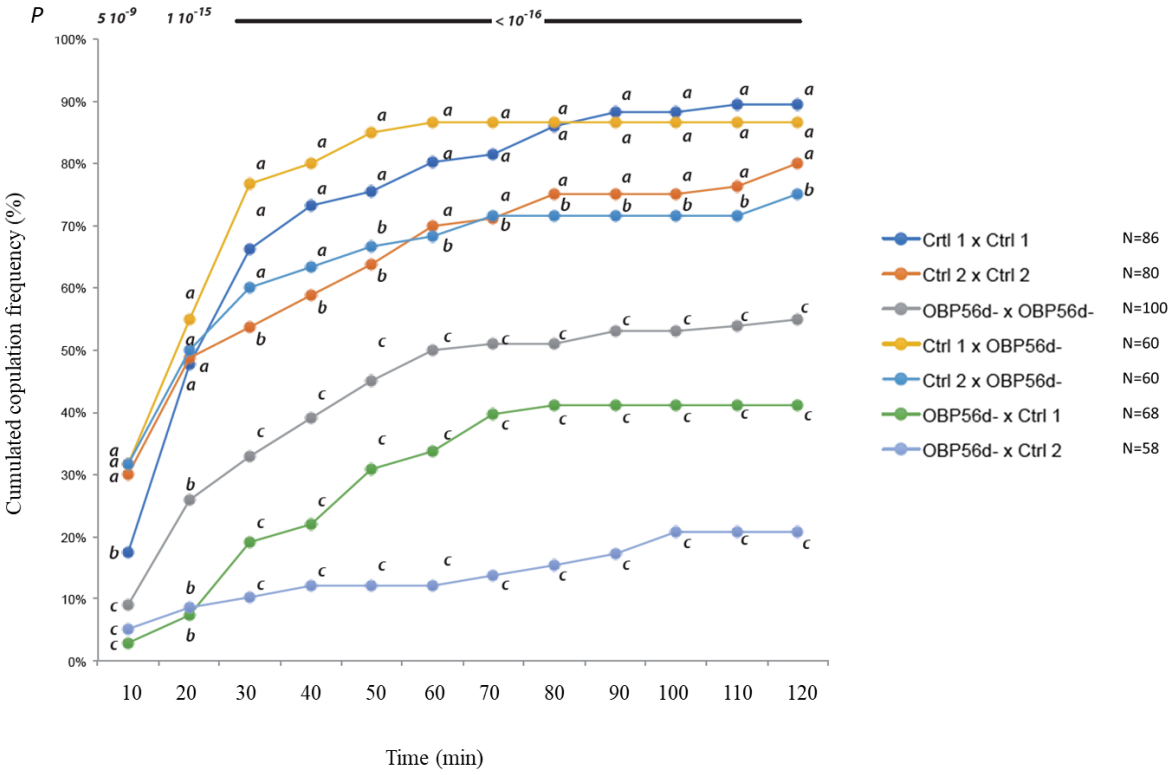

Figure R-30. Copulation kinetics in pairs of flies combining different genotypes

Cumulated copulation frequency was measured during 120min, presented here in fractions each one representing 10min. 4 to 7 days old virgin females and males were used for these tests. All crosses represent female x male pairs (indicated next to each curve).

Therefore, the OBP56d mutation induced an important effect on female but not on male ability to copulate. Moreover, while the performance of mutant females with Ctrl l males was very low, crossed involving mutant males with control females were similar to those involving pairs of control flies. Also, when paired with mutant females, mutant males seemed to show a tendency (not significant) for a higher copulation performance than the two control males, during the two-hours long period. This suggests that the loss of the OBP56d in males did not induce any deleterious effect, at least when measured on both copulation latency and frequency.

4.3.2. Copulation with antennaless females

To evaluate the effect of female antenna in the strong decreased copulation frequency of mutant females, we tested copulation in females chirurgically deprived of their both antenna (Ant-). We performed two crosses (#1) Ctrl1 Ant- females x Ctrl1 males, and (#2) Mutant

Ant- females x Ctrl1 males. For cross#1 pairs, 9/18 (50%) copulated within two hours as compared to only 2/35 (6%) cross#2 pairs. The comparison of these values with those shown by similar genotype pairs but involving intact females (90% [77/86] and 41% [28/68], respectively), indicates that antenna ablation significantly decreased the ability of operated females to copulate within two hours with Ctrl1 males (cross#1: p-value < 0.001; cross#2: p-value < 0.0001).

4.3.3. Fertility (after 2 hours and 12 hours long contact)

Next, we measured the effect of OBP56d$^-$ mutation on the fertility of pairs tested above. Practically, each mated female was kept after the copulation test alone (without the male) in a fresh food vial. In each vial, the presence/absence of progeny was noted 12 to 14 days after the copulation test. Our data indicate that the *OBP56d*$^-$ mutation had no impact on fertility (**Figure R-31**).

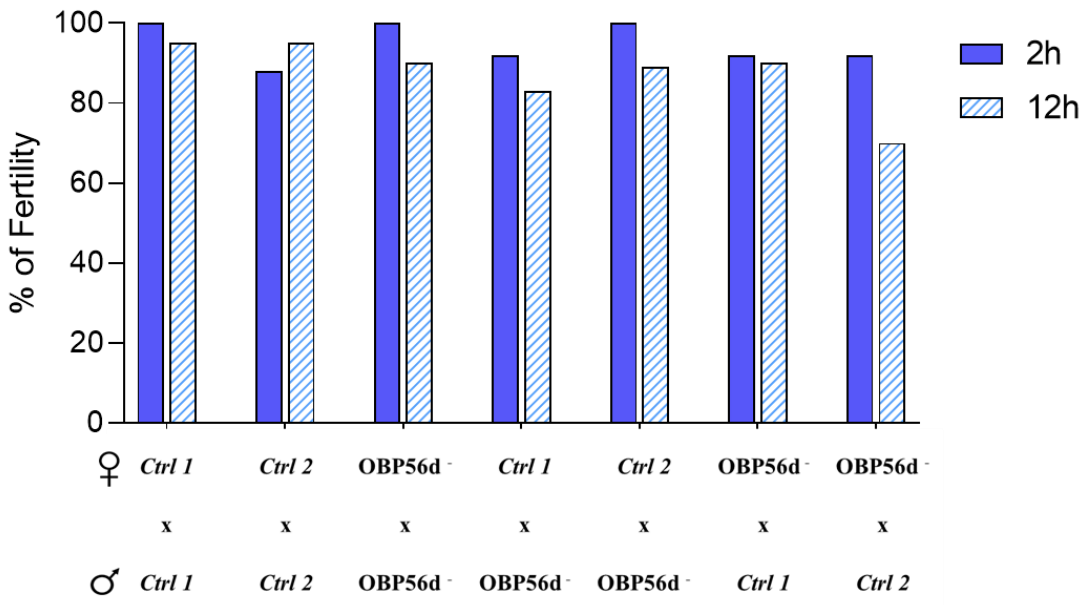

Figure R-31. Fertility in couples of flies paired during 2 and 12 hours

4 to 7 days old virgin females and males were paired. In the two hour experiment, only copulated females were kept individually in fresh food vials and their progeny was checked 12-14 days later. In the 12 hour experiment, pairs were kept overnight, the male was discarted at early morning and the progeny was checked 12-14 days later. Here, we show the frequency for females with progeny (fertility %) based on the total number of vials shown for 2h /12h. For Ctrl 1 x Ctrl 1 (N=25/60); Ctrl 2 x Ctrl 2 (N=24/20); OBP56d- x OBPP56d- (N=16/60); Ctrl 1 x OBP56d- (N=52/40); Ctrl 2 x OBP56d- (N=43/19); OBP56d- x Ctrl 1 (N=24/40); OBP56d- x Ctrl 2 (N=12/20). G^2 of Wilks test applied for each time experiment For 2h: p-value > 0.05; for 12h: p-value > 0.05.

The close observation of the cumulated copulation frequency (as a function of time; see **Figure R-30**) indicates that the difference between high performing pairs and low performing pairs starts very early during the observation period. Taken together with the antenaless experiment, this difference suggests that the behavioural defect shown by mutant females could be due to their altered perception of male signals, possibly—but not only—of male pheromones.

To determine whether females which were reluctant to copulate within the two-hours long period were completely refractory, or not, to male courtship, we performed a fertility test in pairs kept together during 12 hours (overnight) (**Figure R-32**). Beside the measure of fertility, this experiment provided us with an indirect measure of copulation frequency during the 12 hours contact. Practically, pairs of flies, combining similar genotypes (as those used for 2 hours long tests) were introduced at late evening in a fresh food vial and the next morning (after 12 hours), the male was discarded. The presence/absence of adult progeny was checked 12-14 days later, in each vial. Given that our previous "2 hours long" fertility test indicated that around 95% copulating pairs were fertile, we can assume that fertility is a good indicator (proxy) of copulation ability during 12 hours.

Our data indicate that after 12 hours, all types of crosses showed a high level of fertility (therefore of copulation; **Figure R-32**). The crosses which showed a high copulation frequency after 2 hours also showed a similar fertility frequency during 12 hours, supporting the validity of our indicator. Interestingly, the three crosses involving mutant females showed highly increased fertility values after 12 hours compared to data obtained after 2 hours contact. The values showed by "mutant x mutant" and "mutant x Ctrl1" pairs were very similar to those shown by homotypic Ctrl crosses whereas those shown by "mutant x Ctrl2" pairs strongly increased even if they remained a little bit lower than those shown by the other crosses.

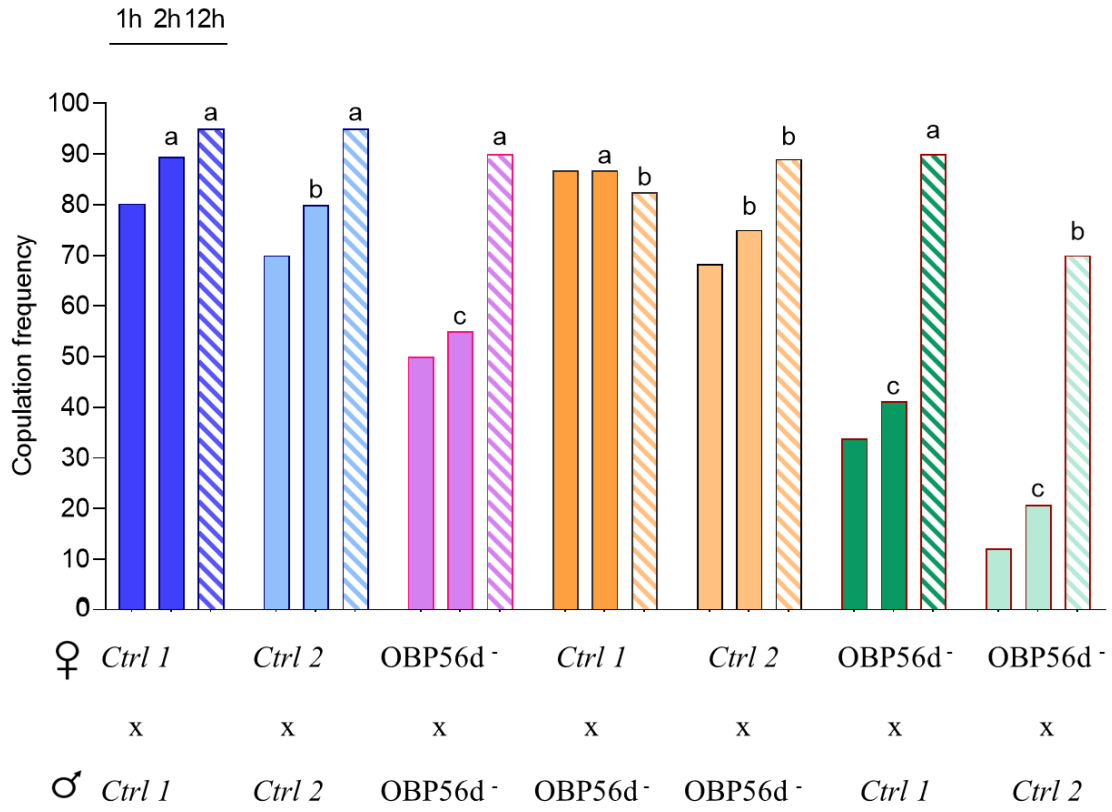

Figure R-32. Copulation frequency for 1h, 2h and 12h

4 to 7 days old virgin females and males were selected. The copulation frequency was measured directly for 1h and 2h by observation, and indirectly through fertility after 12h. For all pairs the copulation frequency was observed in 2h or 12h. G^2 of Wilks test was applied to compare the copulation in two different periods of time (2h and 12h), p-value < 0.0001.

4.3.4. Fecundity

Furthermore, we also counted the total number of adult progeny in each vial for each type of mating pair and we determined the total number of progenies. We also evaluated the sex ratio also, but no significative differences were observed (data not shown). Fecundity was evaluated with two procedures in the two successive series of tests we did perform. In the first series of tests, we pooled all progenies obtained and divided this global fecundity by the number of fertile vials to obtain the mean adult progeny per vial (**Figure R-33**). In the second series of tests, we measured separately, in each vial the progeny and evaluated the distribution of individual progenies (**Figure R-34**).

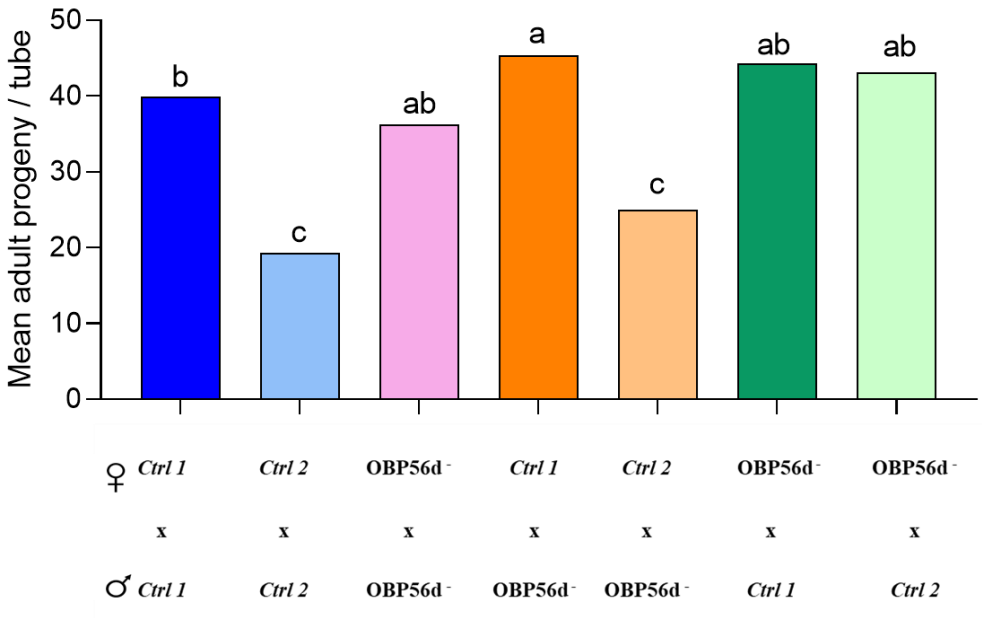

Figure R-33. Adult progeny produced by each type of mating pair

For each cross, the total number of adult progeny was counted. We evaluated numbers based on the global progeny divided by the number of vials with progeny. The total number of tubes for each genotype pairs was: Ctrl 1 x Ctrl 1 (N=69), Ctrl 2 x Ctrl 2 (N=64), OBP56d- x OBpP56d- (N=59), Ctrl 1 x OBP56d- (N=52), Ctrl 2 x OBP56d- (N=43), OBP56d- x Ctrl 1 (N=24) and OBP56d- x Ctrl 2 (N=12). Kruskal-Wallis test followed by a post-hoc Conover-Iman with Bonferroni correction was applied. Different letters indicate significant differences. p-value < 0.0001.

The examination of the global fecundity (procedure 1) indicates that fecundity was significantly decreased in the two pairs involving at least a female progenitor of the Ctrl 2 lines whereas the homotypic "Ctrl1 x Ctrl1" cross produced slightly less progeny than the "Ctrl1 x mutant" cross (**Figure R-33**). The fecundity of transgenic Ctrl 2 females may be decreased due to the presence of Crisp/Cas-9 transgene. However, the fecundity of OBP56d^{-} mutant flies (deriving from Ctrl2 line) was not affected. When evaluating individual adult progeny (per "fertile" vial), we found a significantly lower fecundity in pairs involving Ctrl2 females and two out of three cross involving mutant females (**Figure R-34**). More precisely, crosses involving Ctrl1 females and the homotypic "mutant x mutant" cross showed the higher fecundity as measured in individual progenies.

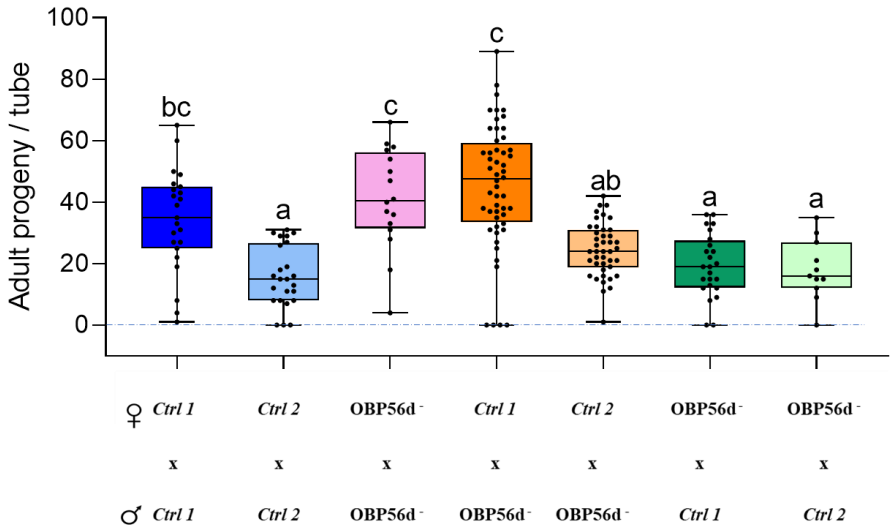

Figure R-34. Adult progeny per tube for all pairs.

For some experiments, we calculated the number of progeny in individual vials. Number of total tubes: Ctrl 1 x Ctrl 1 (N=23), Ctrl 2 x Ctrl 2 (N=24), OBP56d- x OBpP56d- (N=16), Ctrl 1 x OBP56d- (N=52), Ctrl 2 x OBP56d- (N=42), OBP56d- x Ctrl 1 (N=24) and OBP56d- x Ctrl 2 (N=11). Kruskal-Wallis test, post hoc of Conover-Iman with Bonferroni correction was applied. Different letters indicate significant differences. p-value < 0.0001.

Discussion

Feeding and mating are two critical aspects of life which determine the ability of species to multiply, adapt and survive in a constantly changing environment. It is critical for animals to be able to find and discriminate potential food sources and suitable mating partners. Both chemosensory modalities, olfaction and taste, allow animals to orient from a long distance until the proximity of the food/partner of interest. Given the multiplicity of odours and their varying concentrations in the environment, depending on the distance between the animal and its source, both chemosensory systems should possess a fine ability to discriminate. Such fine ability is made possible with the capacity to eliminate out of sensory organs the molecules just detected in the past fractions of seconds. In insects, the peri-receptor enzymes and proteins, which are abundant and diverse, can fulfill these crucial roles. They are mixed in the aqueous lymph bathing olfactory and gustatory receptor neurons housed inside chemosensory hairs. In fact, perireceptor proteins are thought to play several distinct roles, but some of them still need confirmation by more scientific evidence. The most diverse and conserved class of perireceptor proteins are the XMEs (xenobiotic metabolizing enzymes) whose primary function consists to detoxify the intrasensillar lymph. XMEs are therefore involved in clearing off the sensory receptors through the production of metabolites resulting from the degradation of odorant and tastant molecules. Chemosensory proteins (CSPs) is a class of perireceptor proteins whose role still remains ambigous since it could be related to the OBP class. OBPs seem to exert very diverse functions beside their classical involvement as transporter of odorant and pheromone molecules (by OBP/PBP, respectively). The variety of OBP functions in insects, and mostly in *Drosophila*, has been largely expanded during the last decade (Rihani *et al.*, 2021).

During the 3-years long (or rather 3-years short) period of my PhD research project, I chose to focus on a few OBPs which showed either a restricted or a preferential expression both in the peripheral gustatory system together and in the gut. We were particularly interested to test whether feeding ability and satiety could be linked with OBP activity. Moreover, and in relation with the gut-related expression, we were also interested to test the influence of gut-associated microbiota (particularly bacterial microbiota) on the OBP-nutrition relationship. Due to technical adversities and the duration of some time-consuming experiments, we could not really measure OBP influence on nutrition and *vice-versa*. Our data, some of which are still preliminary, indicate that the duration of fasting could influence, but only in rare occurrences, tissues and sex the mRNA expression level of OBP56d. More particularly, we observed a strongly increased expression of OBP56d and of OBP56g in the head of virgin

females fasting 30h compared to all other fasting durations (**Figure R-7.A** and **Figure R-8,** respectively). When the fasting period increases, this could induce a highest number of cells showing autophagy. This cell death phenomenon could affect several tissues and more particularly the gut of flies with an indirect effect on gut-associated OBPs (Moy and Cherry, 2013). Therefore, the long fasting period (30h) could induce the large variation in the male but also in the female head (which contains fat body also affected by the autophagic process; Nagy *et al.*, 2015). A much reduced effect was also detected for OBP56g in the head of flies (between 0 and 16h in males; between 0 and 2h in females; **Figure R-7.A**), but this effect needs to be confirmed by a larger number of replicates. Similarly, a slight effect was detected for OBP56g in gut of females between the "no fasting" condition and the "16 h fasting" condition (**Figure R-7.B**).

However, we could not explore, as we wished, the potential ability of both these OBPs to influence food perception and food uptake. Our *in vitro* binding assay (performed with a fluorescent probe competitor) revealed that OBP56d, and to a lesser extent OBP56g, can bind a large series of long chain fatty acids (**Figure R-22 and Figure R-23,** respectively), but not other compounds tested among the many nutrients potentially available in the food (sugar, bitter compounds, amino acids, antibiotics...) or sex pheromones (**Figure R-21**). It must be stressed out that the difference in binding affinity observed between OBP56d and OBP56g could be partially due to the presence of contaminants in the recombinant OBP56g cavity. In the near future, we need to increase the purity of this OBP to improve its quality and this requires to eliminate the second band (on our gels) which may indicate a protein dimer form.

Unfortunately, the time was missing to test the influence of these OBPs on food preference and particularly whether their alteration would affect behavioural responses in individuals (larvae, adults) towards or against fatty acids (FAs), particularly FAs showing the highest affinity in our biochemical assay. Flybase indicates that OBP56d is only expressed in the larval olfactory system while it is present in both adult chemosensory systems. This was confirmed by an exhaustive study carried out on many OBPs (Gallindo and Smith, 2001). Conversely, these authors reported that OBP56g is expressed both in olfactory and gustatory larval systems and is only present in the adult gustatory system. We believe that testing FA behavioural preference would be much easier in larvae than in adults. In particular, and given that most FAs can be easily mixed in the food, larval preference can be tested in a basic test consisting of a petri dish covered with separated "plain food/FA-rich food" areas. Testing FA preference in adults would be more tricky given that FAs do not dissolve well in the

hydrophilic solvent generally employed to fill the small capillaries used to measure liquid consumption in the "multiCafe" device (Ja *et al.*, 2007). Moreover, a future investigation could stand on data showing Drosophila qualitative FA preference: larvae are attracted to unsaturated fatty acids and strongly repulsed by saturated FAs while adults show a reciprocal preference (Fougeron *et al.*, 2011). However these preference can be altered in insects exposed during early development ($1^{st}/2^{nd}$ instar larvae) on FA-rich diet (Flaven-Pouchon *et al.*, 2014).

Another problem was related to the production of the *OBP56d*$^{-}$ mutant line. This line would have been very useful to carry larval tests described above, but it took a very long time (and several attempts) for the Bestgene Company to produce it. We received this strain only during the spring 2022. Meanwhile, we carried out time-consuming experiments consisting to manipulate and measure the influence of bacterial microbiota on OBP56d and OBP56g expression. We were somewhat disappointed of the restricted effect on OBP56d and OBP56g expression with regard to the number of experiments performed (plain food/axenic food/axenic food + two bacteria species/ axenic food + whole fly guts). Nevertheless, a couple of microbiota manipulations induced highly significant variations while few others showed a strong tendency. The latter ones need to be reinforced before being conclusive. The most significant difference we observed was shown by OBP56d expression in the male gut between control and axenic conditions (**Figure R-13**). Females showed a slighter difference for OBP56g in their head between control and axenic conditions (**Figure R-14**). In these two cases, the flies raised in axenic conditions showed a decreased expression compared to control ones. It is possible to speculate that these variations were detected since they showed a relatively high quantitative expression in the male gut and female head. The other (less) significant differences are more difficult to interpret. In particular, the decreased OBP56d expression in the head of females raised on supplemented axenic media (+ each bacteria or + either sex fly guts) compared to both control and axenic conditions (**Figure R-15.A**). In the gut, only OBP56d varied between conditions with a slight decrease between "axenic media + *A.pomorum*" and axenic media in females (**Figure R-16.B**) and a marked decrease between control and all other conditions in males (**Figure R-16.B**). In summary, these experiments suggest that the total elimination of bacteria from the media (during two generations) induced clear effect in the tissues where OBP showed the highest expression (head in females, gut in males). However, the more subtle manipulation of the media resulting in the addition of a single bacteria species or of fly guts, did not induce such a clear effect likely due to the

possibility that more bacteria species are needed or that more fly guts should be added in the experimental medium to be tested. It is also possible that the presence of the symbiotic Wolbachia bacteria in our control strain introduced a bias in our experiment (see below).

Beside the fact that the significant effects obtained with the axenic medium indicate that the bacterial microbiota interacts directly or indirectly with both OBPs in a sex- and tissue-dependent manner, the contrasted effect induced by some microbiota manipulations could be biased by the abundant presence of Wolbachia in our main control line (w^{1118}). *Drosophila melanogaster* normally hosts two main genera of commensal bacteria, Acetobacter and Lactobacillus (Douglas, 2018, 2015) and Wolbachia-infected flies showed a significantly reduced presence of Acetobacter (Simhadri *et al.*, 2017). In our case, *Lactobacillus plantarum* and *Acetobacter pomorum* were absent from the gut of our control Wolbachia-infested line. More unexpectedly, the OBP56d$^-$ mutant line also showed a strong reduction of both bacteria indicating a possible link between this genetic deletion and the microbiota structure. Conversely, the Izhakiella bacteria, a member of Enterobacteria family (the third main bacteria genera generally found in Drosophila*;* (Douglas, 2018; Jiang *et al.*, 2020), was present in a relatively high proportion in the gut of axenic and OBP56d$^-$ mutant flies. While the bacterial microbiota was reported to be more varied in nature than in laboratory strains (Miguel-Aliaga *et al.*, 2018; Téfit *et al.*, 2018), a difference in the composition between laboratory strains might be also partially induced by the medium quality and frequency of fly transfer to fresh food vials (Broderick and Lemaitre, 2012).

In any case, this raises the urgency to test for the presence/absence of Wolbachia bacteria in all strains dedicated to be used in microbiota experiments, before starting any experiment. Given that Wolbachia is known to affect reproduction, stem cell activity and gut microbiome composition (Simhadri *et al.*, 2017), we tested a Wolbachia-free w^{1118} line (given very recently by Dr Serge Birman). This line showed the same mRNA gut and immunostaining rectal ampulla pattern in both sexes with the OBP56d immunofluorescent probe (data not yet shown). This at least indicates that this tissue-specific expression was not altered by the presence of this symbiotic bacteria. The use of the antibiotics cocktail mostly or totally eliminated Wolbachia from our "axenic" lines and this was not a surprise given that this bacteria is usually eliminated by tetracycline (which was one of the antibiotic used to generate our axenic medium). Similarly, the OBP56d$^-$ mutant also seemed to carry a different bacterial pattern in its gut. This indicates a direct or indirect link between OBP56d gene expression and the presence/abundance of some bacteria in the gut. As a side experiment, we also tested the

bacterial microbiota of two highly diverging *D. melanogaster* strains: the Zimbabwe line (Z30, or Z6 line), which is thought to be the ancestral *D. melanogaster* population (it was collected in the early 1980's and show a strong sexual isolation with all other strains; Wu *et al.*, 1995) and the Dijon2000 line which was collected in 2000 (Svetec and Ferveur, 2005). Despite the fact that both strains were maintained in parallel on the same diet in our lab for more than two decades, they still show a clear-cut difference for their bacterial microbiota (E. Aruçi, D. Agashe, P. Sangebam and JF. Ferveur, unpublished data). This indicates that the food quality by itself cannot totally eliminate existing microbiota difference which thus may be related to some genetic difference between the two strains (Cortot *et al.*, 2019). Genetic difference may be one of the factors explaining the different bacteria pattern between the OBP56d$^-$ genetic mutant and our Wolbachia-contaminated "control" strain. However, we will need to sort out the bias related to the presence of this bacteria, using the recently Wolbachia-free strain to be able to conclude on the respective contribution of genes and Wolbachia on the gut-bacteria pattern.

During the third year of my PhD, when we finally obtained the OBP56d$^-$ mutant strain, we could use mutant flies of both sexes in mating tests. Why did we carry out such behavioural experiments? Two main reasons led us to investigate courtship and copulatory behaviours. Firstly, we found a strong tissue-specific sexual dimorphism: OBP56d was expressed in the male reproductive tract (testis) and in the female (and less in the male) proboscis (using *in situ* fluorescent probes). However, at that time, we did not know that Wolbachia was contaminating our control strain with possible effects on the fluorescent expression in the testis. Secondly: the OBP56d protein was detected in a sexually dimorphic manner in both head chemosensory appendages: the antenna (Anholt and Williams, 2010) and the proboscis (Aruçi *et al.*, 2022) with females showing a much higher level than males. These two reasons raised the tantalizing hypothesis that the OBP56d could be involved in the two sides of sensory communication: emission and perception of one (or several) pheromonal signal(s). Indeed, this is reminiscent of the presence and role of major urinary proteins (MUPs) in some rodent species. MUPs are low-molecular-weight (approximately 19 kDa) members of the large lipocalin family produced by the liver, filtered by the kidneys and secreted into the urine in some rodent species, such as mice and rats (Liberles, 2014). In rodents, MUPs are usually more prevalent in males than in females, implying a male-biased trait (Beynon and Hurst, 2004). Rodents use voided urine to extensively mark their territories for chemosensory communication and particularly to stimulate female sexual behaviour (Hurst *et al.*, 2001).

Similarly, we believe that in Drosophila, some male-specific substances (pheromones?) could be internally processed by the OBP56d in genital structures or/and be transported out of his genital tract by this OBP. When externalized, this (these) male specific substance(s) could be detected by the OBP56d present in the chemosensory sensilla present on female antenna and proboscis. This is a working hypothesis that we tested on the courtship and copulatory behaviours of OBP56d^{-} mutant flies.

More precisely, our behavioural data (based both on direct and indirect observations of copulation) indicate that the OBP56d^{-} mutation severely altered female sexual receptivity to copulate with a male (during 2 hours long period). However, this mutation did not prevent mutant females to copulate (within 12 hours long period). This effect is informative since it means that mutant females did not suffer any physiological defect or heavy behavioural impairment, but that they were less stimulated, than control females, by hypothetical male signal(s). Unfortunately, we had no time to test the few potential candidate molecules, metabolites of male cuticular pheromones (Methyl-laurate, myristate and –palmitate: Dweck *et al.*, 2015), known to induce copulation behaviour. Conversely, we did not find any negative effect of the OBP56d^{-} mutation on mutant male copulatory performance.

A complementary experiment — still preliminary but already showing a clear effect — performed with antennaless mutant and Ctrl females revealed similarly decreased performance of Ctrl males paired with both females. The residual difference shown by antennaless females either paired with Ctrl or mutant males is somewhat similar to the difference shown by intact mutant females with these two male genotypes. This indicates that the strong decrement of the mutant female performance is related to the altered expression of the OBP56d in non-antennal chemosensory appendage(s), maybe the proboscis. This suggests that the female proboscis and antenna both participate to the detection of male pheromone(s). Their conjugated inputs projecting in the brain would add up to induce an adapted behavioural response: female sexual receptivity within a relatively short period of time. This fits with the observation that control antennaless and intact mutant females, partly deprived of their chemosensory perception show an intermediate copulatory response (50 and 41 %, respectively) while antennaless mutant females showed almost no copulation (6%) within two hours. The strongly decreased response shown by antennaless mutant females indicates that most of their ability to react to male pheromone(s) (when they were intact and within two hours) was only (or mostly) due to their antennal perception. To see whether female proboscis

can still serve females to detect male pheromone, we could perform a 12-hour long test with antennaless mutant females.

During the period of my PhD thesis we had some exchanges with Professor Mariana Wolfner and her PhD student Nora Brown who were studying in parallel on the effect of OBP56g on female post-mating response. In a wide-OBP screen, they found that during copulation the OBP56g —but not the OBP56d — is transferred to the female to changes her fecundity. Therefore, we found very interesting the complementary effects — precopulatory for OBP56d and post-copulatory for OBP56g — induced by two closely related transporter proteins on Drosophila reproduction.

We have not yet solved the existence of a possible relationship of expression between the testis and the rectal ampulla. We do not know whether there is a relationship between both tissues, or if their relative proximity is just accidental. The pylorus (a sub-region of hindgut) is an important zone of interaction between the Drosophila host environment and its microbiota. The cuticle of the pyloric region is thought to host enriched microbial communities (Elzinga, 1998) and is implicated in innate immune response via the production of melanin (Wang *et al.*, 2018). In flies, hindgut-specific microbe interaction might influence the OBP56d expression and be transported to the rectum region. A first approach would consist to identify the cell type of the rectal ampulla where the OBP56d is expressed. The rectal ampulla is known for two features: (1) water and minerals reabsorption and (2) ionic transport related to cold resistance in the rectal pads (Andersen *et al.*, 2017). Could the OBP56d be involved in water transport as already shown for OBP59a in the antenna (Jennifer S Sun *et al.*, 2018)? A better characterization of the OBP56d protein would help to evaluate the possibility of a "rectal ampulla-testis" communication way. One attempt to investigate this question consisted to detect for OBP56d presence in the adult faeces, but this attempt remained unsuccessful (data not shown).

To conclude, our study provides novel insights into OBP56d function. OBP56d is expressed in the proboscis, and in sexually dimorphic manner in the male hindgut and gonads. In some cases, OBP56d expression level decreased in the absence of bacterial microbiota. OBP56d binds to long chain fatty acids but we have not yet demonstrated with behavioural data its implication on food preference. Conversely, we showed that its absence strongly decreased female pre-copulatory behaviour without affecting fertility and fecundity. We believe that OBP56d is involved in the transport, release and/or detection of fatty acid-derived

semiochemicals. Future research projects should identify these hypothetical compounds which may have shaped the intersex pheromonal communication this influencing the evolution of Drosophila species.

Perspectives

This thesis raises more questions at the end than those asked when initiating my PhD project. Several investigations need to be continued based on the data shown in the present report.

In particular in the short term, we intent to test female mating behaviour induced by some of the pheromonal metabolites cited above, in a two-level chamber separated by a mesh. On the top level of this chamber, we would place and observe copulation in a mutant female paired with a control male while at the lower level we could place some of the pheromone metabolites. In the lower part of the chamber, we could replace these products by a small number (5-10) of control males, or to an heterosexual pair of control flies, to see whether the increased amount of male chemical stimuli could enhance copulation frequency in mutant females tested during two hours.

In the short term, also, we aim to test the larval response to a variety of fatty acids among those showing the highest affinity for the OBP56d. This test would be mainly based on the compared responses of mutant and control larvae.

We could map more precisely the cells where the OBP56d is expressed both in the male reproductive tissues and in the hindgut (in rectal pads). Similarly, we could try to map more precisely, using secondary cell type markers, OBP56d expression in the female and male proboscis. This should allow us to determine whether there is a complete, or partial, expression overlap between the sexes.

On the longer term, and using the Wolbachia-free w^{1118} strain, we could redo and expand some of the microbiota manipulation. In particular, we could test the simultaneous addition in the medium of the two bacteria (*A. pomorum* + *L. plantarum*) which were separately tested during our PhD project.

Annexe

Annex M.1

Acetobacter pomorum culture: RAE medium

Glucose: 40.00 g

Peptone: 10.00 g

Yeast extract: 10.00 g

Citric acid x H_2O: 1.50 g

Na_2HPO_4 x 2 H_2O: 3.38 g

Glacial acetic acid: 10.00 ml

Absolute ethanol: 10.00 ml

Distilled water: 980.00 ml

Final pH: ~ 3.8 (pH is not adjusted)

Both liquid and solid media are prepared by autoclaving the medium without the addition of glacial acetic acid and absolute ethanol. Glacial acetic acid and absolute ethanol are sterilised either by filtration (Teflon filters) or they may be autoclaved in completely closed screw cap glass bottles sealed with a Teflon coated septum. The preparation of solid media employs a double layer system similar to that described for *Acetobacter europaeus* medium. Substitute the components listed above and prepare a lower, 0.5% agar layer, which is then overlaid with a 1.0% agar layer. Incubate in closed containers to keep the humidity high (> 90%).

Annex M.2

Lactobacillus plantarum culture: MRS broth composition

This is the protocol to make the culture from the scratch, but in our case, we bought the MRS with the same composition.

MRS Broth Composition

Proteose Peptone #3: 10.0 g
Beef Extract: 10.0 g
Yeast Extract: 5.0 g
Dextrose: 20.0 g
Sorbitan Monooleate: 1.0 g
Ammonium Citrate: 2.0 g
Sodium Acetate: 5.0 g
MnSO4 x H2O: 0.05 g
Na2HPO4: 2.0 g
Distilled water: 1000 ml
Final pH: 6.5 +/- 0.2

Annex M.3

Flow cytometry measurement for *Acetobacter pomorum* (A) and *Lactobacillus plantarum* (B)

A.

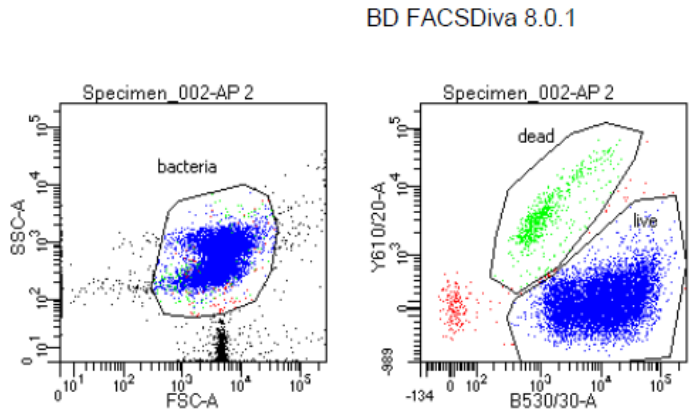

Tube: AP 2

Population	#Events	%Parent	%Total
All Events	10,000	####	100.0
bacteria	8,487	84.9	84.9
dead	635	7.5	6.4
live	7,660	90.3	76.6

B.

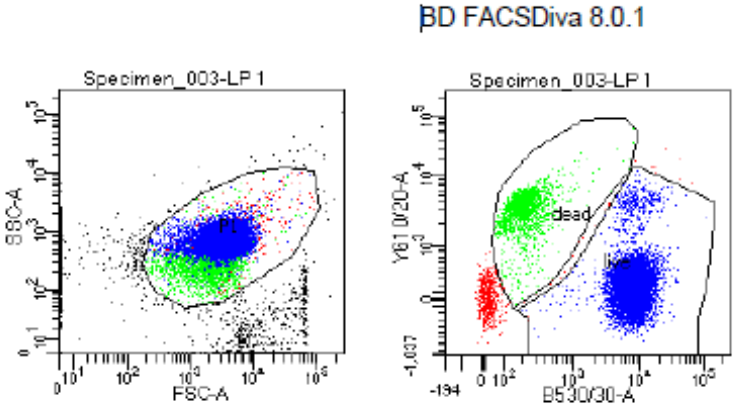

Tube: LP 1

Population	#Events	%Parent	%Total
All Events	12,633	####	100.0
P1	10,105	80.0	80.0
dead	2,402	23.8	19.0
live	7,194	71.2	56.9

Annex M.4

SOC medium composition:

2% Tryptone

0.5% Yeast Extract

10 mM NaCl

2.5 mM KCl

10 mM MgCl2

10 mM MgSO4

20 mM glucose

Article

Proteomic characterization of Drosophila melanogaster proboscis

Enisa Aruçi[1], Jean-Michel Saliou[2], Jean-François Ferveur[3,*] and Loïc Briand[4,]

[1] Centre des Sciences du Goût et de l'Alimentation, CNRS, INRAE, Institut Agro, Université Bourgogne Franche-Comté, F-21000 Dijon, France; enisa.aruci@inrae.fr
[2] University of Lille, CNRS, Inserm, CHU Lille, Institut Pasteur de Lille, UAR CNRS 2014 - US Inserm 41 - PLBS, Lille, France; jean-michel.saliou@pasteur-lille.fr
[3] Centre des Sciences du Goût et de l'Alimentation, CNRS, INRAE, Institut Agro, Université Bourgogne Franche-Comté, F-21000 Dijon, France; jean-francois.Ferveur@u-bourgogne.fr
[4] Centre des Sciences du Goût et de l'Alimentation, CNRS, INRAE, Institut Agro, Université Bourgogne Franche-Comté, F-21000 Dijon, France; loic.briand@inrae.fr

* Correspondence: J-F. F.: jean-francois.Ferveur@u-bourgogne.fr; Tel: +33 380 393 782
L.B.: loic.briand@inrae.fr; Tel.: +33 380 681 615

Citation: Aruçi, E.; Saliou, J.-M.; Ferveur, J.-F; Briand, L. **Pr**oteomic characterization of Drosophila melanogaster proboscis. *Biology* **2022**, *11*, x. https://doi.org/10.3390/xxxxx

Academic Editor: Firstname Lastname

Received: date
Accepted: date
Published: date

Publisher's Note: MDPI stays neutral with regard to jurisdictional claims in published maps and institutional affiliations.

Simple Summary: Insects use chemical signals to locate food, to interact with their environment or for social communication. More precisely, the peripheral sensory olfactory and gustatory systems allow the detection of chemical signals coming from the environment. Volatile or sapid molecules enter the sensory organs and are transported by specialized proteins through the internal aqueous phase to the chemosensory receptors. We used a proteomic analysis to identify the soluble proteins in the proboscis, an organ that is part of the gustatory system of *Drosophila melanogaster.* A total of 586 proteins were identified, and 19 proteins were used for further analysis. We identified two proteins implicated in the transport of molecules such as the odorant-binding proteins OBP19d and OBP56d. Interestingly, OBP56d showed higher expression in female Drosophila, whereas OBP19d showed no sex differences. We also identified proteins implicated in the metabolism of chemicals. Other molecules, such as pheromones, are detected by the proboscis, but our analysis did not identify any of them. In conclusion, we found that the proboscis is involved in the detection of many classes of molecules that can impact feeding and sexual behavior in *Drosophila melanogaster*.

Abstract: *Drosophila melanogaster* flies use their proboscis to taste and distinguish edible compounds from toxic compounds. With their proboscis, flies can detect sex pheromones at a close distance or by contact. Most of the known proteins associated with proboscis detection belong to gustatory receptor families. To extend our knowledge of proboscis-taste proteins involved in chemodetection, we used a proteomic approach to identify soluble proteins from Drosophila females and males. This investigation, performed with hundreds of dissected proboscis, was initiated by chromatographic separation of tryptic peptides followed by tandem mass spectrometry allowing femtomole detection sensitivity. We found 586 proteins, including enzymes involved in intermediary metabolism and proteins dedicated to various functions such as nucleic acid metabolism, ion transport, immunity, digestion, and organ development. Among 60 proteins

potentially involved in chemosensory detection, we identified two odorant-binding proteins (OBPs), i.e., OBP56d (which showed much higher expression in females than in males) and OBP19d. Because OBP56d was also reported to be more highly expressed in the antennae of females, this protein can be involved in the detection of both volatile and contact male pheromone(s). Our proteomic study paves the way to better understand the complex role of Drosophila proboscis in the chemical detection of food and pheromonal compounds.

Keywords: chemosensory system; taste; odorant-binding proteins; mass spectrometry; proteomics

1. Introduction

Insects use their taste system to evaluate food quality and discriminate edible nutrients and toxic ones. The taste system of the model insect *Drosophila melanogaster* is distributed on multiple parts and appendages of the fly body (proboscis, legs, wing margins and ovipositor [1–3]). The proboscis, a foldable appendage extending from the adult head, includes external and internal taste organs. The external taste organs consist of two labella covered with taste sensory hairs, while the internal taste organs consist of three groups of pharyngeal sensory cells: the labral sense organs (LSOs), the dorsal cibarial sense organ (DCSO) and the ventral cibarial sense organ (VCSO) (Figure 1). Sapid molecules are initially detected by the sensory neurons housed in the sensilla covering the proboscis, and their quality is then evaluated by pharyngeal organs. Each taste sensillum is a uni-porous sensillum containing two or four chemosensory neurons whose dendrites harbor highly specialized receptors, such as gustatory receptors (GRs; [4]), ionotropic receptors (IRs; [5]), members of the transient receptor potential family (TRP; [6]), takeout-like receptors [7] and Pickpocket receptors (ppk; [8]). All sensilla also house one mechanosensory neuron. Electrophysiological recording of gustatory sensilla stimulated with a variety of taste stimuli revealed the presence of four types of gustatory receptor neurons (GRNs) that are either sensitive to (1) sugar, (2) water, (3) low or (4) high salt concentrations [9–11]. The dendrites of all these neurons are bathed in a hydrophilic sensillar lymph. This sensillar lymph contains three large families of proteins: xenobiotic metabolizing enzymes (XMEs; [12, 13] and odorant-binding proteins (OBPs; [13–15]), all of which have been hypothesized to be involved in the transport and/or elimination of chemical

stimuli and chemosensory proteins (CSPs; [16]). CSPs show a broad tissue distribution because they are expressed both in sensory and nonsensory organs involved in various functions during development [14], [17], [18]. However, there is no clear evidence that they participate in olfaction or in gustation. Nevertheless, in Drosophila, 4 CSPs were identified, and they may be involved in the storage and release of pheromone molecules [19]. XMEs are involved in detoxification processes and metabolite elimination [12], [20]. OBPs are small soluble proteins that are found in high concentrations in the sensillar lymph of insects [19]. Fifty-two OBP-coding genes have been identified in *Drosophila melanogaster*. Several OBPs were found in nonsensory tissues such as the Drosophila male reproductive tract [21, 22], hindgut [23] and fat body [24]. OBPs can be also expressed during preimaginal development in Drosophila larvae [18].

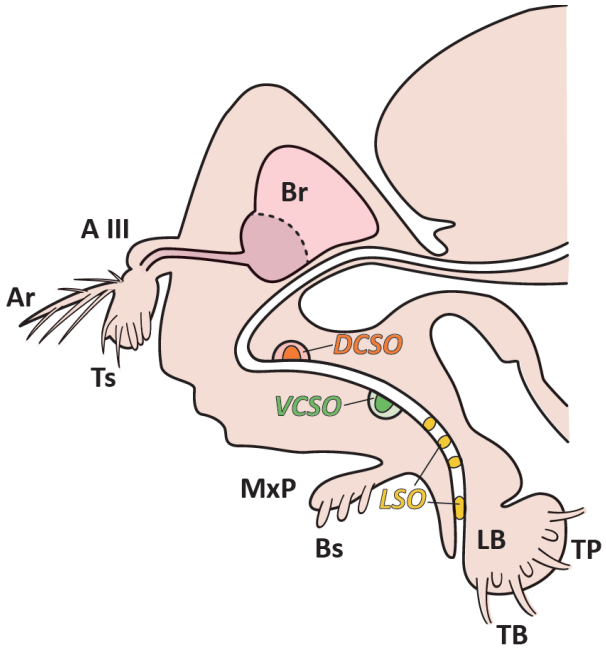

Figure 1. ***Drosophila melanogaster*** **head with olfactory organs, antennae and maxillary palps (Mxp) and gustatory organ, propobscis presented with their sensilla.** Antennae with 3rd antennal segment (A III), arista (Ar) and trichoid sensillum (Ts). Mxp with basiconic sensillum (Bs). The labellum (LB) with taste bristle (TB) and taste peg (TP) and three internal taste organs indicated (i) the labral sense organs (LSOs) in yellow; (ii) the ventral cibarial sense organ (VSCO) in green; and (iii) the dorsal cibarial sense organ (DSCO) in orange. Brain (Br) (Figure adapted from [2])

The best documented function of OBPs is their role in the transport of lipophilic ligands across the aqueous sensilla lymph fluid to dedicated sensory receptors [15], [17], [25, 26].

Several OBPs were shown to play nonolfactory roles [18]. Among them, OBP19c, OBP56g, OBP56b, OBP57b, OBP57e and OBP83c were found to be only expressed in gustatory organs [27]. Moreover, OBP49a, which is expressed in the accessory cells surrounding sweet-responding GRNs, is required to suppress the attractive sugar response after exposure to bitter compounds [28]. Both leg-expressed OBP57d and OBP57e respond in a species-specific manner to C6-C9 fatty acids to elicit egg-laying behavior [29]. Additionally, the proboscis-expressed OBP19b is necessary to transport essential amino acids [30]. OBP59a, which is expressed in the second antennal segment, is implicated in hygrosensation [31, 32]. Other intracellular functions of OBPs remain elusive [33].

To obtain a broader picture of the soluble proteins involved in chemoreception expressed in the *Drosophila melanogaster* proboscis and to identify OBPs and XMEs present in this major taste appendage, we used a proteomics approach. This technique is based on the separation of tryptic peptides by nano-LC followed by tandem mass spectrometry (MS/MS), with femtomole detection sensitivities. We compared the pattern of identified proteins between female and male flies. We found several proteins that are potentially involved in taste, some of which showed sex-specific expression. These proteins include two OBPs, one of which showed clear sexual dimorphism.

2. Materials and Methods

Drosophila stocks and sample preparation

The Canton-S *Drosophila melanogaster* strain (Cs) was kept in a room at 24 ± 0.5 °C and 65 ± 5% relative humidity with a 12-h light/dark cycle. Flies were raised on standard medium culture (1.5% agar–agar, 10% brewer's yeast, 9% corn flour, 0.4% methyl para-hydroxy-benzoate) to ensure development. Virgin female or male flies aged 4 days were dissected. The proboscis were hand-dissected under a microscope and placed in an Eppendorf tube containing 250 µL of 10 mM Tris at pH 8. We obtained duplicate pools of 350 or 550 proboscis dissected from virgin females or virgin males, respectively. Of note, the pair of maxillary palps, normally present on the proboscis, was discarded. These samples were

kept on ice and submitted to ultrasound treatment for 2 min with 5 s pulses every 3 s at 30 W (2 times). The soluble fraction was separated from cell debris or nonsoluble material by centrifugation at 20,000 × g for 30 min at 4 °C. To concentrate all proteins, we performed polyacrylamide gel electrophoresis (SDS–PAGE). A 12% separation gel was used (40% polyacrylamide; Tris 1.5 M pH 8.8; H_2O; 10% SDS; N,N,N,N-tetramethylethyl ethyllenediamine (Temed) and ammonium persulfate (Aps) (10%), and a 12% concentration gel was used (40% polyacrylamide; Tris 0.5 M pH 8.8; H_2O; 10% SDS; Temed and Aps 10%). Twenty microliters of this sample (15 μL of soluble fraction and 5 μL of TDD) were deposited on a gel, and migration was performed at 200 V and 20 mA. Once the samples migrated to the concentration gel, the migration was stopped, and we cut out the band samples in the gel and tested them by mass spectrometry proteomic analysis.

Mass spectrometry proteomic analysis

Proteins were loaded on SDS–PAGE to perform one gel slice trypsin digestion for each sample. Peptides were extracted with 0.1% diluted in formic acid in acetonitrile and evaporated to a volume of 8 μl, which was finally injected into an UltiMate 3000 RSLCnano System (Thermo Fisher Scientific). Peptides were automatically fractionated onto a commercial C18 reversed-phase column (75 μm × 500 mm, 2-μm particle, PepMap100 RSLC column, Thermo Fisher Scientific, temperature 55 °C). Trapping was performed for 4 min at 5 μL/min with solvent A (98% H_2O, 2% acetonitrile and 0.1% formic acid). The peptides were eluted using two solvents, A (0.1% formic acid in water) and B (0.1% formic acid in acetonitrile), at a flow rate of 300 nL/min. Gradient separation lasted 3 min in 3% B, 170 min from 3% to 20% B, 20 min from 20% to 80% B and maintained for 15 min at 80% B. The column was equilibrated for 17 min with 3% buffer B prior to the next sample analysis. The eluted peptides from the C18 column were analyzed by Q-Exactive instruments (Thermo Fisher Scientific). The electrospray voltage was 1.9 kV, and the capillary temperature was 275 °C. Full MS scans were acquired in the Orbitrap mass analyzer over the m/z 400–1200 range with a 70,000 (m/z 200) resolution. The target value was $3.00E^{06}$. The fifteen most intense peaks with charge states between 2 and 5 were fragmented in the higher-energy

collision-activated dissociation cell with a normalized collision energy of 27%, and the tandem mass spectrum was acquired in the Orbitrap mass analyzer with a 17 500 (*m*/*z* 200) resolution. The target value was $1.00E^{05}$. The ion selection threshold was $5.0E^{04}$ counts, and the maximum allowed ion accumulation times were 250 ms for full MS scans and 100 ms for tandem mass spectra. Dynamic exclusion was set to 30 s.

Proteomic data analysis

Raw data collected during nano LC–MS/MS analyses were processed and converted into an *.mgf peak list format with Proteome Discoverer 1.4 (Thermo Fisher Scientific). MS/MS data were analyzed using the search engine Mascot (version 2.4.0, Matrix Science, London, UK) installed on a local server. Searches were performed with a tolerance on mass measurement of 10 ppm for precursor and 0.02 Da for fragment ions against a composite target-decoy database (6064×2 total entries) built with a Drosophila Swissprot database (taxonomy 7215, December 2020, 5946 entries) fused with the sequences of recombinant trypsin and a list of classical contaminants (118 entries). Cysteine carbamidomethylation, methionine oxidation, protein N-terminal acetylation, and cysteine propionamidation were searched as variable modifications. Up to one missed trypsin cleavage was allowed. The identification results were imported into Proline software (http://proline.profiproteomics.fr) [34] for validation. Peptide spectrum matches (PSM) taller than 9 residues and ion scores >15 were retained. The false discovery rate was then optimized to be below 1% at the protein level using the Mascot Modified Mudpit score. Peptide abundances were extracted with Proline software version 2.0 using an m/z tolerance of 10 ppm. Alignment of the LC–MS runs was performed using Loess smoothing. Cross assignment of peptide ion abundances was performed among the samples and controls using an m/z tolerance of 10 ppm and a retention time tolerance of 60 s. Protein abundances were computed using the median ratio fitting of the unique peptide abundances normalized at the peptide level using the median.

3. Results

3.1. Broad identification of soluble proteins from Drosophila melanogaster proboscis

Four proboscis samples (two for each sex) were hand-dissected in four-day-old flies (yielding four pools of approximately 350 females or 550 males). Based on their presence in at least one of the four pools of dissected proboscis, we identified a total of 586 soluble proteins (Table 1; Table S1). Analysis of identified proteins suggests that they originated either from the cytoplasm of disrupted cells or from the extracellular sensillar lymph of taste sensilla. Here, we only show the proteins detected in both samples for each sex. These proteins were classified into 13 categories according to their main known functions (Figure 2). Among all identified proteins, 32.3% are involved in gene expression regulation, nucleic acid metabolism and protein metabolism. These proteins are involved in the regulation of transcription, histone modification, mRNA splicing and protein degradation. We identified actin-, tubulin- and myosin-binding proteins that are involved in the formation of the cytoskeleton structure. They were classified in the "Cytoskeleton organization" category (10.4%). We found proteins involved in cell differentiation or in the regulation of the membrane trafficking pathway from the Golgi apparatus, which were classified in the "Cell function" category (4.8%). We identified proteins involved in electron or proton transportation playing a major role in muscle contraction together with proteins present in actin and thick myosin filaments, which were classified in the "Muscle structure and contraction" category (8.9%).

We also found that 1.7%, 9.2% and 3.9% of the proteins were involved in the metabolism of lipids, energy, and carbohydrates, respectively. All abovementioned proteins are implicated in fatty acid cycles, mitochondrial activity or the glucose cycle. Only 0.3% of the identified proteins were involved in transportation, i.e., the category of "Odorant-binding proteins". We identified protective enzymes associated with antibacterial defense and response against oxidative damage. They were classified into the "Detoxifying enzymes and defense" category (10.4%). We also found two groups of proteins potentially related to chemoreception: (1) proteins involved in the transport of volatile or sapid molecules and (2) enzymes involved in

detoxification processes called XMEs. Other proteins either with another function or with yet unknown function were classified in the "Others" category (10.6%).

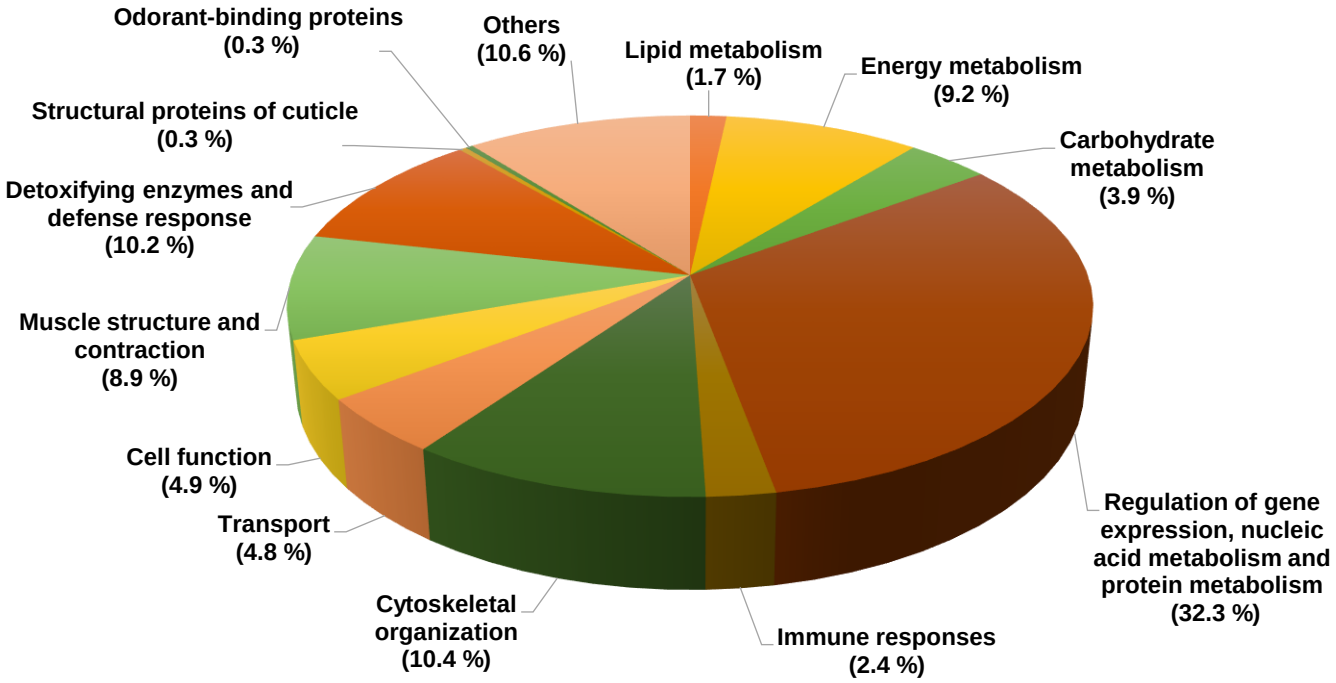

Figure 2. Distribution of all proteins identified in *Drosophila melanogaster* proboscis (proteins identified in females and males are pooled here). The 586 proteins belong to 13 functional categories shown in this pie chart representation (the percentage indicated for each category is relative to the total number of proteins; each protein was counted in only one category).

3.2. Identification of proteins involved in transport and detoxification metabolism

Based on the analysis of the four samples (2 female biological replicates, 2 male biological replicates), we identified 60 proteins potentially involved in chemoreception (Figure 3). These proteins are thought to act in the transport of chemicals and/or to metabolize and eliminate chemicals present in the proboscis. They are shown in Table 1.

Table 1. Proteins that are believed to be involved in the transport of chemicals or that can participate in metabolization and elimination of chemicals present in the proboscis. The mean of the measured abundance of protein is indicated in the right columns.

Accession number	Protein identification	Female mean	Male mean
sp|Q8SY61|OB56D_DROME	General odorant-binding protein 56d	5.09E+06	6.41E+05
sp|P54192|OB19D_DROME	General odorant-binding protein 19d	9.86E+06	7.10E+06
sp|Q95RA9|GILT1_DROME	GILT-like protein 1	1.38E+07	3.45E+06
sp|Q9V521|PPO2_DROME	Phenoloxidase 2	6.06E+07	2.79E+07
sp|Q9V3Z2|SER7_DROME	Serine protease 7	6.70E+05	4.15E+05
sp|Q9V3D2|HEM6_DROME	Oxygen-coproporphyrinogen-III oxidase	3.29E+06	1.26E+06
sp|Q9W265|HOT_DROME	Hydroxyacid-oxoacid transhydrogenase	1.81E+06	
sp|O18404|HCD2_DROME	3-hydroxyacyl-CoA dehydrogenase	4.94E+07	1.90E+07
sp|Q04499|PROD_DROME	Proline dehydrogenase 1	2.68E+06	1.71E+06
sp|Q6AWN0|MTND_DROME	Acireductone dioxygenase	7.14E+05	1.71E+05
sp|P36951|HYI_DROME	Putative hydroxypyruvate isomerase	3.57E+06	1.67E+06
sp|O77458|TPIS_DROYA	Triosephosphate isomerase	5.76E+07	2.27E+07
sp|B3M098|MTNA_DROAN	Methylthioribose-1-phosphate isomerase	1.05E+06	4.21E+05
sp|Q7KML2|ACOX1_DROME	Peroxisomal acyl-coenzyme A oxidase 1	4.97E+07	2.41E+07
sp|Q9V6U9|MECR_DROME	2-enoyl thioester reductase	2.36E+07	4.40E+06
sp|Q01597|G3P_DROHY	Glyceraldehyde-3-phosphate dehydrogenase	2.23E+08	8.95E+07
sp|P07487|G3P2_DROME	Glyceraldehyde-3-phosphate dehydrogenase 2	3.49E+08	1.50E+08
sp|P07486|G3P1_DROME	Glyceraldehyde-3-phosphate dehydrogenase 1	2.91E+08	1.30E+08
sp|O44104|G3P2_DROPS	Glyceraldehyde-3-phosphate dehydrogenase 2	3.70E+08	1.63E+08
sp|P13706|GPDA_DROME	Glycerol-3-phosphate dehydrogenase	1.32E+08	6.49E+07
sp|O02373|UGDH_DROME	UDP-glucose 6-dehydrogenase	7.76E+05	3.19E+05
sp|P54399|PDI_DROME	Protein disulfide-isomerase	9.64E+07	4.18E+07
sp|Q9V429|THIO2_DROME	Thioredoxin-2	3.41E+06	2.07E+06
sp|Q9VSA3|ACADM_DROME	Medium-chain specific acyl-CoA dehydrogenase	9.71E+07	4.54E+07
sp|Q9VWH4|IDH3A_DROME	Isocitrate dehydrogenase	6.06E+07	5.34E+07
sp|P32748|PYRD_DROME	Dihydroorotate dehydrogenase	2.65E+05	1.70E+05
sp|Q9VXJ0|DHB4_DROME	Peroxisomal multifunctional enzyme type 2	1.86E+07	1.14E+07
sp|Q9V3P0|PRDX1_DROME	Peroxiredoxin 1	4.19E+07	1.84E+07
sp|P17336|CATA_DROME	Catalase	1.05E+08	4.20E+07
sp|Q9VG97|GSTD3_DROME	Glutathione S-transferase D3	6.02E+05	2.29E+05
sp|P20432|GSTD1_DROME	Glutathione S-transferase D1	8.75E+07	4.04E+07
sp|P41043|GSTS1_DROME	Glutathione S-transferase S1	2.18E+06	9.93E+05
sp|Q9VZU4|NDUS3_DROME	NADH dehydrogenase	7.11E+06	4.10E+06
sp|Q27597|NCPR_DROME	NADPH--cytochrome P450 reductase	1.31E+06	1.27E+06
sp|P07705|NU3M_DROYA	NADH-ubiquinone oxidoreductase chain 3	6.85E+05	4.46E+05
sp|P91929|NDUAA_DROME	NADH dehydrogenase	5.74E+06	2.43E+06
sp|Q05114|ADH_DROWI	Alcohol dehydrogenase	4.37E+06	1.82E+06
sp|B4M8Y0|ADH_DROVI	Alcohol dehydrogenase	7.10E+06	2.22E+06
sp|P46415|ADHX_DROME	Alcohol dehydrogenase class-3	5.37E+06	2.56E+06
sp|P48584|ADH_DROBO	Alcohol dehydrogenase	2.85E+07	1.90E+07

sp|P09369|ADH2_DROMO	Alcohol dehydrogenase 2	5.41E+07	3.36E+07
sp|P07161|ADH1_DROMU	Alcohol dehydrogenase 1	5.41E+07	3.36E+07
sp|P00334|ADH_DROME	Alcohol dehydrogenase	1.92E+08	1.30E+08
sp|P07159|ADH_DROOR	Alcohol dehydrogenase	1.85E+08	1.25E+08
sp|P10807|ADH_DROLE	Alcohol dehydrogenase	7.30E+07	4.76E+07
sp|Q9W5N0|COA7_DROME	Cytochrome c oxidase	5.51E+05	2.14E+05
sp|Q9V9L1|CP6W1_DROME	Cytochrome P450 6w1	7.56E+05	7.89E+05
sp|Q9V558|CP4P1_DROME	Cytochrome P450 4p1	3.71E+05	2.80E+05
sp|Q9V4N3|CYB5_DROME	Cytochrome b5	1.96E+06	1.86E+06
sp|P19967|CYB5R_DROME	Cytochrome b5	1.71E+05	3.67E+05
sp|Q9VFP1|CP6D5_DROME	Cytochrome P450 6d5	8.61E+06	1.08E+07
sp|Q9VE01|C12A5_DROME	Cytochrome P450 12a5	1.80E+06	1.85E+06
sp|P33270|CP6A2_DROME	Cytochrome P450 6a2	3.40E+06	3.50E+06
sp|Q9VCW1|CP6D4_DROME	Cytochrome P450 6d4	1.05E+06	5.61E+05
sp|Q27606|CP4E2_DROME	Cytochrome P450 4e2	1.90E+05	2.16E+05
sp|Q9VFJ0|CA131_DROME	Cytochrome P450 313a1	5.47E+06	3.35E+07
sp|Q9VLZ7|C4D21_DROME	Cytochrome P450 4d21	1.36E+05	3.54E+06
sp|Q9XY35|QCR9_DROME	Cytochrome b-c1	1.25E+07	9.11E+06
sp|Q9VHS2|COX7A_DROME	Cytochrome c oxidase	6.20E+06	3.43E+06
sp|P84029|CYC2_DROME	Cytochrome c-2	7.44E+07	3.46E+07

To refine our analysis, we only kept the proteins that were simultaneously detected in the two biological replicates, at least in one sex. This procedure yielded a short list of 19 proteins that were putatively involved in chemo-detection: 17 involved in detoxification and two in ligand transport (Table 2). Among detoxification proteins, two are implicated in oxidative stress resistance (catalase, peroxiredoxin), while 15 others belong to one of the three following categories: cytochrome (CYP), alcohol dehydrogenase (ADH), or glutathione S-transferase (GST).

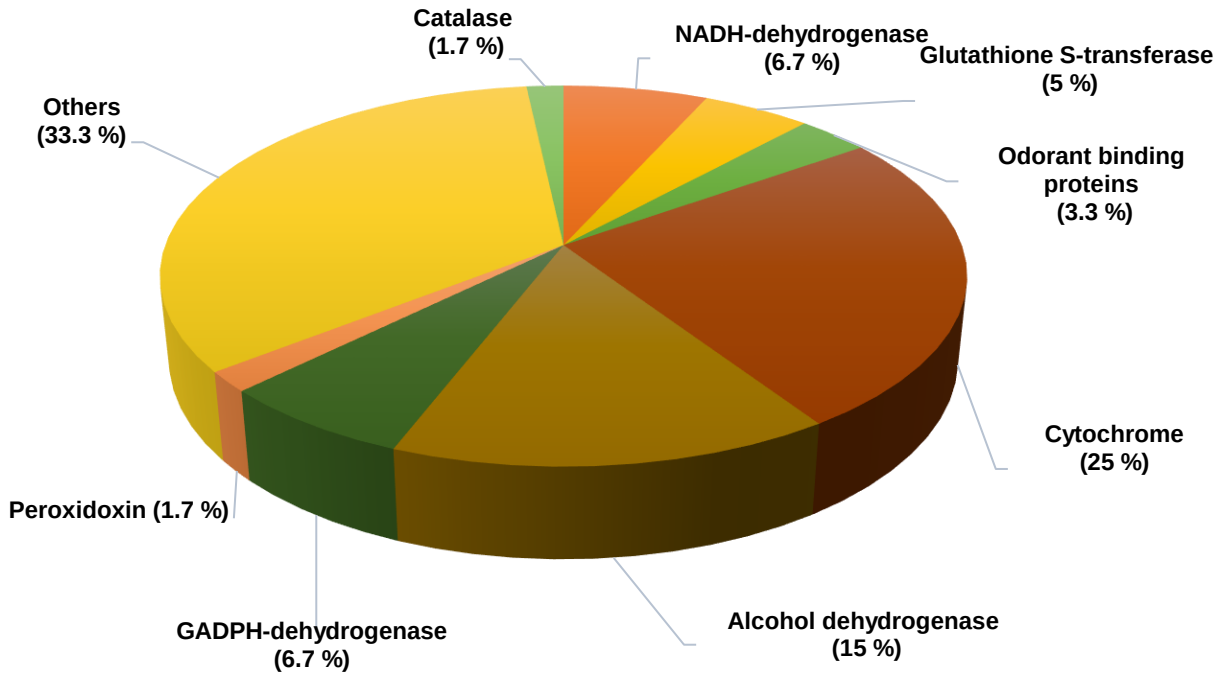

Figure 3. Functional distribution of the 60 proteins putatively involved in "chemoreception". The 60 proteins identified were classified into 8 categories (the percentage indicated for each category is relative to the total number of proteins; each protein was counted in only one category).

More precisely, we found nine cytochromes: five P450 cytochromes and four cytochrome oxidases. The intersex comparison revealed that two P450s (CYP6d5 and CYP313a1) showed higher measured abundance in males than in females, whereas three cytochrome oxidases were more frequently identified in females than in males (Table 2). The remaining cytochromes showed no obvious difference in measured abundance. Among the 3 identified GSTs, only GSTD1 was taken into account for other analyses. It was equally expressed in both sexes. Two OBPs were identified in the proboscis (OBP19d and OBP56d) with OBP56d showing a higher abundance in female proboscis than in male proboscis 5.09×10^6 and 6.41×10^5, respectively; Table 2).

Table 2. The 19 soluble proteins of Drosophila melanogaster proboscis* are potentially involved in the transport and elimination of chemical stimuli.

Accession number	Protein identification	Protein mass (kDa)
sp|Q9V3P0|PRDX1_DROME	Peroxiredoxin 1	21.738
sp|P17336|CATA_DROME	Catalase	57.15
sp|Q8SY61|OB56D_DROME	Odorant-binding protein 56d	14.119
sp|P54192|OB19D_DROME	Odorant-binding protein 19d	16.782
sp|Q9VFP1|CP6D5_DROME	**Cytochrome P450 6d5**	57.384
sp|Q9VE01|C12A5_DROME	Cytochrome P450 12a5	61.355
sp|Q9VCW1|CP6D4_DROME	Cytochrome P450 6d4	59.182
sp|Q9VFJ0|CA131_DROME	**Cytochrome P450 313a1**	56.534
sp|Q9V4N3|CYB5_DROME	Cytochrome b5	15.206
sp|Q9W5N0|COA7_DROME	Cytochrome c oxidase	29.64
sp|P84029|CYC2_DROME	Cytochrome c-2 (Cytochrome c-proximal)	11.735
sp|Q9VHS2|COX7A_DROME	Cytochrome c oxidase subunit 7A	9.902
sp|Q9V558|CP4P1_DROME	Cytochrome P450 4p1	59.433
sp|P20432|GSTD1_DROME	Glutathione S-transferase D1	23.866

sp|B4M8Y0|ADH_DROVI	Alcohol dehydrogenase	27.608
sp|P09369|ADH2_DROMO	Alcohol dehydrogenase 2	27.605
sp|P07161|ADH1_DROMU	Alcohol dehydrogenase 1	27.495
sp|P00334|ADH_DROME	Alcohol dehydrogenase	27.761
sp|P46415|ADHX_DROME	Alcohol dehydrogenase 3	40.389

*Underlined entries designate an expression at least 2 times more important in females than in males; bold font indicates an expression at least 2 times more important in males than in females.

T

4.Discussion

CYPs are often reported to be broadly tuned detoxifying enzymes [12]. More than eighty P450 cytochrome genes have been identified in *Drosophila melanogaster.* Sex-specific differences in cytochromes can be related to their implication in the metabolism of hormone precursors, pheromones or lipids [35]. In Drosophila, it was shown that the loss of function of P450 cytochromes induces specific defects in mechano- and chemosensory perception [36]. CYP303a1 is essential for the development and structure of external sensory organs that mediate the reception of mechanosensory and chemosensory stimuli. This P450 cytochrome, which is only expressed in sensory bristles, may play a role in morphogenesis and cell differentiation [36]. ADH enzymes of classes 1, 2 and 3 were also identified in our proteomic analysis. Among the five ADH enzymes identified in both sexes, two showed higher expression in females (ADH and ADH class 3). ADHs are involved in the metabolic processing of alcohols and aldehydes. They were shown to be necessary for ethanol detection. For example, the level of ADH activity affects Drosophila oviposition preference on food containing a relatively high ethanol concentration [37]. GSTs are ubiquitously expressed enzymes required in detoxification processes. They catalyze the conjugation of glutathione to various molecules. The Drosophila GSTD1 enzyme is involved in resistance to the insecticide dichloro-diphenyl-trichloroethane (DDT) [38]. It is classified in the Delta group of GSTs and appears to be

highly expressed in antennae and proboscis [39]. The presence of GSTD1 was identified in other non-chemosensory organs, like in the gut, carcass and head without appendages, suggesting that it has a general function and is important for insecticide resistance [40, 41].

The two OBPs identified in the proboscis (OBP19d and OBP56d) are not exclusive to the taste system because they are also expressed in the olfactory system [42, 43]. Our analysis did not reveal sex differences in OBP19d expression. A similar result was found in *D. melanogaster* antennae [42]. In this species, OBP19d is localized both in hair-shaped and peg-type taste sensilla [44]. OBP19d is abundantly expressed in all adult gustatory organs on the labellum, legs, and wings and in the internal taste organs on the proboscis. In the hair-shaped sensilla, OBP19d is localized in the crescent-shaped lumen of the sensilla but not in the lumen where the dendrites of the gustatory neurons are found, suggesting that a function in stimulus transport is unlikely in these sensilla [44]. This indicates that OBPs have roles other than the transport of lipophilic tastant ligands.

OBP56d showed a higher abundance in female proboscis than in male proboscis. This fits with the observation that OBP56d mRNA is higher in the female than in the male proboscis (Aruçi et al., in preparation). However, such relationship is not always verified. OBP56d expression was also found in olfactory organs (of the antenna and maxillary palp) and in the gustatory sensilla of the anterior wing margin, tarsae and larval dorsal organs [43]. The higher expression of the OBP56d protein also found in the female antenna [42] indicates that OBP56d is involved both in taste and olfaction. Moreover, its sex-biased expression suggests that it is involved in the detection of male pheromone(s) in females. The fact that the OBP56d gene is also expressed in nonhead tissues such as the adult hindgut and testis [23] raises the tantalizing hypothesis that this OBP is involved not only in the sensory detection of sex pheromones but also in physiological functions such as nutrition and reproduction. For instance, two other OBPs highly related to OBP56d (OBP56f and OBP56g) have been observed in the male seminal fluid. Both are transferred to the female during copulation to subsequently affect egg-laying behavior [45–47]. Another study revealed that the z-7-tricosene (7-T) pheromone elicits a similar electrophysiological signal as bitter substances in the same taste sensilla of the proboscis, suggesting that 7-T tastes bitter to the fly [48]. These two

types of molecules induce dose-dependent inhibition of male–male homosexual courtship.

Two other *D. melanogaster* OBPs are also involved in sexual behaviors. OBP76a (also named Lush) participates in the olfactory detection of the *cis*-vaccenyl acetate male pheromone (cVA) through a pH-dependent interaction with a sensory neuron membrane protein (SNMP; [49, 50]). Lush OBP was initially discovered based on its role in alcohol detection: wild-type flies showed active olfactory avoidance to concentrated alcohol, whereas *lush* mutants did not [51]. Another antenna-expressed OBP (OBP69a), which shows sexually dimorphic expression in *D. melanogaster* flies, also participates in cVA detection. More precisely, exposure of flies to cVA tended to increase OBP69a levels in females and to decrease its levels in males. Increased OBP69a expression led to increased female receptivity to copulation and aggressive behavior in males [52]. These examples suggest that dimorphic expression of OBP may have a role in fly sexual behavior.

We believe that our proteomic analysis missed several proteins expressed at a minute level in the proboscis. For instance, despite the high number of dissected proboscis, we did not detect OBP19b, which is nevertheless present in this taste organ given that it is involved in the detection of amino acids by proboscis taste sensilla [30]. While the evaluation of the level of protein expression based on mRNA expression could be a useful approach in some cases, it remains difficult to carry out given possible post-translational modification and also for technical reasons due to devices used to detect proteins or mRNA levels. A similar comparison could have been carried out in antennae given that two studies measured the levels of mRNA and proteins in these appendages [53]. However, this is not possible here given that no extensive mRNA characterization has been yet carried out on Drosophila proboscis. Other OBPs (OBP56g, OBP19c, OBP83c), which are also present in the proboscis, were not detected in our proteomic screen [28], [43]. This indicates that the expression level of these proteins was too low to be detected with our technique. In our study, the lower level of expression was 1.36×10^5 (Cytochrome P450 4d21; Table 1). Protein detection could be limited by masking peptide fragments in nanoLC–MS/MS analyses. This can explain the failure to detect proteins below a detection threshold. A similar bias was observed in the antenna proteomic screen [42]. These authors detected an

increased number of OBPs when they used an increasing number of antennae in each sample. Another study based on the RNA-seq method was also unable to detect several OBPs, including OBP19d and OBP56d, in fly antennae [53].

5. Conclusions

Our proteomic analysis revealed the presence of many enzymes potentially involved in chemoreception. In particular, we identified putative tastant carriers, including two OBPs. Interestingly, the sexually dimorphic expression observed for OBP56d suggests that it may be involved in the detection and processing of hydrophobic sex-specific pheromone(s) detected by contact. The second (non-sex specific) OBP (OBP19d) is likely involved in food quality detection. Together, these data indicate that the proboscis is a complex organ involved in the detection of general tastant molecules as well as sex pheromones. Further work is needed to characterize the biochemical properties and physiological functions of these OBPs to determine their precise roles in insect chemoreception.

5. Patents

Supplementary Materials: The following supporting information can be downloaded at www.mdpi.com/xxx/s1. Table S1: List of identified soluble proteins in proboscis.

Author Contributions: Conceptualization, E.A., J-F.F., L.B.; methodology E.A., J-M.S., J-F.F., L.B.; validation, E.A., J-M.S., J-F.F. and L.B.; formal analysis, E.A., J-M.S., J-F.F. and L.B.; investigation, E.A., J-M.S., J-F.F. and L.B.; data curation, E.A. and J-M.S.; writing—original draft preparation, E.A., J.-F. and L.B.; writing—review and editing, E.A., J-M.S., J-F.F. and L.B.; visualization, E.A., J-F.F. and L.B.; supervision, J-F. and L.B.; project administration, L.B.; funding acquisition, L.B. All authors have read and agreed to the published version of the manuscript.

Funding: This research was funded by the Institut National de la Recherche pour l'Agriculture, l'Alimentation et l'Environnement (INRAE) and the Burgundy council, as well as a fellowship from the Burgundy council (A.L.).

Institutional Review Board Statement: Not applicable.

Informed Consent Statement: Not applicable.

Data Availability Statement: All data in this paper were analyzed using the search engine Mascot (version 2.4.0, Matrix Science, London, UK). For the visualization of the results, we used XLSTAT 2022.2.1. The datasets generated and analyzed during this study are available from the corresponding author on request.

Acknowledgments: We thank F. Neiers for helping in the preparation of samples and C. Everaerts for his help in the preparation of proboscis figure.

Conflicts of Interest: The authors declare no conflict of interest

References

[1] H. Raad, J.-F. Ferveur, N. Ledger, M. Capovilla, and A. Robichon, "Functional Gustatory Role of Chemoreceptors in Drosophila Wings," *Cell Reports*, vol. 15, no. 7, pp. 1442–1454, May 2016, doi: 10.1016/j.celrep.2016.04.040.

[2] R. F. Stocker, "The organization of the chemosensory system in Drosophila melanogaster: a rewiew," *Cell Tissue Res*, vol. 275, no. 1, pp. 3–26, Jan. 1994, doi: 10.1007/BF00305372.

[3] L. B. Vosshall and R. F. Stocker, "Molecular Architecture of Smell and Taste in *Drosophila*," *Annu. Rev. Neurosci.*, vol. 30, no. 1, pp. 505–533, Jul. 2007, doi: 10.1146/annurev.neuro.30.051606.094306.

[4] H. Amrein and N. Thorne, "Gustatory Perception and Behavior in Drosophila melanogaster," *Current Biology*, vol. 15, no. 17, pp. R673–R684, Sep. 2005, doi: 10.1016/j.cub.2005.08.021.

[5] R. Benton, K. S. Vannice, C. Gomez-Diaz, and L. B. Vosshall, "Variant Ionotropic Glutamate Receptors as Chemosensory Receptors in Drosophila," *Cell*, vol. 136, no. 1, pp. 149–162, Jan. 2009, doi: 10.1016/j.cell.2008.12.001.

[6] T. Voets, K. Talavera, G. Owsianik, and B. Nilius, "Sensing with TRP channels," *Nat Chem Biol*, vol. 1, no. 2, pp. 85–92, Jul. 2005, doi: 10.1038/nchembio0705-85.

[7] K. Fujikawa, K. Seno, and M. Ozaki, "A novel Takeout-like protein expressed in the taste and olfactory organs of the blowfly, Phormia regina," *FEBS Journal*, vol. 273, no. 18, pp. 4311–4321, Sep. 2006, doi: 10.1111/j.1742-4658.2006.05422.x.

[8] T. Liu, X. Guo, Y. Bu, Y. Zhou, Y. Duan, and Q. Yang, "Structural and biochemical insights into an insect gut-specific chitinase with antifungal activity," *Insect Biochemistry and Molecular Biology*, vol. 119, p. 103326, Apr. 2020, doi: 10.1016/j.ibmb.2020.103326.

[9] N. Fujishiro and H. Kijima, "IMPULSE FREQUENCY AND ACTION POTENTIAL AMPLITUDE IN LABELLAR CHEMOSENSORY NEURONES OF DROSOPHILA MELANOGASTER," p. 9, 1984.

[10] N. Meunier, F. Marion-Poll, J.-P. Rospars, and T. Tanimura, "Peripheral coding of bitter taste inDrosophila," *J. Neurobiol.*, vol. 56, no. 2, pp. 139–152, Aug. 2003, doi: 10.1002/neu.10235.

[11] S. R. Shanbhag and R. Naresh Singh, "Functional implications of the projections of neurons from individual labellar sensillum of Drosophila melanogaster as revealed by neuronal-marker horseradish peroxidase," *Cell Tissue Res*, vol. 267, no. 2, pp. 273–282, Feb. 1992, doi: 10.1007/BF00302965.

[12] J.-M. Heydel *et al.*, "Odorant-Binding Proteins and Xenobiotic Metabolizing Enzymes: Implications in Olfactory Perireceptor Events: Odorant-Binding Proteins and Metabolizing Enzymes," *Anat. Rec.*, vol. 296, no. 9, pp. 1333–1345, Sep. 2013, doi: 10.1002/ar.22735.

[13] P. Pelosi, "Odorant-Binding Proteins," *1994*, p. 30, 1994.

[14] P. Pelosi, "Diversity of Odorant-binding Proteins and Chemosensory Proteins in Insects," *Chemical Senses*, vol. 30, no. Supplement 1, pp. i291–i292, Jan. 2005, doi: 10.1093/chemse/bjh229.
[15] R. G. Vogt and L. M. Riddiford, "Pheromone binding and inactivation by moth antennae," *Nature*, vol. 293, no. 5828, pp. 161–163, Sep. 1981, doi: 10.1038/293161a0.
[16] S. Angeli *et al.*, "Purification, structural characterization, cloning and immunocytochemical localization of chemoreception proteins from Schistocerca gregaria," *Eur J Biochem*, vol. 262, no. 3, pp. 745–754, Jun. 1999, doi: 10.1046/j.1432-1327.1999.00438.x.
[17] N. F. Brito, M. F. Moreira, and A. C. A. Melo, "A look inside odorant-binding proteins in insect chemoreception," *Journal of Insect Physiology*, vol. 95, pp. 51–65, Dec. 2016, doi: 10.1016/j.jinsphys.2016.09.008.
[18] K. Rihani, J.-F. Ferveur, and L. Briand, "The 40-Year Mystery of Insect Odorant-Binding Proteins," *Biomolecules*, vol. 11, no. 4, p. 509, Mar. 2021, doi: 10.3390/biom11040509.
[19] P. Pelosi, J.-J. Zhou, L. P. Ban, and M. Calvello, "Soluble proteins in insect chemical communication," *Cell. Mol. Life Sci.*, vol. 63, no. 14, pp. 1658–1676, Jul. 2006, doi: 10.1007/s00018-005-5607-0.
[20] S. M. Rollmann, T. F. C. Mackay, and R. R. H. Anholt, "Pinocchio, a novel protein expressed in the antenna, contributes to olfactory behavior in *Drosophila melanogaster*: Pinocchio Contributes to Olfaction," *J. Neurobiol.*, vol. 63, no. 2, pp. 146–158, May 2005, doi: 10.1002/neu.20123.
[21] G. D. Findlay, X. Yi, M. J. MacCoss, and W. J. Swanson, "Proteomics Reveals Novel Drosophila Seminal Fluid Proteins Transferred at Mating," *PLoS Biol*, vol. 6, no. 7, p. e178, Jul. 2008, doi: 10.1371/journal.pbio.0060178.
[22] N. Takemori and M.-T. Yamamoto, "Proteome mapping of the ***Drosophila melanogaster*** male reproductive system," *Proteomics*, vol. 9, no. 9, pp. 2484–2493, May 2009, doi: 10.1002/pmic.200800795.
[23] V. R. Chintapalli, J. Wang, and J. A. T. Dow, "Using FlyAtlas to identify better Drosophila melanogaster models of human disease," *Nat Genet*, vol. 39, no. 6, pp. 715–720, Jun. 2007, doi: 10.1038/ng2049.
[24] H.-L. Chen, U. Stern, and C.-H. Yang, "Molecular control limiting sensitivity of sweet taste neurons in *Drosophila*," *Proc Natl Acad Sci USA*, vol. 116, no. 40, pp. 20158–20168, Oct. 2019, doi: 10.1073/pnas.1911583116.
[25] D. Gonzalez *et al.*, "The Drosophila odorant-binding protein 28a is involved in the detection of the floral odour ß-ionone," *Cell. Mol. Life Sci.*, Sep. 2019, doi: 10.1007/s00018-019-03300-4.
[26] R. A. Steinbrecht, "Odorant-Binding Proteins: Expression and Function," *Annals NY Acad Sci*, vol. 855, no. 1 OLFACTION AND, pp. 323–332, Nov. 1998, doi: 10.1111/j.1749-6632.1998.tb10591.x.

[27] D. S. Hekmat-Scafe, "Genome-Wide Analysis of the Odorant-Binding Protein Gene Family in Drosophila melanogaster," *Genome Research*, vol. 12, no. 9, pp. 1357–1369, Sep. 2002, doi: 10.1101/gr.239402.
[28] Y. T. Jeong *et al.*, "An Odorant-Binding Protein Required for Suppression of Sweet Taste by Bitter Chemicals," *Neuron*, vol. 79, no. 4, pp. 725–737, Aug. 2013, doi: 10.1016/j.neuron.2013.06.025.
[29] T. Matsuo, S. Sugaya, J. Yasukawa, T. Aigaki, and Y. Fuyama, "Odorant-Binding Proteins OBP57d and OBP57e Affect Taste Perception and Host-Plant Preference in Drosophila sechellia," *PLoS Biol*, vol. 5, no. 5, p. e118, Apr. 2007, doi: 10.1371/journal.pbio.0050118.
[30] K. Rihani *et al.*, "A conserved odorant binding protein is required for essential amino acid detection in Drosophila," *Commun Biol*, vol. 2, no. 1, p. 425, 2019, doi: 10.1038/s42003-019-0673-2.
[31] J. S. Sun, N. K. Larter, J. S. Chahda, D. Rioux, A. Gumaste, and J. R. Carlson, "Humidity response depends on the small soluble protein Obp59a in Drosophila," *eLife*, vol. 7, p. e39249, Sep. 2018, doi: 10.7554/eLife.39249.
[32] P. Xu, R. Atkinson, D. N. M. Jones, and D. P. Smith, "Drosophila OBP LUSH Is Required for Activity of Pheromone-Sensitive Neurons," *Neuron*, vol. 45, no. 2, pp. 193–200, Jan. 2005, doi: 10.1016/j.neuron.2004.12.031.
[33] W. S. Leal, "Odorant Reception in Insects: Roles of Receptors, Binding Proteins, and Degrading Enzymes," *Annu. Rev. Entomol.*, vol. 58, no. 1, pp. 373–391, Jan. 2013, doi: 10.1146/annurev-ento-120811-153635.
[34] D. Bouyssié *et al.*, "Proline: an efficient and user-friendly software suite for large-scale proteomics," *Bioinformatics*, vol. 36, no. 10, pp. 3148–3155, May 2020, doi: 10.1093/bioinformatics/btaa118.
[35] M. A. Ortiz de Montellano, "Inhibition of Cytochrome P450 Enzymes," p. 60, 1995.
[36] A. T. Willingham and T. Keil, "A tissue specific cytochrome P450 required for the structure and function of Drosophila sensory organs," *Mechanisms of Development*, vol. 121, no. 10, pp. 1289–1297, Oct. 2004, doi: 10.1016/j.mod.2004.04.017.
[37] M. L. Siegal and D. L. Hartl, "Oviposition-Site Preference in Drosophila Following Interspecific Gene Transfer of the Alcohol dehydrogenase Locus," p. 6, 1999.
[38] A. H. Tang and C. P. Tu, "Biochemical characterization of Drosophila glutathione S-transferases D1 and D21.," *Journal of Biological Chemistry*, vol. 269, no. 45, pp. 27876–27884, Nov. 1994, doi: 10.1016/S0021-9258(18)46868-8.
[39] E. Gonis *et al.*, "Expression Patterns of Drosophila Melanogaster Glutathione Transferases," *Insects*, vol. 13, no. 7, p. 612, Jul. 2022, doi: 10.3390/insects13070612.
[40] Z. Alias and A. G. Clark, "Studies on the glutathione S-transferase proteome of adultDrosophila melanogaster: Responsiveness to chemical challenge," *Proteomics*, vol. 7, no. 19, pp. 3618–3628, Oct. 2007, doi: 10.1002/pmic.200700070.

[41] W. Y. Low *et al.*, "Recognition and Detoxification of the Insecticide DDT by Drosophila melanogaster Glutathione S-Transferase D1," *Journal of Molecular Biology*, vol. 399, no. 3, pp. 358–366, Jun. 2010, doi: 10.1016/j.jmb.2010.04.020.
[42] R. R. H. Anholt and T. I. Williams, "The Soluble Proteome of the Drosophila Antenna," *Chemical Senses*, vol. 35, no. 1, pp. 21–30, Jan. 2010, doi: 10.1093/chemse/bjp073.
[43] K. Galindo and D. P. Smith, "A Large Family of Divergent Drosophila Odorant-Binding Proteins Expressed in Gustatory and Olfactory Sensilla," p. 14, 2001.
[44] S. Shanbhag, P. S.-K., P. C., and S. R., "Gustatory organs of Drosophila melanogaster : fine structure and expression of the putative odorant-binding protein PBPRP2," *Cell and Tissue Research*, vol. 304, no. 3, pp. 423–437, May 2001, doi: 10.1007/s004410100388.
[45] F. W. Avila, L. K. Sirot, B. A. LaFlamme, C. D. Rubinstein, and M. F. Wolfner, "Insect Seminal Fluid Proteins: Identification and Function," *Annu. Rev. Entomol.*, vol. 56, no. 1, pp. 21–40, Jan. 2011, doi: 10.1146/annurev-ento-120709-144823.
[46] I. Sepil *et al.*, "Quantitative Proteomics Identification of Seminal Fluid Proteins in Male Drosophila melanogaster," *Molecular & Cellular Proteomics*, vol. 18, pp. S46–S58, Mar. 2019, doi: 10.1074/mcp.RA118.000831.
[47] M. F. Wolfner, "The gifts that keep on giving: physiological functions and evolutionary dynamics of male seminal proteins in Drosophila," *Heredity*, vol. 88, no. 2, pp. 85–93, Feb. 2002, doi: 10.1038/sj.hdy.6800017.
[48] F. Lacaille *et al.*, "An Inhibitory Sex Pheromone Tastes Bitter for Drosophila Males," *PLoS ONE*, vol. 2, no. 8, p. e661, Aug. 2007, doi: 10.1371/journal.pone.0000661.
[49] R. Benton, K. S. Vannice, and L. B. Vosshall, "An essential role for a CD36-related receptor in pheromone detection in Drosophila," *Nature*, vol. 450, no. 7167, pp. 289–293, Nov. 2007, doi: 10.1038/nature06328.
[50] M. E. Rogers, R. A. Steinbrecht, and R. G. Vogt, "Expression of SNMP-1 in olfactory neurons and sensilla of male and female antennae of the silkmoth Antheraea polyphemus," *Cell and Tissue Research*, vol. 303, no. 3, pp. 433–446, Mar. 2001, doi: 10.1007/s004410000305.
[51] M.-S. Kim, A. Repp, and D. P. Smith, "LUSH Odorant-Binding Protein Mediates Chemosensory Responses to Alcohols in Drosophila melanogaster," *Genetics*, vol. 150, no. 2, pp. 711–721, Oct. 1998, doi: 10.1093/genetics/150.2.711.
[52] T. A. Hopf, S. Morinaga, S. Ihara, K. Touhara, D. S. Marks, and R. Benton, "Amino acid coevolution reveals three-dimensional structure and functional domains of insect odorant receptors," *Nat Commun*, vol. 6, no. 1, p. 6077, May 2015, doi: 10.1038/ncomms7077.
[53] F. Younus *et al.*, "Identification of candidate odorant degrading gene/enzyme systems in the antennal transcriptome of Drosophila melanogaster," *Insect Biochemistry and Molecular Biology*, vol. 53, pp. 30–43, Oct. 2014, doi: 10.1016/j.ibmb.2014.07.003.

References

Abaffy, T., Matsunami, H. and Luetje, C.W. 2006. Functional analysis of a mammalian odorant receptor subfamily. *J Neurochem*, **97**: 1506–1518.

Abdelfattah, A., Wisniewski, M., Schena, L. and Tack, A.J.M. 2021. Experimental evidence of microbial inheritance in plants and transmission routes from seed to phyllosphere and root. *Environ Microbiol*, **23**: 2199–2214.

Adams, M.D., Celniker, S.E., Holt, R.A., Evans, C.A. and Gocayne, J.D. 2000. The Genome Sequence of Drosophila melanogaster. *Science*, **287**: 2185–2195.

Adler, E., Hoon, M.A., Mueller, K.L., Chandrashekar, J., Ryba, N.J.P. and Zuker, C.S. 2000. A Novel Family of Mammalian Taste Receptors. *Cell*, **100**: 693–702.

Agranyoni, O., Meninger-Mordechay, S., Uzan, A., Ziv, O., Salmon-Divon, M., Rodin, D., Raz, O., Koman, I., Koren, O., Pinhasov, A. and Navon-Venezia, S. 2021. Gut microbiota determines the social behavior of mice and induces metabolic and inflammatory changes in their adipose tissue. *npj Biofilms Microbiomes*, **7**: 28.

Al-Assal, K., Martinez, A.C., Torrinhas, R.S., Cardinelli, C. and Waitzberg, D. 2018. Gut microbiota and obesity. *Clinical Nutrition Experimental*, **20**: 60–64.

Andersen, M.K., MacMillan, H.A., Donini, A. and Overgaard, J. 2017. Cold tolerance of *Drosophila* species is tightly linked to epithelial K+ transport capacity of the Malpighian tubules and rectal pads. *Journal of Experimental Biology*, jeb.168518.

Anholt, R.R.H. and Williams, T.I. 2010. The Soluble Proteome of the Drosophila Antenna. *Chemical Senses*, **35**: 21–30.

Arboleya, S., Suárez, M., Fernández, N., Mantecón, L., Solís, G., Gueimonde, M. and de los Reyes-Gavilán, C.G. 2018. C-section and the Neonatal Gut Microbiome Acquisition: Consequences for Future Health. *Ann Nutr Metab*, **73**: 17–23.

Arthur, J.C., Perez-Chanona, E., Mühlbauer, M., Tomkovich, S., Uronis, J.M., Fan, T.-J., Campbell, B.J., Abujamel, T., Dogan, B., Rogers, A.B., Rhodes, J.M., Stintzi, A., Simpson, K.W., Hansen, J.J., Keku, T.O., Fodor, A.A. and Jobin, C. 2012. Intestinal Inflammation Targets Cancer-Inducing Activity of the Microbiota. *Science*, **338**: 120–123.

Aruçi, E., Saliou, J.-M., Ferveur, J.-F. and Briand, L. 2022. Proteomic Characterization of Drosophila melanogaster Proboscis. *Biology*, **11**: 1687.

Avila, F.W., Sirot, L.K., LaFlamme, B.A., Rubinstein, C.D. and Wolfner, M.F. 2011. Insect Seminal Fluid Proteins: Identification and Function. *Annu. Rev. Entomol.*, **56**: 21–40.

Azuma, H., Thien, L.B. and Kawano, S. 1999. Floral scents, leaf volatiles and thermogenic flowers in Magnoliaceae. *Plant Species Biol*, **14**: 121–127.

Baillie, A.G.S., Coburn, C.T. and Abumrad, N.A. 1996. Reversible Binding of Long-chain Fatty Acids to Purified FAT, the Adipose CD36 Homolog. *Journal of Membrane Biology*, **153**: 75–81.

Baothman, O.A., Zamzami, M.A., Taher, I., Abubaker, J. and Abu-Farha, M. 2016. The role of Gut Microbiota in the development of obesity and Diabetes. *Lipids Health Dis*, **15**: 108.

Barceló-Coblijn, G. and Murphy, E.J. 2009. Alpha-linolenic acid and its conversion to longer chain n−3 fatty acids: Benefits for human health and a role in maintaining tissue n−3 fatty acid levels. *Progress in Lipid Research*, **48**: 355–374.

Bar-On, Y.M., Phillips, R. and Milo, R. 2018. The biomass distribution on Earth. *Proc. Natl. Acad. Sci. U.S.A.*, **115**: 6506–6511.

Bartelt, R.J., Schaner, A.M. and Jackson, L.L. 1985. cis-Vaccenyl acetate as an aggregation pheromone inDrosophila melanogaster. *J Chem Ecol*, **11**: 1747–1756.

Bassler, B.L. 1999. How bacteria talk to each other: regulation of gene expression by quorum sensing. *Current Opinion in Microbiology*, **2**: 582–587.

Belloir, C., Neiers, F. and Briand, L. 2017. Sweeteners and sweetness enhancers. *Current Opinion in Clinical Nutrition & Metabolic Care*, **20**: 279–285.

Benoit, J.B., Vigneron, A., Broderick, N.A., Wu, Y., Sun, J.S., Carlson, J.R., Aksoy, S. and Weiss, B.L. 2017. Symbiont-induced odorant binding proteins mediate insect host hematopoiesis. *eLife*, **6**: e19535.

Benton, R., Sachse, S., Michnick, S.W. and Vosshall, L.B. 2006. Atypical Membrane Topology and Heteromeric Function of Drosophila Odorant Receptors In Vivo. *PLoS Biol*, **4**: e20.

Benton, R., Vannice, K.S., Gomez-Diaz, C. and Vosshall, L.B. 2009. Variant Ionotropic Glutamate Receptors as Chemosensory Receptors in Drosophila. *Cell*, **136**: 149–162.

Beynon, R.J. and Hurst, J.L. 2004. Urinary proteins and the modulation of chemical scents in mice and rats. *Peptides*, **25**: 1553–1563.

Bianchet, M.A., Bains, G., Pelosi, P., Pevsner, J., Snyder, S.H., Monaco, H.L. and Amzel, L.M. 1996. The three-dimensional structure of bovine odorant binding protein and its mechanism of odor recognition. *Nat Struct Mol Biol*, **3**: 934–939.

Billeter, J.-C., Atallah, J., Krupp, J.J., Millar, J.G. and Levine, J.D. 2009. Specialized cells tag sexual and species identity in Drosophila melanogaster. *Nature*, **461**: 987–991.

Billeter, J.-C. and Levine, J.D. 2015. The role of cVA and the Odorant binding protein Lush in social and sexual behavior in Drosophila melanogaster. *Front. Ecol. Evol.*, **3**.

Blaser, M.J. and Parsonnet, J. 1994. Parasitism by the “Slow” Bacterium Helicobacter pylon Leads to Altered Gastric Homeostasis and Neoplasia. 5.

Bloemberg, G.V. and Lugtenberg, B.J.J. 2001. Molecular basis of plant growth promotion and biocontrol by rhizobacteria. *Current Opinion in Plant Biology*, **4**: 343–350.

Blum, J.E., Fischer, C.N., Miles, J. and Handelsman, J. 2013. Frequent Replenishment Sustains the Beneficial Microbiome of Drosophila melanogaster. *mBio*, **4**: e00860-13.

Bojsen-Møller, F. 1975. Demonstration of terminalis, olfactory, trigeminal and perivascular nerves in the rat nasal septum: INNERVATION OF RAT NASAL SEPTUM. *J. Comp. Neurol.*, **159**: 245–256.

Bolter, C.J., Dicke, M., Van Loon, J.J.A., Visser, J.H. and Posthumus, M.A. 1997. Attraction of Colorado Potato Beetle to Herbivore-Damaged Plants During Herbivory and After Its Termination. *J Chem Ecol*, **23**: 1003–1023.

Bosch, O.J., Geier, M. and Boeckh, J. 2000. Contribution of Fatty Acids to Olfactory Host Finding of Female Aedes aegypti. *Chemical Senses*, **25**: 323–330.

Briand, L., Nespoulous, C., Huet, J.-C., Takahashi, M. and Pernollet, J.-C. 2001. Ligand binding and physico-chemical properties of ASP2, a recombinant odorant-binding protein from honeybee (*Apis mellifera* L.): Odorant binding by a honeybee OBP. *European Journal of Biochemistry*, **268**: 752–760.

Briand, L., Trotier, D. and Pernollet, J.-C. 2004. Aphrodisin, an aphrodisiac lipocalin secreted in hamster vaginal secretions. *Peptides*, **25**: 1545–1552.

Brieger, G. and Butterworth, F.M. 1970. *Drosophila melanogaster* : Identity of Male Lipid in Reproductive System. *Science*, **167**: 1262–1262.

Briscoe, C.P., Tadayyon, M., Andrews, J.L., Benson, W.G., Chambers, J.K., Eilert, M.M., Ellis, C., Elshourbagy, N.A., Goetz, A.S., Minnick, D.T., Murdock, P.R., Sauls, H.R., Shabon, U., Spinage, L.D., Strum, J.C., Szekeres, P.G., Tan, K.B., Way, J.M., Ignar, D.M., *et al.* 2003. The Orphan G Protein-coupled Receptor GPR40 Is Activated by Medium and Long Chain Fatty Acids. *Journal of Biological Chemistry*, **278**: 11303–11311.

Brito, N.F., Moreira, M.F. and Melo, A.C.A. 2016. A look inside odorant-binding proteins in insect chemoreception. *Journal of Insect Physiology*, **95**: 51–65.

Broderick, N.A. and Lemaitre, B. 2012. Gut-associated microbes of Drosophila melanogaster. *Gut Microbes*, **3**: 307–321.

Brulé, M., Glaz, M., Belloir, C., Poirier, N., Moitrier, L., Neiers, F. and Briand, L. 2020. Bacterial expression and purification of vertebrate odorant-binding proteins. In: *Methods in Enzymology*, pp. 125–150.

Buchholz, F., Antonielli, L., Kostić, T., Sessitsch, A. and Mitter, B. 2019. The bacterial community in potato is recruited from soil and partly inherited across generations. *PLoS ONE*, **14**: e0223691.

Buchon, N., Osman, D., David, F.P.A., Yu Fang, H., Boquete, J.-P., Deplancke, B. and Lemaitre, B. 2013. Morphological and Molecular Characterization of Adult Midgut Compartmentalization in Drosophila. *Cell Reports*, **3**: 1725–1738.

Buchon, N., Silverman, N. and Cherry, S. 2014. Immunity in Drosophila melanogaster — from microbial recognition to whole-organism physiology. *Nat Rev Immunol*, **14**: 796–810.

Buck, L. and Axel, R. 1991. A Novel Multigene Family May Encode Odorant Receptors: A Molecular Basis for Odor Recognition. 13.

Buck, L.B. 1996. Information Coding in the Vertebrate Olfactory System. 28.

Bufe, B., Schumann, T. and Zufall, F. 2012. Formyl Peptide Receptors from Immune and Vomeronasal System Exhibit Distinct Agonist Properties. *Journal of Biological Chemistry*, **287**: 33644–33655.

Cameron, P., Hiroi, M., Ngai, J. and Scott, K. 2010. The molecular basis for water taste in Drosophila. *Nature*, **465**: 91–95.

Canessa, C.M., Schild, L., Buell, G., Thorens, B., Gautschi, I., Horisberger, J.-D. and Rossier, B.C. 1994. Amiloride-sensitive epithelial Na+ channel is made of three homologous subunits. *Nature*, **367**: 463–467.

Cartoni, C., Yasumatsu, K., Ohkuri, T., Shigemura, N., Yoshida, R., Godinot, N., le Coutre, J., Ninomiya, Y. and Damak, S. 2010. Taste Preference for Fatty Acids Is Mediated by GPR40 and GPR120. *Journal of Neuroscience*, **30**: 8376–8382.

Chale-Rush, A., Burgess, J.R. and Mattes, R.D. 2007. Evidence for Human Orosensory (Taste?) Sensitivity to Free Fatty Acids. *Chemical Senses*, **32**: 423–431.

Chandler, J.A. and James, P.M. 2013. Discovery of Trypanosomatid Parasites in Globally Distributed Drosophila Species. *PLoS ONE*, **8**: e61937.

Chandler, J.A., Morgan Lang, J., Bhatnagar, S., Eisen, J.A. and Kopp, A. 2011. Bacterial Communities of Diverse Drosophila Species: Ecological Context of a Host–Microbe Model System. *PLoS Genet*, **7**: e1002272.

Chandrashekar, J., Hoon, M.A., Ryba, N.J.P. and Zuker, C.S. 2006. The receptors and cells for mammalian taste. *Nature*, **444**: 288–294.

Chandrashekar, J., Kuhn, C., Oka, Y., Yarmolinsky, D.A., Hummler, E., Ryba, N.J.P. and Zuker, C.S. 2010. The cells and peripheral representation of sodium taste in mice. *Nature*, **464**: 297–301.

Chandrashekar, J., Mueller, K.L., Hoon, M.A., Adler, E., Feng, L., Guo, W., Zuker, C.S. and Ryba, N.J.P. 2000. T2Rs Function as Bitter Taste Receptors. *Cell*, **100**: 703–711.

Chang, R.B., Waters, H. and Liman, E.R. 2010. A proton current drives action potentials in genetically identified sour taste cells. *Proc. Natl. Acad. Sci. U.S.A.*, **107**: 22320–22325.

Charlu, S., Wisotsky, Z., Medina, A. and Dahanukar, A. 2013. Acid sensing by sweet and bitter taste neurons in Drosophila melanogaster. *Nat Commun*, **4**: 2042.

Chen, K., Luan, X., Liu, Q., Wang, J., Chang, Xinxia, Snijders, A.M., Mao, J.-H., Secombe, J., Dan, Z., Chen, J.-H., Wang, Z., Dong, X., Qiu, C., Chang, Xiaoai, Zhang, D., Celniker, S.E. and Liu, X. 2019. Drosophila Histone Demethylase KDM5 Regulates Social Behavior through Immune Control and Gut Microbiota Maintenance. *Cell Host & Microbe*, **25**: 537-552.e8.

Chen, Y.-C.D. and Dahanukar, A. 2019. Recent advances in the genetic basis of taste detection in Drosophila. *Cell. Mol. Life Sci.*, doi: 10.1007/s00018-019-03320-0.

Chen, Z., Wang, Q. and Wang, Z. 2010. The Amiloride-Sensitive Epithelial Na+ Channel PPK28 Is Essential for Drosophila Gustatory Water Reception. *Journal of Neuroscience*, **30**: 6247–6252.

Chevalier, G., Siopi, E., Guenin-Macé, L., Pascal, M., Laval, T., Rifflet, A., Boneca, I.G., Demangel, C., Colsch, B., Pruvost, A., Chu-Van, E., Messager, A., Leulier, F., Lepousez, G., Eberl, G. and Lledo, P.-M. 2020. Effect of gut microbiota on depressive-like behaviors in mice is mediated by the endocannabinoid system. *Nat Commun*, **11**: 6363.

Cognigni, P., Bailey, A.P. and Miguel-Aliaga, I. 2011. Enteric Neurons and Systemic Signals Couple Nutritional and Reproductive Status with Intestinal Homeostasis. *Cell Metabolism*, **13**: 92–104.

Cohen, E., Allen, S.R., Sawyer, J.K. and Fox, D.T. 2018. Fizzy-Related dictates A cell cycle switch during organ repair and tissue growth responses in the Drosophila hindgut. *eLife*, **7**: e38327.

Cohen, E., Sawyer, J.K., Peterson, N.G., Dow, J.A.T. and Fox, D.T. 2020. Physiology, Development, and Disease Modeling in the *Drosophila* Excretory System. *Genetics*, **214**: 235–264.

Cortot, J., Farine, J.-P., Houot, B., Everaerts, C. and Jean-Francois Ferveur. 2019. Experimental Introgression To Evaluate the impact of Sex Specific Traits on Drosophila melanogaster Incipient Speciation.

Couto, A., Alenius, M. and Dickson, B.J. 2005. Molecular, Anatomical, and Functional Organization of the Drosophila Olfactory System. *Current Biology*, **15**: 1535–1547.

Cremon, C., Barbaro, M.R., Ventura, M. and Barbara, G. 2018. Pre- and probiotic overview. *Current Opinion in Pharmacology*, **43**: 87–92.

Croset, V., Schleyer, M., Arguello, J.R., Gerber, B. and Benton, R. 2016. A molecular and neuronal basis for amino acid sensing in the Drosophila larva. *Sci Rep*, **6**: 34871.

Cryan, J.F. and Dinan, T.G. 2015. More than a Gut Feeling: the Microbiota Regulates Neurodevelopment and Behavior. *Neuropsychopharmacol*, **40**: 241–242.

Dahanukar, A., Lei, Y.-T., Kwon, J.Y. and Carlson, J.R. 2007. Two Gr Genes Underlie Sugar Reception in Drosophila. *Neuron*, **56**: 503–516.

Davoodi, S., Galenza, A., Panteluk, A., Deshpande, R., Ferguson, M., Grewal, S. and Foley, E. 2019. The Immune Deficiency Pathway Regulates Metabolic Homeostasis in *Drosophila*. *J.I.*, **202**: 2747–2759.

de Carvalho, C. and Caramujo, M. 2018. The Various Roles of Fatty Acids. *Molecules*, **23**: 2583.

de Renobales, M. and Blomquist, G.J. 1984. Biosynthesis of medium chain fatty acids in Drosophila melanogaster. *Archives of Biochemistry and Biophysics*, **228**: 407–414.

Delbare, S.Y.N., Ahmed-Braimah, Y.H., Wolfner, M.F. and Clark, A.G. 2020. Interactions between the microbiome and mating influence the female's transcriptional profile in Drosophila melanogaster. *Sci Rep*, **10**: 18168.

Delompré, T., Belloir, C., Martin, C., Salles, C. and Briand, L. 2022. Detection of Bitterness in Vitamins Is Mediated by the Activation of Bitter Taste Receptors. *Nutrients*, **14**: 4141.

Demerec, M. (1950). Biology of Drosophila (New York: John Wiley & Sons).

Dethier VG. 1971. The physiology of insect senses. Chapman and Hal.

Dewan, A., Pacifico, R., Zhan, R., Rinberg, D. and Bozza, T. 2013. Non-redundant coding of aversive odours in the main olfactory pathway. *Nature*, **497**: 486–489.

Dobson, A.J., Chaston, J.M., Newell, P.D., Donahue, L., Hermann, S.L., Sannino, D.R., Westmiller, S., Wong, A.C.-N., Clark, A.G., Lazzaro, B.P. and Douglas, A.E. 2015. Host genetic determinants of

microbiota-dependent nutrition revealed by genome-wide analysis of Drosophila melanogaster. *Nat Commun*, **6**: 6312.

Dobson, H.E.M. and Bergstrom, G. 2000. The ecology and evolution of pollen odors. 25.

Dobson, H.E.M., Danielson, E.M. and Wesep, I.D.V. 1999. Pollen odor chemicals as modulators of bumble bee foraging on Rosa rugosa Thunb. (Rosaceae). *Plant Species Biol*, **14**: 153–166.

Doudna, J.A. and Charpentier, E. 2014. The new frontier of genome engineering with CRISPR-Cas9. *Science*, **346**: 1258096.

Douglas, A.E. 2018. Contradictory Results in Microbiome Science Exemplified by Recent *Drosophila* Research. *mBio*, **9**: e01758-18.

Douglas, A.E. 2015. Multiorganismal Insects: Diversity and Function of Resident Microorganisms. *Annu. Rev. Entomol.*, **60**: 17–34.

Douglas, A.E. 2019. Simple animal models for microbiome research. *Nat Rev Microbiol*, **17**: 764–775.

Duménil, C., Woud, D., Pinto, F., Alkema, J.T., Jansen, I., Van Der Geest, A.M., Roessingh, S. and Billeter, J.-C. 2016. Pheromonal Cues Deposited by Mated Females Convey Social Information about Egg-Laying Sites in Drosophila Melanogaster. *J Chem Ecol*, **42**: 259–269.

Duncan, S.H., Lobley, G.E., Holtrop, G., Ince, J., Johnstone, A.M., Louis, P. and Flint, H.J. 2008. Human colonic microbiota associated with diet, obesity and weight loss. *Int J Obes*, **32**: 1720–1724.

Dunipace, L., Meister, S., McNealy, C. and Amrein, H. 2001. Spatially restricted expression of candidate taste receptors in the Drosophila gustatory system. *Current Biology*, **11**: 822–835.

Dutta, D., Dobson, A.J., Houtz, P.L., Gläßer, C., Revah, J., Korzelius, J., Patel, P.H., Edgar, B.A. and Buchon, N. 2015. Regional Cell-Specific Transcriptome Mapping Reveals Regulatory Complexity in the Adult Drosophila Midgut. *Cell Reports*, **12**: 346–358.

Dweck, H.K.M., Ebrahim, S.A.M., Thoma, M., Mohamed, A.A.M., Keesey, I.W., Trona, F., Lavista-Llanos, S., Svatoš, A., Sachse, S., Knaden, M. and Hansson, B.S. 2015. Pheromones mediating copulation and attraction in *Drosophila*. *Proc. Natl. Acad. Sci. U.S.A.*, **112**.

Elzinga, R.J. 1998. Microspines in the alimentary canal of arthropoda, onychophora, annelida. *International Journal of Insect Morphology and Embryology*, **27**: 341–349.

Everard, A., Belzer, C., Geurts, L., Ouwerkerk, J.P., Druart, C., Bindels, L.B., Guiot, Y., Derrien, M., Muccioli, G.G., Delzenne, N.M., de Vos, W.M. and Cani, P.D. 2013. Cross-talk between *Akkermansia muciniphila* and intestinal epithelium controls diet-induced obesity. *Proc. Natl. Acad. Sci. U.S.A.*, **110**: 9066–9071.

Falk, R., Bleiser-Avivi, N. and Atidia, J. 1976. Labellar taste organs of *Drosophila melanogaster*: TASTE ORAGNS OF DORSOPHILA. *J. Morphol.*, **150**: 327–341.

Farine, J.-P., Habbachi, W., Cortot, J., Roche, S. and Ferveur, J.-F. 2017. Maternally-transmitted microbiota affects odor emission and preference in Drosophila larva. *Sci Rep*, **7**: 6062.

Ferveur, J.-F. 1997. The pheromonal role of cuticular hydrocarbons inDrosophila melanogaster. *Bioessays*, **19**: 353–358.

Ferveur, J.-F. and Sureau, G. 1996. Simultaneous influence on male courtship of stimulatory and inhibitory pheromones produced by live sex-mosaic *Drosophila melanogaster*. *Proc. R. Soc. Lond. B*, **263**: 967–973.

Fischer, C.N., Trautman, E.P., Crawford, J.M., Stabb, E.V., Handelsman, J. and Broderick, N.A. 2017. Metabolite exchange between microbiome members produces compounds that influence Drosophila behavior. *eLife*, **6**: e18855.

Fischler, W., Kong, P., Marella, S. and Scott, K. 2007. The detection of carbonation by the Drosophila gustatory system. *Nature*, **448**: 1054–1057.

Flaven-Pouchon, J., Garcia, T., Abed-Vieillard, D., Farine, J.-P., Ferveur, J.-F. and Everaerts, C. 2014. Transient and Permanent Experience with Fatty Acids Changes Drosophila melanogaster Preference and Fitness. *PLoS ONE*, **9**: e92352.

Flower, D.R. 1996. The lipocalin protein family: structure and function. *Biochemical Journal*, **318**: 1–14.

Flower, D.R., North, A.C.T. and Sansom, C.E. 2000. The lipocalin protein family: structural and sequence overview. *Biochimica et Biophysica Acta (BBA) - Protein Structure and Molecular Enzymology*, **1482**: 9–24.

Foster, J.A. and McVey Neufeld, K.-A. 2013. Gut–brain axis: how the microbiome influences anxiety and depression. *Trends in Neurosciences*, **36**: 305–312.

Fougeron, A.-S., Ferveur, J.-F. and Bousquet, F. 2011. Réponses comportementales et préférences envers les acides gras à longue chaîne chez Drosophila melanogaster. 127.

Fukano, Y. 2017. Vine tendrils use contact chemoreception to avoid conspecific leaves. 8.

Fürnkranz, M., Lukesch, B., Müller, H., Huss, H., Grube, M. and Berg, G. 2012. Microbial Diversity Inside Pumpkins: Microhabitat-Specific Communities Display a High Antagonistic Potential Against Phytopathogens. *Microb Ecol*, **63**: 418–428.

Gaillard, D., Laugerette, F., Darcel, N., El-Yassimi, A., Passilly-Degrace, P., Hichami, A., Khan, N.A., Montmayeur, J. and Besnard, P. 2008. The gustatory pathway is involved in CD36-mediated orosensory perception of long-chain fatty acids in the mouse. *FASEB j.*, **22**: 1458–1468.

Galindo, K. and Smith, D.P. 2001. A Large Family of Divergent Drosophila Odorant-Binding Proteins Expressed in Gustatory and Olfactory Sensilla. 14.

Ganger, M.T., Dietz, G.D. and Ewing, S.J. 2017. A common base method for analysis of qPCR data and the application of simple blocking in qPCR experiments. *BMC Bioinformatics*, **18**: 534.

Gao, Q., Yuan, B. and Chess, A. 2000. Convergent projections of Drosophila olfactory neurons to specific glomeruli in the antennal lobe. *Nat Neurosci*, **3**: 780–785.

Gendre, N., Lüer, K., Friche, S., Grillenzoni, N., Ramaekers, A., Technau, G.M. and Stocker, R.F. 2004. Integration of complex larval chemosensory organs into the adult nervous system of *Drosophila*. *Development*, **131**: 83–92.

Getchell, T., Margolis, F. and Getchell, M. 1984. Perireceptor and receptor events in vertebrate olfaction. *Progress in Neurobiology*, **23**: 317–345.

Gilbertson, T.A., Fontenot, D.T., Liu, L., Zhang, H. and Monroe, W.T. 1997. Fatty acid modulation of K+ channels in taste receptor cells: gustatory cues for dietary fat. *American Journal of Physiology-Cell Physiology*, **272**: C1203–C1210.

Glusman, G., Yanai, I., Rubin, I. and Lancet, D. 2001. The Complete Human Olfactory Subgenome. *Genome Res.*, **11**: 685–702.

Gnainsky, Y., Zfanya, N., Elgart, M., Omri, E., Brandis, A., Mehlman, T., Itkin, M., Malitsky, S., Adamski, J. and Soen, Y. 2021. Systemic Regulation of Host Energy and Oogenesis by Microbiome-Derived Mitochondrial Coenzymes. *Cell Reports*, **34**: 108583.

Gobert, V., Gottar, M., Matskevich, A.A., Rutschmann, S., Royet, J., Belvin, M., Hoffmann, J.A. and Ferrandon, D. 2003. Dual Activation of the *Drosophila* Toll Pathway by Two Pattern Recognition Receptors. *Science*, **302**: 2126–2130.

Gomez-Diaz, C., Reina, J.H., Cambillau, C. and Benton, R. 2013. Ligands for Pheromone-Sensing Neurons Are Not Conformationally Activated Odorant Binding Proteins. *PLoS Biol*, **11**: e1001546.

Gonzalez, D., Rihani, K., Neiers, F., Poirier, N., Fraichard, S., Gotthard, G., Chertemps, T., Maïbèche, M., Ferveur, J.-F. and Briand, L. 2019. The Drosophila odorant-binding protein 28a is involved in the detection of the floral odour ß-ionone. *Cell. Mol. Life Sci.*, doi: 10.1007/s00018-019-03300-4.

Gould, A.L., Zhang, V., Lamberti, L., Jones, E.W., Obadia, B., Korasidis, N., Gavryushkin, A., Carlson, J.M., Beerenwinkel, N. and Ludington, W.B. 2018. Microbiome interactions shape host fitness. *Proc. Natl. Acad. Sci. U.S.A.*, **115**.

Grangeteau, C., Yahou, F., Everaerts, C., Dupont, S., Farine, J.-P., Beney, L. and Ferveur, J.-F. 2018. Yeast quality in juvenile diet affects Drosophila melanogaster adult life traits. *Sci Rep*, **8**: 13070.

Green, P.R. and Geer, B.W. 1979. Changes in the fatty-acid composition of *Drosophila melanogaster* during development and ageing. *Archives Internationales de Physiologie et de Biochimie*, **87**: 485–491.

Greene, M.J. and Gordon, D.M. 2003. Cuticular hydrocarbons inform task decisions. *Nature*, **423**: 32–32.

Greenfield, N.J. 2006. Using circular dichroism spectra to estimate protein secondary structure. *Nat Protoc*, **1**: 2876–2890.

Grillet, M., Dartevelle, L. and Ferveur, J.-F. 2006. A Drosophila male pheromone affects female sexual receptivity. *Proc. R. Soc. B.*, **273**: 315–323.

Groussin, M., Mazel, F., Sanders, J.G., Smillie, C.S., Lavergne, S., Thuiller, W. and Alm, E.J. 2017. Unraveling the processes shaping mammalian gut microbiomes over evolutionary time. *Nat Commun*, **8**: 14319.

Guiraudie-Capraz, G., Pho, D.B. and Jallon, J.-M. 2007. Role of the ejaculatory bulb in biosynthesis of the male pheromone *cis* -vaccenyl acetate in *Drosophila melanogaster*. *Integrative Zoology*, **2**: 89–99.

Hale, V.L., Tan, C.L., Niu, K., Yang, Y., Knight, R., Zhang, Q., Cui, D. and Amato, K.R. 2018. Diet Versus Phylogeny: a Comparison of Gut Microbiota in Captive Colobine Monkey Species. *Microb Ecol*, **75**: 515–527.

Hallem, E.A., Dahanukar, A. and Carlson, J.R. 2006. INSECT ODOR AND TASTE RECEPTORS. *Annu. Rev. Entomol.*, **51**: 113–135.

Hansen, A. and Reutter, K. 2004. Chemosensory Systems in Fish: Structural, Functional and Ecological Aspects. In: *The Senses of Fish* (G. von der Emde, J. Mogdans, and B. G. Kapoor, eds), pp. 55–89.

Hara, T.J. 1994. Olfaction and gustation in fish: an overview. *Acta Physiologica Scandinavica*, **152**: 207–217.

Harada, E., Haba, D., Aigaki, T. and Matsuo, T. 2008. Behavioral analyses of mutants for two odorant-binding protein genes, Obp57d and Obp57e, in Drosophila melanogaster. *Genes Genet. Syst.*, **83**: 257–264.

Harada, E., Nakagawa, J., Asano, T., Taoka, M., Sorimachi, H., Ito, Y., Aigaki, T. and Matsuo, T. 2012. Functional Evolution of Duplicated Odorant-Binding Protein Genes, Obp57d and Obp57e, in Drosophila. *PLoS ONE*, **7**: e29710.

Hegedus, D., Erlandson, M., Gillott, C. and Toprak, U. 2009. New Insights into Peritrophic Matrix Synthesis, Architecture, and Function. *Annu. Rev. Entomol.*, **54**: 285–302.

Hekmat-Scafe, D.S. 2002. Genome-Wide Analysis of the Odorant-Binding Protein Gene Family in Drosophila melanogaster. *Genome Research*, **12**: 1357–1369.

Henriques, S.F., Serra, L., Francisco, A.P., Carvalho-Santos, Z., Baltazar, C., Elias, A.P., Anjos, M., Zhang, T., Maddocks, O.D.K. and Ribeiro, C. 2019. *Metabolic cross-feeding allows a gut microbial community to overcome detrimental diets and alter host behaviour*.

Herndon, L.A. and Wolfner, M.F. 1995. A Drosophila seminal fluid protein, Acp26Aa, stimulates egg laying in females for 1 day after mating. *Proceedings of the National Academy of Sciences*, **92**: 10114–10118.

Herrada, G. and Dulac, C. 1997. A Novel Family of Putative Pheromone Receptors in Mammals with a Topographically Organized and Sexually Dimorphic Distribution. 11.

Heydel, J.-M., Coelho, A., Thiebaud, N., Legendre, A., Bon, A.-M.L., Faure, P., Neiers, F., Artur, Y., Golebiowski, J. and Briand, L. 2013. Odorant-Binding Proteins and Xenobiotic Metabolizing Enzymes: Implications in Olfactory Perireceptor Events: Odorant-Binding Proteins and Metabolizing Enzymes. *Anat. Rec.*, **296**: 1333–1345.

Heydel, J.-M., Holsztynska, E.J., Legendre, A., Thiebaud, N., Artur, Y. and Bon, A.-M.L. 2010. UDP-glucuronosyltransferases (UGTs) in neuro-olfactory tissues: expression, regulation, and function. *Drug Metabolism Reviews*, **42**: 74–97.

Hirasawa, A., Tsumaya, K., Awaji, T., Katsuma, S., Adachi, T., Yamada, M., Sugimoto, Y., Miyazaki, S. and Tsujimoto, G. 2005. Free fatty acids regulate gut incretin glucagon-like peptide-1 secretion through GPR120. *Nat Med*, **11**: 90–94.

Hiroi, M., Meunier, N., Marion-Poll, F. and Tanimura, T. 2004. Two antagonistic gustatory receptor neurons responding to sweet-salty and bitter taste inDrosophila. *J. Neurobiol.*, **61**: 333–342.

Hoon, M.A., Adler, E., Battey, J.F., Ryba, N.J.P. and Zuker, C.S. 1999. Putative Mammalian Taste Receptors: A Class of Taste-Specific GPCRs with Distinct Topographic Selectivity. 11.

Hopkins, C.R. 1967. The fine-structural changes observed in the rectal papillae of the mosquito Aedes aegypti, L. and their relation to the epithelial transport of water and inorganic ions. *Journal of the Royal Microscopical Society*, **86**: 235–252.

Horio, N., Yoshida, R., Yasumatsu, K., Yanagawa, Y., Ishimaru, Y., Matsunami, H. and Ninomiya, Y. 2011. Sour Taste Responses in Mice Lacking PKD Channels. *PLoS ONE*, **6**: e20007.

Houot, B., Gigot, V., Robichon, A. and Ferveur, J.-F. 2017. Free flight odor tracking in Drosophila: Effect of wing chemosensors, sex and pheromonal gene regulation. *Sci Rep*, **7**: 40221.

Hurst, J.L., Payne, C.E., Nevison, C.M., Marie, A.D., Humphries, R.E., Robertson, D.H.L., Cavaggioni, A. and Beynon, R.J. 2001. Individual recognition in mice mediated by major urinary proteins. *Nature*, **414**: 631–634.

Imler, J.-L. 2014. Overview of Drosophila immunity: A historical perspective. *Developmental & Comparative Immunology*, **42**: 3–15.

Inoshita, T. and Tanimura, T. 2006. Cellular identification of water gustatory receptor neurons and their central projection pattern in *Drosophila*. *Proc. Natl. Acad. Sci. U.S.A.*, **103**: 1094–1099.

Ja, W.W., Carvalho, G.B., Mak, E.M., de la Rosa, N.N., Fang, A.Y., Liong, J.C., Brummel, T. and Benzer, S. 2007. Prandiology of Drosophila and the CAFE assay. *Proceedings of the National Academy of Sciences*, **104**: 8253–8256.

Jeong, Y.T., Shim, J., Oh, S.R., Yoon, H.I., Kim, C.H., Moon, S.J. and Montell, C. 2013. An Odorant-Binding Protein Required for Suppression of Sweet Taste by Bitter Chemicals. *Neuron*, **79**: 725–737.

Jiang, L., Wang, D., Kim, J.-S., Lee, J.H., Kim, D.-H., Kim, S.W. and Lee, J. 2020. Reclassification of genus Izhakiella into the family Erwiniaceae based on phylogenetic and genomic analyses. *International Journal of Systematic and Evolutionary Microbiology*, **70**: 3541–3546.

Jiao, Y., Moon, S.J., Wang, X., Ren, Q. and Montell, C. 2008. Gr64f Is Required in Combination with Other Gustatory Receptors for Sugar Detection in Drosophila. *Current Biology*, **18**: 1797–1801.

Johnson, B.A., Woo, C.C., Hingco, E.E., Pham, K.L. and Leon, M. 1999. Multidimensional chemotopic responses to n-aliphatic acid odorants in the rat olfactory bulb. *J. Comp. Neurol.*, **409**: 529–548.

Jones, P.M. and George, A.M. 2004. The ABC transporter structure and mechanism: perspectives on recent research. *Cellular and Molecular Life Sciences (CMLS)*, **61**: 682–699.

Kang, D.-W., Park, J.G., Ilhan, Z.E., Wallstrom, G., LaBaer, J., Adams, J.B. and Krajmalnik-Brown, R. 2013. Reduced Incidence of Prevotella and Other Fermenters in Intestinal Microflora of Autistic Children. *PLoS ONE*, **8**: e68322.

Keebaugh, E.S., Yamada, R. and Ja, W.W. 2019. The Nutritional Environment Influences the Impact of Microbes on Drosophila melanogaster Life Span. *mBio*, **10**: e00885-19.

Kelly, S.M., Jess, T.J. and Price, N.C. 2005. How to study proteins by circular dichroism. *Biochimica et Biophysica Acta (BBA) - Proteins and Proteomics*, **1751**: 119–139.

Keverne EB. The vomeronasal organ. Science 1999; **286:**716–20

Kim, Hyeyon, Kim, Haein, Kwon, J.Y., Seo, J.T., Shin, D.M. and Moon, S.J. 2018. Drosophila Gr64e mediates fatty acid sensing via the phospholipase C pathway. *PLoS Genet*, **14**: e1007229.

Kim, S.H., Lee, Y., Akitake, B., Woodward, O.M., Guggino, W.B. and Montell, C. 2010. *Drosophila* TRPA1 channel mediates chemical avoidance in gustatory receptor neurons. *Proc. Natl. Acad. Sci. U.S.A.*, **107**: 8440–8445.

Kimchi, T., Xu, J. and Dulac, C. 2007. A functional circuit underlying male sexual behaviour in the female mouse brain. *Nature*, **448**: 1009–1014.

Kleino, A. and Silverman, N. 2014. The Drosophila IMD pathway in the activation of the humoral immune response. *Developmental & Comparative Immunology*, **42**: 25–35.

Knudsen, J.T., Eriksson, R., Gershenzon, J. and Ståhl, B. 2006. Diversity and Distribution of Floral Scent. *The Botanical Review*, **72**: 1–120.

Kõiv, V., Roosaare, M., Vedler, E., Ann Kivistik, P., Toppi, K., Schryer, D.W., Remm, M., Tenson, T. and Mäe, A. 2015. Microbial population dynamics in response to Pectobacterium atrosepticum infection in potato tubers. *Sci Rep*, **5**: 11606.

Kratzing, J.E. 1978. The olfactory apparatus of the bandicoot (Isoodon macrourus): fine structure and presence of a septal olfactory organ. 13.

Krieger, J., Klink, O., Mohl, C., Raming, K. and Breer, H. 2003. A candidate olfactory receptor subtype highly conserved across different insect orders. *Journal of Comparative Physiology A: Sensory, Neural, and Behavioral Physiology*, **189**: 519–526.

Laffitte, A., Neiers, F. and Briand, L. 2016. Characterization of taste compounds: chemical structures and sensory properties. In: *Flavour* (E. Guichard, C. Salles, M. Morzel, and A.-M. Le Bon, eds), pp. 154–191.

Larsson, M.C., Domingos, A.I., Jones, W.D., Chiappe, M.E., Amrein, H. and Vosshall, L.B. 2004. Or83b Encodes a Broadly Expressed Odorant Receptor Essential for Drosophila Olfaction. *Neuron*, **43**: 703–714.

Larter, N.K., Sun, J.S. and Carlson, J.R. 2016. Organization and function of Drosophila odorant binding proteins. *eLife*, **5**: e20242.

Laturney, M. and Billeter, J.-C. 2016. Drosophila melanogaster females restore their attractiveness after mating by removing male anti-aphrodisiac pheromones. *Nat Commun*, **7**: 12322.

Laugerette, F., Montmayeur, J.-P. and Besnard, P. 2005. CD36 involvement in orosensory detection of dietary lipids, spontaneous fat preference, and digestive secretions. *Journal of Clinical Investigation*, **115**: 3177–3184.

Laughlin, J.D., Ha, T.S., Jones, D.N.M. and Smith, D.P. 2008. Activation of Pheromone-Sensitive Neurons Is Mediated by Conformational Activation of Pheromone-Binding Protein. *Cell*, **133**: 1255–1265.

Le Poul, E., Loison, C., Struyf, S., Springael, J.-Y., Lannoy, V., Decobecq, M.-E., Brezillon, S., Dupriez, V., Vassart, G., Van Damme, J., Parmentier, M. and Detheux, M. 2003. Functional Characterization of Human Receptors for Short Chain Fatty Acids and Their Role in Polymorphonuclear Cell Activation. *Journal of Biological Chemistry*, **278**: 25481–25489.

Leal, W.S., Nikonova, L. and Peng, G. 1999. Disul¢de structure of the pheromone binding protein from the silkworm moth, Bombyx mori. *FEBS Letters*, 6.

Lee, Y., Kang, M.J., Shim, J., Cheong, C.U., Moon, S.J. and Montell, C. 2012. Gustatory Receptors Required for Avoiding the Insecticide L-Canavanine. *Journal of Neuroscience*, **32**: 1429–1435.

Lee, Y., Moon, S.J. and Montell, C. 2009. Multiple gustatory receptors required for the caffeine response in Drosophila. *Proceedings of the National Academy of Sciences*, **106**: 4495–4500.

Leftwich, P.T., Clarke, N.V.E., Hutchings, M.I. and Chapman, T. 2017. Gut microbiomes and reproductive isolation in *Drosophila*. *Proc. Natl. Acad. Sci. U.S.A.*, **114**: 12767–12772.

Leitão-Gonçalves, R., Carvalho-Santos, Z., Francisco, A.P., Fioreze, G.T., Anjos, M., Baltazar, C., Elias, A.P., Itskov, P.M., Piper, M.D.W. and Ribeiro, C. 2017. Commensal bacteria and essential amino acids control food choice behavior and reproduction. *PLoS Biol*, **15**: e2000862.

Lemaitre, B. and Hoffmann, J. 2007. The Host Defense of *Drosophila melanogaster*. *Annu. Rev. Immunol.*, **25**: 697–743.

Ley, R.E., Bäckhed, F., Turnbaugh, P., Lozupone, C.A., Knight, R.D. and Gordon, J.I. 2005. Obesity alters gut microbial ecology. *Proc. Natl. Acad. Sci. U.S.A.*, **102**: 11070–11075.

Liberles, S.D. 2014. Mammalian Pheromones. *Annu. Rev. Physiol.*, **76**: 151–175.

Liberles, S.D. 2015. Trace amine-associated receptors: ligands, neural circuits, and behaviors. *Current Opinion in Neurobiology*, **34**: 1–7.

Liman, E.R., Zhang, Y.V. and Montell, C. 2014. Peripheral Coding of Taste. *Neuron*, **81**: 984–1000.

Lindemann, B. 2001. Receptors and transduction in taste. *Nature*, **413**: 219–225.

Liu, L., Leonard, A.S., Motto, D.G., Feller, M.A., Price, M.P., Johnson, W.A. and Welsh, M.J. 2003. Contribution of Drosophila DEG/ENaC Genes to Salt Taste. *Neuron*, **39**: 133–146.

Liu, P., Shah, B.P., Croasdell, S. and Gilbertson, T.A. 2011. Transient Receptor Potential Channel Type M5 Is Essential for Fat Taste. *Journal of Neuroscience*, **31**: 8634–8642.

Ludington, W.B. and Ja, W.W. 2020. Drosophila as a model for the gut microbiome. *PLoS Pathog*, **16**: e1008398.

Malnic, B., Hirono, J., Sato, T. and Buck, L.B. 1999. Combinatorial Receptor Codes for Odors. 11.

Marcillac, F. and Ferveur, J.-F. 2004. A set of female pheromones affects reproduction before, during and after mating in *Drosophila*. *Journal of Experimental Biology*, **207**: 3927–3933.

Martin, C.R. and Mayer, E.A. 2017. Gut-Brain Axis and Behavior. In: *Nestlé Nutrition Institute Workshop Series* (E. Isolauri, P. M. Sherman, and W. A. Walker, eds), pp. 45–54.

Marui, T., Harada, S. and Kasahara, Y. 1983. Gustatory specificity for amino acids in the facial taste system of the carp,Cyprinus carpio L. *J. Comp. Physiol.*, **153**: 299–308.

Masek, P. and Keene, A.C. 2013. Drosophila Fatty Acid Taste Signals through the PLC Pathway in Sugar-Sensing Neurons. *PLoS Genet*, **9**: e1003710.

Matsunami, H., Montmayeur, J.-P. and Buck, L.B. 2000. A family of candidate taste receptors in human and mouse. *Nature*, **404**: 601–604.

Mattick, J.S. 2002. Type IV Pili and Twitching Motility. *Annu. Rev. Microbiol.*, **56**: 289–314.

McMullen, J.G., Peters-Schulze, G., Cai, J., Patterson, A.D. and Douglas, A.E. 2020. How gut microbiome interactions affect nutritional traits of *Drosophila melanogaster*. *J Exp Biol*, **223**: jeb227843.

Melo, A.C.A. 2004. Identification of a Chemosensory Receptor from the Yellow Fever Mosquito, Aedes aegypti, that is Highly Conserved and Expressed in Olfactory and Gustatory Organs. *Chemical Senses*, **29**: 403–410.

Meunier, N., Ferveur, J.-F. and Marion-Poll, F. 2000. Sex-specific non-pheromonal taste receptors in Drosophila. *Current Biology*, **10**: 1583–1586.

Meunier, N., Marion-Poll, F., Rospars, J.-P. and Tanimura, T. 2003. Peripheral coding of bitter taste inDrosophila. *J. Neurobiol.*, **56**: 139–152.

Miguel-Aliaga, I., Jasper, H. and Lemaitre, B. 2018. Anatomy and Physiology of the Digestive Tract of *Drosophila melanogaster*. *Genetics*, **210**: 357–396.

Miguel-Aliaga, I., Thor, S. and Gould, A.P. 2008. Postmitotic Specification of Drosophila Insulinergic Neurons from Pioneer Neurons. *PLoS Biol*, **6**: e58.

Mitri, C., Soustelle, L., Framery, B., Bockaert, J., Parmentier, M.-L. and Grau, Y. 2009. Plant Insecticide L-Canavanine Repels Drosophila via the Insect Orphan GPCR DmX. *PLoS Biol*, **7**: e1000147.

Miyamoto, T., Slone, J., Song, X. and Amrein, H. 2012. A Fructose Receptor Functions as a Nutrient Sensor in the Drosophila Brain. *Cell*, **151**: 1113–1125.

Mombaerts, P. 2004. Genes and ligands for odorant, vomeronasal and taste receptors. *Nat Rev Neurosci*, **5**: 263–278.

Montell, C. 2009. A taste of the Drosophila gustatory receptors. *Current Opinion in Neurobiology*, **19**: 345–353.

Moore, P.J., Reagan-Wallin, N.L., Haynes, K.F. and Moore, A.J. 1997. Odour conveys status on cockroaches. *Nature*, **389**: 25–25.

Morimoto, J., Simpson, S.J. and Ponton, F. 2017. Direct and trans-generational effects of male and female gut microbiota in *Drosophila melanogaster*. *Biol. Lett.*, **13**: 20160966.

Moy, R.H. and Cherry, S. 2013. Antimicrobial Autophagy: A Conserved Innate Immune Response in ***Drosophila***. *J Innate Immun*, **5**: 444–455.

Murakami, R. and Shiotsuki, Y. 2001. Ultrastructure of the hindgut ofDrosophila larvae, with special reference to the domains identified by specific gene expression patterns. *J. Morphol.*, **248**: 144–150.

Murgier, J., Everaerts, C., Farine, J.-P. and Ferveur, J.-F. 2019. Live yeast in juvenile diet induces species-specific effects on Drosophila adult behaviour and fitness. *Sci Rep*, **9**: 8873.

Mussabekova, A., Daeffler, L. and Imler, J.-L. 2017. Innate and intrinsic antiviral immunity in Drosophila. *Cell. Mol. Life Sci.*, **74**: 2039–2054.

Nagy, P., Varga, Á., Kovács, A.L., Takáts, S. and Juhász, G. 2015. How and why to study autophagy in Drosophila: It's more than just a garbage chute. *Methods*, **75**: 151–161.

Nakamura, M.T. and Nara, T.Y. 2003. Essential fatty acid synthesis and its regulation in mammals. *Prostaglandins, Leukotrienes and Essential Fatty Acids*, **68**: 145–150.

Nelson, G., Hoon, M.A., Chandrashekar, J., Zhang, Y., Ryba, N.J.P. and Zuker, C.S. 2001. Mammalian Sweet Taste Receptors. *Cell*, **106**: 381–390.

Nespoulous, C. 2004. Odorant Binding and Conformational Changes of a Rat Odorant-binding Protein. *Chemical Senses*, **29**: 189–198.

Newell, P.D. and Douglas, A.E. 2014. Interspecies Interactions Determine the Impact of the Gut Microbiota on Nutrient Allocation in Drosophila melanogaster. *Appl. Environ. Microbiol.*, **80**: 788–796.

Nishida, A.H. and Ochman, H. 2018. Rates of gut microbiome divergence in mammals. *Mol Ecol*, **27**: 1884–1897.

Obadia, B., Güvener, Z.T., Zhang, V., Ceja-Navarro, J.A., Brodie, E.L., Ja, W.W. and Ludington, W.B. 2017. Probabilistic Invasion Underlies Natural Gut Microbiome Stability. *Current Biology*, **27**: 1999-2006.e8.

Obata, F., Fons, C.O. and Gould, A.P. 2018. Early-life exposure to low-dose oxidants can increase longevity via microbiome remodelling in Drosophila. *Nat Commun*, **9**: 975.

Ortega, Á., Zhulin, I.B. and Krell, T. 2017. Sensory Repertoire of Bacterial Chemoreceptors. *Microbiol Mol Biol Rev*, **81**: e00033-17.

Patrick, M.L., Aimanova, K., Sanders, H.R. and Gill, S.S. 2006. P-type Na+/K+-ATPase and V-type H+-ATPase expression patterns in the osmoregulatory organs of larval and adult mosquito *Aedes aegypti*. *Journal of Experimental Biology*, **209**: 4638–4651.

Pelosi, P. 2005. Diversity of Odorant-binding Proteins and Chemosensory Proteins in Insects. *Chemical Senses*, **30**: i291–i292.

Pelosi, P. 1994. Odorant-Binding Proteins. *1994*, 30.

Pelosi, P., Pisanelli, A.M., Baldaccini, N.E. and Gagliardo, A. 1981. Binding of [^J-l-isobutyl-S-methoxypyrazine to cow olfactory mucosa. 9.

Pelosi, P., Zhou, J.-J., Ban, L.P. and Calvello, M. 2006. Soluble proteins in insect chemical communication. *Cell. Mol. Life Sci.*, **63**: 1658–1676.

Piper, M.D.W., Blanc, E., Leitão-Gonçalves, R., Yang, M., He, X., Linford, N.J., Hoddinott, M.P., Hopfen, C., Soultoukis, G.A., Niemeyer, C., Kerr, F., Pletcher, S.D., Ribeiro, C. and Partridge, L. 2014. A holidic medium for Drosophila melanogaster. *Nat Methods*, **11**: 100–105.

Porter, S.L., Wadhams, G.H. and Armitage, J.P. 2011. Signal processing in complex chemotaxis pathways. *Nat Rev Microbiol*, **9**: 153–165.

Portman, K.L., Long, J., Carr, S., Briand, L., Winzor, D.J., Searle, M.S. and Scott, D.J. 2014. Enthalpy/Entropy Compensation Effects from Cavity Desolvation Underpin Broad Ligand Binding Selectivity for Rat Odorant Binding Protein 3. *Biochemistry*, **53**: 2371–2379.

Qin, J., Li, R., Raes, J., Arumugam, M., Burgdorf, K.S., Manichanh, C., Nielsen, T., Pons, N., Levenez, F., Yamada, T., Mende, D.R., Li, J., Xu, J., Li, S., Li, D., Cao, J., Wang, B., Liang, H., Zheng, H., *et al.* 2010. A human gut microbial gene catalogue established by metagenomic sequencing. *Nature*, **464**: 59–65.

Qiu, Y.T., van Loon, J.J.A., Takken, W., Meijerink, J. and Smid, H.M. 2006. Olfactory Coding in Antennal Neurons of the Malaria Mosquito, Anopheles gambiae. *Chemical Senses*, **31**: 845–863.

Raad, H., Ferveur, J.-F., Ledger, N., Capovilla, M. and Robichon, A. 2016. Functional Gustatory Role of Chemoreceptors in Drosophila Wings. *Cell Reports*, **15**: 1442–1454.

Raguso, R.A. and Pichersky, E. 1999. New Perspectives in Pollination Biology: Floral Fragrances. A day in the life of a linalool molecule: Chemical communication in a plant-pollinator system. Part 1: Linalool biosynthesis in flowering plants. *Plant Species Biol*, **14**: 95–120.

Rasmussen, L.E.L. 1988. Chemosensory responses in two species of elephants to constituents of temporal gland secretion and musth urine. *J Chem Ecol*, **14**: 1687–1711.

Rasmussen, L.E.L. and Schulte, B.A. 1998. Chemical signals in the reproduction of Asian žElephas maximus/ and African žLoxodonta africana/ elephants. 16.

Reedy, A.R., Luo, L., Neish, A.S. and Jones, R.M. 2019. Commensal microbiota induced redox signaling activates proliferative signals in the intestinal stem cell microenvironment. *Development*, dev.171520.

Ridley, E.V., Wong, A.C.-N., Westmiller, S. and Douglas, A.E. 2012. Impact of the Resident Microbiota on the Nutritional Phenotype of Drosophila melanogaster. *PLoS ONE*, **7**: e36765.

Rihani, K., Ferveur, J.-F. and Briand, L. 2021. The 40-Year Mystery of Insect Odorant-Binding Proteins. *Biomolecules*, **11**: 509.

Rihani, K., Fraichard, S., Chauvel, I., Poirier, N., Delompré, T., Neiers, F., Tanimura, T., Ferveur, J.-F. and Briand, L. 2019. A conserved odorant binding protein is required for essential amino acid detection in Drosophila. *Commun Biol*, **2**: 425.

Rimal, S., Sang, J., Poudel, S., Thakur, D., Montell, C. and Lee, Y. 2019. Mechanism of Acetic Acid Gustatory Repulsion in Drosophila. *Cell Reports*, **26**: 1432-1442.e4.

Rivière, S., Challet, L., Fluegge, D., Spehr, M. and Rodriguez, I. 2009. Formyl peptide receptor-like proteins are a novel family of vomeronasal chemosensors. *Nature*, **459**: 574–577.

Robertson, H.M., Warr, C.G. and Carlson, J.R. 2003. Molecular evolution of the insect chemoreceptor gene superfamily in *Drosophila melanogaster*. *Proc. Natl. Acad. Sci. U.S.A.*, **100**: 14537–14542.

Rothschild, L.J. and Mancinelli, R.L. 2001. Life in extreme environments. **409**: 10.

Roy, S. and Trinchieri, G. 2017. Microbiota: a key orchestrator of cancer therapy. *Nat Rev Cancer*, **17**: 271–285.

Rustan, A.C. and Drevon, C.A. 2005. Fatty Acids: Structures and Properties. In: *eLS* (John Wiley & Sons, Ltd, ed).

Sato, K., Pellegrino, M., Nakagawa, Takao, Nakagawa, Tatsuro, Vosshall, L.B. and Touhara, K. 2008. Insect olfactory receptors are heteromeric ligand-gated ion channels. *Nature*, **452**: 1002–1006.

Savarit, F., Sureau, G., Cobb, M. and Ferveur, J.-F. 1999. Genetic elimination of known pheromones reveals the fundamental chemical bases of mating and isolation in *Drosophila*. *Proc. Natl. Acad. Sci. U.S.A.*, **96**: 9015–9020.

Sawyer, J.K., Cohen, E. and Fox, D.T. 2017. Inter-organ regulation of *Drosophila* intestinal stem cell proliferation by a hybrid organ boundary zone. *Development*, dev.153114.

Scaloni, A., Monti, M., Angeli, S. and Pelosi, P. 1999. Structural Analysis and Disulfide-Bridge Pairing of Two Odorant-Binding Proteins from Bombyx mori. *Biochemical and Biophysical Research Communications*, **266**: 386–391.

Schaal, B., Coureaud, G., Langlois, D., Giniès, C., Sémon, E. and Perrier, G. 2003. Chemical and behavioural characterization of the rabbit mammary pheromone. *Nature*, **424**: 68–72.

Schwenk, K. 1995. Oftongues and noses: chemoreceptionin lizardsand snakes. 6.

Scott D. Doughman, Srirama Krupanidhi, and Carani B. Sanjeevi. 2007. Omega-3 Fatty Acids for Nutrition and Medicine: Considering Microalgae Oil as a Vegetarian Source of EPA and DHA. *CDR*, **3**: 198–203.

Scott, K., Brady, R., Cravchik, A., Morozov, P., Rzhetsky, A., Zuker, C. and Axel, R. 2001. A Chemosensory Gene Family Encoding Candidate Gustatory and Olfactory Receptors in Drosophila. 13.

Selkrig, J., Mohammad, F., Ng, S.H., Chua, J.Y., Tumkaya, T., Ho, J., Chiang, Y.N., Rieger, D., Pettersson, S., Helfrich-Förster, C., Yew, J.Y. and Claridge-Chang, A. 2018. The Drosophila microbiome has a limited influence on sleep, activity, and courtship behaviors. *Sci Rep*, **8**: 10646.

Semmler, A.B.T., Whitchurch, C.B. and Mattick, J.S. 1999. A re-examination of twitching motility in Pseudomonas aeruginosa. *Microbiology*, **145**: 2863–2873.

Servant, G., Kenakin, T., Zhang, L., Williams, M. and Servant, N. 2020. The function and allosteric control of the human sweet taste receptor. In: *Advances in Pharmacology*, pp. 59–82.

Shanbhag, S.R., Muller, B. and Steinbrecht, R.A. 1999. Atlas of olfactory organs of Drosophila melanogaster 1. Types, external organization, innervation and distribution of olfactory sensilla. *International Journal of Insect Morphology and Embryology*, 21.

Sharon, G., Cruz, N.J., Kang, D.-W., Gandal, M.J., Wang, B., Kim, Y.-M., Zink, E.M., Casey, C.P., Taylor, B.C., Lane, C.J., Bramer, L.M., Isern, N.G., Hoyt, D.W., Noecker, C., Sweredoski, M.J., Moradian, A., Borenstein, E., Jansson, J.K., Knight, R., *et al.* 2019. Human Gut Microbiota from Autism Spectrum Disorder Promote Behavioral Symptoms in Mice. *Cell*, **177**: 1600-1618.e17.

Sharon, G., Segal, D., Ringo, J.M., Hefetz, A., Zilber-Rosenberg, I. and Rosenberg, E. 2010. Commensal bacteria play a role in mating preference of Drosophila melanogaster. *Proceedings of the National Academy of Sciences*, **107**: 20051–20056.

Shen, J., Obin, M.S. and Zhao, L. 2013. The gut microbiota, obesity and insulin resistance. *Molecular Aspects of Medicine*, **34**: 39–58.

Shi, P. and Zhang, J. 2006. Contrasting Modes of Evolution Between Vertebrate Sweet/Umami Receptor Genes and Bitter Receptor Genes. *Molecular Biology and Evolution*, **23**: 292–300.

Shin, S.C., Kim, S.-H., You, H., Kim, B., Kim, A.C., Lee, K.-A., Yoon, J.-H., Ryu, J.-H. and Lee, W.-J. 2011. *Drosophila* Microbiome Modulates Host Developmental and Metabolic Homeostasis via Insulin Signaling. *Science*, **334**: 670–674.

Shorter, J.R., Dembeck, L.M., Everett, L.J., Morozova, T.V., Arya, G.H., Turlapati, L., St. Armour, G.E., Schal, C., Mackay, T.F.C. and Anholt, R.R.H. 2016. Obp56h modulates Mating Behavior in Drosophila melanogaster. *G3*, **6**: 3335–3342.

Silbering, A.F., Rytz, R., Grosjean, Y., Abuin, L., Ramdya, P., Jefferis, G.S.X.E. and Benton, R. 2011. Complementary Function and Integrated Wiring of the Evolutionarily Distinct Drosophila Olfactory Subsystems. *Journal of Neuroscience*, **31**: 13357–13375.

Simhadri, R.K., Fast, E.M., Guo, R., Schultz, M.J., Vaisman, N., Ortiz, L., Bybee, J., Slatko, B.E. and Frydman, H.M. 2017. The Gut Commensal Microbiome of Drosophila melanogaster Is Modified by the Endosymbiont *Wolbachia*. *mSphere*, **2**: e00287-17.

Simopoulos, A. 2016. An Increase in the Omega-6/Omega-3 Fatty Acid Ratio Increases the Risk for Obesity. *Nutrients*, **8**: 128.

Simopoulos, A.P. 2002. The importance of the ratio of omega-6/omega-3 essential fatty acids. *Biomedicine & Pharmacotherapy*, **56**: 365–379.

Slone, J., Daniels, J. and Amrein, H. 2007. Sugar Receptors in Drosophila. *Current Biology*, **17**: 1809–1816.

Smallegange, R.C., Qiu, Y.T., Bukovinszkiné-Kiss, G., Van Loon, J.J.A. and Takken, W. 2009. The Effect of Aliphatic Carboxylic Acids on Olfaction-Based Host-Seeking of the Malaria Mosquito Anopheles gambiae sensu stricto. *J Chem Ecol*, **35**: 933–943.

Sorensen, P.W., Hara, T.J. and Stacey, N.E. 1991. Sex pheromones selectively stimulate the medial olfactory tracts of male goldfish. *Brain Research*, **558**: 343–347.

Steinberg, T.H. 2009. Chapter 31 Protein Gel Staining Methods. In: *Methods in Enzymology*, pp. 541–563.

Steinbrecht, R.A. 1998. Odorant-Binding Proteins: Expression and Function. *Annals NY Acad Sci*, **855**: 323–332.

Stocker, R.F. 1994. The organization of the chemosensory system in Drosophila melanogaster: a rewiew. *Cell Tissue Res*, **275**: 3–26.

Stoffolano, J.G. and Haselton, A.T. 2013. The Adult Dipteran Crop: A Unique and Overlooked Organ. *Annu. Rev. Entomol.*, **58**: 205–225.

Storelli, G., Defaye, A., Erkosar, B., Hols, P., Royet, J. and Leulier, F. 2011. Lactobacillus plantarum Promotes Drosophila Systemic Growth by Modulating Hormonal Signals through TOR-Dependent Nutrient Sensing. *Cell Metabolism*, **14**: 403–414.

Storelli, G., Strigini, M., Grenier, T., Bozonnet, L., Schwarzer, M., Daniel, C., Matos, R. and Leulier, F. 2018. Drosophila Perpetuates Nutritional Mutualism by Promoting the Fitness of Its Intestinal Symbiont Lactobacillus plantarum. *Cell Metabolism*, **27**: 362-377.e8.

Sturz, A.V. 1995. The role of endophytic bacteria during seed piece decay and potato tuberization. *Plant Soil*, **175**: 257–263.

Sun, Jennifer S, Larter, N.K., Chahda, J.S., Rioux, D., Gumaste, A. and Carlson, J.R. 2018. Humidity response depends on the small soluble protein Obp59a in Drosophila. *eLife*, **7**: e39249.

Sun, Jennifer S., Xiao, S. and Carlson, J.R. 2018. The diverse small proteins called odorant-binding proteins. *Open Biol.*, **8**: 180208.

Svetec, N. and Ferveur, J.-F. 2005. Social experience and pheromonal perception can change male–male interactions in *Drosophila melanogaster*. *Journal of Experimental Biology*, **208**: 891–898.

Taga, M.E. and Bassler, B.L. 2003. Chemical communication among bacteria. 6.

Takashima, S., Adams, K.L., Ortiz, P.A., Ying, C.T., Moridzadeh, R., Younossi-Hartenstein, A. and Hartenstein, V. 2011. Development of the Drosophila entero-endocrine lineage and its specification by the Notch signaling pathway. *Developmental Biology*, **353**: 161–172.

Takashima, S., Gold, D. and Hartenstein, V. 2013. Stem cells and lineages of the intestine: a developmental and evolutionary perspective. *Dev Genes Evol*, **223**: 85–102.

Téfit, M.A., Gillet, B., Joncour, P., Hughes, S. and Leulier, F. 2018. Stable association of a Drosophila -derived microbiota with its animal partner and the nutritional environment throughout a fly population's life cycle. *Journal of Insect Physiology*, **106**: 2–12.

Tegoni, M., Ramoni, R., Bignetti, E., Spinelli, S. and Cambillau, C. 1996. Domain swapping creates a third putative combining site in bovine odorant binding protein dimer. *Nat Struct Mol Biol*, **3**: 863–867.

Tennessen, J.M. and Thummel, C.S. 2011. Coordinating Growth and Maturation — Insights from Drosophila. *Current Biology*, **21**: R750–R757.

Thorne, N. 2005. Function and Expression of the Drosophila Gr Genes in the Perception of Sweet, Bitter and Pheromone Compounds. *Chemical Senses*, **30**: i270–i272.

Tordoff, M.G., Shao, H., Alarcón, L.K., Margolskee, R.F., Mosinger, B., Bachmanov, A.A., Reed, D.R. and McCaughey, S. 2008. Involvement of T1R3 in calcium-magnesium taste. *Physiological Genomics*, **34**: 338–348.

Toshima, N. and Tanimura, T. 2012. Taste preference for amino acids is dependent on internal nutritional state in *Drosophila melanogaster*. *Journal of Experimental Biology*, **215**: 2827–2832.

Trotier, D. 2011. Vomeronasal organ and human pheromones. *European Annals of Otorhinolaryngology, Head and Neck Diseases*, **128**: 184–190.

Tsuruta, M., Kawada, T., Fukuwatari, T. and Fushiki, T. 1999. The Orosensory Recognition of Long-Chain Fatty Acids in Rats. *Physiology & Behavior*, **66**: 285–288.

Tu, Y.-H., Cooper, A.J., Teng, B., Chang, R.B., Artiga, D.J., Turner, H.N., Mulhall, E.M., Ye, W., Smith, A.D. and Liman, E.R. 2018. An evolutionarily conserved gene family encodes proton-selective ion channels. *Science*, **359**: 1047–1050.

Turlings, T.C., Loughrin, J.H., McCall, P.J., Röse, U.S., Lewis, W.J. and Tumlinson, J.H. 1995. How caterpillar-damaged plants protect themselves by attracting parasitic wasps. *Proc. Natl. Acad. Sci. U.S.A.*, **92**: 4169–4174.

Turnbaugh, P.J., Bäckhed, F., Fulton, L. and Gordon, J.I. 2008. Diet-Induced Obesity Is Linked to Marked but Reversible Alterations in the Mouse Distal Gut Microbiome. *Cell Host & Microbe*, **3**: 213–223.

Turnbaugh, P.J., Hamady, M., Yatsunenko, T., Cantarel, B.L., Duncan, A., Ley, R.E., Sogin, M.L., Jones, W.J., Roe, B.A., Affourtit, J.P., Egholm, M., Henrissat, B., Heath, A.C., Knight, R. and Gordon, J.I. 2009. A core gut microbiome in obese and lean twins. *Nature*, **457**: 480–484.

Turnbaugh, P.J., Ley, R.E., Mahowald, M.A., Magrini, V., Mardis, E.R. and Gordon, J.I. 2006. An obesity-associated gut microbiome with increased capacity for energy harvest. *Nature*, **444**: 1027–1031.

Tzou, P., Ohresser, S., Ferrandon, D., Capovilla, M., Reichhart, J.-M., Lemaitre, B., Hoffmann, J.A. and Imler, J.-L. 2000. Tissue-Specific Inducible Expression of Antimicrobial Peptide Genes in Drosophila Surface Epithelia. *Immunity*, **13**: 737–748.

Uma, G., Babu, M.M., Prakash, V.S.G., Nisha, S.J. and Citarasu, T. 2020. Nature and bioprospecting of haloalkaliphilics: a review. *World J Microbiol Biotechnol*, **36**: 66.

Vandesompele, J., Preter, K.D., Roy, N.V. and Paepe, A.D. 2002. Accurate normalization of real-time quantitative RT-PCR data by geometric averaging of multiple internal control genes. 12.

Vidal, B., Aghayeva, U., Sun, H., Wang, C., Glenwinkel, L., Bayer, E.A. and Hobert, O. 2018. An atlas of Caenorhabditis elegans chemoreceptor expression. *PLoS Biol*, **16**: e2004218.

Vijay-Kumar, M., Aitken, J.D., Carvalho, F.A., Cullender, T.C., Mwangi, S., Srinivasan, S., Sitaraman, S.V., Knight, R., Ley, R.E. and Gewirtz, A.T. 2010. Metabolic Syndrome and Altered Gut Microbiota in Mice Lacking Toll-Like Receptor 5. *Science*, **328**: 228–231.

Vincent, F., Spinelli, S., Ramoni, R., Grolli, S., Pelosi, P., Cambillau, C. and Tegoni, M. 2000. Complexes of porcine odorant binding protein with odorant molecules belonging to different chemical classes. *Journal of Molecular Biology*, **300**: 127–139.

Vogt, R.G. and Riddiford, L.M. 1981. Pheromone binding and inactivation by moth antennae. *Nature*, **293**: 161–163.

Vosshall, L.B., Amrein, H., Morozov, P.S., Rzhetsky, A. and Axel, R. 1999. A Spatial Map of Olfactory Receptor Expression in the Drosophila Antenna. *Cell*, **96**: 725–736.

Vosshall, L.B. and Hansson, B.S. 2011. A Unified Nomenclature System for the Insect Olfactory Coreceptor. *Chemical Senses*, **36**: 497–498.

Vosshall, L.B. and Stocker, R.F. 2007. Molecular Architecture of Smell and Taste in *Drosophila*. *Annu. Rev. Neurosci.*, **30**: 505–533.

Vosshall, L.B., Wong, A.M. and Axel, R. 2000. An Olfactory Sensory Map in the Fly Brain. *Cell*, **102**: 147–159.

Wakil, S.J., Stoops, J.K. and Joshi, V.C. 1983. Fatty Acid Synthesis and its Regulation. 43.

Wang, J., Batourina, E., Schneider, K., Souza, S., Swayne, T., Liu, C., George, C.D., Tate, T., Dan, H., Wiessner, G., Zhuravlev, Y., Canman, J.C., Mysorekar, I.U. and Mendelsohn, C.L. 2018. Polyploid Superficial Cells that Maintain the Urothelial Barrier Are Produced via Incomplete Cytokinesis and Endoreplication. *Cell Reports*, **25**: 464-477.e4.

Westwood, J.H., Yoder, J.I., Timko, M.P. and dePamphilis, C.W. 2010. The evolution of parasitism in plants. *Trends in Plant Science*, **15**: 227–235.

Wisotsky, Z., Medina, A., Freeman, E. and Dahanukar, A. 2011. Evolutionary differences in food preference rely on Gr64e, a receptor for glycerol. *Nat Neurosci*, **14**: 1534–1541.

Wolfner, M.F. 2002. The gifts that keep on giving: physiological functions and evolutionary dynamics of male seminal proteins in Drosophila. *Heredity*, **88**: 85–93.

Wolfner, M.F. 1997. Tokens of love: Functions and regulation of drosophila male accessory gland products. *Insect Biochemistry and Molecular Biology*, **27**: 179–192.

Wong, A.C.-N., Dobson, A.J. and Douglas, A.E. 2014. Gut microbiota dictates the metabolic response of *Drosophila* to diet. *Journal of Experimental Biology*, jeb.101725.

Wong, A.C.-N., Wang, Q.-P., Morimoto, J., Senior, A.M., Lihoreau, M., Neely, G.G., Simpson, S.J. and Ponton, F. 2017. Gut Microbiota Modifies Olfactory-Guided Microbial Preferences and Foraging Decisions in Drosophila. *Current Biology*, **27**: 2397-2404.e4.

Wong, C.N.A., Ng, P. and Douglas, A.E. 2011. Low-diversity bacterial community in the gut of the fruitfly Drosophila melanogaster: Bacterial community in Drosophila melanogaster. *Environmental Microbiology*, **13**: 1889–1900.

Wu, C.I., Hollocher, H., Begun, D.J., Aquadro, C.F., Xu, Y. and Wu, M.L. 1995. Sexual isolation in Drosophila melanogaster: a possible case of incipient speciation. *Proc. Natl. Acad. Sci. U.S.A.*, **92**: 2519–2523.

Wu, K., Zhang, J., Zhang, Q., Zhu, S., Shao, Q., Clark, K.D., Liu, Y. and Ling, E. 2015. Plant phenolics are detoxified by prophenoloxidase in the insect gut. *Sci Rep*, **5**: 16823.

Xu, C., Li, C.Y.-T. and Kong, A.-N.T. 2005. Induction of phase I, II and III drug metabolism/transport by xenobiotics. *Arch Pharm Res*, **28**: 249–268.

Xu, W., Zhang, H.-J. and Anderson, A. 2012. A Sugar Gustatory Receptor Identified from the Foregut of Cotton Bollworm Helicoverpa armigera. *J Chem Ecol*, **38**: 1513–1520.

Yamada, R., Deshpande, S.A., Bruce, K.D., Mak, E.M. and Ja, W.W. 2015. Microbes Promote Amino Acid Harvest to Rescue Undernutrition in Drosophila. *Cell Reports*, **10**: 865–872.

Yamaguchi, S. 1967. The Synergistic Taste Effect of Monosodium Glutamate and Disodium 5'-Inosinate. *J Food Science*, **32**: 473–478.

Yang, W. and Briegel, A. 2020. Diversity of Bacterial Chemosensory Arrays. *Trends in Microbiology*, **28**: 68–80.

Yarmolinsky, D.A., Zuker, C.S. and Ryba, N.J.P. 2009. Common Sense about Taste: From Mammals to Insects. *Cell*, **139**: 234–244.

Yoshikawa, K., Nakagawa, H., Mori, N., Watanabe, H. and Touhara, K. 2013. An unsaturated aliphatic alcohol as a natural ligand for a mouse odorant receptor. *Nat Chem Biol*, **9**: 160–162.

Young, J.M., Massa, H.F., Hsu, L. and Trask, B.J. 2010. Extreme variability among mammalian V1R gene families. *Genome Res.*, **20**: 10–18.

Zhang, H.-J., Anderson, A.R., Trowell, S.C., Luo, A.-R., Xiang, Z.-H. and Xia, Q.-Y. 2011. Topological and Functional Characterization of an Insect Gustatory Receptor. *PLoS ONE*, **6**: e24111.

Zhang, X. and Firestein, S. 2002. The olfactory receptor gene superfamily of the mouse. *Nat Neurosci*, **5**: 124–133.

Zhang, Y.V., Ni, J. and Montell, C. 2013. The Molecular Basis for Attractive Salt-Taste Coding in *Drosophila*. *Science*, **340**: 1334–1338.

Zhou, D., Pan, Q., Shen, F., Cao, H., Ding, W., Chen, Y. and Fan, J. 2017. Total fecal microbiota transplantation alleviates high-fat diet-induced steatohepatitis in mice via beneficial regulation of gut microbiota. *Sci Rep*, **7**: 1529.

Zhou, J.-J. 2010. Odorant-Binding Proteins in Insects. In: *Vitamins & Hormones*, pp. 241–272.

Zhou, J.-J., Huang, W., Zhang, G.-A., Pickett, J.A. and Field, L.M. 2004. "Plus-C" odorant-binding protein genes in two Drosophila species and the malaria mosquito Anopheles gambiae. *Gene*, **327**: 117–129.

Zhu, J., Arena, S., Spinelli, S., Liu, D., Zhang, G., Wei, R., Cambillau, C., Scaloni, A., Wang, G. and Pelosi, P. 2017. Reverse chemical ecology: Olfactory proteins from the giant panda and their interactions with putative pheromones and bamboo volatiles. *Proc. Natl. Acad. Sci. U.S.A.*, **114**.

Abstract

Implication of an odorant-binding protein in precopulatory behaviour and interaction with the bacterial microbiota

*Keywords: Drosophila, chemoreception, O*BP, *gustatory system, gut microbiota, courtship behaviour*

Chemoreception allows animals to detect nutritive food and avoid toxic compounds. Volatile and non-volatile chemical compounds, which are detected by olfactory and gustatory sensory organs, can trigger feeding and reproductive behaviours in animals such as *Drosophila melanogaster*. Inside chemosensory organs, perireceptor proteins like odorant-binding proteins (OBPs) serve to transport odorant and tastant molecule to dedicated receptors. OBPs are not only involved in chemoreception but also in several other functions. A recent study revealed an interaction between insect microbiota and OBP expression while another one showed that microbes can promote nutrient harvesting on food.

In our project, we used Drosophila *melanogaster as a model organism,* to find a link between the presence of bacteria, the expression of OBPs and behavioural performance of flies. More particularly, we investigated the expression of OBP56d and OBP56g, both present in the adult chemosensory system and in the gut, and we measured their influence on reproductive-related behaviours. We used both *in vitro* and *in vivo* approaches to characterize several aspects pertaining to OBP expression in adult gustatory appendages, gut and reproductive organs.

The expression of OBP56g and OBP56d was measured and compared in the thorax, head, and gut of virgin females and males and of mated females subjected to fasting of different durations (0h, 2h, 16h, and 30h). A focus on OBP56d expression revealed a particularly strong expression in the male hindgut and in the proboscis of both sexes. To test the effect of bacterial microbiota on OBP56d and OBP56g expression, our first experiment consisted to raise a control *D.melanogaster* strain, during two generations on an antibiotic-rich diet.

Both OBPs were cloned, produced with a bacterial heterologous expression system and purified. Their binding properties were studied with a competitive fluorescence binding assay. Among many compounds tested OBP56d, and to a lesser extend OBP56g, showed a strong affinity for long chain fatty acids with no clear preference according to the presence and number of unsaturation(s).

The use of *in situ* fluorescent probes confirmed the expression of OBP56d in the male hindgut. Moreover, we discovered OBP56d expression in the testis, and this led us to test mating behaviour. More particularly, we tested copulation in pairs of flies combining control and *OBP56d*$^{-}$ mutant flies. The *OBP56d*$^{-}$ mutation strongly decreased female copulation in experiments lasting 2 hours but not in those lasting 12 hours indicating that the *OBP56d*$^{-}$ mutation was likely slowing down female capacity to detect or to interpret male stimulating pheromone(s) whose identity remains still unknown. However, the *OBP56d*$^{-}$ mutation did not affect fly fertility and fecundity.

Overall, our PhD project provides novel insights on the roles of OBPs in precopulatory behaviour and some hints on the impact of microbiota on their expression.

Résumé

Implication d'une protéine de liaison aux odorants dans le comportement précopulatoire et l'interaction avec le microbiote bactérien

Mots clés : Drosophila, chemioperception, protéine de liaison aux odorants, system gustatif, microbiote bactérien, comportement de parade nuptiale

La chemioperception permet aux animaux de détecter les aliments nutritifs et d'éviter les composés toxiques. Les composés chimiques volatils et non volatils, qui sont détectés par les organes sensoriels olfactifs et gustatifs, peuvent déclencher des comportements alimentaires et reproducteurs chez des animaux tels que Drosophila melanogaster. À l'intérieur des organes chemiosensoriels, les protéines périréceptrices telles que les protéines de liaison aux odeurs (OBP) servent à transporter les molécules odorantes et gustatives vers des récepteurs dédiés. Les OBP ne sont pas seulement impliqués dans la chemioperception mais également dans plusieurs autres fonctions. Une étude récente a révélé une interaction entre le microbiote des insectes et l'expression de l'OBP tandis qu'une autre a montré que les microbes peuvent favoriser la récolte des nutriments sur les aliments.

Dans notre projet, nous avons utilisé Drosophila melanogaster comme organisme modèle, pour trouver un lien entre la présence de bactéries, l'expression des OBP et les performances comportementales des mouches. Plus particulièrement, nous avons étudié l'expression de OBP56d et OBP56g, les deux présentent dans le système chemiosensoriel adulte et dans l'intestin, et nous avons mesuré leur influence sur les comportements liés à la reproduction. Nous avons utilisé des approches in vitro et in vivo pour caractériser plusieurs aspects relatifs à l'expression de l'OBP dans les appendices gustatifs adultes, l'intestin et les organes reproducteurs. L'expression d'OBP56g et d'OBP56d a été mesurée et comparée dans le thorax, la tête et l'intestin de femelles et de mâles vierges et de femelles accouplées soumises à des jeûnes de différentes durées (0h, 2h, 16h et 30h). Une concentration sur l'expression d'OBP56d a révélé une expression particulièrement forte dans l'intestin postérieur des mâles et dans la trompe des deux sexes.

Pour tester l'effet du microbiote bactérien sur l'expression d'OBP56d et d'OBP56g, notre première expérience a consisté à élever la lignée témoin de *D.melanogaster*, pendant deux générations sur un régime riche en antibiotiques. Les deux OBP ont été clonés, produits avec un système d'expression hétérologue bactérien et purifiés. Leurs propriétés de liaison ont été étudiées avec un test de liaison par fluorescence compétitive. Parmi de nombreux composés testés, OBP56d, et dans une moindre mesure OBP56g, ont montré une forte affinité pour les acides gras à longue chaîne sans préférence nette selon la présence et le nombre d'insaturation(s). L'utilisation de sondes fluorescentes in situ a confirmé l'expression d'OBP56d dans l'intestin postérieur mâle.

De plus, nous avons découvert l'expression d'OBP56d dans les testicules, ce qui nous a conduit à tester le comportement d'accouplement. Plus particulièrement, nous avons testé la copulation chez des couples de mouches combinant des mouches témoins et OBP56d-mutantes. La mutation OBP56d a fortement diminué la copulation des femelles dans les expériences d'une durée de 2 heures mais pas dans celles d'une durée de 12 heures indiquant que la mutation OBP56d ralentissait probablement la capacité de la femelle à détecter ou à interpréter la ou les phéromones stimulantes mâles dont l'identité reste encore inconnue. Cependant, la mutation OBP56d n'a pas affecté la fertilité et la fécondité des mouches.

Dans l'ensemble, notre projet de doctorat fournit de nouvelles informations sur les rôles des OBP dans le comportement précopulatoire et quelques indices sur l'impact du microbiote sur leur expression.